



12-2000

## **Structure-function studies of the saccharomyces cerevisiae pheromone receptor, ste2p, using novel $\alpha$ -factor analogs**

Loren Keith Henry

Follow this and additional works at: [https://trace.tennessee.edu/utk\\_graddiss](https://trace.tennessee.edu/utk_graddiss)

---

### **Recommended Citation**

Henry, Loren Keith, "Structure-function studies of the saccharomyces cerevisiae pheromone receptor, ste2p, using novel  $\alpha$ -factor analogs. " PhD diss., University of Tennessee, 2000.  
[https://trace.tennessee.edu/utk\\_graddiss/8293](https://trace.tennessee.edu/utk_graddiss/8293)

This Dissertation is brought to you for free and open access by the Graduate School at TRACE: Tennessee Research and Creative Exchange. It has been accepted for inclusion in Doctoral Dissertations by an authorized administrator of TRACE: Tennessee Research and Creative Exchange. For more information, please contact [trace@utk.edu](mailto:trace@utk.edu).

To the Graduate Council:

I am submitting herewith a dissertation written by Loren Keith Henry entitled "Structure-function studies of the *saccharomyces cerevisiae* pheromone receptor, *ste2p*, using novel  $\alpha$ -factor analogs." I have examined the final electronic copy of this dissertation for form and content and recommend that it be accepted in partial fulfillment of the requirements for the degree of Doctor of Philosophy, with a major in Life Sciences.

Jeffery M. Becker, Major Professor

We have read this dissertation and recommend its acceptance:

John W. Koontz, May Ann Handel, Cynthia B. Peterson

Accepted for the Council:


Carolyn R. Hodges

Vice Provost and Dean of the Graduate School

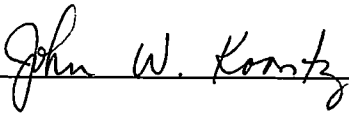
(Original signatures are on file with official student records.)

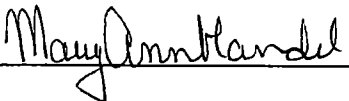
To the Graduate Council:

I am submitting a dissertation written by Loren Keith Henry entitled "Structure-Function Studies of the *Saccharomyces cerevisiae* Pheromone Receptor, Ste2p, using Novel  $\alpha$ -factor Analogs." I have examined the final copy of this dissertation for form and content and recommend that it be accepted in partial fulfillment of the requirements for the degree of Doctor of Philosophy, with a major in Life Sciences.

  
\_\_\_\_\_  
Jeffrey M. Becker, Major Professor

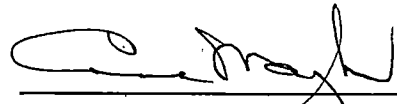
We have read this dissertation  
And recommend its acceptance:

  
\_\_\_\_\_

  
\_\_\_\_\_

  
\_\_\_\_\_

Accepted for the Council:

  
\_\_\_\_\_  
Interim Vice Provost and  
Dean of The Graduate School

**Structure-Function Studies of the  
*Saccharomyces cerevisiae* Phermone Receptor, Ste2p,  
using novel  $\alpha$ -factor analogs**

A Dissertation  
Presented for the  
Doctor of Philosophy  
Degree

The University of Tennessee, Knoxville

L. Keith Henry  
December 2000

Copyright © Loren Keith Henry, 2000  
All rights reserved

## DEDICATION

This dissertation is dedicated in memory of my parents

Mr. John Lewis Henry

and

Mrs. Grace Marie Henry

who gave me the courage to reach for my dreams and the strength to persevere  
along the journey.

## ACKNOWLEDGEMENTS

I would like to thank several people who have been instrumental in my personal growth as a researcher and as a member of society. I would first like to thank my committee members: Dr. Handel, Dr. Koontz and Dr. Peterson. Their guidance, insight and forthrightness have been invaluable to me during my graduate studies. Most of all, I thank them for being interested in my ideas and treating me more as a colleague than as a student.

My appreciation goes out to Dr. Fred Naider for his keen mind, critical thinking and objectivity during these studies. Also, I would like to thank Dr. Naider and members of his lab for the peptide syntheses that made these studies possible.

The importance of picking the right lab for your graduate studies cannot be overstated and I can say without reservation that the Becker lab is the best. The lab members over the years seem to possess both tangible and intangible qualities that have made the environment conducive for camaraderie, self-development, enthusiasm and progressive thinking. There have been some very special people from the Becker lab that I would like to especially thank. To start, I would like to convey my appreciation for these people as friends and as scientists by using a quote from Isaac Newton, "*If I have seen further...it is by standing upon the shoulders of Giants*". Thanks goes to my dear friend Dr. Angela McKinney-

Williams who started the work on crosslinking  $\alpha$ -factor to Ste2p. She has been like a sister to me and holds a special place in my heart. My utmost appreciation and respect goes to my friend, Dr. Melinda Hauser. She has been a tome of knowledge and a tower of strength for me <and many others>. Special thanks goes to my friend Dr. David Barnes, who truly has the intangibles. He has had more influence on me than he will ever know. Thanks to my great friend and CDC connection, Greg Anderson. He came through many times when I needed a laugh or a smile just to go on. Thanks to David Miller, who taught me the ropes both in research and in administration, and to Hui-Fen Lu, who showed me that quiet dignity can be deafening. Appreciation to Dr. Steve Wright for crosslinking help. Thanks to several past members of the Becker lab who were role models in many ways. Dr. Mark “anti-technology ray gun” Lubkowitz, Dr. Greg “organization is everything” Abel, Dr. Kumar “joke a day” Alagrammam, Dr. Angus Dawe, Dr. Guy Caldwell and Jeff Wiles.

A special appreciation goes to those currently in the Becker lab. I will always remember my enthusiastic conversations with Byung-Kwon “the thinker” Lee on topics such as Ste2,  $\alpha$ -factor, the theory of relativity, quantum mechanics and Korean socio-economics. Lee’s wife is the ultimate source for great lab meeting snacks. Special gratitude goes to my “Indonesian Connection” Vanny Narita. Vanny always has something positive or funny to say. Thanks to Amy “allergy” Donhardt for all your help and sharing musical tastes, sort of. Also,



thanks to Sarah “dancing mouse” Kauffman and “Evil” Keith Goldstein. Much appreciation goes to Ayca Strader, who had to persevere having the closest proximity to me. Thanks to Cagdas Son for continuing the work on Ste2p crosslinking and for taking over computer duties. Great things are yet to come. Thanks to Jason Cathelyn, Brandon Belcher, Summer Galloway, Nathan “Big Ten” VerBerkmoes, Joshua Sharp Wes Parris, Allen Craig, Shannon Matulis, Stephanie Hulen, Amy Kieser and Alison Jakes.

To my mentor, teacher, and friend, Dr. Jeff Becker, I offer my sincere admiration and gratitude. In many ways, Jeff has been there in place of the father I lost too soon. He has provided me with strength, support and direction. Jeff gave me a chance when he did not have to and probably shouldn't have. That solitary act of kindness has always been a treasure to me and continues to give me hope that one day I too can make such a difference in someone's life. We have shared great tragedy and triumph together and as a result learned what is truly important in the grand scheme of things. I know that I am proud to call Jeff my friend.

Finally, I would like to thank my wife, Jennifer. She has been and continues to be supportive, caring, loving and most of all, patient. Many times I think I asked too much of her. On numerous occasions, I have been told that I lucked out by having a wife who actually enjoys sports and who can deal with the pressures of being married to a graduate student. Well, I'm not just lucky. I am

blessed. I am certain that without Jennifer and her love I would not have reached this point. Thank you!

## ABSTRACT

G- protein coupled receptors (GPCRs) are heptahelical membrane proteins that allow cells to sense and respond to a variety of environmental stimuli. Study of GPCRs has begun to elucidate their important role in human disease and has allowed for the development of a number of clinical treatments.

The yeast *Saccharomyces cerevisiae* which uses peptide pheromones and GPCRs to mediate sexual reproduction between haploid cells presents a model system for the study of GPCRs. The studies presented here detail the use of novel peptide analogs to investigate the structure-function relationship between the Ste2p receptor and its ligand, the  $\alpha$ -factor pheromone.

Characterization of a gamut of  $\alpha$ -factor analogs resulted in the identification of several analogs with biological activity and sub-micromolar binding affinity (Kd) identifying them as good candidates for use in photoaffinity labeling studies to map the  $\alpha$ -factor binding site in the Ste2p receptor.

Photoaffinity labeling with the analog [Bpa<sup>1</sup> Y<sup>3</sup> (<sup>125</sup>I) R<sup>7</sup> Nle<sup>12</sup> F<sup>13</sup>]  $\alpha$ -factor and subsequent receptor fragmentation showed that position one of the  $\alpha$ -factor peptide crosslinked to a fragment of the receptor from amino acid 190 to 294.

Formation of a dimeric  $\alpha$ -factor molecule by covalent attachment of the epsilon amines of Lys<sup>7</sup> via an aminohexanoic acid bridge resulted in a ligand which showed specific binding to the Ste2p receptor and the ability to activate the

pheromone signal cascade. The binding affinity and biological activity of this  $\alpha$ -factor dimer suggest that the Lys<sup>7</sup> residue in  $\alpha$ -factor is relatively exposed to solvent and not buried into the receptor. These findings support the current model of the structure of  $\alpha$ -factor when it is bound to the Ste2p receptor.

Further characterization of a novel class of  $\alpha$ -factor analogs termed synergist has revealed that these ligands do not enhance biological activity by modulating the rates of association or dissociation of agonists to the Ste2p receptor. Furthermore, the synergists do not increase the total amount of agonist binding to Ste2p since the total amount of [<sup>3</sup>H]  $\alpha$ -factor associated to Ste2p does not change in the presence or absence of synergist. The new information from these studies has allowed for several models of synergist action to be proposed.

## TABLE OF CONTENTS

CHAPTER		PAGE
	<b>PART I: GENERAL INTRODUCTION</b>	1
I	LITERATURE REVIEW	2
	LIST OF REFERENCES	16
	 <b>PART II: POSITION 13 ANALOGS OF THE TRIDECAPEPTIDE MATING PHEROMONE FROM <i>SACCHAROMYCES CEREVISIAE</i>: DESIGN OF AN IODINATABLE LIGAND FOR RECEPTOR BINDING</b>	 22
I	INTRODUCTION	23
II	MATERIALS AND METHODS	27
III	RESULTS	35
IV	DISCUSSION	50
	LIST OF REFERENCES	55
	 <b>PART III: IDENTIFICATION OF AN <math>\alpha</math>-FACTOR BINDING SITE ON THE Ste2p PHEROMONE RECEPTOR BY DIRECT PHOTO-AFFINITY LABELING WITH [Bpa<sup>1</sup> Y<sup>3</sup> R<sup>7</sup> F<sup>13</sup>] <math>\alpha</math>-FACTOR</b>	 66
I	INTRODUCTION	67
II	MATERIALS AND METHODS	70
III	RESULTS	82
IV	DISCUSSION	119
	LIST OF REFERENCES	125
	 <b>PART IV: DESIGN, SYNTHESIS AND CHARACTERIZATION OF A NOVEL DIMERIC <math>\alpha</math>-FACTOR LIGAND</b>	 132
I	INTRODUCTION	133
II	MATERIALS AND METHODS	137
III	RESULTS	143
IV	DISCUSSION	166
	LIST OF REFERENCES	171
	 <b>PART V: CHARACTERIZATION OF A NOVEL GROUP OF SYNERGISTIC LIGANDS FOR Ste2p, THE <math>\alpha</math>-FACTOR RECEPTOR IN <i>SACCHAROMYCES CEREVISIAE</i>.</b>	 178
I	INTRODUCTION	179
II	MATERIALS AND METHODS	186
III	RESULTS	199
IV	DISCUSSION	226
	LIST OF REFERENCES	238

**PART IV: GENERAL CONCLUSIONS AND  
DISCUSSION**

**244**

**VITA**

**267**

## LIST OF TABLES

TABLE		PAGE
	<b>PART II: POSITION 13 ANALOGS OF THE TRIDECAPEPTIDE MATING PHEROMONE FROM <i>SACCHAROMYCES CEREVISIAE</i>: DESIGN OF AN IODINATABLE LIGAND FOR RECEPTOR BINDING</b>	
1	Chemical and physical properties of $\alpha$ -factor analogs.....	28
2	Biological activities and binding affinities of $\alpha$ -factor analogs...	36
	<b>PART III: IDENTIFICATION OF AN <math>\alpha</math>-FACTOR BINDING SITE ON THE Ste2p PHEROMONE RECEPTOR BY DIRECT PHOTO-AFFINITY LABELING WITH [Bpa<sup>1</sup> Y<sup>3</sup> R<sup>7</sup> F<sup>13</sup>] <math>\alpha</math>-FACTOR</b>	
1	Physiochemical properties of photoactivatable peptides.....	71
2	Biological activity and binding affinity of $\alpha$ -factor analogs.....	87
	<b>PART IV: DESIGN, SYNTHESIS AND CHARACTERIZATION OF A NOVEL DIMERIC <math>\alpha</math>-FACTOR LIGAND</b>	
1	Synergist effect on growth arrest activity of $\alpha$ -factor dimer in <i>S. cerevisiae</i> strain RC629 and RC631.....	154
	<b>PART V: CHARACTERIZATION OF A NOVEL GROUP OF SYNERGISTIC LIGANDS FOR Ste2p, THE <math>\alpha</math>-FACTOR RECEPTOR IN <i>SACCHAROMYCES CEREVISIAE</i>.</b>	
1	Ligand structures.....	184
2	Effect of overexpression of <i>SST2</i> on action of synergist and $\alpha$ -factor in growth arrest assay with strain LM23-3AZ.....	214

## LIST OF FIGURES

FIGURE		PAGE
<b>PART I: GENERAL INTRODUCTION</b>		
1	Ribbon drawing of rhodopsin.....	5
2	Pheromone mediated mating in <i>Saccharomyces cerevisiae</i> .....	8
3	Pheromone signal trasduction pathway.....	10
4	Functional domains of the $\alpha$ -factor ligand.....	13
 <b>PART II: POSITION 13 ANALOGS OF THE TRIDECAPEPTIDE MATING PHEROMONE FROM <i>SACCHAROMYCES CEREVISIAE</i>: DESIGN OF AN IODINATABLE LIGAND FOR RECEPTOR BINDING</b>		
1	Growth arrest of <i>S. cerevisiae</i> by $\alpha$ -factor and various analogs	38
2	Dose response to $\alpha$ -factor and analogs determined by reporter gene <i>lacZ</i> (beta-galactosidase).....	41
3	Competition binding assay.....	44
4	Saturation and competition binding assays with [Tyr <sup>1</sup> ( <sup>125</sup> I)-Phe <sup>13</sup> ] $\alpha$ -factor .....	48
 <b>PART III: IDENTIFICATION OF AN <math>\alpha</math>-FACTOR BINDING SITE ON THE Ste2p PHEROMONE RECEPTOR BY DIRECT PHOTO-AFFINITY LABELING WITH [Bpa<sup>1</sup> Y<sup>3</sup> R<sup>7</sup> F<sup>13</sup>] <math>\alpha</math>-FACTOR</b>		
1	Binding affinity of Bpa substituted $\alpha$ -factor analogs.....	84
2	Growth arrest of <i>S. cerevisiae</i> DK102pNED cells by $\alpha$ -factor and various analogs.....	85
3	Competition binding assay of various $\alpha$ -factor analogs vs ( <sup>125</sup> I)-[Tyr <sup>1</sup> Arg <sup>7</sup> Phe <sup>13</sup> ] $\alpha$ -factor using DK102pNED cells.....	91
4	HPLC analysis of products from iodination of tyrosine substituted $\alpha$ -factor analogs.....	94



FIGURE		PAGE
5	Competition binding analysis of ( <sup>125</sup> I)-[Bpa <sup>1</sup> Tyr <sup>3</sup> Arg <sup>7</sup> Phe <sup>13</sup> ] α-factor and non-radiolabeled α-factor.....	96
6	Total radioactive counts of ( <sup>125</sup> I)-[Bpa <sup>1</sup> Tyr <sup>3</sup> Arg <sup>7</sup> Phe <sup>13</sup> ] α-factor bound to membranes following crosslinking in the presence and absence of non-radiolabeled α-factor.....	99
7	Autoradiogram of SDS-PAGE analysis of UV irradiated DK102pNED membranes in the presence of ( <sup>125</sup> I)-[Bpa <sup>1</sup> Tyr <sup>3</sup> Arg <sup>7</sup> Phe <sup>13</sup> ] α-factor.....	101
8	Western blot analysis of crosslinked BJ2168pNED1 membranes	103
9	Autoradiograph of SDS-PAGE 10-20% tricine gel analysis of BJ2168pNED1 membranes photolabeled with ( <sup>125</sup> I)-[Bpa <sup>1</sup> Tyr <sup>3</sup> Arg <sup>7</sup> Phe <sup>13</sup> ] α-factor.....	106
10	Schematic of chemical cleavage of Ste2p.....	108
11	Western blot analysis of BNPS-skatole digested BJ2168pNED1 membranes.....	111
12	Autoradiograph of BJ2168pNED1 membranes photocrosslinked with ( <sup>125</sup> I)-[Bpa <sup>1</sup> Tyr <sup>3</sup> Arg <sup>7</sup> Phe <sup>13</sup> ] α-factor and treated with BNPS-skatole.....	113
13	Autoradiographs of BJ2168pNED1 membranes photocrosslinked with ( <sup>125</sup> I)-[Bpa <sup>1</sup> Tyr <sup>3</sup> Arg <sup>7</sup> Phe <sup>13</sup> ] α-factor and treated with cyanogens bromide.....	116
<b>PART IV: DESIGN, SYNTHESIS AND CHARACTERIZATION OF A NOVEL DIMERIC α-FACTOR LIGAND</b>		
1	Diagram of primary structure of α-factor dimer.....	144
2	Growth arrest assay of <i>S. cerevisiae</i> by α-factor and α-factor dimer.....	147

FIGURE		PAGE
3	Dose response to $\alpha$ -factor and $\alpha$ -factor dimer by reporter gene lacZ (beta-galactosidase).....	149
4	Competition binding assay with ( $^{125}$ I)-[Tyr <sup>1</sup> Phe <sup>13</sup> ] $\alpha$ -factor.....	151
5	Effect of the $\alpha$ -factor antagonist desW <sup>1</sup> desH <sup>2</sup> $\alpha$ -factor on $\alpha$ -factor and $\alpha$ -factor dimer in growth arrest assay.....	156
6	HPLC analysis of $\alpha$ -factor and $\alpha$ -factor dimer following incubation with RC629 and DK102pNED1 cells.....	159
 <b>PART V: CHARACTERIZATION OF A NOVEL GROUP OF SYNERGISTIC LIGANDS FOR Ste2p, THE <math>\alpha</math>-FACTOR RECEPTOR IN <i>SACCHAROMYCES CEREVISIAE</i>.</b> 		
1	Illustration of growth arrest used to characterize the activity of $\alpha$ -factor analogs.....	189
2	Schematic for disruption of the <i>STE2</i> open reading frame using a PCR amplified disruption cassette of the selectable marker <i>kan<sup>r</sup></i> resistance gene.....	192
3	Map of pCSST2 plasmid used for overexpression of <i>SST2</i> .....	196
4	Rate of association of [ $^3$ H] $\alpha$ -factor in the presence and absence of synergist ([desM <sup>12</sup> des W <sup>13</sup> ] $\alpha$ -factor).....	200
5	Rate of dissociation of [ $^3$ H] $\alpha$ -factor in the presence and absence of synergist ([desM <sup>12</sup> des W <sup>13</sup> ] $\alpha$ -factor).....	204
6	Western blot analysis of trypsin digest of Ste2p over time in the presence and absence of $\alpha$ -factor and/or synergist.....	207
7	Biological testing of KHSYN1 Ste2p deletion strain using growth arrest assay.....	211
8	Test of synergist in growth arrest assay with various strains of <i>S. cerevisiae</i> .....	217

<b>FIGURE</b>		<b>PAGE</b>
9	Dose response growth arrest assay by co-spotting of $\alpha$ -factor and synergist in strains RC629 and LM23-3AZ.....	219
10	Saturation binding analysis with various strains of <i>S. cerevisiae</i>	224
11	Model I – Sst2p sequestration.....	231
12	Model II – heteroactivation of Ste2p dimer.....	234
<b>GENERAL CONCLUSIONS AND DISCUSSION</b>		
1	Predicted membrane topology of the $\alpha$ -factor receptor.....	249

# **PART I**

## **GENERAL INTRODUCTION**

## CHAPTER I

### LITERATURE REVIEW

G-protein coupled receptors (GPCRs) are integral membrane proteins that traverse the cell membrane seven times. GPCRs function by responding to ligand binding or photons of light by inducing the activation of a heterotrimeric G-protein. The subunits ( $\alpha$ ,  $\beta$ ,  $\gamma$ ) of the activated G-protein then act upon other proteins to initiate a pyramidal signal cascade. These receptors are found throughout biology from single celled yeast to humans and are able to sense a diverse range of compounds including ions, amino acids, monoamines, lipid messengers, purines, neuropeptides, peptide hormones, and glycoprotein hormones [1]. Additionally, there are hundreds to thousands of different olfactory GPCRs that detect odorant compounds [2]. Based on these criteria, it is easy to see why GPCRs constitute the largest family of known receptors [3].

Analysis of cloned GPCRs has resulted in the sub-classification of the receptor super-family into classes based on common structural/sequence features and the ligands the receptors bind [4]. The super-family has been divided into five classes: Class A – rhodopsin like, Class B – secretin like, Class C – metabotropic –glutamate like, Class D – fungal pheromone receptors and Class E – cAMP receptors (Dictyostelium). Some of the more well know GPCR receptors include

the  $\beta$ -adrenergic, serotonin, dopamine, odorant, and rhodopsin receptors [5, 6]. The sheer number and variety of signals that are transduced through GPCRs in humans make it easy to see how GPCR dysfunction plays a major role in many human diseases and why over 50% of all modern medicines are directed at GPCRs [7, 8]. Furthermore, it has been estimated that the human genome contains over 5000 GPCR genes [3] but the majority of these remain to be cloned and/or characterized. From these observations, it is clear that future studies of GPCRs should make a dramatic impact on understanding and treatment of a variety of diseases.

While there have been significant breakthroughs in the study of the regulation of GPCRs, like the discovery of  $\beta$ -arrestin like molecules [9], there still remains a void of information concerning the structure-function relationship between GPCRs and their cognate ligands. To date, no complete binding pocket has been described for GPCRs [3]. The search to elucidate complete ligand binding sites brings out a disparity between the different GPCRs. While not complete, there have been significant advancements in the identification of receptor-ligand contact residues with GPCRs that bind small molecules such as biogenic amines. However, there is almost no information concerning the binding of peptidyl ligands.

Peptide ligands, which include neuropeptide Y, somatostatin, bradykinin, opioids, and substance P for humans and the a-factor and  $\alpha$ -factor pheromones

from yeast, are role players in a variety of different physiological pathways and responses in many different organisms. A greater understanding of how peptide ligands interact with their GPCRs has the potential to contribute to significant advances in treatment of many human disorders. For instance, by understanding how a peptidyl ligand activates a receptor, it may be possible to design non-peptide mimetics that could be easily delivered to the necessary sites without having the short biological half-life problem that currently makes most peptidyl treatments prohibitive. However, there are several factors that have hampered progress in this area.

Most of the structural information concerning GPCRs has come from the high resolution X-ray diffraction studies of the heptahelical light receptor/proton transporter, bacteriorhodopsin [10, 11]. Bacteriorhodopsin is not a true GPCR as it does not couple to a heterotrimeric G-protein and acts more as a proton transporter than a receptor. However, comparisons have been drawn between bacteriorhodopsin and GPCRs based upon the rhodopsin GPCRs in higher eukaryotes. Low resolution X-ray diffraction studies of bovine and frog rhodopsin [12, 13] have helped to modify and refine the bacteriorhodopsin model into a better representation of "true" GPCRs. Recently, the bovine rhodopsin GPCR protein was crystallized [14]. Palczewski *et al.* have reported solving the three dimensional structure at 2.8 angstrom resolution (figure 1). This new structural information in combination with previous structural data from the studies above

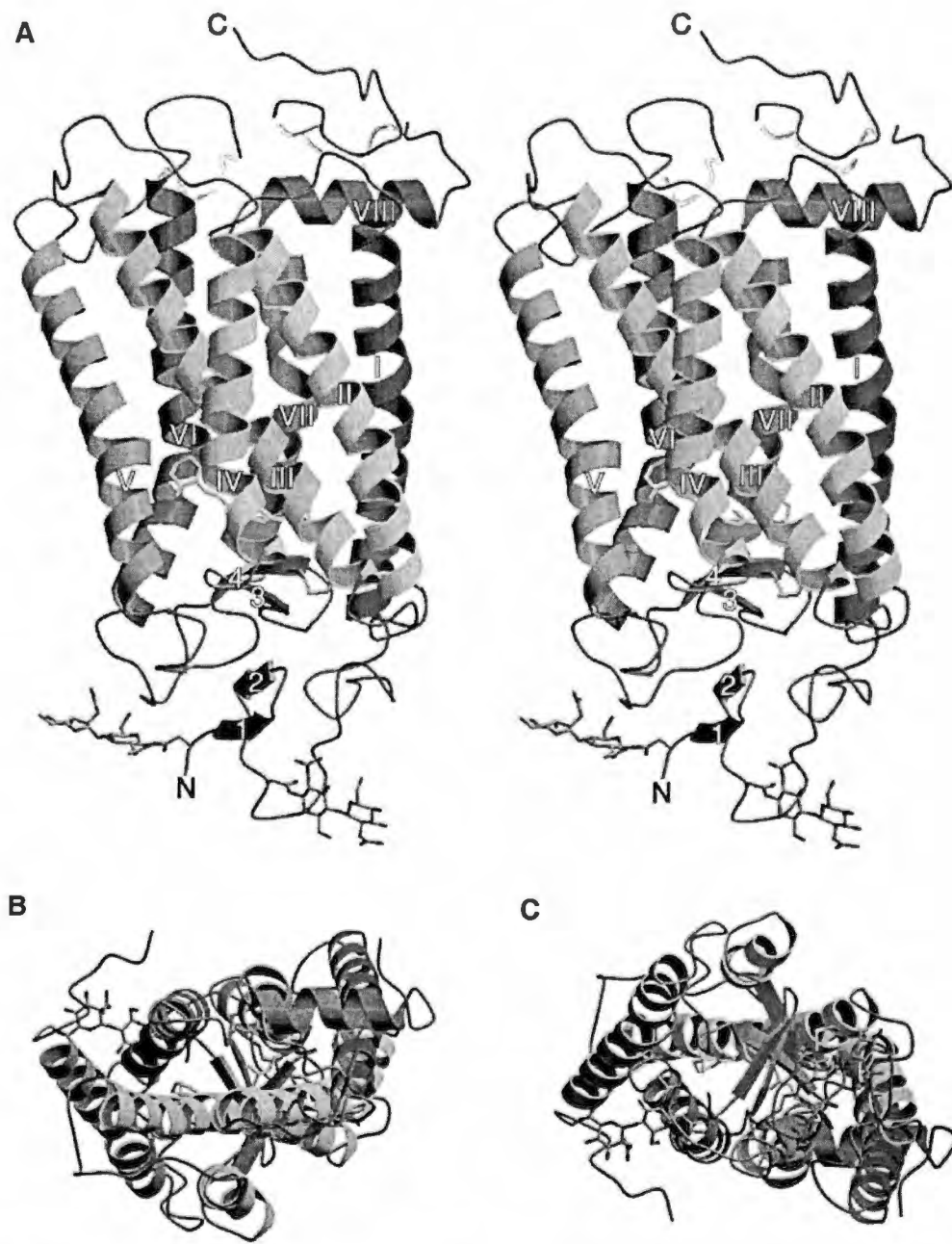


Fig 1. Ribbon drawings of rhodopsin. (A) Parallel to the plane of the membrane (stereoview). A view into the membrane plane is seen from the cytoplasmic (B) and intradiscal side (C) of the membrane. Source: Palczewski, K et al. *Science*. 2000.



should allow for a greater understanding as to how the structure of GPCRs correlate to their function. However, rhodopsins represent only one subfamily of GPCRs. Many of the clinically relevant GPCRs bind ligands quite different from retinal, a light activated molecule complexed to rhodopsins. Further structural information of the different classes of GPCRs could give great insight into how receptor structure correlates to its signaling function.

Another challenge facing GPCR research is the lack of an isolated system in which to study the receptors. In higher eukaryotes, the presence of receptor subtypes, known and unknown, within the same biological system complicate biochemical and physiological studies. In any one tissue, it is possible to have multiple receptors binding the same ligand but with different affinities and resulting in a wide range of physiological responses. These receptor subtypes make analysis of experimental data problematic. In light of the continuing need for structure-function information and the lack of isolated systems to perform the biochemical and biophysical studies, single celled yeast provide a model system for the study of GPCRs.

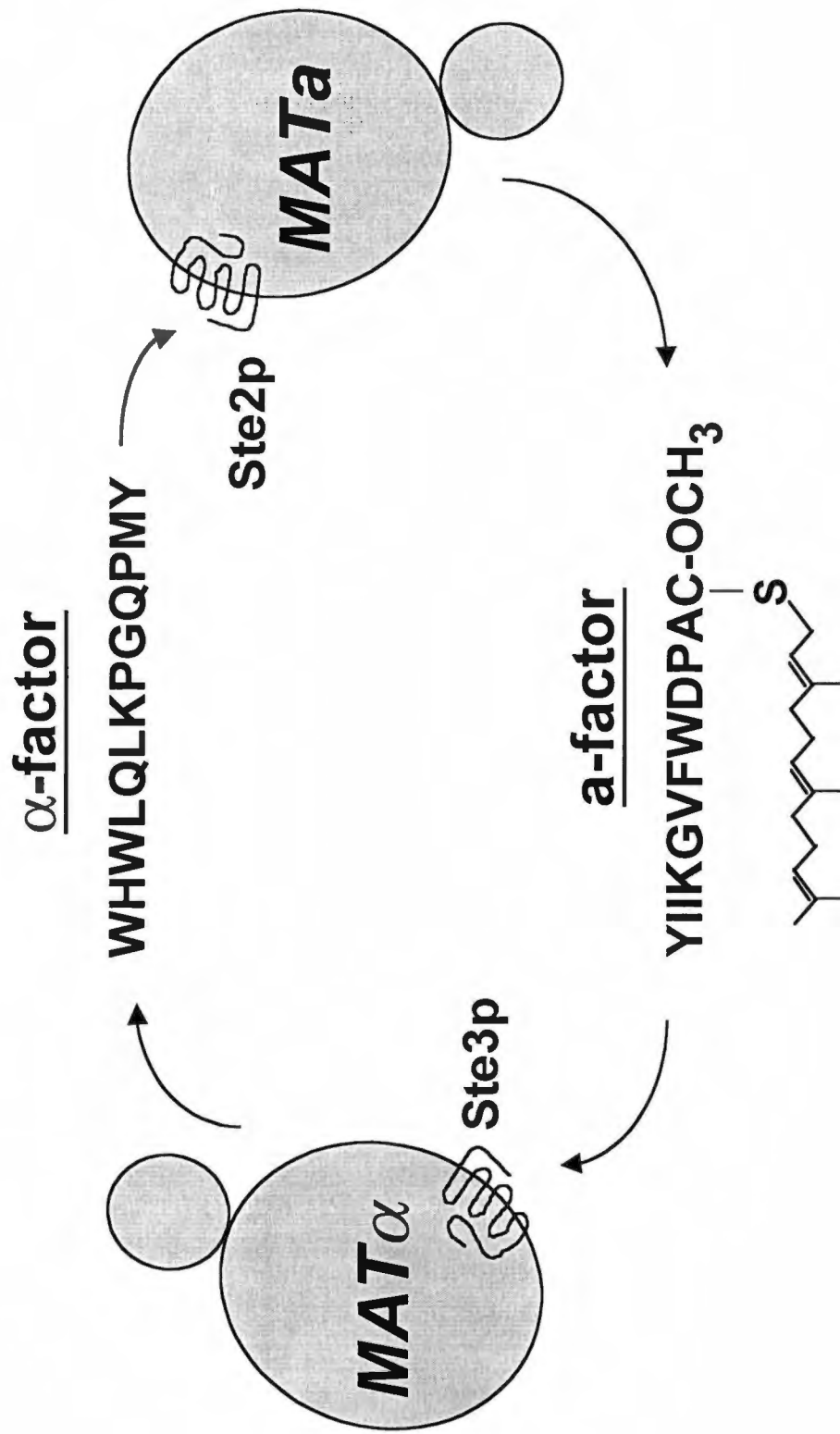
The yeast *Saccharomyces cerevisiae* has been used by many as a model organism for higher eukaryotes to study a range of phenomenon. Commonly referred to as Brewer's or Baker's yeast, *Saccharomyces* can grow as a haploid or diploid [15, 16]. Haploid cells exist in two mating cell types MATa and MAT $\alpha$ . The secretion and reciprocal detection of peptide pheromones initiate mating and

eventual fusion of the two haploids. **a**-cells secrete **a**-factor, a hydrophobic farnesylated, carboxymethylated, dodecapeptide with the sequence YIIKGVFWDPAC(Farnesyl)-OCH<sub>3</sub> while  $\alpha$ -cells secrete  $\alpha$ -factor, a tridecapeptide with the sequence WHWLQLKPGQPMY. **a**-factor and  $\alpha$ -factor bind to heptahelical receptors on the surface of opposite mating cells. **a**-factor binds to the receptor Ste3p while  $\alpha$ -factor binds to Ste2p [17] (see illustration in figure 2).

Binding of the pheromone to the receptor of the opposite mating type induces activation of a signal cascade resulting in several changes in the cell such as: growth arrest in G1 phase of the cell cycle, increased production of agglutinins, induction of mating specific genes and cell elongation. This signal is transduced via a complicated yet well studied protein kinase cascade [18] (see figure 3). It has been determined from sequencing of its entire genome that *S. cerevisiae* has only three GPCRs. Two of these, Ste2p and Ste3p, as stated previously respond to peptide pheromones. The third GPCR, Gpr1p, appears to be a carbohydrate sensor and while it shares some common downstream components with the pheromone signal cascade, there is no crosstalk between the two pathways as Gpr1p is coupled to the G-protein (Gpa2p) [19, 20] unlike the pheromone receptors which are coupled to Gpa1p. The two pheromone GPCRs share the same downstream components but only one of the two receptors based on the cell mating type is expressed at any one time in the haploid cell. Therefore, study of GPCRs in yeast

**Figure 2. Pheromone mediated mating in *Saccharomyces cerevisiae*.**

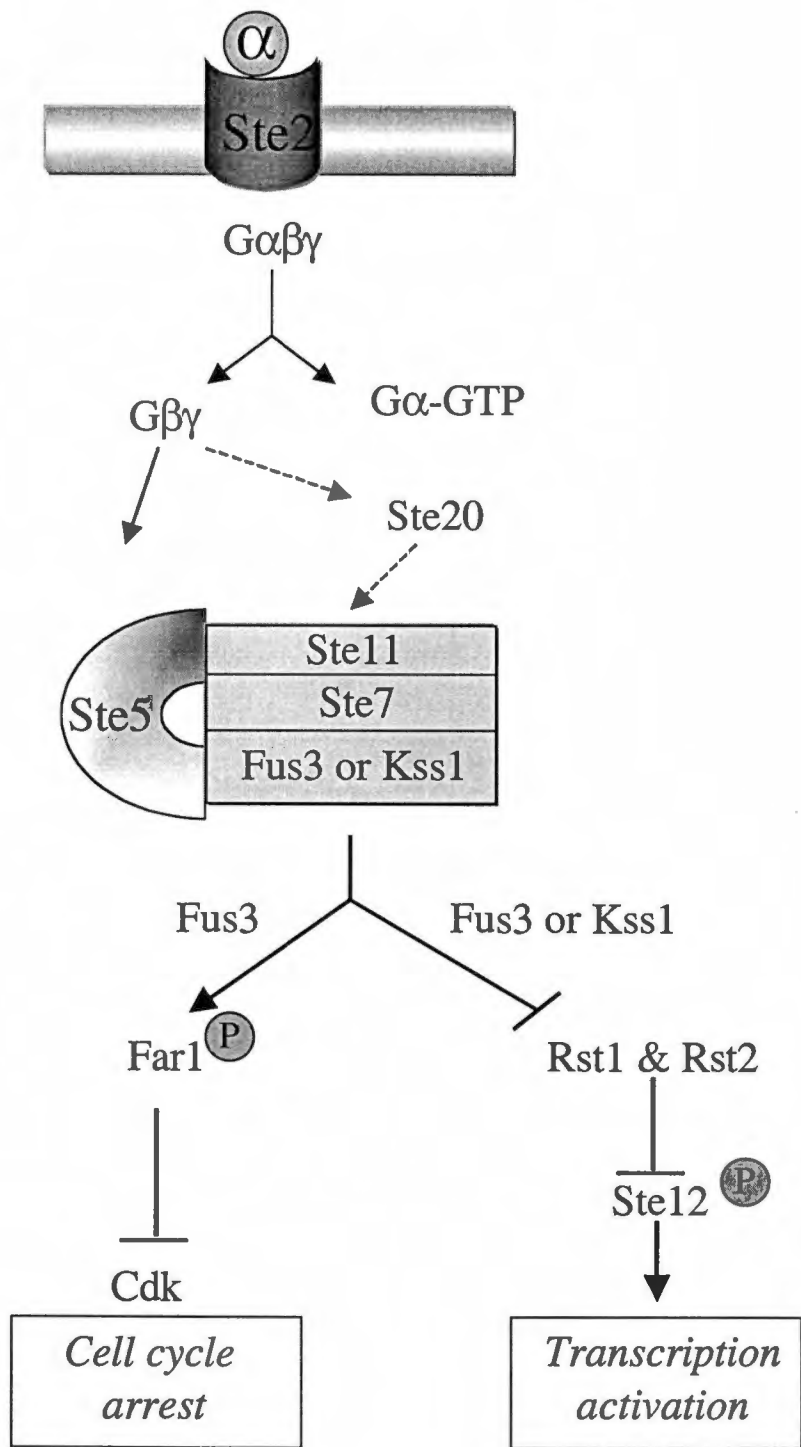
Graphical representation of pheromone/receptor mediated communication between a and  $\alpha$  haploid cells prior to mating.



**Figure 3. Pheromone signal transduction pathway.**

Schematic representation showing the major players in the kinase signal cascade following activation of the Ste2p receptor. Arrows represent activation. Flatheaded lines represent repression.

Source: Banuett, F. *Microbiol Mol Biol Rev* (1998).



does not present the problems with hundreds of GPCRs and multiple subtypes as in some higher eukaryotic systems.

There are several methods commonly used for elucidating structure-function relationships between receptors and peptide ligands including receptor mutagenesis, nuclear magnetic resonance, and fluorescence probes. However, the bulk of this dissertation will be focused on the use of peptide analogs to study the Ste2p pheromone receptor. Careful analysis of peptide analogs in combination with receptor mutagenesis can be a powerful tool in elucidating ligand-receptor interactions by analyzing how changes in the peptide ligand result in changes in the interaction with wild-type vs. mutant residues in a receptor.

Much information has been gained from the use of peptide analogs of  $\alpha$ -factor [21-24]. These analogs have allowed for the discovery of several antagonists, partial agonists and a ligand with novel function which is able to enhance the activity of  $\alpha$ -factor but, alone, has no agonistic activity in wild-type cells. This novel analog has been termed a synergist. Additionally, the information gained from these studies has allowed assignment of general functional domains in the  $\alpha$ -factor peptide in which the N-terminus of the peptide appears to be mainly involved in activation of the receptor, the C-terminus contributes mostly to binding affinity and the middle of the peptide is thought to give the peptide a bent conformation (figure 4). The apparent role of each of these domains has provided a road map to follow for future studies on binding and/or receptor activation. This

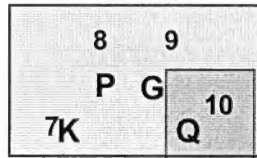
**Figure 4. Functional domains of the  $\alpha$ -factor ligand.**

Studies of  $\alpha$ -factor analogs have revealed a grouping of residues according to their major function in structure, activity and binding affinity. The different groupings are designated by the shadowed boxes and identifying text. The residues in the N-terminal signaling domain while contributing to overall binding appear to mainly function by interacting with the receptor to result in activation of the G-protein. The C-terminal domain functions mainly allow for high affinity binding of the ligand to the receptor. The loop domain corresponds to residues of the peptide which are thought to produce a bend in the ligand.

Source: Adapted from Abel *et al.* 1998, *J. Pept. Res.*

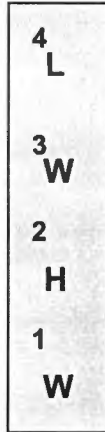


*Loop domain*



6  
L

5  
Q



*C-terminal  
Binding domain*

*N-terminal  
Signaling domain*

dissertation will describe use of novel  $\alpha$ -factor ligands, developed based on previous analog studies, as tools and probes to study receptor binding and activation. Parts II and III detail the construction, characterization and use of  $\alpha$ -factor probes which contain the photo-crosslinkable group, benzoylphenylalanine, for use in determining ligand-receptor contact sites. Part IV describes the construction and characterization of a dimeric  $\alpha$ -factor ligand consisting of two  $\alpha$ -factor molecules linked by an aminohexanoic bridge and Part V details further characterization of a group of  $\alpha$ -factor analogs termed synergists (see above). Finally, Part VI is a holistic evaluation of what was learned from these studies and what future studies could be performed to gain further understanding of the Ste2p receptor and its ligand  $\alpha$ -factor.

## REFERENCES

1. Foreman, J.C. and T. Johansen, *Textbook of receptor pharmacology*. 1996, Boca Raton: CRC Press. 300.
2. Dryer, L. and A. Berghard, *Odorant receptors: a plethora of G-protein-coupled receptors*. *Trends Pharmacol Sci*, 1999. **20**(10): p. 413-7.
3. Marchese, A., S.R. George, L.F. Kolakowski, Jr., K.R. Lynch, and B.F. O'Dowd, *Novel GPCRs and their endogenous ligands: expanding the boundaries of physiology and pharmacology [published erratum appears in Trends Pharmacol Sci 1999 Nov;20(11):447]*. *Trends Pharmacol Sci*, 1999. **20**(9): p. 370-5.
4. Horn, F., J. Weare, M.W. Beukers, S. Horsch, A. Bairoch, W. Chen, O. Edvardsen, F. Campagne, and G. Vriend, *GPCRDB: an information system for G protein-coupled receptors*. *Nucleic Acids Res*, 1998. **26**(1): p. 277-281.
5. Morris, A.J. and C.C. Malbon, *Physiological regulation of G protein-linked signaling [published erratum appears in Physiol Rev 2000*

*Jan;80(1):following table of contents].* *Physiol Rev*, 1999. **79(4)**: p. 1373-430.

6. Malbon, C.C., M. Berrios, S.J. Guest, J.R. Hadcock, G.M. Morris, P.A. Galvin-Parton, and H.Y. Wang, *Signal transduction via G-protein-linked receptors: physiological regulation from the plasma membrane to the genome.* *Chin J Physiol*, 1991. **34(1)**: p. 105-20.
7. Gudermann, T., B. Nurnberg, and G. Schultz, *Receptors and G proteins as primary components of transmembrane signal transduction. Part 1. G-protein-coupled receptors: structure and function.* *J Mol Med*, 1995. **73(2)**: p. 51-63.
8. Flower, D.R., *Modelling G-protein-coupled receptors for drug design.* *Biochim Biophys Acta*, 1999. **1422(3)**: p. 207-34.
9. Lohse, M.J., J.L. Benovic, J. Codina, M.G. Caron, and R.J. Lefkowitz, *beta-Arrestin: a protein that regulates beta-adrenergic receptor function.* *Science*, 1990. **248(4962)**: p. 1547-50.

10. Henderson, R., J.M. Baldwin, T.A. Ceska, F. Zemlin, E. Beckmann, and K.H. Downing, *Model for the structure of bacteriorhodopsin based on high-resolution electron cryo-microscopy*. J Mol Biol, 1990. **213**(4): p. 899-929.
11. Henderson, R., J.M. Baldwin, T.A. Ceska, F. Zemlin, E. Beckmann, and K.H. Downing, *An atomic model for the structure of bacteriorhodopsin*. Biochem Soc Trans, 1990. **18**(5): p. 844.
12. Corless, J.M., D.R. McCaslin, and B.L. Scott, *Two-dimensional rhodopsin crystals from disk membranes of frog retinal rod outer segments*. Proc Natl Acad Sci U S A, 1982. **79**(4): p. 1116-20.
13. Dratz, E.A., J.F. Van Breemen, K.M. Kamps, W. Keegstra, and E.F. Van Bruggen, *Two-dimensional crystallization of bovine rhodopsin*. Biochim Biophys Acta, 1985. **832**(3): p. 337-42.
14. Palczewski, K., T. Kumasaka, T. Hori, C.A. Behnke, H. Motoshima, B.A. Fox, I. Le Trong, D.C. Teller, T. Okada, R.E. Stenkamp, M. Yamamoto, and M. Miyano, *Crystal structure of rhodopsin: A G protein-coupled receptor [see comments]*. Science, 2000. **289**(5480): p. 739-45.

15. Sprague, G.F., Jr., R. Jensen, and I. Herskowitz, *Control of yeast cell type by the mating type locus: positive regulation of the alpha-specific STE3 gene by the MAT alpha 1 product*. Cell, 1983. **32**(2): p. 409-15.
16. Thorner, J., *Pheromonal regulation of development in Saccharomyces cerevisiae*. In *The Molecular biology of the yeast Saccharomyces: Life cycle and inheritance*, ed. J.N. Strathern. 1981: Cold Spring Harbor Laboratory Press.
17. Blumer, K.J., J.E. Reneke, and J. Thorner, *The STE2 gene product is the ligand-binding component of the alpha-factor receptor of Saccharomyces cerevisiae*. J Biol Chem, 1988. **263**(22): p. 10836-42.
18. Banuett, F., *Signalling in the yeasts: an informational cascade with links to the filamentous fungi*. Microbiol Mol Biol Rev, 1998. **62**(2): p. 249-74.
19. Lorenz, M.C., X. Pan, T. Harashima, M.E. Cardenas, Y. Xue, J.P. Hirsch, and J. Heitman, *The G protein-coupled receptor gpr1 is a nutrient sensor that regulates pseudohyphal differentiation in Saccharomyces cerevisiae*. Genetics, 2000. **154**(2): p. 609-22.

20. Lorenz, M.C., N.S. Cutler, and J. Heitman, *Characterization of alcohol-induced filamentous growth in Saccharomyces cerevisiae*. Mol Biol Cell, 2000. **11**(1): p. 183-99.
21. Xue, C.B., A. McKinney, H.F. Lu, Y. Jiang, J.M. Becker, and F. Naider, *Probing the functional conformation of the tridecapeptide mating pheromone of Saccharomyces cerevisiae through study of disulfide-constrained analogs*. Int J Pept Protein Res, 1996. **47**(3): p. 131-41.
22. Yang, W., A. McKinney, J.M. Becker, and F. Naider, *Systematic analysis of the Saccharomyces cerevisiae alpha-factor containing lactam constraints of different ring size*. Biochemistry, 1995. **34**(4): p. 1308-15.
23. Abel, M.G., Y.L. Zhang, H.F. Lu, F. Naider, and J.M. Becker, *Structure-function analysis of the Saccharomyces cerevisiae tridecapeptide pheromone using alanine-scanned analogs*. J Pept Res, 1998. **52**(2): p. 95-106.

24. Eriotou-Bargiota, E., C.B. Xue, F. Naider, and J.M. Becker, *Antagonistic and synergistic peptide analogues of the tridecapeptide mating pheromone of Saccharomyces cerevisiae*. *Biochemistry*, 1992. **31**(2): p. 551-7.



## PART II

### POSITION 13 ANALOGS OF THE TRIDECAPEPTIDE MATING PHEROMONE FROM *SACCHAROMYCES CEREVISIAE*: DESIGN OF AN IODINATABLE LIGAND FOR RECEPTOR BINDING<sup>§</sup>

<sup>§</sup>Part II was published in its entirety as S. Liu, L. K. Henry, B. K. Lee, S. H. Wang, B. Arshava, J.M. Becker and F. Naider. 2000. Position 13 analogs of the tridecapeptide mating pheromone from *Saccharomyces cerevisiae*: design of an iodinated ligand for receptor binding. *J. Pep. Res.* **56**: p24-34 Dr. Naider's laboratory was responsible for synthesis and purification of the peptides used in the study. B.K. Lee was responsible for the characterization of the position 13 replacement analogs. Keith Henry was responsible for development of radioiodinated binding assay, iodination and characterization of tyrosine substitution position analogs, and determination of biological and binding activities of iodinated analogs.

# CHAPTER I

## INTRODUCTION

Hepta-helical receptors are ubiquitous sensors in living cells for a diverse array of signal molecules including peptides, alkaloids, proteins, amino acids and choline esters (1,2) . This diverse family of signal transducers currently is predicted to have more than 1000 members many of which interact with heterotrimeric G proteins located on the cytoplasmic side of the plasma membrane (3-5). Although much is now known concerning the general function of hepta-helical receptors, few studies have provided a detailed description of the atomic contacts involved in ligand receptor interaction. Furthermore, the mechanism by which ligand binding results in downstream activation of the signaling pathway is not described in detail for any member of this protein family.

The yeast *Saccharomyces cerevisiae* is a sexual organism which manifests a conjugative response when opposite mating type cells, **MATa** and **MAT $\alpha$** , are mixed together. The mating process is driven by exchange of diffusible mating factors, the **a**-factor (Tyr-Ile-Ile-Lys-Gly-Val-Phe-Trp-Asp-Pro-Ala-Cys[farnesyl]OCH<sub>3</sub>)<sup>1</sup> and the  $\alpha$ -factor (Trp-His-Trp-Leu-Gln-Leu-Lys-Pro-Gly-Gln-Pro-Met-Tyr), which interact with reciprocal receptors (Ste3p and Ste2p, respectively) on the opposite cell type (6,7). Receptor binding results in activation of G proteins which leads to a series of events including G1 growth arrest, cellular

elongation, gene induction, agglutinin biosynthesis and ultimately cell fusion. The hepta-helical receptors (Ste2p and Ste3p) have been cloned (8,9) and identified to be unique members of this family of proteins classified in subgroup D (3). Moreover, Ste2p was recently expressed in high copy number, purified to near homogeneity and reconstituted in active form in synthetic membrane vesicles (10). The availability of relatively large quantities of this receptor protein and of highly developed genetic tools for working with *S. cerevisiae* have stimulated the use of the  $\alpha$ -factor receptor as a paradigm to learn about the biochemistry of hepta-helical receptors.

Previous investigations on  $\alpha$ -factor - Ste2p interactions have involved both measurement of biological activities of synthetic analogs and assessment of their binding to the receptor (11-15). The receptor binding assay presently used for  $\alpha$ -factor involves use of either tritiated pheromone prepared synthetically (16) or  $^{35}\text{S}$  labeled  $\alpha$ -factor prepared biosynthetically (17,18). Neither of these ligands is completely satisfactory. The tritiated pheromone is expensive to prepare and has a specific activity limited to 10-20 Ci/mmol. The biosynthetic ligand is difficult to obtain in quantity and cannot be prepared readily in forms containing amino acid analogs such as photoactivatable groups useful for receptor studies. These limitations make it problematic to use these probes in affinity labeling studies designed to determine contacts between residues of  $\alpha$ -factor and the Ste2p binding site. An obvious alternative to the above ligands would be preparation of iodinated

$\alpha$ -factor. However, iodination of Tyr<sup>13</sup> was reported to virtually eliminate the biological activity of the pheromone (19). Moreover, structure-activity studies concluded that the phenolic OH of Tyr<sup>13</sup> was important for biological activity since substitution of Tyr by Phe resulted in nearly 10<sup>4</sup> decrease in activity as judged in a morphogenesis assay (20). Recently, the importance of the Tyr side chain was further indicated in an Ala scan analysis of  $\alpha$ -factor (15). Replacement of Tyr<sup>13</sup> with Ala or *D*-Ala led to a 500-fold and greater than 3000-fold decrease in receptor affinity, respectively.

The above observations stymied efforts to prepare a receptor ligand with high specific activity (>1000 Ci/mmol). Recently, however, we have reevaluated the importance of the Tyr side chain. We reasoned that the phenolic group served either as a center of electron density or a hydrogen bonding moiety. Therefore, we studied the effect of replacement with a variety of functionalized aromatic rings. In this paper we report on  $\alpha$ -factor analogs in which Tyr was replaced with *p*-fluorophenylalanine, *p*-aminophenylalanine, *p*-nitrophenylalanine or *m*-fluorophenylalanine. Peptides containing phenylalanine or serine at position 13 served as controls. The results allowed us to design new analogs of  $\alpha$ -factor which retain relatively high biological activity and receptor affinity after iodination. One of these analogs [Tyr(<sup>125</sup>I)<sup>1</sup>, Phe<sup>13</sup>] $\alpha$ -factor gave saturable binding to the Ste2p receptor which could be specifically competed by  $\alpha$ -factor. This probe represents

the first of a new series of ligands, which can be used to study  $\alpha$ -factor- receptor interactions.

## CHAPTER II

### MATERIALS AND METHODS

*Organisms.* *S. cerevisiae* LM102 (21) [*MATa ste2-dl bar1 leu2 ura3 his4 trp1 met1 fus1::lacZ(URA3)*] transformed with pGA314[*STE2*] (22) was used for the growth arrest, gene induction, and competition binding assays of various  $\alpha$ -factor analogs. *S. cerevisiae* DK102[*MATa ste2::HIS3 bar1 leu2 ura3 lys2 ade2 his3 trp1*] transformed with pNED1[*STE2*] (10) was used in binding studies with the radioiodinated alpha factor analogs.

*Synthesis of [Nle<sup>12</sup>] $\alpha$ -factor analogs.* *L*-norleucine, which is isosteric with *L*-methionine, was incorporated at position 12 to replace the original *L*-methionine in all analogs. This replacement was shown previously to result in an analog with equal activity and receptor affinity to that of the native pheromone (16). The structures of the synthetic  $\alpha$ -factor analogs are given in Table 1. Since all analogs have Nle in place of Met<sup>12</sup> this residue is eliminated from the abbreviated names for simplicity. The replacement of Met by Nle improves the synthesis and the stability of the resulting peptide. The solid phase syntheses of all the  $\alpha$ -factor analogs were carried out automatically on an Applied Biosystems 433A peptide synthesizer (Applied Biosystems, Foster City, California) using preloaded *N*- $\alpha$ -Fmoc-Phe -Wang resins<sup>1</sup> (0.65 mmol/gram resin, Advanced

Table 1. Chemical and Physical Properties of  $\alpha$ -factor analogs

Peptide <sup>a</sup>	Abbreviated Name	HPLC <sup>b</sup> k'	M.W. (Calc.)	Mass (Found)	TLC <sup>c</sup> (R <sub>f</sub> )
Trp-His-Trp-Leu-Gln-Leu-Lys-Pro-Gly-Gln-Pro-Nle-Phe(pF)	<i>p</i> -F-Phe <sup>13</sup>	5.7	1668.9	1669	0.22
Tyr-His-Trp-Leu-Gln-Leu-Lys-Pro-Gly-Gln-Pro-Nle-Phe(pF)	Tyr <sup>1</sup> , <i>p</i> -F-Phe <sup>13</sup>	4.7	1645.9	1645.5	0.25
Trp-His-Trp-Leu-Gln-Leu-Lys-Pro-Gly-Gln-Pro-Nle-Phe	Phe <sup>13</sup>	5.6	1650.0	1650.9	0.20
Trp-His-Trp-Leu-Gln-Leu-Lys-Pro-Gly-Gln-Pro-Nle-Phe(pNH <sub>2</sub> )	<i>p</i> -NH <sub>2</sub> -Phe <sup>13</sup>	3.2	1664.9	1664.8	0.18
Trp-His-Trp-Leu-Gln-Leu-Lys-Pro-Gly-Gln-Pro-Nle-Phe(pF)	Tyr <sup>3</sup> , <i>p</i> -F-Phe <sup>13</sup>	3.1	1645.9	1644.9	0.16
Trp-His-Trp-Leu-Gln-Leu-Lys-Pro-Gly-Gln-Pro-Nle-Scr	Ser <sup>13</sup>	3.7	1588.9	1589.8	0.12
Trp-His-Trp-Leu-Gln-Leu-Lys-Pro-Gly-Gln-Pro-Nle-Phe(pNO <sub>2</sub> )	<i>p</i> -NO <sub>2</sub> -Phe <sup>13</sup>	5.8	1696.0	1695.9	0.11
Trp-His-Trp-Leu-Gln-Leu-Lys-Pro-Gly-Gln-Pro-Nle-Phe(mF)	<i>m</i> -F-Phe <sup>13</sup>	5.9	1668.9	1668.7	0.12
Tyr-His-Trp-Leu-Gln-Leu-Lys-Pro-Gly-Gln-Pro-Nle-Phe	Tyr <sup>1</sup> , Phe <sup>13</sup>	4.7	1626.9	1626.9	0.12
Trp-His-Trp-Leu-Gln-Leu-Lys-Pro-Gly-Gln-Pro-Nle-Phe	Tyr <sup>3</sup> , Phe <sup>13</sup>	2.8	1626.9	1626.7	0.15
Tyr(I <sub>2</sub> )-His-Trp-Leu-Gln-Leu-Arg-Pro-Gly-Gln-Pro-Nle-Phe	Tyr(I <sub>2</sub> ), Phe <sup>13</sup>	6.3	1906.5	1906.5	0.15
Trp-His-Tyr(I <sub>2</sub> )-Leu-Gln-Leu-Arg-Pro-Gly-Gln-Pro-Nle-Phe	Tyr <sup>3</sup> (I <sub>2</sub> ), Phe <sup>13</sup>	5.6	1906.5	1906.9	0.12

<sup>a</sup>The structure of the native  $\alpha$ -factor is: Trp-His-Trp-Leu-Gln-Leu-Lys-Pro-Gly-Gln-Pro-Met-Tyr. <sup>b</sup>HPLC was run on a C<sub>18</sub> reversed-phase column. The gradient used with CH<sub>3</sub>CN (CH<sub>3</sub>CN:H<sub>2</sub>O: 0.025% CF<sub>3</sub>COOH) was from 20% - 40% CH<sub>3</sub>CN in 20 min. The gradient used with CH<sub>3</sub>OH (CH<sub>3</sub>OH:H<sub>2</sub>O: 0.025% CF<sub>3</sub>COOH) was from 50-80% CH<sub>3</sub>OH in 30 min.

<sup>c</sup>The gradient was from 30-80% CH<sub>3</sub>OH in 30 min. <sup>d</sup>The gradient was from 30-100% CH<sub>3</sub>OH in 30 min. <sup>e</sup>TLC - was run on silica thin layers. The mobile phase was CH<sub>3</sub>OH/CHCl<sub>3</sub>/AcOH (2:1:2).

ChemTech, Louisville, Kentucky) except for the syntheses of the *p*-NO<sub>2</sub>-Phe<sup>13</sup>, *p*-F-Phe<sup>13</sup>, *m*-F-Phe<sup>13</sup> and Ser<sup>13</sup> analogs. In these cases, the desired Fmoc-protected amino acid was loaded onto a Wang-resin using *p*-(*N,N*-dimethylamino)pyridine-catalyzed esterification with dicyclohexylcarbodiimide in NMP followed by benzoic anhydride capping. 9-Fluorenylmethoxycarbonyl (Fmoc) was employed for all *N*-α-protections while the side chain protecting groups were Trp(tBoc), His(Trt), Gln(Trt) and Lys(tBoc). The '0.1-mmol FastMoc' chemistry of Applied Biosystems was utilized for the peptide chain elongation with an HBTU/HOBt/DIEA catalyzed single-coupling using 4 equivalents of protected amino acid and a 30 min. coupling time followed by an Ac<sub>2</sub>O/HOBt/DIEA capping (10 min). The *p*-NH<sub>2</sub>-Phe<sup>13</sup> analog was prepared by catalytically reducing the *p*-NO<sub>2</sub>-Phe<sup>13</sup> analog using 10% Pd/C in a Parr Hydrogenation apparatus at 30 psi of hydrogen gas for one hour. The hydrogenation was judged to be complete using HPLC and the product was purified by semipreparative HPLC as described below.

*Peptide Cleavage.* The *N*-α-deprotected peptide resin was washed thoroughly with NMP and dichloromethane and dried *in vacuo* for 2 hours. The cleavage was carried out in a mixture of trifluoroacetic acid (10 ml), crystalline phenol (0.75 g), ethane-1,2-dithiol (0.25 ml), thioanisole (0.5 ml) and water (0.5 ml) at room temperature for 1.5 hours. After evaporation of trifluoroacetic acid



under reduced pressure, the residue was precipitated and thoroughly washed with ethyl ether and extracted into 20% aqueous acetonitrile.

*Purification and Characterization.* The crude peptide was purified by reversed phase HPLC (Hewlett-Packard Series 1050) on a semi-preparative Waters  $\mu$ Bondapak C18 (19x300 mm) column. Wavelength set for peptide detection was 220 nm. The cleavage product (45 mg) was dissolved in about 4 ml of aqueous acetonitrile (20%) containing 0.025% TFA and applied onto the column. Elution of the peptide utilized a linear gradient from 0 to 55% acetonitrile (both the water and acetonitrile reservoirs contained 0.025% TFA) over 2 hours at a flow rate of 5 ml/min. The fractions were collected and analyzed at 220 nm by reversed phase HPLC (Hewlett-Packard Series 1050) on an analytical Waters  $\mu$ Bondapak C18 column (3.9x300 mm). Fractions of over 99% homogeneity were combined and lyophilized. The peptide purity was judged with analytical HPLC using two different solvent systems. Electron spray mass spectrometry was carried out at Peptidogenics Inc. Amino acid analyses were performed by the Biopolymers Laboratory at the Brigham and Womans Hospital, Boston, Massachusetts.

*Growth arrest (halo) assay.* Yeast nitrogen base medium (Difco) without amino acids (SD medium) supplemented with histidine (20  $\mu$ g/ml), leucine (30  $\mu$ g/ml) and methionine (20  $\mu$ g/ml) was overlaid with 4 ml of *S. cerevisiae* LM102 cell suspension ( $2.5 \times 10^5$  cells/ml of Nobel agar). Filter disks (sterile blanks

from Difco), 8 mm in diameter, were impregnated with 10  $\mu$ l portions of peptide solutions at various concentrations and placed onto the overlay. The plates were incubated at 30°C for 24 -36 h and then observed for clear zones (halos) around the disks. The data were expressed as the diameter of the halo including the diameter of the disk. Therefore, a minimum value for growth arrest is 9 mm, which represents the disk diameter (8 mm) and a small zone of inhibition. All assays were carried out at least three times with no more than a 2 mm variation in halo size at a particular amount applied for each peptide. The values reported represent the mean of these tests. Similar ranks of biological activities were obtained for these analogs within an assay as measured by growth arrest (halo) or gene induction (see below). In the latter assay cells were suspended in liquid medium thereby eliminating any contribution of diffusion through agar potentially present in the halo assay.

*Effect of  $\alpha$ -Factor Analogs on Gene Induction. S. cerevisiae LM102* carries a *FUS1* gene that is inducible by mating pheromone and which is fused to the reporter gene  $\beta$ -galactosidase. Cells were grown overnight in SD medium at 30°C to  $5 \times 10^6$  cells/ml, washed by centrifugation, and grown for one doubling (hemocytometer count) at 30°C. Induction was performed by adding 0.5 ml of peptide at various concentrations to 4.5 ml of concentrated cells ( $1 \times 10^8$  cells/ml). The mixtures were vortexed and placed at 30°C with shaking for 2 h. After this time, cells were harvested by centrifugation, and each pellet was resuspended and

assayed for  $\beta$ -galactosidase production (expressed as Miller units) in triplicate by a modified (23) standard protocol (24, 25). Each experiment was carried out at least three times with the results similar in each assay.

*Binding competition assay for [ $^3$ H] $\alpha$ -factor.* This assay was performed using strain LM102 and tritiated  $\alpha$ -factor prepared by reduction of [dehydroproline<sup>8</sup>, Nle<sup>12</sup>] $\alpha$ -factor as described previously (16). In general, cells were grown at 30°C overnight and harvested at  $1 \times 10^7$  cells/ml by centrifugation at 5,000 x g at 4°C. The pelleted cells were washed two times in ice cold YM-1 medium (15) and resuspended to  $4 \times 10^7$  cells/ml. The binding assay was started by addition of [ $^3$ H] $\alpha$ -factor and various concentration of nonlabeled peptide (140  $\mu$ l) to a 560  $\mu$ l cell suspension so that the final concentration of radioactive peptide was  $6 \times 10^{-9}$  M (20 Ci/mmol). Analog concentrations were adjusted using UV absorption at 280 nm and the corresponding extinction coefficients. After a 30 min incubation, triplicate samples of 200  $\mu$ l were filtered and washed over glass fiber filtermats using the Standard Cell Harvester (Skatron Instruments, Sterling, VA) and placed in scintillation vials for counting. Each experiment was carried out at least three times with the results similar in each assay. Binding of labeled  $\alpha$ -factor to filters in the absence of cells was less than 20 cpm. The  $K_i$  values were calculated by using the equation of Cheng and Prusoff, where  $K_i = EC_{50} / (1 + [\text{ligand}] / K_d)$  (26).

*Synthesis of Iodinated  $\alpha$ -factor Peptides.* Peptides were iodinated with Iodogen<sup>®</sup> tubes from Pierce, Inc. using conditions recommended by the manufacturer. Briefly, Iodogen tubes were pre-wet with Tris Iodination Buffer (TIB)(25mM Tris pH 7.5, 0.4M NaCl). TIB was decanted and 100  $\mu$ l of fresh TIB was added directly to the bottom of the Iodogen tube and either 10  $\mu$ l of Na<sup>127</sup>I (1.86 mg/ml) or 10  $\mu$ l of Na<sup>125</sup>I (100  $\mu$ Ci/ $\mu$ l pH 10) was added and incubated for 6 minutes with gentle swirling every 30 seconds. Activated iodide was transferred to a siliconized microfuge tube containing 100  $\mu$ l of the peptide (0.5 mmol/L in TIB) and incubated for 6 minutes with gentle mixing every 30 seconds. Scavenging buffer (50  $\mu$ l at 10 mg/ml tyrosine in TIB) was added and incubated for 5 minutes with mixing at minutes 1 and 4. Following incubation, 1 ml of TIB containing 5 mM EDTA was added. The remaining unreacted iodine was separated from peptide using a Waters Sep-Pak<sup>®</sup> C18 mini-column. The eluted products were separated by HPLC using H<sub>2</sub>O/acetonitrile/0.025% TFA with an acetonitrile percentage of 20 to 35% over 30 minutes at 1.4 ml/min on a Waters  $\mu$ Bondapak C18 reversed phase analytical column (3.9x300mm). <sup>127</sup>I labeled peptides were quantitated by UV spectrophotometry using appropriate extinction coefficients. Radioiodinated peptides were labeled using carrier free Na<sup>125</sup>I and the resulting mono-iodinated peptides were quantitated by converting total dpm associated with the HPLC purified peptide to mmole of peptide using the specific activity of carrier free Na<sup>125</sup>I (2159 Ci/mmole).

*Binding Assays for <sup>125</sup>I labeled α-factor.* DK102 pNED1 cells (grown in MLT medium) (10) and DK102 cells (grown in MLT medium supplemented with tryptophan) were harvested at  $1 \times 10^7$  cells/ml by centrifugation and resuspended to  $6.25 \times 10^7$  cells/ml in 0.5M potassium phosphate buffer (PPBi) (pH6.24) containing 10mM TAME, 10mM sodium azide, 10 mM potassium fluoride, 1% BSA (fraction IV) and placed at 4°C. In competition binding assays, [Tyr<sup>1</sup>(<sup>125</sup>I), Phe<sup>13</sup>]α-factor ( $2.4 \times 10^{-9}$  M final concentration) was pre-mixed with various concentrations of cold competitor. In saturation binding assays, [Tyr<sup>1</sup>(<sup>125</sup>I), Phe<sup>13</sup>]α-factor was diluted with cold [Tyr<sup>1</sup>(<sup>127</sup>I), Phe<sup>13</sup>]α-factor to a specific activity of 12 Ci/mole to obtain sufficient peptide concentrations. Cells in PPBi were then added to peptide solutions to a final density of  $6.25 \times 10^6$  cells/ml and incubated for 45 minutes at room temperature. Following incubation, reaction mixes were transferred (3 x 200 μl) to wells of a 0.45 μm MultiScreen –HV, 96 well plate (Millipore MHVBN4510) pre-blocked with BSA using PPBi. Samples were vacuum filtered, washed with PPBi (2 x 200 μl) and counted on a LKB-Wallac CliniGamma 1272 gamma counter. Using this methodology non-specific binding of radiolabeled peptide to the filter was at background levels. Specific binding was determined by subtracting counts associated with the DK102 (ste2-) strain from counts bound to the DK102pNED1 (STE2<sup>+</sup>) strain.

## CHAPTER III

### RESULTS

*Synthesis of  $\alpha$ -Factor Analogs.* The automated solid phase synthesis of all analogs resulted in crude peptides with purities ranging from 80% - 90% except in the case of the diiodoTyr containing analogs. The synthesis of these compounds using a standard protocol resulted in very heterogeneous crude peptides with three or four major peaks. This problem was eliminated when Lys<sup>7</sup> of wild-type  $\alpha$ -factor was replaced with Arg. This replacement has been previously shown to have no effect on either the biological activity or the receptor affinity of the pheromone (16, 27). The *p*-aminophenylalanine containing analog was prepared by catalytic reduction of the *p*-nitrophenylalanine containing precursor. The hydrogenation was quantitative as judged using analytical HPLC and the reduced peptide had the calculated molecular weight as judged by electrospray mass spectroscopy. All final peptides were greater than 99% homogeneous using analytical HPLC in either an acetonitrile/water/trifluoroacetic acid or methanol/water/acetonitrile/trifluoroacetic acid gradient system. The peptides were also homogeneous on silica thin layers using a methanol/methylene chloride/acetic acid mobile phase and ninhydrin or ultraviolet light for detection. The peptides gave the expected molecular weights within 1 dalton and had amino acid ratios within 15% of the

theoretical values for all natural residues. The F-Phe residues were within 25% of theory and no attempt was made to quantify iodinated tyrosine or nitrophenylalanine substituents by amino acid analysis. The presence of Trp was qualitatively confirmed using absorbance measurements at 280 nm. In the case of the *p*-NO<sub>2</sub>-Phe<sup>13</sup> analog the nitrophenyl substituent added significantly to the absorbance at this wavelength and the extinction coefficient was nearly 60% higher than that found for  $\alpha$ -factor. The physical and analytical data on the various peptides are summarized in Table 1.

*Bioactivities of Position-13 Analogs.* The biological activities of the position-13 analogs were determined by growth arrest and gene induction assays (Table 2). The growth arrest activities were measured as halo size at different amounts of peptide pheromone and plotted on a semi-logarithmic plot. The plots were all linear and the slopes for all analogs were nearly parallel (Representative data shown in Fig. 1). Furthermore, the analogs were stable in all assays because we used *sst1* mutants lacking in the  $\alpha$ -factor inactivating Bar1 protease. There are some discrepancies between the biological activities obtained with the lacZ and halo assays with a few of the peptide analogs. The differences were not due to diffusion of peptides in agar in the halo assay because results similar to those of the halo assay were obtained in growth arrest assays done in liquid medium (data not shown). Others performing similar studies (21) observed a comparable lack of relationship between these assays. The differences have been attributed to

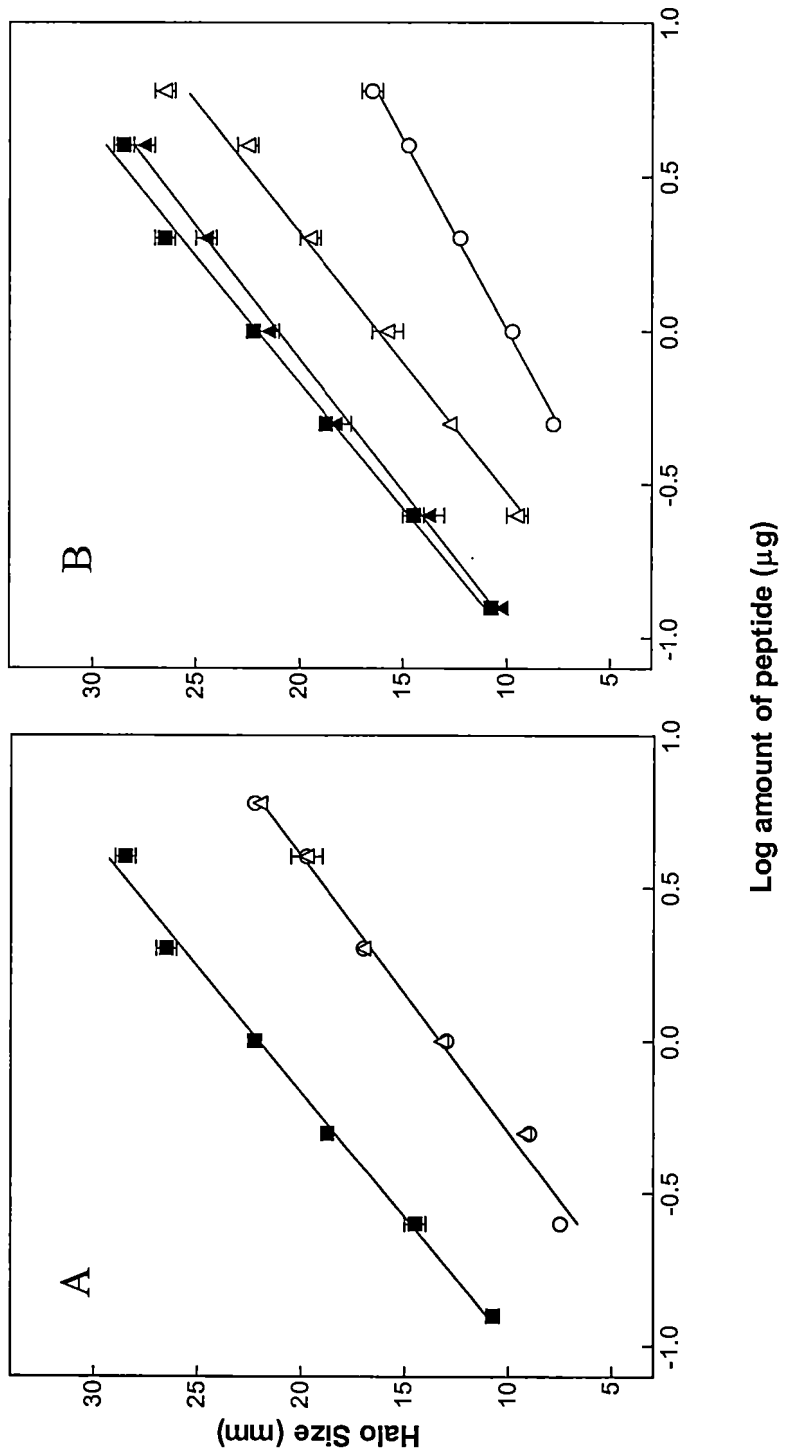
Table 2. Biological activities and binding affinities of  $\alpha$ -factor analogs

Peptide	Halo Assay (ug peptide for a 15mm halo)	$\beta$ -galactosidase Assay (% activity at $10^{-7}$ M)	Binding Assay (Ki; nM)
$\alpha$ -factor	$0.26 \pm 0.03$	100	$11 \pm 3$
<i>p</i> -F-Phe <sup>13</sup>	$0.46 \pm 0.04$	$110 \pm 5$	$16 \pm 3$
Tyr <sup>1</sup> , <i>p</i> -F-Phe <sup>13</sup>	$1.45 \pm 0.22$	$69 \pm 0$	$94 \pm 8.5$
<i>p</i> -NH <sub>2</sub> -Phe <sup>13</sup>	$0.47 \pm 0.03$	$95 \pm 8$	$36 \pm 3$
Tyr <sup>3</sup> , <i>p</i> -F-Phe <sup>13</sup>	$0.19 \pm 0.04$	$79 \pm 5$	$127 \pm 25$
Ser <sup>13</sup>	$1.49 \pm 0.11$	$55 \pm 4$	$>1000$
<i>p</i> -NO <sub>2</sub> -Phe <sup>13</sup>	$0.36 \pm 0.03$	$94 \pm 6$	$58 \pm 7$
<i>m</i> -F-Phe <sup>13</sup>	$0.38 \pm 0.02$	$86 \pm 3$	$59 \pm 6$
Phe <sup>13</sup>	$0.29 \pm 0.05$	$120 \pm 8$	$22 \pm 3.5$
Tyr <sup>1</sup> , Phe <sup>13</sup>	$3.30 \pm 0.25$	$13 \pm 2$	$181 \pm 26$
Tyr <sup>3</sup> , Phe <sup>13</sup>	$0.60 \pm 0.12$	$28 \pm 2$	$200 \pm 25$
Tyr <sup>1</sup> (I <sub>2</sub> ), Phe <sup>13</sup>	$1.10 \pm 0.15$	$38 \pm 2$	$330 \pm 32$
Tyr <sup>3</sup> (I <sub>2</sub> ), Phe <sup>13</sup>	$1.02 \pm 0.13$	$97 \pm 9$	$30 \pm 4$
Tyr <sup>1</sup> (I <sub>1</sub> ), Phe <sup>13</sup>	$0.90 \pm 0.10$	$33 \pm 3$	$81 \pm 9$



**Figure 1. Growth arrest of *S. cerevisiae* by  $\alpha$ -factor and various analogs.**

The halo of growth arrest is plotted in response to various amounts of peptide as indicated in the figure. Fig. 1A shows  $\alpha$ -factor (■) and the diiodinated analogs: Tyr<sup>1</sup> (I<sub>2</sub>), Phe<sup>13</sup> ( $\Delta$ ), Tyr<sup>3</sup>(I<sub>2</sub>), Phe<sup>13</sup> (O). Fig 1B shows  $\alpha$ -factor (■) and the analogs: Tyr<sup>1</sup>, Phe<sup>13</sup> (O), Tyr<sup>3</sup>, Phe<sup>13</sup> ( $\Delta$ ) and Phe<sup>13</sup> ( $\blacktriangle$ ).

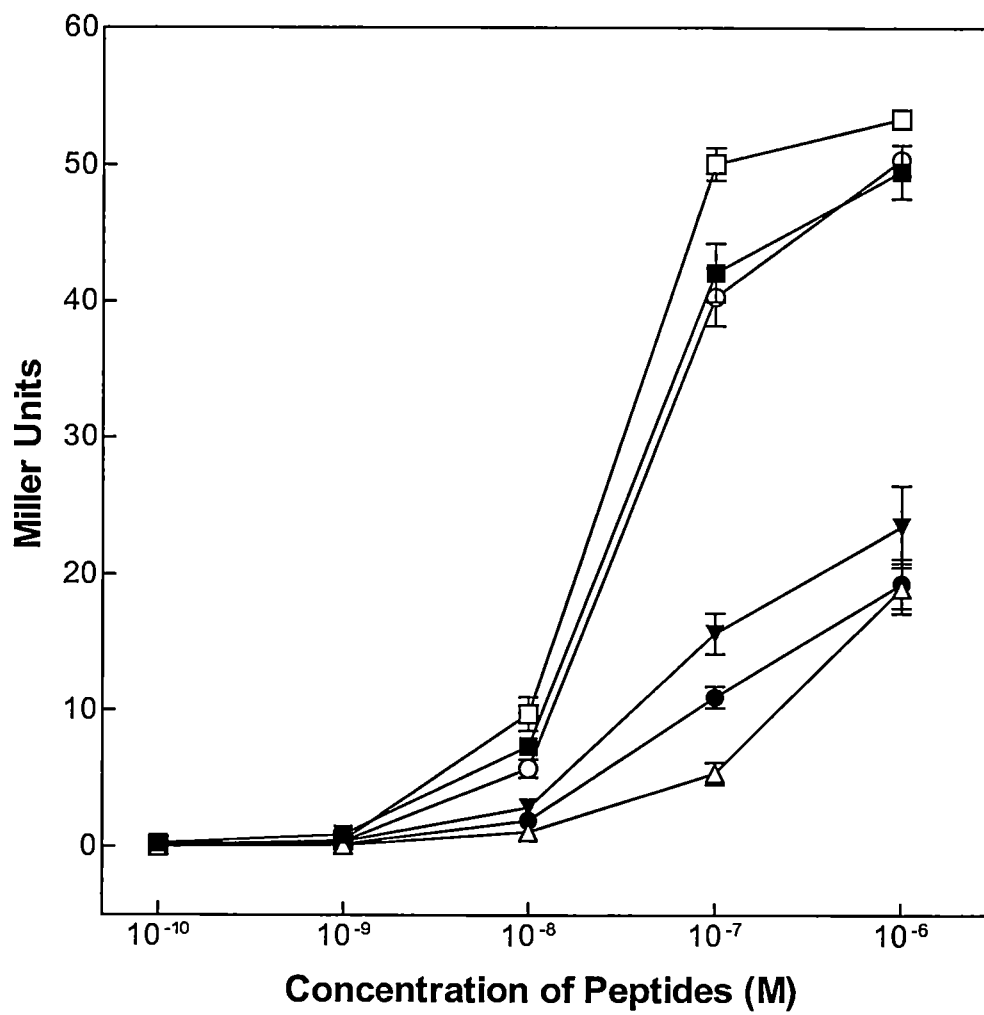


independent thresholds required to initiate the biological responses of growth inhibition (halo assay) versus gene induction (lacZ) probably due to differences in regulation of the two pathways. As summarized in Table 2, replacement of Tyr<sup>13</sup> with *p*-F-Phe, *m*-F-Phe, *p*-NO<sub>2</sub>-Phe, *p*-NH<sub>2</sub>-Phe, or Phe resulted in peptides which caused a 15 mm growth arrest halo from 0.29 μg peptide to 0.47 μg in the growth arrest assay compared to 0.26 μg for the parent α-factor. These same analogs exhibit 80%-120% of the activity of the α-factor in the gene induction assay. Thus the OH of Tyr is clearly not necessary for high biological activity as it can be eliminated completely or it can be replaced by a variety of groups including F and NH<sub>2</sub>. Even the relatively large NO<sub>2</sub> moiety did not markedly decrease the biological activity of this analog. The analog containing Ser<sup>13</sup> had the lowest biological activity of any of the singly-substituted position 13 analogs tested in both the growth arrest and gene induction assays (Table 2).

*Bioactivities of Multiple Replacement Analogs.* A principal goal of this study was the development of probes for the α-factor receptor. Having learned that Tyr<sup>13</sup> could be replaced with Phe we wished to determine whether Tyr could be placed at other positions in [Phe<sup>13</sup>]α-factor. Accordingly we synthesized two analogs in which Trp<sup>1</sup> or Trp<sup>3</sup> were replaced by Tyr. As indicated in Table 2, Figure 1b, and Figure 2 these analogs had significantly lower activity than [Phe<sup>13</sup>]α-factor exhibiting 2-10 fold lower activity than α-factor in the growth

**Figure 2. Dose response to  $\alpha$ -factor and analogs determined by reporter gene *lacZ* ( $\beta$ -Galactosidase).**

$\beta$ -galactosidase activity in Miller Units was measured in cultures incubated with various amounts of peptide as shown:  $\alpha$ -factor (■), Tyr<sup>1</sup>, Phe<sup>13</sup> ( $\Delta$ ), Tyr<sup>1</sup>(I<sub>2</sub>), Phe<sup>13</sup> ( $\nabla$ ), Tyr<sup>3</sup>, Phe<sup>13</sup> (●), Tyr<sup>3</sup>(I<sub>2</sub>), Phe<sup>13</sup> (O), Phe<sup>13</sup> ( $\square$ ).

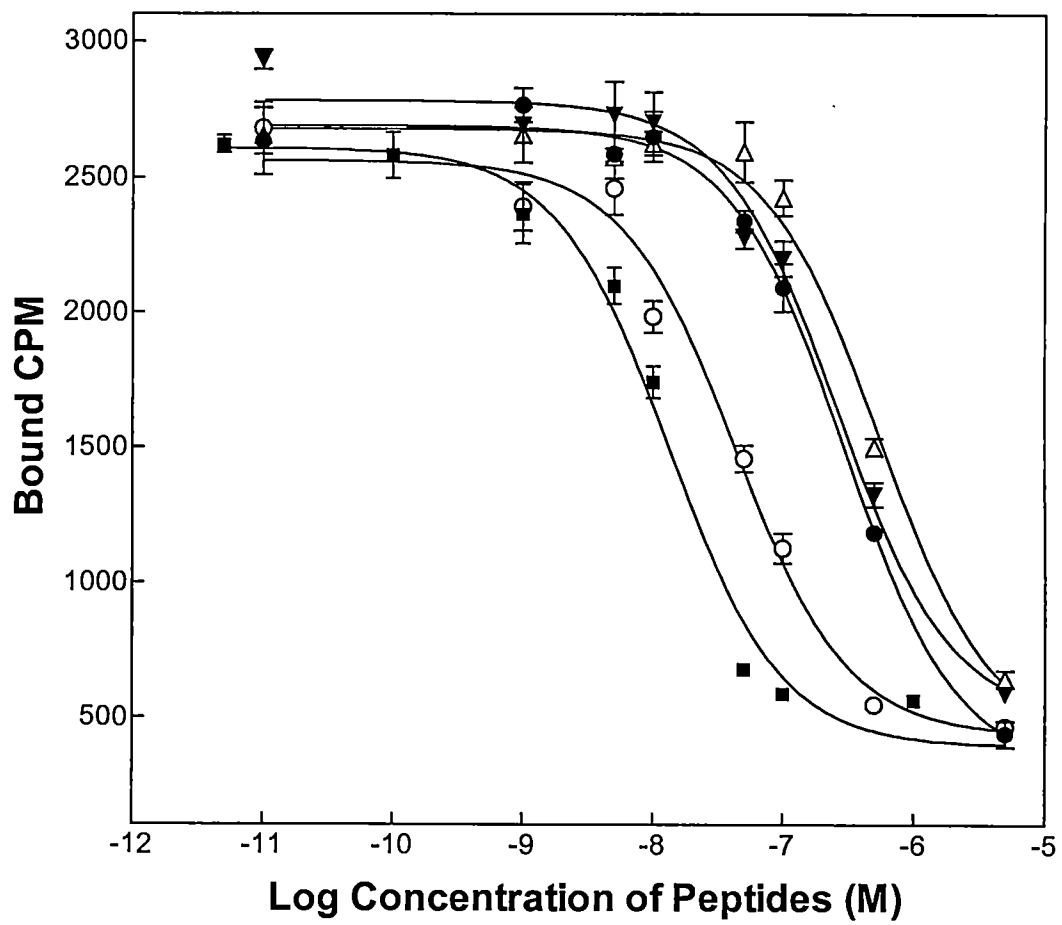


arrest assay and only 13-28 % potency in the gene induction assay. Interestingly, the Tyr<sup>1</sup>(I<sub>2</sub>), Phe<sup>13</sup>, and Tyr<sup>3</sup>(I<sub>2</sub>), Phe<sup>13</sup> analogs exhibited higher potency than the Tyr<sup>1</sup>, Phe<sup>13</sup> and Tyr<sup>3</sup>, Phe<sup>13</sup> analogs, respectively, in the gene induction assay. In fact the latter compound is nearly as active as  $\alpha$ -factor in this assay. However, whereas iodination of Tyr<sup>1</sup> also increased activity in the growth arrest assay iodination of Tyr<sup>3</sup> resulted in a decrease in activity in this same assay. There is some indication in the data that the biological response of the Tyr<sup>1</sup>,Phe<sup>13</sup>, the Tyr<sup>3</sup>, Phe<sup>13</sup> and the Tyr<sup>1</sup> (I<sub>2</sub>),Phe<sup>13</sup> analogs have not reached a plateau at the highest concentrations tested. However, due to the poor solubility of these peptides, higher concentrations were not tested. Whether these peptides are capable of fully stimulating a biological response is not known.

*Receptor Affinities of  $\alpha$ -Factor Analogs.* The affinity of the position 13 and multiple position analogs for the Ste2p receptor was determined by measuring the relative abilities of these compounds to compete with [<sup>3</sup>H] $\alpha$ -factor. As exemplified in Figure 3 the pheromones were able to eliminate more than 80% of the binding of the radioactive  $\alpha$ -factor. This result is similar to that found when cold  $\alpha$ -factor is used as the competitor. The binding competition resulted in sharp curves whose slopes were parallel to each other. The concentration of competitor causing 50% displacement of  $\alpha$ -factor was determined from these curves and converted to K<sub>I</sub> values using the approach of Cheng and Prusoff (26). The results show that replacement of Tyr<sup>13</sup> with Phe or *p*-F-Phe had almost no effect on

**Figure 3. Competition binding assay.**

Binding of the analogs was performed in competition with [<sup>3</sup>H]α-factor. The binding curves are for α-factor (■), Tyr<sup>1</sup>, Phe<sup>13</sup> (●), Tyr<sup>1</sup>(I<sub>2</sub>), Phe<sup>13</sup> (Δ), Tyr<sup>3</sup>, Phe<sup>13</sup> (▼), Tyr<sup>3</sup>(I<sub>2</sub>), Phe<sup>13</sup> (O).





receptor affinity (Table 2). Incorporation of NH<sub>2</sub> in place of the Tyr OH caused about a three-fold decrease in affinity while a nitro group at the para position resulted in approximately a five-fold decrease. When the fluorine group was placed in the *meta* position of the phenyl ring the affinity was also about five-fold lower than when it was in the *para* position. In contrast to the analogs containing a substituted phenyl ring at position 13, incorporation of Ser at this position resulted in a large decrease (>100-fold) in receptor affinity.

The high affinity of Phe<sup>13</sup> and *p*-F-Phe<sup>13</sup> analogs encouraged us to place Tyr at positions 1 and 3 in place of the Trp residues of these pheromones. In both the Phe and the *p*-F-Phe series the incorporation of Tyr at positions 1 or 3 resulted in a drop in affinity of about 6-10 fold. This still represented receptor affinities in the 100 nM range. Thus, these compounds were potential substrates for radioiodination. Prior to preparing radioactive substrates we synthesized diiodinated standards containing <sup>127</sup>I. During the synthesis we experienced problems when Lys was in position 7. This problem was eliminated when Arg was placed in this position (See peptide synthesis). Interestingly, diiodination of Tyr<sup>1</sup> resulted in a two-fold decrease whereas diiodination of Tyr<sup>3</sup> resulted in a large increase in receptor affinity (Table 2).

*Synthesis and Binding of Radioiodinated ([Tyr<sup>1</sup>(<sup>125</sup>I),Phe<sup>13</sup>]α-Factor.*

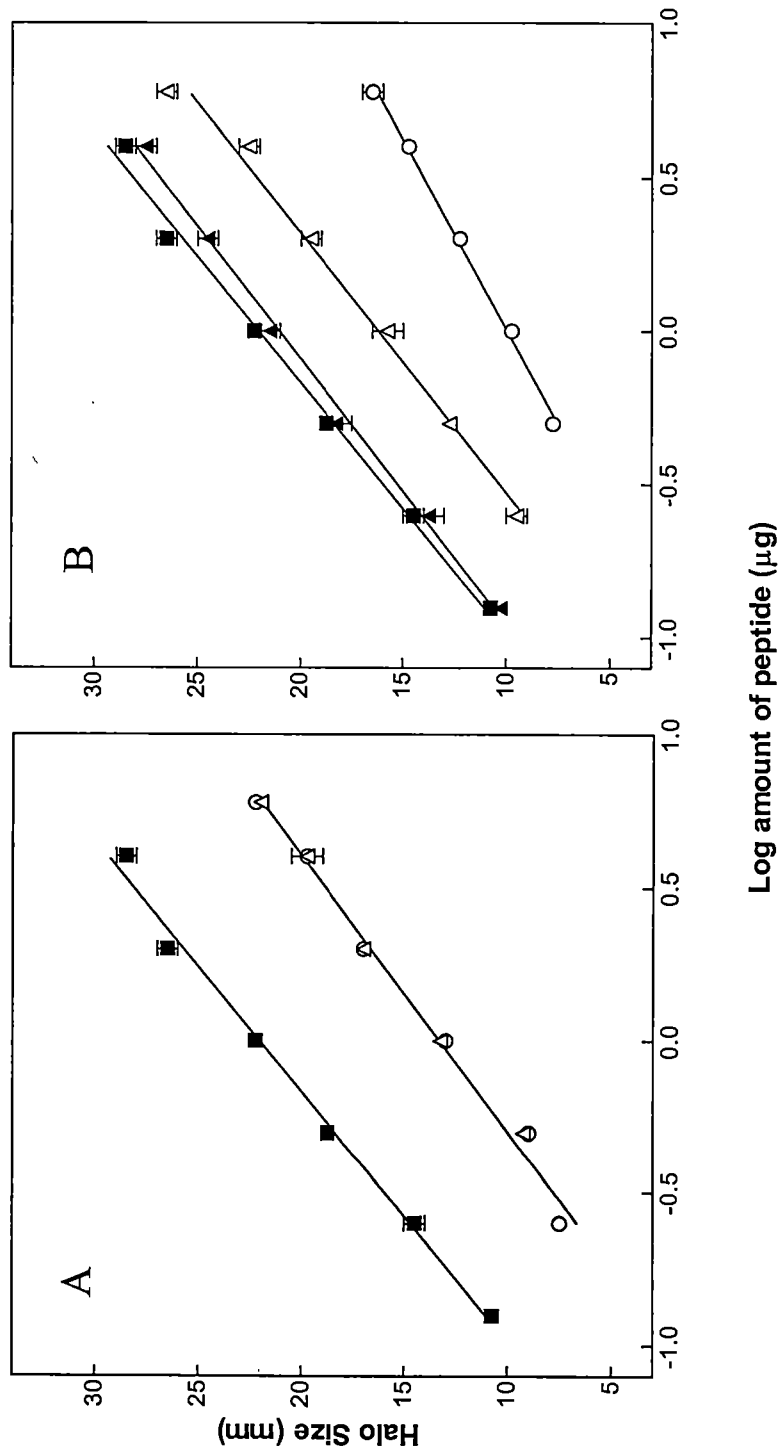
Based on the significant receptor affinities and bioactivities of the diiodinated analogs of α-factor we attempted to radioiodinate the Tyr<sup>1</sup>, Phe<sup>13</sup> and Tyr<sup>3</sup>, Phe<sup>13</sup>

analogs. All attempts with the latter compound resulted in multiple products as judged by HPLC and we were not able to isolate pure labeled receptor probes. However, the Tyr<sup>1</sup>, Phe<sup>13</sup> analog could be successfully monoiodinated using IODOGEN<sup>®</sup> tubes. The monoiodinated compound exhibited a retention time intermediate to those for the underivatized and doubly derivatized compound (data not shown). This non-radioactive monoiodinated peptide moved at the same retention time as the radiolabeled compound and had the expected molecular weight as determined by mass spectrometry. Its biological activities are indicated in Table 2.

The [Tyr<sup>1</sup>(<sup>125</sup>I), Phe<sup>13</sup>]α-factor specifically bound to the α-factor receptor and showed saturation binding with a  $K_D = 81$  nM in a whole cell binding assay (Fig. 4a). A similar  $K_D$  of 108 nM was found when cell membranes were used for binding (data not shown). The binding of monoiodinated α-factor could be displaced by both the unlabelled diiodinated pheromone and α-factor (Figure 4b). The  $K_i$  determined for α-factor in this experiment was 7.7 nM which is consistent with the affinity of α-factor that we normally find in our receptor binding analyses. A known α-factor antagonist [Trp-Leu-Gln-Leu-Lys-Pro-Gly-Gln-Pro-Nle-Tyr] also displaced labeled [Tyr<sup>1</sup>(<sup>125</sup>I), Phe<sup>13</sup>]α-factor from the receptor (Fig 4b) whereas Trp-His-Trp-Leu-Gln-Leu-Lys-Pro-Gly-Gln-Pro, an α-factor analog that does not bind to Ste2p (28), could not release the iodinated ligand from this protein (data not shown).

**Figure 4. Saturation and competition binding assays with [Tyr<sup>1</sup>(<sup>125</sup>I), Phe<sup>13</sup>]α-factor.**

Cells were incubated with increasing amount of [Tyr<sup>1</sup>(<sup>125</sup>I), Phe<sup>13</sup>]α-factor as described in the Experimental Procedures and the dpm associated with the Ste2p receptor were plotted against the pheromone concentration. The inset represents the total counts bound to cells with receptor (DK102pNED1, ■) and total counts bound to cells without receptor (DK102, ▲) [Panel A]. Competition for binding of [Tyr<sup>1</sup>(<sup>125</sup>I), Phe<sup>13</sup>]α-factor to Ste2p receptor was performed using α-factor (■), Tyr<sup>1</sup>(<sup>127</sup>I<sub>2</sub>), Phe<sup>13</sup> (▲), and Trp-Leu-Gln-Leu-Lys-Pro-Gly-Gln-Pro-Nle-Tyr (▼) as competitors (Panel B). The concentration of the radioactive pheromone was  $2.4 \times 10^{-9}$  M and the concentration of the competitors is indicated in the figure.



## CHAPTER IV

### DISCUSSION

The  $\alpha$ -factor receptor from the yeast *S. cerevisiae* is a representative of Class D within the GPCR family of heptahelical receptors (3-5). This subgroup consists solely of fungal receptors which are characterized by the absence of disulfide bridges in the functional protein. Very little work has been done on this family of receptors and its characterization is of interest in defining distinguishing features of the different subgroups and the relationship between receptor structure and function.

Although Ste2p has been subjected to a variety of mutagenesis studies (21, 22, 29-35) there is little knowledge on the pheromone binding site. Structure - activity relationship studies combined with conformational analysis on the  $\alpha$ -factor suggest that the two termini of the pheromone are important for receptor binding and that the pheromone is bent when it binds to its receptor (12, 15, 36-38). However, there is no direct evidence for contacts between residues of the peptide ligand and residues of the receptor. At present a method of choice for discerning such contacts is photoaffinity crosslinking of bound agonist into the receptor and characterizing the crosslinking site using biochemical techniques (39-45). This approach requires the availability of a photoactivatable ligand with a tag

that can be used to follow ligand incorporation by subsequent analytical procedures. Although biotin has been suggested as one approach for such a tag, the sensitivity of its detection is two to three orders lower than that of  $^{125}\text{I}$ . Recent reports indicated that biotin was not useful in receptor analysis of the integrin receptor  $\alpha_v\beta_3$  (46). Studies on  $\alpha$ -factor - Ste2p interactions have previously been stymied by the lack of an iodinated agonist. Therefore, design and characterization of such a probe was the principal goal of the present study.

*Can Tyr<sup>13</sup> of  $\alpha$ -factor be replaced by other residues?* Since iodination of  $\alpha$ -factor results in an inactive ligand with low receptor affinity, we evaluated replacement of Tyr<sup>13</sup> with amino acids containing other aromatic side chains. In contrast to previous reports (20), we found that incorporation of a variety of aromatic amino acids including Phe at position 13 resulted in pheromones with high biological activity and high receptor affinities. An analog with Ser<sup>13</sup> exhibited poor activity and more than a 100-fold drop in receptor affinity. In a previous study it was noted that [Ala<sup>13</sup>] $\alpha$ -factor had low biological activity and did not bind well to Ste2p (15). These results suggest that the phenolic hydroxyl group of residue 13 is not involved in a direct interaction with the receptor and that an aromatic side chain at this position seems to be required for high affinity binding to Ste2p. Interestingly, even the Ser<sup>13</sup> and Ala<sup>13</sup> analogs, which bind poorly, can trigger biological responses. Thus, the aromatic side chain at residue 13 is not necessary for downstream signal transduction from the  $\alpha$ -factor receptor. At

present very little is known about the nature of the binding site for  $\alpha$ -factor. The fact that aromatic residues in both positions 1 and 13 have been associated with a high receptor affinity (12, 15), taken together with the hypothesis of a bent pheromone, suggests that an aromatic cluster between residues near the chain ends might occur on binding to Ste2p. This cluster would likely interact with a hydrophobic surface in the receptor. In addition, it is possible that there may be contacts between Arg or Lys side chains in the extracellular receptor loops with the aromatic rings of the pheromone forming cation -  $\pi$  interactions. Such cation- $\pi$  interactions have been suggested to supply significant stabilization energies in proteins and in protein ligand interactions (47).

*Are multiple substitutions at the N and C termini of the pheromone accepted by Ste2p?* To obtain an iodinated ligand one strategy would be to remove Tyr from position 13 and place it at other positions of  $\alpha$ -factor. Therefore, starting with the Phe<sup>13</sup> or *p*-F-Phe<sup>13</sup> analogs we determined whether it would be possible to substitute Tyr for the Trp residues in positions 1 and 3 and still retain high receptor affinity. We found that substitution of Tyr at position one or three of either [Phe<sup>13</sup>] $\alpha$ -factor or [*p*-F-Phe<sup>13</sup>] $\alpha$ -factor resulted in a 6-10-fold reduction in receptor affinity and that diiodination of these compounds did not lead to a significant further reduction in the binding constant. These observations suggest that  $\alpha$ -factor analogs with multiple changes in the aromatic residues at position 13 and positions 1 or 3 would be potential ligands for use in a receptor binding assay.

Most importantly, the cold diiodinated pheromone still had a binding affinity in the 100 nM range indicating that it could be used directly to develop a radioactive probe.

*Can iodinated  $\alpha$ -factor analogs bind specifically to Ste2p?* Attempts to use iodinated  $\alpha$ -factor in a radioactive binding assay started with [Tyr<sup>1</sup>(I<sub>2</sub>)] $\alpha$ -factor prepared by exchange from the <sup>127</sup>I containing peptide (48). Specific binding of iodinated  $\alpha$ -factor to receptor was masked by high levels of non-specific binding of iodinated  $\alpha$ -factor to filters used in the binding assay. In previous studies such sticking to filters was not encountered with tritiated  $\alpha$ -factor. For binding studies with iodinated  $\alpha$ -factor we developed methods that eliminated non-specific binding of the iodinated peptide. We switched to a charged, low-protein binding filter (Durapore membranes, Millipore Corp.) and incorporated BSA (1% w/v) into the binding medium.

In another report significant differences in specific binding were observed for a peptide hormone containing a monoiodinated as compared to a diiodinated tyrosine derivative (49). In order to obtain a monoiodinated receptor probe we used IODOGEN<sup>®</sup> to radiolabel the Tyr<sup>1</sup>, Phe<sup>13</sup> analog and isolated [Tyr<sup>1</sup>(<sup>125</sup>I), Phe<sup>13</sup>] $\alpha$ -factor. This ligand gave saturable binding to Ste2p. Binding was competed by  $\alpha$ -factor and an antagonist, but not by an  $\alpha$ -factor analog known not to bind to Ste2p. The K<sub>D</sub> values determined with whole cells (81 nM) and membranes (108 nM) as calculated by fitting the binding isotherm indicated that



the monoiodinated pheromone binds to the receptor as well as or better than either Tyr<sup>1</sup>,Phe<sup>13</sup> or Tyr<sup>1</sup>(I)<sub>2</sub>,Phe<sup>13</sup> (Table 2).

In a previous study with [Bpa<sup>3</sup>, Arg<sup>7</sup>]α-factor we found that replacement of Trp<sup>1</sup> with diiodoTyrosine resulted in a peptide with an approximately 20-fold decrease in affinity for Ste2p compared to α-factor (50). Moreover, this latter peptide had nearly the same growth arresting activity as [Bpa<sup>3</sup>, Arg<sup>7</sup>]α-factor. These findings are consistent with the results found for the [Phe<sup>13</sup>]α-factor and [*p*-F-Phe<sup>13</sup>]α-factor series. They suggest that peptides containing Phe<sup>13</sup>, Bpa and an iodinateable tyrosine should retain reasonably high (100 nanomolar) receptor affinities and therefore should be potential photoaffinity labels for Ste2p.

In conclusion, we have successfully prepared a new radioligand for the α-factor receptor which has very high specific activity. This peptide can be radiolabeled by a simple procedure that is employed in many laboratories. This iodinateable α-factor analog will be a useful tool for researchers interested in studying wildtype and mutant Ste2p.

## REFERENCES

- 1) Wess, J. (1997) G protein-coupled receptors: molecular mechanisms involved in receptor activation and selectivity of G protein recognition. *FASEB J.* **11**, 346-354.
- 2) Hall, R.A., Premont, R.T. and Lefkowitz RJ (1999) Heptahelical receptor signaling: beyond the G protein paradigm. *J. Cell. Biol.* **145**, 927-32.
- 3) Kenakin, T. (1996) The classification of seven transmembrane receptors in recombinant expression systems. *Pharmacol. Rev.*, **48**, 413-463.
- 4) Strader, C.D., Fong, T.M., Graziano, M. P., and Tota, M.R. (1995) The family of G protein-coupled receptors. *FASEB J.* **9**, 745-754.
- 5) Strader, C.D., Fong, T.M., Tota, M.R., Underwood, D., and Dixon, R. A. F. (1994) Structure and function of G protein-coupled receptors. *Annu. Rev. Biochem.* **63**, 101-132.
- 6) Blumer, K. J., and Thorner, J. (1991) Receptor G protein signaling in yeast. *Annu. Rev. Physiol.* **53**, 37-57.

- 7) Dohlman, H. G., Thorner, J., Caron, M. G. and Lefkowitz, R. J. (1991) Model systems for the study of seven-transmembrane-segment receptors. *Annu. Rev. Biochem.* **60**, 653-688.
- 8) Burkholder, A. C. and Hartwell, L. H. (1985) The yeast  $\alpha$ -factor receptor: structural properties deduced from the sequence of the *STE2* gene. *Nucleic Acids Res.* **13**, 8463-8475.
- 9) Nakayama N., Miyajima, A. and Arai, K. (1985) Nucleotide sequences of *STE2* and *STE3*, cell type-specific sterile genes from *Saccharomyces cerevisiae*. *EMBO J.* **4**, 2643-2648.
- 10) David, N. E., Gee, M., Andersen, B., Naider, F., Thorner, J. and Stevens, R. C. (1997) Expression and purification of the *Saccharomyces cerevisiae*  $\alpha$ -factor receptor (Ste2p), a 7-transmembrane-segment G protein-coupled receptor. *J. Biol. Chem.* **272**, 15553-15561.
- 11) Naider, F. and Becker, J.M. (1986) Structure-function relationships of the *Saccharomyces cerevisiae*  $\alpha$ -factor. *CRC Critical Reviews in Biochemistry* **21**, 225-248.

- 12) Zhang, Y. L., Lu, H.-F., Becker, J. M. and Naider, F. (1997) Position one analogs of the *Saccharomyces cerevisiae* tridecapeptide pheromone. *J. Peptide Res.* **50**, 319-328.
- 13) Manfredi, J. P., Klein, C., Herrero, J. J., Byrd, D. R., Trueheart, J., Wiesler, W. T., Fowlkes, D. M. and Broach, J. R. (1993) Yeast  $\alpha$  mating factor structure-activity relationship derived from genetically selected peptide agonists and antagonists of Ste2p. *Mol. Cell. Biol.* **16**, 4700-4709.
- 14) Levin, Y., Khare, R. K., Able, G., Hill, D., Eriotou-Bargiota, E., Becker, J. and Naider, F. (1993) Histidine<sup>2</sup> of the  $\alpha$ -factor of *Saccharomyces cerevisiae* is not essential for binding to its receptor or for biological activity. *Biochemistry*, **32**, 8199-8206.
- 15) Abel, M.G., Zhang, Y.L., Lu, H.F., Naider, F. and Becker, J.M. (1998) Structure-function analysis of the *Saccharomyces cerevisiae* tridecapeptide pheromone using alanine-scanned analogs. *J. Peptide Res.* **52**, 95-106.
- 16) Raths, S. K., Naider, F. and Becker, J. M. (1988) Peptide analogues compete with the binding of  $\alpha$ -factor to its receptor in *Saccharomyces cerevisiae*. *J. Biol. Chem.* **263**, 17333-17341.

- 17) Jenness, D.D., Burkholder, A.C., and Hartwell, L.H. (1983) Binding of  $\alpha$ -factor pheromone to yeast a cells: Chemical and genetic evidence for an  $\alpha$ -factor receptor. *Cell* **35**, 521-529.
- 18) Blumer, K. J., Reneke, J. E. and Thorner, J. (1988) The *STE2* gene product is the ligand-binding component of the  $\alpha$ -factor receptor of *Saccharomyces cerevisiae*. *J. Biol. Chem.* **263**, 10836-10842.
- 19) Lipke, P.N. (1976) Morphogenetic effects of  $\alpha$ -factor on *S. cerevisiae* a-cells. Ph.D. Thesis University of California, Berkeley.
- 20) Masui, Y., Chino, N., Kita, H., and Sakakibara, S. (1979) Amino acid substitution of mating factor of *Saccharomyces cerevisiae* structure-activity relationship. *Biochem. Biophys. Res. Comm.* **86**, 982-987.
- 21) Marsh, L. (1992) Substitutions in the hydrophobic core of the  $\alpha$ -factor receptor of *Saccharomyces cerevisiae* permit response to *Saccharomyces kluyveri*  $\alpha$ -factor and to antagonist. *Mol. Cell. Biol.* **12**, 3959-3966.

- 22) Abel, M.G., Lee, B.K., Naider, F. and Becker, J.M. (1998) Mutations affecting ligand specificity of the G-protein-coupled receptor for the *Saccharomyces cerevisiae* tridecapeptide pheromone. *Biochim. Biophys. Acta* **1448**, 12-26.
- 23) Kippert, F. (1995) A rapid permeabilization procedure for accurate quantitative determination of beta-galactosidase activity in yeast cells. *FEMS Microbiol. Lett.* **128**, 201-206.
- 24) Guarente, L. (1983) Yeast promoters and lacZ fusions designed to study expression of cloned genes in yeast. *Meth. Enzymol.* **101**, 167-180.
- 25) Miller, J.H. (1972) Experiments in Molecular Genetics, Cold Spring Harbor Laboratory, Cold Spring Harbor, New York.
- 26) Cheng, Y. and Prusoff, W.H. (1973) Relationship between the inhibition constant (K<sub>1</sub>) and the concentration of inhibitor which causes 50 percent inhibition (I<sub>50</sub>) of an enzymatic reaction. *Biochem. Pharmacol.* **22**, 3099-3108.
- 27) Samokhin, G.P., Lizlova, L.V., Bepalova, J.D., Titov, M.I., and Smirnov, V.N. (1979) Substitution of Lys7 by Arg does not affect biological activity of  $\alpha$ -factor, a yeast mating pheromone. *FEMS, Microbiol. Lett.* **5**, 435-438.

- 28) Eriotou-Bargiota, E., Xue, C.-B., Naider, F., and Becker, J.M. (1992)  
Antagonistic and synergistic peptide analogues of the tridecapeptide mating pheromone of *Saccharomyces cerevisiae*. *Biochemistry* **31**, 551-557.
- 29) Clark, C. D., Palzkill, T. and Botstein, D. (1994) Systematic mutagenesis of the yeast mating pheromone receptor third intracellular loop. *J. Biol. Chem.* **269**, 1-11.
- 30) Sen, M. and Marsh, L. (1994) Noncontiguous domains of the alpha-factor receptor of yeasts confer ligand specificity. *J. Biol. Chem.* **269**, 968-973.
- 31) Stefan, C. J. and Blumer, K. J. (1994). The third cytoplasmic loop of a yeast G-protein-coupled receptor controls pathway activation, ligand discrimination, and receptor internalization. *Mol. Cell. Biol.* **14**, 3339-3349.
- 32) Konopka, J. B., Margarit, S. M. and Dube, P. (1996) Mutation of Pro-258 in transmembrane domain 6 constitutively activates the G protein-coupled alpha-factor receptor. *Proc. Natl. Acad. Sci. USA*, **93**, 6764-6769.

- 33) Sen, M., Shah, A., and Marsh, L. (1997) Two types of alpha-factor receptor determinants for pheromone specificity in the mating-incompatible yeasts *S. cerevisiae* and *S. kluyveri*. *Curr. Genet.* **31**, 235-240.
- 34) Sommers, C.M. and Dumont, M. E. (1997) Genetic interactions among the transmembrane segments of the G protein coupled receptor encoded by the yeast STE2 gene. *J. Mol. Biol.* **266**, 559-575.
- 35) Martin, N.P., Leavitt, L.M., Sommers, C.M., and Dumont, M. E. (1999) Assembly of G protein-coupled receptors from fragments: identification of functional receptors with discontinuities in each of the loops connecting transmembrane segments. *Biochem.* **38**, 682-695.
- 36) Jelicks, L.A., Naider, F., Shenbagamurthi, P., Becker, J.M., and Broido, M.S. (1988) A type II beta-turn in a flexible peptide proton assignment and conformational analysis of the alpha-factor from *Saccharomyces cerevisiae* in solution. *Biopolymers* **27**, 431-449.



- 37) Naider, F., Jelicks, L.A., Becker, J.M., and Broido, M.S. (1989) Biologically significant conformation of the *Saccharomyces cerevisiae* alpha factor. Biopolymers **28**, 487-497.
- 38) Zhang, Y.L., Marepalli, H.R., Lu, H.F., Becker, J.M., and Naider, F. (1998) Synthesis, biological activity, and conformational analysis of peptidomimetic analogues of the *Saccharomyces cerevisiae* alpha-factor tridecapeptide. *Biochemistry* **37**, 12465-12476.
- 39) Williams, K.P and Shoelson, S.E. (1993) Bpa<sup>B25</sup> insulins: photoactivatable analogues that quantitatively crosslink, radiolabel, and activate the insulin receptor. *J. Biol. Chem.* **268**, 5361-5364.
- 40) Zhou, A.T., Besalle, R., Bisello, A., Nakamoto, C., Rosenblatt, M., Suva, L.J., and Chorev, M. (1997) Direct mapping of an agonist-binding domain within the parathyroid hormone/parathyroid hormone-related protein receptor by photoaffinity crosslinking. *Proc. Natl. Acad. Sci. USA.* **94**, 3644-3649.
- 41) Bisello, A., Adams, A., Mierke, D., Pellegrini, M., Rosenblatt, M., Suva, L. and Chorev, M., (1998) Parathyroid hormone-receptor interactions identified

directly by photocrosslinking and molecular modeling studies. *J. Biol. Chem.* **273**, 22498-22505.

42) Dong, M., Wang, Y., Pinon, D., Hadac, E. and Miller, L. (1999)

Demonstration of a direct interaction between residue 22 in the carboxyl terminal half of secretin and the amino terminal tail of the secretin receptor using photoaffinity labeling. *J. Biol. Chem.* **274**, 903-909.

43) McNicoll, N., Gagnon, J., Rondeau, J.J., Ong, H. and DeLean, A. (1996)

Localization by photoaffinity labeling of natriuretic peptide receptor - A binding domain. *Biochemistry* **35**, 12950-12956.

44) Blanton, M.P., Li, Y.M., Stimson, E.R., Maggio, J.E. and Cohen, J.B. (1994)

Agonist induced photoincorporation of a *p*-benzoylphenylalanine derivative of substance P into membrane-spanning region 2 of the torpedo nicotinic acetylcholine receptor  $\epsilon$  subunit. *Mol. Pharmacol.* **46**, 1048-1055.

45) Anders, J., Bluggel, M., Meyer, H.E., Kuhne, R., ter Laak, A.M., Kojro, E. and

Fahrenholz, F. (1999) Direct identification of the agonist binding site in the human brain choecystokinin B receptor. *Biochemistry* **38**, 6043-6055.

- 46) Bitan, G., Scheibler, L., Greenberg, Z., Rosenblatt, M., and Chorev, M. (1999) Mapping the Integrin  $\alpha_v\beta_3$ -Ligand Interface by Photoaffinity Cross-Linking. *Biochemistry*; **38**, 3414-3420.
- 47) Dougherty, D.A. (1996) Cation-pi interactions in chemistry and biology: a new view of benzene, Phe, Tyr and Trp. *Science* **271**, 163-168.
- 48) Breslav, M., McKinney, A., Becker, J.M., and Naider . F. (1996) A New Method for Radioiodination of Peptides. *Analytical Biochemistry* **239**, 213-217.
- 49) Goldman, M.E., Chorev, M., Reagan, J.E., Levy, J.J., and Rosenblatt M. (1988) Evaluation of novel parathyroid hormone analogs using a bovine renal membrane receptor binding assay. *Endocrinology* **123**, 1468-1475.

50)Jiang, Y., Breslav, M., Khare, R.K., McKinney, A., Becker, J.M., and Naider, F. (1995) Synthesis of alpha-factor analogues containing photoactivatable and labeling groups. *Int. J. Peptide Protein Res.* **45**, 106-115.

## PART III

### IDENTIFICATION OF AN $\alpha$ -FACTOR BINDING REGION IN THE Ste2p PHEROMONE RECEPTOR BY DIRECT PHOTO-AFFINITY LABELING WITH [Bpa<sup>1</sup> Y<sup>3</sup> R<sup>7</sup> F<sup>13</sup>] $\alpha$ -FACTOR.

Part III represents collaborative work with the laboratory of Dr. Fred Naider at the City University of New York, Staten Island. Keith Henry performed all the studies in the part with the exception of synthesis of the peptides used in this study. The peptide syntheses were carried out by Dr. Sanjay Khare in Dr. Naider's lab. While not involved in performing the syntheses, Keith Henry was involved in guiding which peptides were synthesized for this study.

## CHAPTER I

### INTRODUCTION

G-protein coupled receptors (GPCRs) comprise one of the largest superfamilies of proteins with over a 1000 members having been discovered from a diversity of organisms. And while there has been considerable amounts of data published on the GPCR ligand binding sites for biogenic amines [1-4], almost no information exists concerning the binding sites of peptide responsive GPCRs. However, recently there have been several reports which are starting to address this issue with the use of photoreactive chemical groups called photophores [5-16]. These studies detail the design, synthesis and radioiodination of peptide ligand probes containing the photoactivatable-crosslinking moiety benzoylphenylalanine (Bpa) and their use to determine direct contacts between the peptide ligand and domains of the cognate receptor. For instance, a recent study by Mouldous *et al.* [16] investigating interaction between the heptadecapeptide nociceptin and the Opioid Receptor-Like (ORL1) GPCR made use of a Bpa containing nociceptin analog ([Bpa<sup>10</sup>, Tyr<sup>14</sup>] nociceptin) and found that the photoactivatable Bpa moiety crosslinked to a six amino acid fragment [amino acids 296-302]. Identification of these crosslinked receptor fragments is a first but critical step in the elucidation of direct residue to residue contacts between ligand and receptor.

GPCRs can bind a variety of molecules including biogenic amines, peptides, and sugars [4]. The unicellular yeast *Saccharomyces cerevisiae* contains two Class IV GPCRs used by haploid cells in the detection and response to pheromones secreted by cells of the opposite mating type during sexual reproduction. One of these receptors, Ste2p, responds to the  $\alpha$ -factor peptide pheromone (WHWLQLKPGQPMY) while the other receptor, Ste3p, responds to the post-translationally modified  $\alpha$ -factor peptide (YIIKGVFWD PAC(S-farnesyl)-OCH<sub>3</sub>).

Here, we describe the construction and characterization of a series of radioiodinatable Bpa containing  $\alpha$ -factor analogs. One of the analogs [Bpa<sup>1</sup>Tyr<sup>3</sup>(<sup>125</sup>I),Arg<sup>7</sup> Phe<sup>13</sup>]  $\alpha$ -factor was used to determine direct contacts between the  $\alpha$ -factor peptide and fragments of the Ste2p receptor. The data show that the Bpa of [Bpa<sup>1</sup>Tyr<sup>3</sup>(<sup>125</sup>I),Arg<sup>7</sup> Phe<sup>13</sup>]  $\alpha$ -factor crosslinks somewhere within residues 190-218 and/or 251-294 which correspond to the second and third extracellular loops of the Ste2p receptor.

There is precedent that the study of the pheromone receptors in yeast has led to many critical findings concerning the biology of GPCRs, such as discovery of the Regulator of G-protein Signaling (RGS) family of proteins [17, 18]. Additionally, Ste2p arguably serves as a model protein for the study of GPCRs, as (1) its functional domains are arranged similar to GPCRs, (2) interactions between the 5<sup>th</sup> and 6<sup>th</sup> transmembrane domains (TMD) appear to be critical for proper

signal transduction to the G-protein and (3) close packing of the 5<sup>th</sup> and 6<sup>th</sup> TMDs appears to be structurally similar to that of rhodopsin [19]. All of these factors suggest that while most GPCRs do not share sequence homology, they do have strong structural and functional similarity. Therefore, knowledge gained from this study and subsequent crosslinking studies of Ste2p, such as the elucidation of contact residues between receptor and ligand, should provide pertinent insight into structure-function relationships in binding and activation of peptide responsive GPCRs.



## CHAPTER II

### MATERIALS AND METHODS

*Organisms.* *S. cerevisiae* DK102[*MATa ste2::HIS3 bar1 leu2 ura3 lys2 ade2 his3 trp1*] transformed with pNED1[*STE2*] [20] was used in binding studies and in the growth arrest assays of various  $\alpha$ -factor analogs. Strain LM23-3AZ [*MATa FUS1::lacZ bar1-1*] from Lorraine Marsh, Albert Einstein College of Medicine, New York, NY was used in *FUS1*-lacZ gene induction assays. Strain BJ2168 transformed with pNED1[*STE2*] [20] was used in crosslinking assays.

*Synthesis of Bpa containing [Nle<sup>12</sup>] $\alpha$ -factor analogs.* All reagents and solvents used for the solid phase peptide synthesis of the photoactivatable peptides mentioned in Table 1 were analytical grade and were purchased from Advanced Chem Tech (Louisville, KY), VWR Scientific (Piscataway, NJ) and Aldrich Chemical Co. (Milwaukee, WI). High performance liquid chromatography (HPLC) grade dichloromethane (CH<sub>2</sub>Cl<sub>2</sub>), acetonitrile (ACN), methanol (MeOH) and water were purchased from VWR scientific (Piscataway, NJ) and Fisher Scientific (Springfield, NJ).

*L*-norleucine (Nle), which is isosteric with *L*-methionine, was incorporated at position 12 to replace the original *L*-methionine in all analogs in order to

**Table 1: Physicochemical Properties of Photoactivatable Peptides**

No'	PEPTIDES	MW <sup>p</sup>	MS <sup>q</sup>	K(a) <sup>r</sup>	K(b) <sup>r</sup>	Amino Acid Analysis
1	Bpa1Y3R7Nle12F13	1720.03	1721.1	4.74	3.79	Y: 0.92(1); H: 0.93(1); L: 1.99(2); Q: 2.16(2); R: 0.89(1); P: 1.99(2); G: 0.99(1); Nle: 1.21(1); F: 0.98(1)
2	Y1Bpa3R7Nle12F13	1719.09	1720.3	4.61	2.99	Y: 0.91(1); H: 0.94(1); L: 1.98(2); Q: 2.13(2); R: 0.88(1); P: 1.97(2); G: 0.99(1); Nle: 1.23(1); F: 0.99(1)
3	Y1Bpa5R7Nle12F13	1779.12	1779.4	4.39	5.04	Y: 0.97(1); H: 0.81(1); L: 2.00(2); Q: 1.08(1); R: 0.96(1); P: 1.97(2); G: 0.99(1); Nle: 1.23(1); F: 0.99(1)
4	Y1R7Nle12Bpa13	1759.06	1760	5.19	3.83	Y: 0.95(1); H: 0.95(1); L: 1.95(2); Q: 2.11(2); R: 0.94(1); P: 1.92(2); G: 0.99(1); Nle: 1.19(1)
5	K7(Y)Nle12F13	1813.03	1814.5	4.99	4.69	Y: 0.89(1); H: 0.95(1); L: 1.98(2); Q: 2.11(2); K: 0.93(1); P: 1.93(2); G: 0.99(1); Nle: 1.23(1); F: 1.00(1)
6	K7(-AHA-Y)Nle12F13	1926.19	1927.1	4.97	3.42	Y: 0.79(1); H: 0.96(1); L: 1.99(2); Q: 2.17(2); K: 0.84(1); P: 1.98(2); G: 0.99(1); Nle: 1.25(1); F: 1.01(1)
7	Bpa3K7(Y)Nle12F13	1878.14	1879.7	5.33	4.38	Y: 0.91(1); H: 0.96(1); L: 1.99(2); Q: 2.15(2); K: 0.92(1); P: 1.91(2); G: 0.99(1); Nle: 1.23(1); F: 0.97(1)
8	Bpa3K7(-AHA-Y)Nle12F13	1991.54	1992.8	5.37	4.65	Y: 0.82(1); H: 0.99(1); L: 2.01(2); Q: 2.18(2); K: 0.86(1); P: 1.94(2); G: 0.99(1); Nle: 1.23(1); F: 0.99(1)
9	Bpa1Y3(I2)R7Nle12F13	1972.05	1973	41.5	4.92	Y: 0.38(1); H: 1.04(1); L: 2.16(2); Q: 2.37(2); R: 0.38(1); P: 2.14(2); G: 1.08(1); Nle: 1.34(1); F: 1.09(1)
10	Y1(I2)Bpa3R7Nle12F13	1972.21	1972.7	2.66	3.19	Y: 0.93(1); H: 0.97(1); L: 1.99(2); Q: 2.13(2); R: 0.92(1); P: 1.91(2); G: 0.96(1); Nle: 1.22(1); F: 0.98(1)
11	Y1(I2)Bpa5R7Nle12F13	2030.13	2030.7	2.92	5.56	Y: 0.91(1); H: 0.96(1); L: 1.99(2); Q: 1.08(2); R: 0.96(1); P: 1.93(2); G: 0.97(1); Nle: 1.21(1); F: 0.98(1)
12	Y1(I2)R7Nle12Bpa13	2011.08	2011.7	5.50	6.42	Y: 0.92(1); H: 0.89(1); L: 1.96(2); Q: 2.13(2); R: 0.89(1); P: 2.02(2); G: 0.97(1); Nle: 1.21(1)

p) Monoisotopic molecular weight

q) Molecular mass was determined using electron ionization mass spectroscopy (ESI-MS)

r) K is defined as (V<sub>p</sub>-V<sub>f</sub>)/V<sub>f</sub> where V<sub>p</sub>= the elution volume for the peptide and V<sub>f</sub>= the breakthrough volume.

K-values (a) was determined on a C<sub>18</sub> μ -Bondpack column using a 10-50 % acetonitrile gradient (0.025% trifluoroacetic acid ) over 15 min and (b) was determined using 50-80% methanol gradient (0.025% trifluoroacetic acid ) over 30 min.

prevent oxidation of the sulfur atom of this amino acid. Oxidation occurs during synthesis of various analogs leading to peptides of reduced biological activity and stability. This replacement of Met by Nle was shown previously to result in an analog with equal activity and receptor affinity to that of the native pheromone [21]. Since all analogs have Nle in place of Met<sup>12</sup> this residue is eliminated from the abbreviated names for simplicity. All analogs were synthesized in the laboratory of Dr. Fred Naider at the City University of New York, College of Staten Island. Automated synthesis of all of the peptides mentioned in Table 1 were carried out on an Applied Biosystem 433A peptide synthesizer (Applied Biosystem, Foster City, California), using preloaded N- $\alpha$ -Fmoc-Phe-Wang resin (0.70 mmol/gm, Advanced ChemTech, Louisville, Kentucky) for all of the peptides except peptides number- 4 and -12 which were synthesized using preloaded N- $\alpha$ -Fmoc-Bpa-Wang resin (0.5 mmol/gm, Advanced Chem Tech, Louisville, Kentucky). In case of analogues 5 and 6 initially the protected peptidyl resin ( Boc-Trp(Boc)-His(Trt)-Trp(Boc)-Leu-Gln(Trt)-Leu-Lys(Mtt)-Pro-Gly-Gln(Trt)-Pro-Nle-Phe-Wang resin) was synthesized on peptide synthesizer. In order to attach - Tyrosine and amino hexanoic acid-Tyrosine at the side chain of Lysine at position-7, the Mtt group was cleaved using 1% trifluoroacetic acid/ dichloromethane/ triisopropylsilane mixture [22]. TFA salt was neutralized using 2% diisopropyl ethyl amine in dimethylformamide and after washing with dimethyl formamide, methanol and dimethyl formamide, Tyrosine and

–aminohexanoic acid-Tyrosine (AHA-Tyr) were coupled manually using HBTU/DIEA procedure and completion of the coupling reaction was monitored by the Kaiser's test [23]. Direct attachment or attachment via AHA of tyrosine to the epsilon amine of Lys<sup>7</sup> was performed to distance the iodlatable Tyr residue from the backbone of the peptide in hopes of obtaining cleaner iodination products (see below) and are referred to hereafter as tethered ligands. Finally the simultaneous cleavage of the peptide with all protecting groups and from the resin was carried out with the procedure discussed in section pertaining to peptide cleavage below. Similar strategy and procedure was applied for the synthesis of analogues- 7 and 8, in this case the protected peptidyl resin was Boc-Trp(Boc)-His(Trt)-Bpa-Leu-Gln(Trt)-Leu-Lys(Mtt)-Pro-Gly-Gln(Trt)-Pro-Nle-Phe-Wang resin. All other protected amino acids used including Fmoc-Bpa, Fmoc-His(Trt)OH, Fmoc-Tyr(But)OH, Fmoc-Tyr(I<sub>2</sub>)OH, Fmoc-Leu-OH, Fmoc-Gln(Trt)OH, Fmoc-Arg(Pmc)OH, Fmoc-Pro-OH, Fmoc-Gly-OH and Fmoc-Nle-OH, Fmoc- Amino hexanoic acid and Boc-Tyr(But) OH were obtained from Advanced ChemTech, Louisville, Kentucky. The 0.1 mmol FastMoc chemistry of Applied Biosystem was used for the elongation of the peptide chain with an HBTU/HOBt/DIEA catalyzed, single coupling step using 10 equivalents of protected amino acids for 30 min. Of all of the peptides were synthesized peptide no'-1 was found to be a suitable ligand for crosslinking studies and a detail

synthetic procedure for this peptide [Bpa<sup>1</sup>Y<sup>3</sup>R<sup>7</sup>Nle<sup>12</sup>F<sup>13</sup>]  $\alpha$ -factor is described below.

*Cleavage of peptide:* The N- $\alpha$ -deprotected peptidyl resin for the peptide no'-1 was washed thoroughly with 1-methyl-2-Pyrrolidinone and dichloro methane and dried in *vacuo* for 2 hours. The peptide was cleaved from the resin support with simultaneous side chain deprotection using a cleavage cocktail containing trifluoroacetic acid (10 ml), crystalline phenol (0.75 gm), thioanisole (0.5 ml) and water (0.5ml) at room temperature for 1.5 hours. 1,2- ethane dithiol was omitted, because it was known to transform Bpa- containing peptides to cyclic dithioketal derivatives [24]. The filtrates from the cleavage reaction were collected, combined with trifluoroacetic acid washes of the resin and concentrated under reduced pressure and treated with cold ether to precipitate the crude product.

*Purification and Characterization:* The crude peptide so obtained was purified by reversed phase HPLC (Hewlett-Packard Series 1050) on a semi preparative waters  $\mu$ -bond pack C18 (19x300 mm) column with detection at 220 nm. The crude product (50 mg) was dissolved in about 4ml of aqueous acetonitrile (20%) containing 0.025% TFA, applied on to the column, and eluted with a linear gradient of water and acetonitrile containing 0.025% TFA from 0 - 70% acetonitrile over 2 hours at a flow rate of 5 ml/min. The fractions were collected and analyzed at 220 nm by reversed phase HPLC (Hewlett-Packard Series 1050)

on an analytical waters  $\mu$ -bondpack C18 column (3.9x300 mm). Fractions of over 99% homogeneity were pooled and subjected to lyophilisation. The purity of final peptide was assessed by analytical HPLC using two different solvent systems (10-55% acetonitrile gradient (15 min) with 0.025% trifluoroacetic acid and 50-80% (30 min) methanol gradient with 0.025% trifluoroacetic acid). Amino acid analysis (Biopolymer lab, Brigham and Women's Hospital, Cambridge, Massachusetts) and Electron spray ionization mass spectrometry (ESI-MS Peptido Genic Inc, CA) were used to characterize the purified peptide.

*Growth arrest (halo) assay.* Solid MLT medium [yeast nitrogen base without amino acids (Difco), 6.7 g/L; casamino acids (Difco), 10 g/L; glucose, 20 g/L; adenine sulfate (ICN), 0.058 g/L; arginine, 0.026 g/L; asparagine, 0.058 g/L; aspartic acid, 0.14 g/L; glutamic acid, 0.14 g/L; histidine, 0.028 g/L; isoleucine, 0.058 g/L; leucine, 0.083 g/L; lysine, 0.042 g/L; methionine, 0.028 g/L, phenylalanine, 0.69 g/L; serine, 0.52 g/L; threonine, 0.28 g/L; tyrosine, 0.042 g/L; valine, 0.21 g/L; and uracil, 0.028 g/L] [25] was overlaid with 4 ml of *S. cerevisiae* DK102pNED cell suspension ( $2.5 \times 10^5$  cells/ml of Nobel agar). Filter disks (sterile blanks from Difco), 8 mm in diameter, were impregnated with 10  $\mu$ l portions of peptide solutions at various concentrations and placed onto the overlay. The plates were incubated at 30<sup>0</sup>C for 24 -36 h and then observed for clear zones (halos) around the disks. The data were expressed as the diameter of the halo including the diameter of the disk. Therefore, a minimum value for growth arrest

is 9 mm, which represents the disk diameter (8 mm) and a small zone of inhibition. All assays were carried out at least three times with no more than a 2 mm variation in halo size at a particular amount applied for each peptide. The values reported represent the mean of these tests. Similar ranks of biological activities were obtained for these analogs within an assay as measured by growth arrest (halo) or gene induction (see below). In the latter assay, cells were suspended in liquid medium thereby eliminating any contribution of diffusion through agar potentially present in the halo assay.

*Effect of  $\alpha$ -Factor Analogs on Gene Induction.* *S. cerevisiae* LM23-3AZ carries a *FUS1* gene that is inducible by mating pheromone and which is fused to the reporter gene  $\beta$ -galactosidase. Cells were grown overnight in MLT at 30°C to  $5 \times 10^6$  cells/ml, washed by centrifugation, and grown for one doubling at 30°C. Induction was performed by adding 15  $\mu$ l of 10X peptide at various concentrations to 135  $\mu$ l of concentrated cells ( $2 \times 10^8$  cells/ml) in a 96 well microtiter plate. The mixtures were placed at 30°C with shaking for 2 h. After this time, cells were harvested by centrifugation, and each pellet was resuspended in Z-Buffer containing  $\beta$ -mercaptoethanol [26] and assayed for  $\beta$ -galactosidase production (expressed as Miller units) in triplicate. Each experiment was carried out at least three times with the results similar in each assay.

*Binding competition assay with [ $^3$ H] $\alpha$ -factor.* This assay was performed using strain DK102pNED and tritiated  $\alpha$ -factor prepared by reduction of

[dehydroproline<sup>8</sup>, Nle<sup>12</sup>] $\alpha$ -factor as described previously [21]. In general, cells were grown at 30<sup>0</sup>C overnight and harvested at 1 x 10<sup>7</sup> cells/ml by centrifugation at 5,000 x g at 4<sup>0</sup>C. The pelleted cells were washed two times in ice cold buffer [PPBi, 0.5M potassium phosphate (pH 6.24) containing 10 mM TAME, 10 mM sodium azide, 10 mM potassium fluoride, 1% BSA (fraction IV)] and resuspended to 4 x 10<sup>7</sup> cells/ml. The binding assay was started by addition of [<sup>3</sup>H] $\alpha$ -factor and various concentration of nonlabeled peptide (140  $\mu$ l) to a 560  $\mu$ l cell suspension so that the final concentration of radioactive peptide was 6 x 10<sup>-9</sup> M (20 Ci/mmmole). Analog concentrations were adjusted using UV absorption at 280 nm and the corresponding extinction coefficients. After a 30 min incubation, triplicate samples of 200  $\mu$ l were filtered and washed over glass fiber filtermats using the Standard Cell Harvester (Skatron Instruments, Sterling, VA) and placed in scintillation vials for counting. Each experiment was carried out at least three times with the results similar in each assay. Binding of labeled  $\alpha$ -factor to filters in the absence of cells was less than 20 cpm. The Ki values were calculated by using the equation of Cheng and Prusoff, where  $K_i = EC_{50} / (1 + [ligand] / K_d)$  (26).

*Synthesis of Iodinated  $\alpha$ -factor Peptides.* Peptides were iodinated with Iodogen<sup>®</sup> tubes from Pierce, Inc. using conditions recommended by the manufacturer. Briefly, Iodogen tubes were pre-wet with 2X Tris Iodination Buffer (TIB)(50mM Tris pH 7.5, 0.8M NaCl). TIB was decanted and 100  $\mu$ l of fresh TIB was added directly to the bottom of the Iodogen tube and either 10  $\mu$ l of Na<sup>127</sup>I



(1.86 mg/ml) or 10  $\mu\text{l}$  of  $\text{Na}^{125}\text{I}$  (100  $\mu\text{Ci}/\mu\text{l}$  pH 10) was added and incubated for 15 minutes with gentle swirling every 30 seconds. Activated iodide was transferred to a siliconized microfuge tube containing 100  $\mu\text{l}$  of the peptide (0.5 mmol/L in TIB) and incubated for 20 minutes with gentle mixing every 30 seconds. Scavenging buffer (50  $\mu\text{l}$  at 10 mg/ml tyrosine in TIB) was added and incubated for 5 minutes with mixing at minutes 1 and 4. Following incubation, 1 ml of TIB containing 5 mM EDTA was added. The remaining unreacted iodine was separated from peptide using a Waters Sep-Pak® C18 mini-column. The eluted products were separated by HPLC using  $\text{H}_2\text{O}/\text{acetonitrile}/0.025\%$  TFA with an acetonitrile percentage of 20 to 35% over 30 minutes at 1.4 ml/min on a Waters  $\mu\text{Bondapak}$  C18 reversed phase analytical column (3.9x300mm).  $^{127}\text{I}$  labeled peptides were quantitated by UV spectrophotometry using appropriate extinction coefficients. Radioiodinated peptides were labeled using carrier free  $\text{Na}^{125}\text{I}$  and the resulting mono-iodinated peptides were quantitated by converting total dpm associated with the HPLC purified peptide to mmole of peptide using the specific activity of carrier free  $\text{Na}^{125}\text{I}$  (2159 Ci/mmmole).

*Binding Assays with  $^{125}\text{I}$  labeled  $\alpha$ -factor.* DK102 pNED1 cells (grown in MLT medium) (10) and DK102 cells (grown in MLT medium supplemented with tryptophan) were harvested at  $1 \times 10^7$  cells/ml by centrifugation and resuspended to  $6.25 \times 10^7$  cells/ml in PPBi buffer (pH6.24) and placed at 4°C. In competition binding assays, [ $\text{Bpa}^1\text{Tyr}^3(^{125}\text{I}),\text{Arg}^7\text{Phe}^{13}$ ] $\alpha$ -factor ( $2.4 \times 10^{-9}$  M final

concentration) was pre-mixed with various concentrations of cold competitor. In saturation binding assays, radiolabeled  $\alpha$ -factor analogs were diluted with cold analog to obtain sufficient peptide concentrations. Cells in PPBi were then added to peptide solutions to a final density of  $6.25 \times 10^6$  cells/ml and incubated for 45 minutes at room temperature. Following incubation, reaction mixes were transferred (3 x 200  $\mu$ l) to wells of a 0.45  $\mu$ m MultiScreen –HV, 96 well plate (Millipore MHVBN4510) pre-blocked with PPBi. Samples were vacuum filtered, washed with PPBi (2 x 200  $\mu$ l) and counted on a LKB-Wallac CliniGamma 1272 gamma counter. Using this methodology non-specific binding of radiolabeled peptide to the filter was at background levels. Specific binding was determined by subtracting counts associated with the DK102 (ste2-) strain from counts bound to the DK102pNED1 (STE2<sup>+</sup>) strain.

*Crosslinking of [Bpa<sup>1</sup>Tyr<sup>3</sup>(<sup>125</sup>I),Arg<sup>7</sup>Phe<sup>13</sup>] $\alpha$ -factor to Ste2p.*

BJ2168pNED1 membranes (220  $\mu$ g) [20] were incubated with 975  $\mu$ l of PPBi buffer (with 0.1%BSA) in siliconized microfuge tubes (Midwest Scientific) for 10 minutes at ambient temperature. [Bpa<sup>1</sup>Tyr<sup>3</sup>(<sup>125</sup>I),Arg<sup>7</sup>Phe<sup>13</sup>] $\alpha$ -factor (10 and 20 million CPM) was added to the membranes and reaction was incubated for 2 hours at room temperature with gentle mixing. The reaction mixture was aliquoted into three wells of a chilled 24 well Costar culture plate (Cat# 3526) preblocked with PPBi (0.1% BSA). Separation of the reaction mixtures into separate wells kept the depth of the samples low (~2mm) for efficient UV penetration of the sample. The

samples were held at 4°C by placing on a prechilled enzyme caddy and surrounded with ice. The samples were irradiated without the culture plate lid at 365 nm for 1 hour at a distance of 12 cm in a Stratlinker (Stratagene, La Jolla, CA). Membrane samples were recombined in siliconized microfuge tubes and washed twice by centrifugation (14,000 x g) with PPBi (0.1% BSA). Membrane pellets were dissolved in 2X sample buffer (0.25M Tris-HCl, pH 8.8; 0.005% bromphenol blue; 5% glycerol; 1.25% β-mercaptoethanol ;2% SDS). Samples were heated to 37°C for 10 minutes and separated by SDS-PAGE (10% gel; 30 mAmps). In competition crosslinking experiments, cold [Nle<sup>12</sup>] α-factor was added with radioiodinated peptide. For subsequent receptor digestion analysis, the gel was exposed to a phosphorimager screen (STORM, Molecular Dynamics) and the band of radioactivity corresponding to Ste2p was excised and placed into dialysis tubing (15,000 MWCO) with buffer [0.2M Tris acetate (pH7.4); 1.0% SDS; 100 mM dithiothreitol]. Electroelution was performed by placing dialysis tubing containing the gel in a horizontal electrophoresis chamber (34 cm(L) X 21(W) X 10 cm (D)) containing running buffer [50 mM Tris acetate (pH 7.4); 0.1% SDS; 0.5 mM sodium thioglycolate]. Elution was carried out at 100 volts for three hours. The buffer in the dialysis tubing was transferred to a Millipore Ultrafree-15 centrifuge filter device (30,000 MWCO) and concentrated by centrifugation. Concentrated sample was washed three times with 50 mM Tris-

HCl (pH 7.5). Half of the sample was further treated with PNGaseF (Glyco) per supplier's instructions.

*Digestion of Crosslinked Ste2p.* Deglycosylated and untreated crosslinked samples were digested with either BNPS-skatole or CNBr. For BNPS-skatole digestions, samples were dissolved in 70% acetic acid and approximately 10mg of BNPS-skatole (Sigma) was added. For CNBr digestion, samples were dissolved in 70% formic acid and a few crystals of CNBr (Sigma) were added. Both BNPS-skatole and CNBr reactions took place under nitrogen and complete darkness. After 24 hours of digestion, samples were dried by vacuum centrifugation, resuspended in 50  $\mu$ l of 0.5M Tris pH 8.25 and re-dried. Samples were then dissolved in Tris-tricine sample buffer from Novex (San Diego, CA) and run on both 16% and 10-20% tricine gels (Novex). Gels were dried and exposed to a phosphorimager screen for 1-4 days.

## CHAPTER III

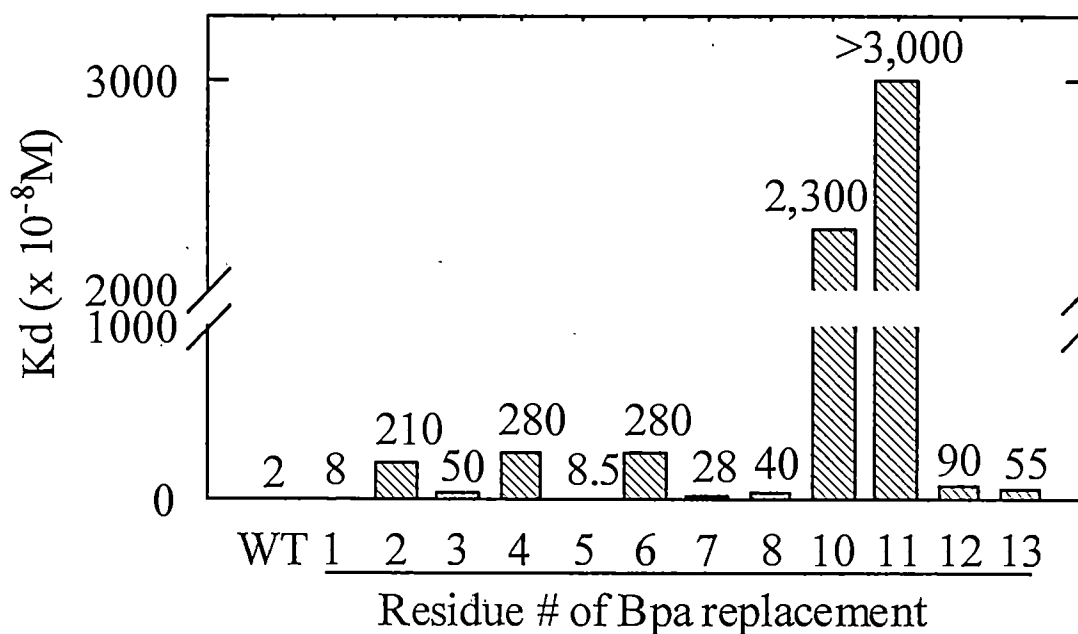
### RESULTS

*Synthesis of  $\alpha$ -Factor Analogs.* The automated solid phase synthesis of all peptides yielded 60-70% crude peptide except in the case of diiodoTyr- containing peptides as well as spacer peptides where the purity of the crude peptides is < 50%. All peptides were purified by reversed phase HPLC employing an acetonitrile-water (each containing 0.025 % trifluoroacetic acid) linear gradient elution from 10% to 70% over 2 h with the flow rate of 5 ml min<sup>-1</sup>. The fractions of each resolved peak over 99% homogeneity using analytical HPLC in either an acetonitrile/H<sub>2</sub>O/TFA or methanol/H<sub>2</sub>O/TFA gradient system were pooled, lyophilized and subjected to amino acid analysis and electron spray ionization mass spectrometry (ESI-MS), which identified and verified the peptides. The physicochemical data of all peptides are summarized in Table 1.

*Bioactivities of Position-13 Bpa Analogs.* In this study,  $\alpha$ -factor analogs were used which contained a phenylalanine in place of the normal tyrosine at position 13. Previous studies with  $\alpha$ -factor showed that iodination of the tyrosine at position 13 resulted in a biologically inactive compound. Previous work (Part II) investigated the replacement of Tyr<sup>13</sup> with Phe and showed that the conservative replacement had little to no effect on biological activity or binding

affinity of  $\alpha$ -factor. This finding allowed for a Tyr residue to be placed elsewhere in the peptide in hopes that at the alternate position Tyr would retain biological activity following iodination. The Trp residues at positions 1 and 3, which are prime candidates for replacement by tyrosine, were individually substituted with tyrosine in the [Phe<sup>13</sup>]  $\alpha$ -factor analog and found to maintain biological activity and binding affinity even after iodination. This information was combined with previous data involving characterization of a complete series of Bpa substitutions for residues in  $\alpha$ -factor (Hui-Fen Lu, unpublished results). The K<sub>d</sub> of each analog was determined and is shown in Figure 1. These data were used to direct where incorporation of Bpa would be best tolerated in the tyrosine-phenylalanine substitutions discussed above. Bpa replacements at positions 1 (Trp), 3 (Trp), 5 (Gln), 7 (Lys), 8 (Pro), 12 (Met), and 13 (Tyr) were well tolerated as the fold decrease in K<sub>d</sub> of these substitutions versus  $\alpha$ -factor ranged from 4 to 45-fold. Based on these data, incorporation of Bpa at residues 1, 3, 5, and 13 were chosen for initial studies using [Phe<sup>13</sup>]  $\alpha$ -factor as the starting template.

Growth arrest assays and *FUS1* gene induction assays were performed to determine the biological activity of the analogs (Table 2). Activity in the growth arrest assay was measured by spotting dilutions of peptide onto paper disks (concentration disks, 6mm diameter, Difco) and measuring the resulting halo after incubation. The results were plotted on a semilogarithmic graph. The plots were all linear and exhibited similar slopes (representative data shown in Figure 2).



**Figure 1. Binding affinity of Bpa substituted  $\alpha$ -factor analogs.**

A series of  $\alpha$ -factor analogs were synthesized which contained Bpa substituted at each position. The binding affinity of each analog was tested by assaying its ability to compete with [<sup>3</sup>H]  $\alpha$ -factor analogs for binding to Ste2p. The numbers above each bar represents the Kd (x 10<sup>-8</sup>M) of that analog.

Source: Hui-Fen Lu, unpublished data

**Figure 2. Growth arrest of *S. cerevisiae* DK102pNED cells by  $\alpha$ -factor and various analogs.**

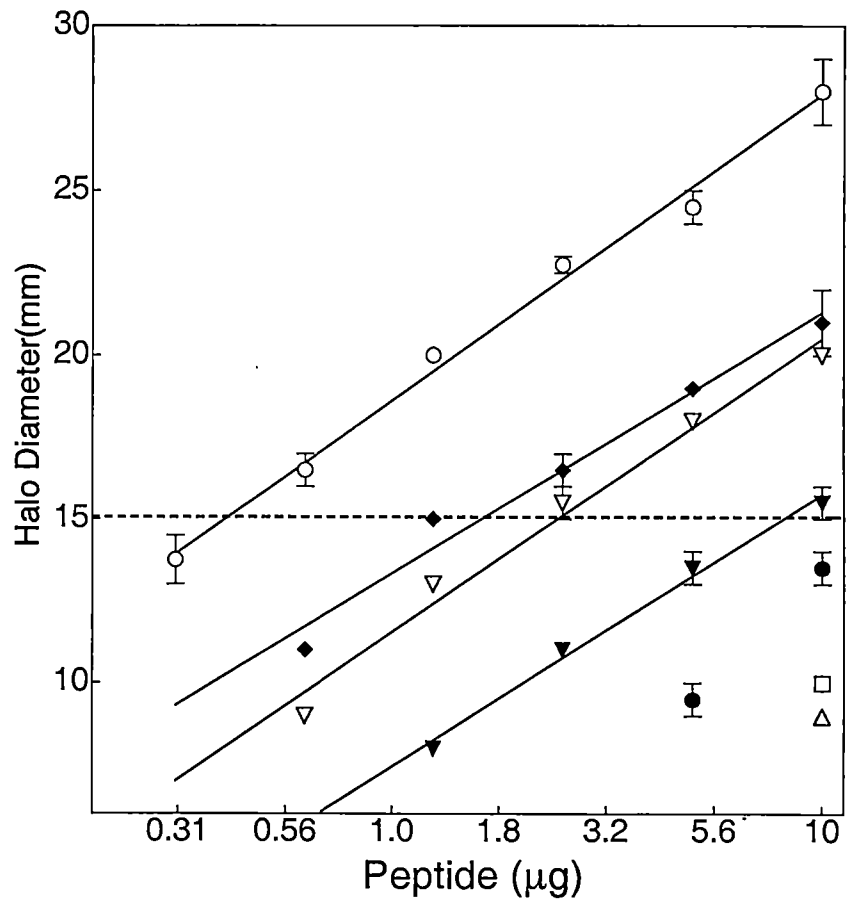
The diameter of the halos are plotted versus amount of peptide spotted as shown:

$\alpha$ -factor (O), [K<sup>7</sup>(Y)F<sup>13</sup>]  $\alpha$ -factor (▲), [Bpa<sup>3</sup>K<sup>7</sup>(Y)F<sup>13</sup>]  $\alpha$ -factor (▽),

[K<sup>7</sup>(AHA-Y)F<sup>13</sup>]  $\alpha$ -factor (◆), [Bpa<sup>3</sup>K<sup>7</sup>(AHA-Y)F<sup>13</sup>]  $\alpha$ -factor (●), [Y<sup>1</sup>Bpa<sup>5</sup>R<sup>7</sup>F<sup>13</sup>]

$\alpha$ -factor (□) and [(I<sub>2</sub>)Y<sup>1</sup>Bpa<sup>5</sup>R<sup>7</sup>F<sup>13</sup>]  $\alpha$ -factor (△).





**Table 2. Biological activity of  $\alpha$ -factor analogs**

Peptide	Growth Arrest <sup>a</sup> ( $\mu$ g peptide)	<i>FUSI</i> -lacZ <sup>b</sup> Induction Potency [nM]	Binding Affinity <sup>c</sup> K <sub>i</sub> [nM]
$\alpha$ -factor	0.41	3.1	9
Bpa <sup>1</sup> Y <sup>3</sup> R <sup>7</sup> F <sup>13</sup>	0.97	4.4	127
Y <sup>1</sup> Bpa <sup>3</sup> R <sup>7</sup> F <sup>13</sup>	Inactive	149	157
Y <sup>1</sup> Bpa <sup>5</sup> R <sup>7</sup> F <sup>13</sup>	>10	184	150
Y <sup>1</sup> R <sup>7</sup> Bpa <sup>13</sup>	Inactive	Inactive	132
K <sup>7</sup> (Y)F <sup>13</sup>	2.4	14	5
K <sup>7</sup> (AHA-Y)F <sup>13</sup>	1.6	15	57
Bpa <sup>3</sup> K <sup>7</sup> (Y)F <sup>13</sup>	8.1	37	23
Bpa <sup>3</sup> K <sup>7</sup> (AHA-Y)F <sup>13</sup>	Inactive	171	1900
Bpa <sup>1</sup> (I <sub>2</sub> )Y <sup>3</sup> R <sup>7</sup> F <sup>13</sup>	1.5	14	199
(I <sub>2</sub> ) Y <sup>1</sup> Bpa <sup>3</sup> R <sup>7</sup> F <sup>13</sup>	7.3 <sup>d</sup>	19	216
(I <sub>2</sub> ) Y <sup>1</sup> Bpa <sup>5</sup> R <sup>7</sup> F <sup>13</sup>	>10	26	22
(I <sub>2</sub> ) Y <sup>1</sup> R <sup>7</sup> Bpa <sup>13</sup>	Inactive	33	315
DesW <sup>1</sup> desH <sup>2</sup>	Inactive	Inactive	6

<sup>a</sup> Values represent  $\mu$ g of peptide necessary to produce a halo with a diameter of 15 mm.

<sup>b</sup> Values represent nM concentration of ligand to give 50% maximal activity in a *FUSI*-lacZ gene induction assay.

<sup>c</sup> Binding affinities were determined by calculation of K<sub>i</sub> in competition binding assays using <sup>125</sup>I-Y<sup>1</sup>R<sup>7</sup>F<sup>13</sup>  $\alpha$ -factor.

<sup>d</sup> The zone of growth inhibition was partially filled in giving the halo a fuzzy appearance.

Peptide analogs used in this assay were stable under the conditions tested as strains used in this analysis lacked the Bar1p protease which cleaves  $\alpha$ -factor.

Substitution of Trp<sup>1</sup> and Trp<sup>3</sup> with Bpa and Tyr or di-iodo-Tyr, respectively, resulted in biologically active analogs with relatively high binding affinity. For instance, the peptide analog [Bpa<sup>1</sup>Tyr<sup>3</sup>Arg<sup>7</sup>Phe<sup>13</sup>]  $\alpha$ -factor showed only a 2.3-fold decrease in its ability to cause growth arrest and 1.3-fold decrease in ability to induce the reporter gene *FUS1-lacZ*. The di-iodinated [Bpa<sup>1</sup>Tyr<sup>3</sup>Arg<sup>7</sup>Phe<sup>13</sup>]  $\alpha$ -factor showed a 3.7 and 4.5-fold decrease in the growth arrest and gene induction assays, respectively. Interestingly, reciprocal substitution in which Tyr or di-iodo-Tyr is placed at position one and Bpa at position 3 resulted in a greater decrease in activity. [Tyr<sup>1</sup>Bpa<sup>3</sup>Arg<sup>7</sup>Phe<sup>13</sup>]  $\alpha$ -factor was not active at the highest amount tested in the growth arrest assay and showed a 48-fold decrease in *FUS1-lacZ* induction. The di-iodination of [Tyr<sup>1</sup>Bpa<sup>3</sup>Arg<sup>7</sup>Phe<sup>13</sup>]  $\alpha$ -factor restored some of the biological activity with only a 17-fold and 6-fold reduction versus native  $\alpha$ -factor in the halo assay and gene induction assay, respectively. Interestingly, the halo generated in the growth arrest assay by di-iodo-[Tyr<sup>1</sup>Bpa<sup>3</sup>Arg<sup>7</sup>Phe<sup>13</sup>]  $\alpha$ -factor was fuzzy (growth was observed within the halo but growth was markedly reduced compared to the growth in unaffected areas of the plate) as opposed to the normally clear halo seen with other  $\alpha$ -factor agonists indicating that di-iodo-[Tyr<sup>1</sup>Bpa<sup>3</sup>Arg<sup>7</sup>Phe<sup>13</sup>]  $\alpha$ -factor may be a partial agonist. The [Tyr<sup>1</sup>Bpa<sup>5</sup>Arg<sup>7</sup>Phe<sup>13</sup>]  $\alpha$ -factor analog exhibited activity at the highest amounts tested in the halo assay but even the

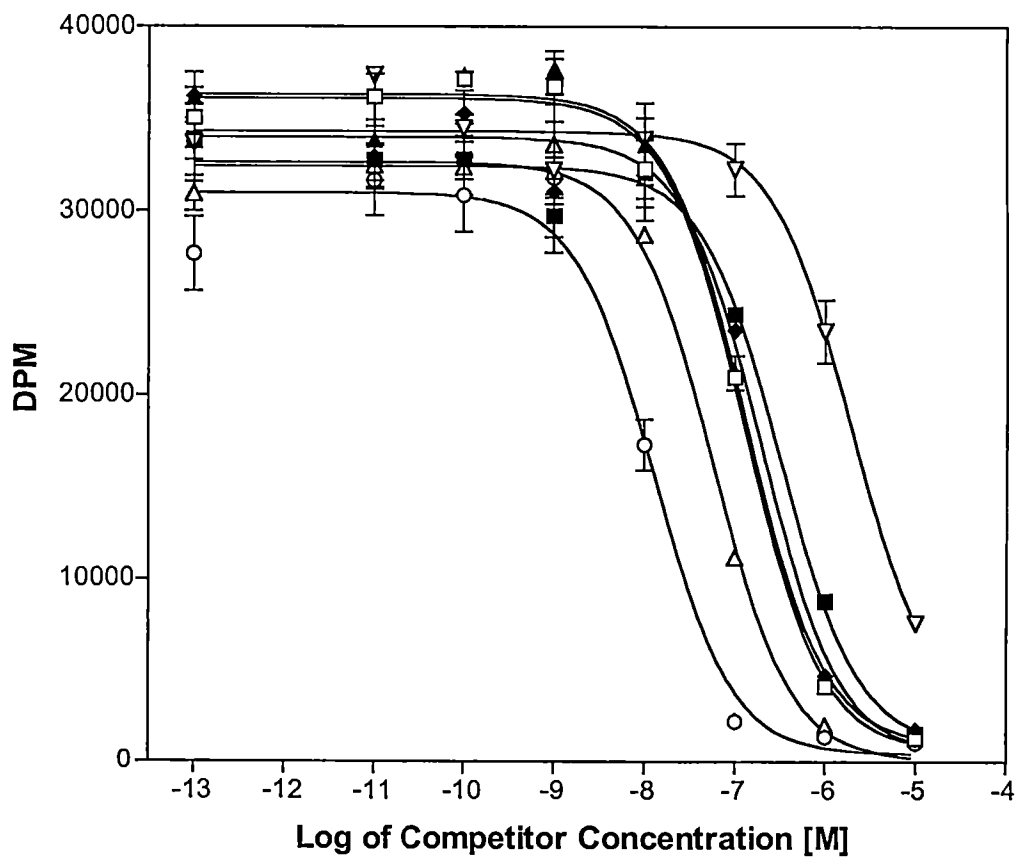
highest amount spotted was insufficient to yield a 15 mm halo. *FUS1-lacZ* induction was also quite reduced for [Tyr<sup>1</sup>Bpa<sup>5</sup>Arg<sup>7</sup>Phe<sup>13</sup>]  $\alpha$ -factor with an EC<sub>50</sub> of 184 nM vs. 3.1 for native  $\alpha$ -factor. The di-iodinated form gave similar results to the non-iodinated analog for the halo assay but as indicated by its EC<sub>50</sub> (26 nM vs. 184 nM of non-iodinated species) iodination restored some of the gene induction activity. A similar pattern is seen with substitution of the thirteenth position with Bpa. [Tyr<sup>1</sup>Arg<sup>7</sup>Bpa<sup>13</sup>]  $\alpha$ -factor and the di-iodinated form are inactive in the halo assay at the highest amounts tested. However, while [Tyr<sup>1</sup>Arg<sup>7</sup>Bpa<sup>13</sup>]  $\alpha$ -factor is inactive in the gene induction assay, a gain of activity is seen when the peptide is iodinated (EC<sub>50</sub> 33 nM). With the exception of [Bpa<sup>3</sup>Lys<sup>7</sup>(AHA-Y)Phe<sup>13</sup>]  $\alpha$ -factor, the tethered ligands which had either a Tyr or a AHA-Tyr group attached to the epsilon amine of Lys at position seven showed between a 4 and 20 fold decrease of activity in growth arrest assay and only a 5 to 12 fold decrease in the gene induction assay over native  $\alpha$ -factor. [Bpa<sup>3</sup>Lys<sup>7</sup>(AHA-Y)Phe<sup>13</sup>]  $\alpha$ -factor was inactive in the growth arrest assay and showed a 55-fold decrease in activity in gene induction assay compared to native  $\alpha$ -factor. While in some cases iodination enhanced biological activity and/or binding affinity, overall, there was no recognizable pattern that predicted the effect iodination would have on any given peptide.

*Binding affinities of  $\alpha$ -factor analogs.* Binding affinities of the peptides were determined by competition and saturation binding assays as described previously [25] and are given in Table 2 and representative graphs shown in Figure 3. In general, substitution of Bpa at positions 1, 3, 5 and 13 resulted in only 15- to 17-fold reduction in binding affinity versus native  $\alpha$ -factor. With the exception of (I<sub>2</sub>)-[Tyr<sup>1</sup>Bpa<sup>5</sup>Arg<sup>7</sup>Phe<sup>13</sup>]  $\alpha$ -factor which showed increased binding, di-iodination of the Bpa analogs resulted in a slight reduction (1.5- to 2.4-fold) in binding compared to the non-iodinated peptides. An interesting observation was made with the tethered ligands. The [Lys<sup>7</sup>(Y)Phe<sup>13</sup>] and [Lys<sup>7</sup>(AHA-Y)Phe<sup>13</sup>] peptides showed only a marginal decrease in binding affinity with respect to  $\alpha$ -factor. This is also true for [Bpa<sup>3</sup>Lys<sup>7</sup>(Y)Phe<sup>13</sup>]. However, [Bpa<sup>3</sup>Lys<sup>7</sup>(AHA-Y)Phe<sup>13</sup>]  $\alpha$ -factor showed a 33-fold decrease in binding compared to [Lys<sup>7</sup>(AHA-Y)Phe<sup>13</sup>]. This is a substantial drop in binding affinity when considering substitution of Bpa in position 3 of the Lys<sup>7</sup>(Y) analogs only resulted in a 4.6-fold difference in binding affinity (compare [Lys<sup>7</sup>(Y)Phe<sup>13</sup>] and [Bpa<sup>3</sup>Lys<sup>7</sup>(Y)Phe<sup>13</sup>]). This suggests that extension of the side chain of Lys<sup>7</sup> using the AHA group may result in some steric interaction with the Bpa<sup>3</sup> and the Lys<sup>7</sup>(AHA-Y) group that is not seen with [Lys<sup>7</sup>(Y)] or [Lys<sup>7</sup>(AHA-Y)Phe<sup>13</sup>].

*Iodination and purification of  $\alpha$ -factor analogs.* Several of the Bpa-containing analogs were chosen to mono-iodinate based on the criteria that they have relatively good biological activity and binding affinities in the sub-

**Figure 3. Competition binding assay of various  $\alpha$ -factor analogs vs.  $^{125}\text{I}$ -  
[Tyr<sup>1</sup>Arg<sup>7</sup>Phe<sup>13</sup>] $\alpha$ -factor using DK102pNED cells.**

The plots represent DPM in relationship to concentration of cold competitors which were:  
 $\alpha$ -factor (○), [Y<sup>1</sup>R<sup>7</sup>Bpa<sup>13</sup>]  $\alpha$ -factor (▲), [Bpa<sup>3</sup>K<sup>7</sup>(AHA-Y)F<sup>13</sup>]  $\alpha$ -factor (▽),  
[(I<sub>2</sub>)Bpa<sup>1</sup>Y<sup>3</sup>R<sup>7</sup>F<sup>13</sup>]  $\alpha$ -factor (◆), [(I<sub>2</sub>)Y<sup>1</sup>R<sup>7</sup>Bpa<sup>13</sup>]  $\alpha$ -factor (■) and  
[K<sup>7</sup>(AHA-Y)F<sup>13</sup>]  $\alpha$ -factor (△).



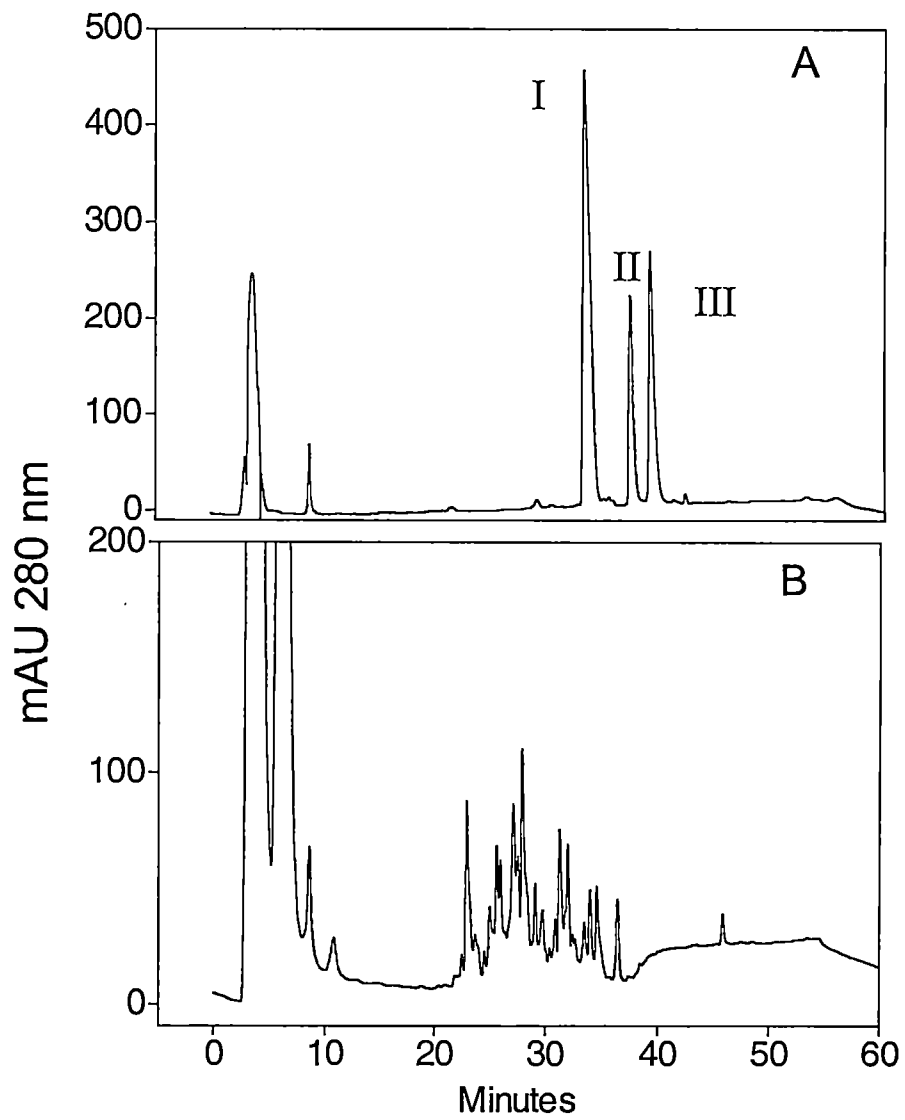
micromolar range. As we recently reported, some  $\alpha$ -factor analogs are resistant to chemical iodination [25]. The peptides [Bpa<sup>1</sup>Tyr<sup>3</sup>Arg<sup>7</sup>Phe<sup>13</sup>], [Tyr<sup>1</sup>Bpa<sup>5</sup>Arg<sup>7</sup>Phe<sup>13</sup>], and [Tyr<sup>1</sup>Arg<sup>7</sup>Bpa<sup>13</sup>]  $\alpha$ -factor were successfully iodinated but mono-iodinated [Tyr<sup>1</sup>Bpa<sup>3</sup>Arg<sup>7</sup>Phe<sup>13</sup>] was unable to be produced (representative chromatograms presented in Figure 4). The tethered analogs [Lys<sup>7</sup>(Y)Phe<sup>13</sup>], [Lys<sup>7</sup>(AHA-Y)Phe<sup>13</sup>], [Bpa<sup>3</sup>Lys<sup>7</sup>(Y)Phe<sup>13</sup>], and [Bpa<sup>3</sup>Lys<sup>7</sup>(AHA-Y)Phe<sup>13</sup>] were constructed to create distance between the iodination site of the Tyr residue and the backbone of the peptide in attempts to eliminate the problems with chemical iodination. Surprisingly, remote placement of the Tyr residue did not alleviate the iodination problem yielding similar results to that of the [Tyr<sup>1</sup>Bpa<sup>3</sup>Arg<sup>7</sup>Phe<sup>13</sup>] peptide. The mass of the mono-iodinated peptides was verified by electrospray mass spectrometry (data not shown).

*Displacement of <sup>125</sup>I-[Bpa<sup>1</sup>Tyr<sup>3</sup>Arg<sup>7</sup>Phe<sup>13</sup>]  $\alpha$ -factor by  $\alpha$ -factor in competition binding assays.* <sup>125</sup>I-[Bpa<sup>1</sup>Tyr<sup>3</sup>Arg<sup>7</sup>Phe<sup>13</sup>]  $\alpha$ -factor was shown to be displaced by non-radiolabeled  $\alpha$ -factor in a competition binding assay. The experiment was performed in triplicate and the results are plotted in Figure 5. The amount of bound peptide of processed samples is expressed in DPM and reported in relation to the amount of cold competitor added. Greater than 90% competition was observed and the shape of the curve is consistent with competitive binding inhibition indicating the radioligand is specific for Ste2p. The success in iodination of [Bpa<sup>1</sup>Tyr<sup>3</sup>Arg<sup>7</sup>Phe<sup>13</sup>]  $\alpha$ -factor and its relatively good biological



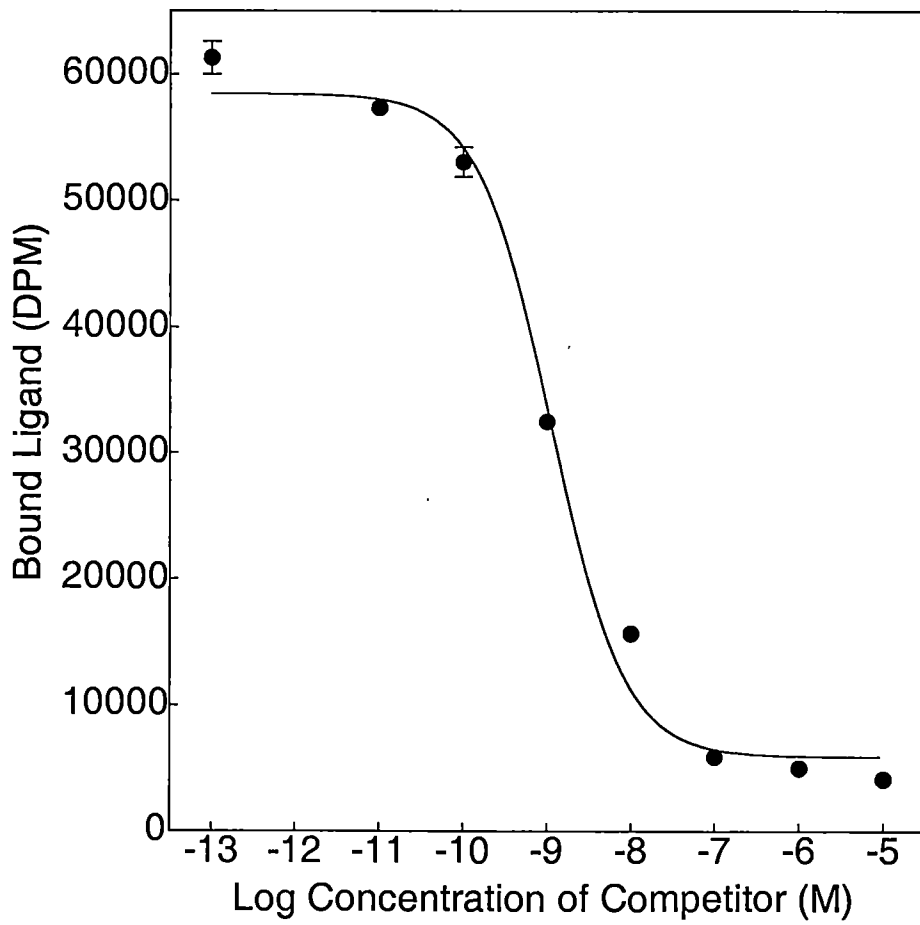
**Figure 4. HPLC analysis of products from iodination of tyrosine substituted  $\alpha$ -factor analogs.**

$\alpha$ -factor analogs were chemically iodinated using Iodogen<sup>TM</sup> reagent and products separated by HPLC. Figures A and B represent typical chromatograms: (A) iodination of [Bpa<sup>1</sup>Tyr<sup>3</sup>Arg<sup>7</sup>Phe<sup>13</sup>] $\alpha$ -factor; I – non iodinated peptide, II- mono-iodinated peptide, III di-iodinate peptide. (B) iodination of [Tyr<sup>1</sup>Bpa<sup>3</sup>Arg<sup>7</sup>Phe<sup>13</sup>] $\alpha$ -factor.



**Figure 5. Competition binding analysis of [Bpa<sup>1</sup>Tyr<sup>3</sup>(<sup>125</sup>I)Arg<sup>7</sup>Phe<sup>13</sup>]  $\alpha$ -factor and non-radiolabeled  $\alpha$ -factor.**

Plot represents amount of bound radiolabeled probe (DPM) in relationship to concentration of non-radiolabeled  $\alpha$ -factor. Data were analyzed with the graph program Prism using single site competition binding equation.



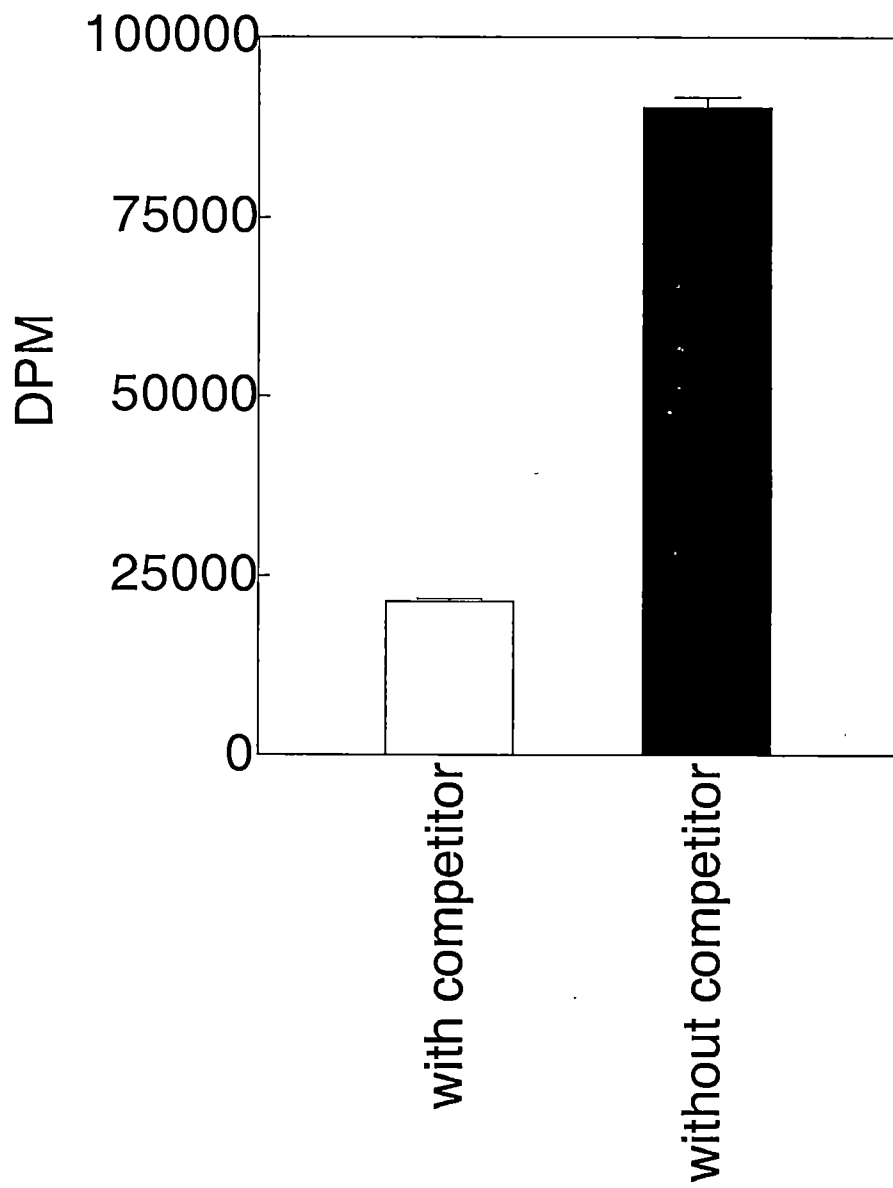
activity and binding affinity made it the top candidate for use in the crosslinking studies.

*Crosslinking of  $^{125}\text{I}$ -[Bpa<sup>1</sup>Tyr<sup>3</sup>Arg<sup>7</sup>Phe<sup>13</sup>]  $\alpha$ -factor to Ste2p.* DK102pNED membranes were photocrosslinked with  $^{125}\text{I}$ -[Bpa<sup>1</sup>Tyr<sup>3</sup>Arg<sup>7</sup>Phe<sup>13</sup>]  $\alpha$ -factor. A small portion (20  $\mu\text{l}$ ) of the reaction mixture was removed following crosslinking and tested for total binding by processing over Multiscreen™ durapore membranes [25]. The radioactive counts of the samples with and without competitor reveal a 76% reduction in crosslinked product in the presence of 100-fold excess competitor (Figure 6). The remainder of the reaction mixture was analyzed by SDS-PAGE and a crosslinked product which migrated to the expected size of Ste2p + probe (54 kD) was detected by autoradiography (Figure 7). No crosslinking products were observed with samples that were not UV irradiated (Figure 7 – lanes 3-4). Co-incubation of DK102pNED membranes [STE2<sup>+</sup>] with radiolabeled probe and cold  $\alpha$ -factor resulted in a decrease in crosslinked product showing that the crosslinking to Ste2p was specific. (Figure 7 - lane 1 vs. lane 2). Western analysis using anti-Flag antibodies to detect Ste2p showed that all lanes had equivalent amounts of the receptor (Figure 8).

*Fragmentation analysis of crosslinked Ste2p.* Based on the crosslinking results showing specific crosslinking of the radiolabeled probe  $^{125}\text{I}$ -[Bpa<sup>1</sup>Tyr<sup>3</sup>Arg<sup>7</sup>Phe<sup>13</sup>]  $\alpha$ -factor to the Ste2p receptor, digestion of the receptor was initiated to identify the crosslinked fragment(s) of the receptor. V8 protease

**Figure 6. Total radioactive counts of  $^{125}\text{I}$ -[Bpa<sup>1</sup>Tyr<sup>3</sup>Arg<sup>7</sup>Phe<sup>13</sup>]  $\alpha$ -factor bound to membranes following crosslinking in the presence and absence of non-radiolabeled  $\alpha$ -factor.**

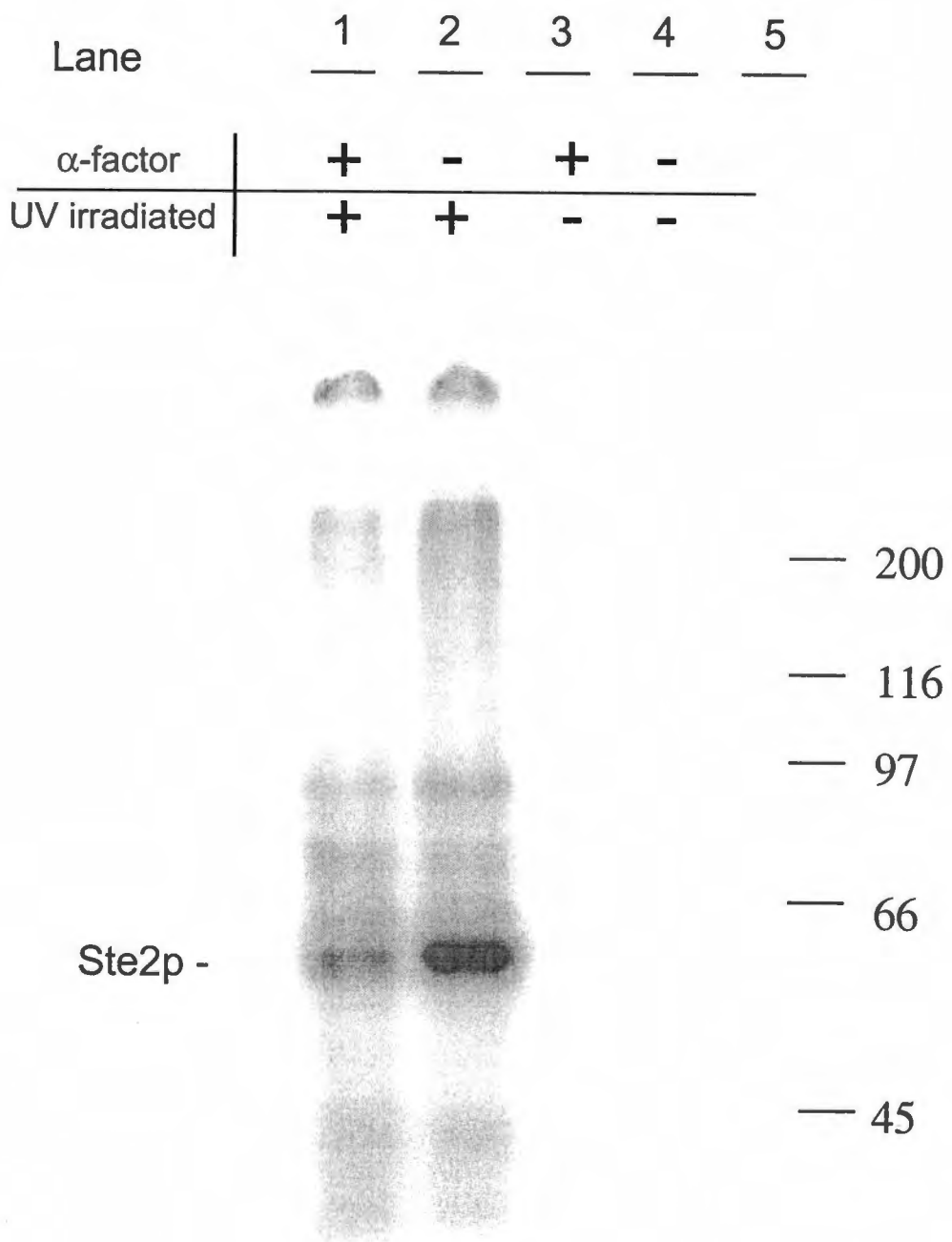
Bars represent amount of ligand associated with DK102pNED1 membranes expressed in DPM. One sample was crosslinked in the presence of non-radiolabeled  $\alpha$ -factor (open bar) while the other sample contained only labeled ligand (solid bar).



**Figure 7. Autoradiogram of SDS-PAGE analysis of UV irradiated DK102pNED membranes in the presence of  $^{125}\text{I}$  [Bpa<sup>1</sup>Tyr<sup>3</sup>Arg<sup>7</sup>Phe<sup>13</sup>]  $\alpha$ -factor.**

All membranes were incubated with  $^{125}\text{I}$  [Bpa<sup>1</sup>Tyr<sup>3</sup>Arg<sup>7</sup>Phe<sup>13</sup>]  $\alpha$ -factor. Some samples were also UV irradiated or contained  $\alpha$ -factor. All samples were analyzed by SDS-PAGE. The gel was dried and exposed to phosphorimager screen for 36 hours. The samples are: UV irradiated plus excess nonradiolabeled  $\alpha$ -factor (lane 1), UV irradiated (lane2), excess nonradiolabeled  $\alpha$ -factor without UV irradiation (lane 3), without excess non-radiolabeled  $\alpha$ -factor and without UV irradiation (lane 4) and molecular weight markers (lane 5).

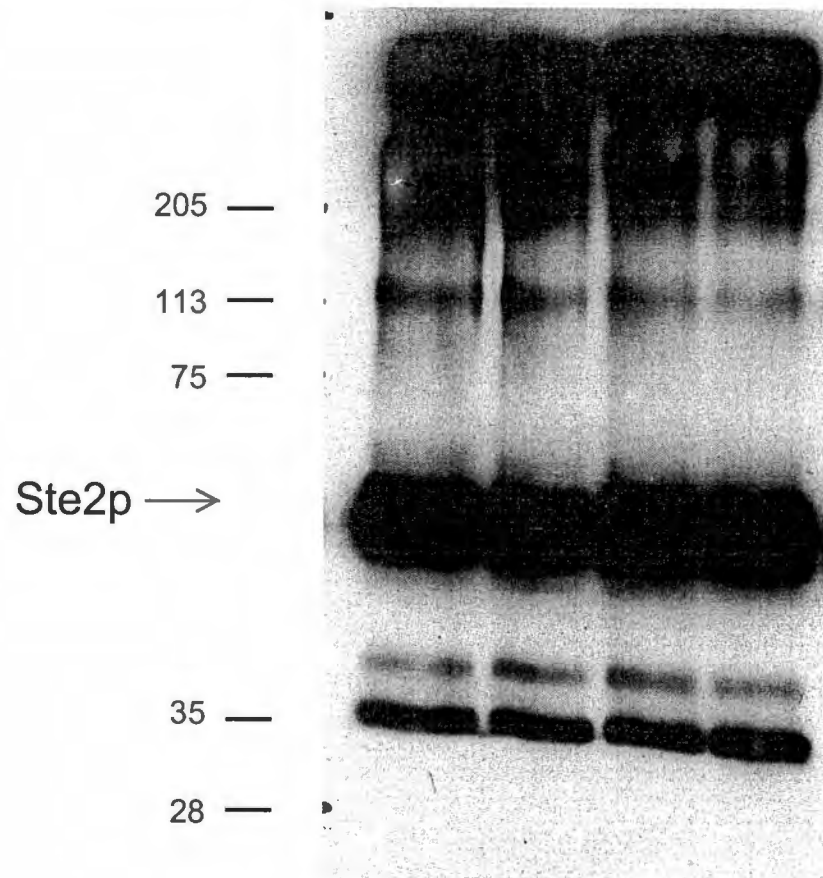




**Figure 8. Western blot analysis of crosslinked BJ2168pNED1 membranes.**

10  $\mu$ l portions of the samples used in crosslinking experiment were solubilized in sample buffer and separated by SDS-PAGE (10% gel, 35 mAmps). Protein was transferred to Immobilon P membrane from Millipore using a Hoefer mini gel tank blotter. Blots were probed with anti-FLAG epitope antibody. The anti-FLAG antibodies were detected by probing with secondary antibody (horseradish peroxidase conjugated goat anti-rabbit). Secondary antibody was detected by treating the blot with ECl chemiluminescent detection reagent from ICN and exposing the blot to X-ray film. Lane designations are as shown in figure. Intact Ste2p is indicated by an arrow.

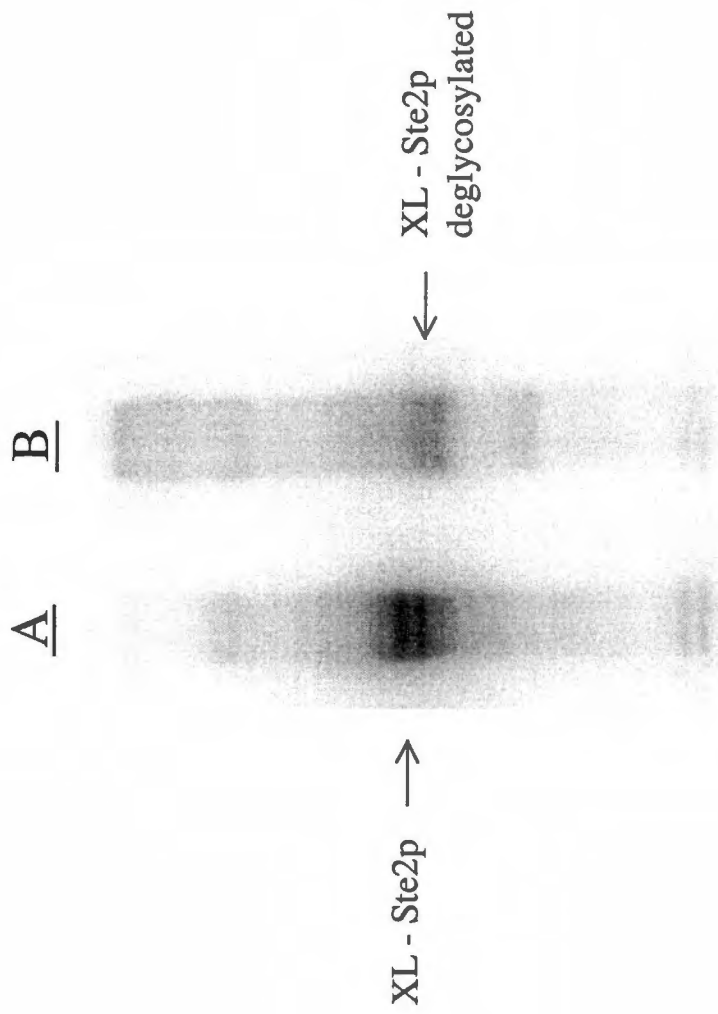
Lane	1	2	3	4
$\alpha$ -factor	+	-	+	-
UV irradiated	+	+	-	-



and trypsin were used in early attempts to fragment the receptor. However, complete digestion of the receptor was not achieved even in the presence of amounts of SDS or acetonitrile that were not inhibitory to protease activity (data not shown). As alternative methods to fragmenting the crosslinked receptor, chemical cleavage with CNBr and BNPS-skatole was performed. These methods take place under acidic conditions presumably allowing for unfolding of the receptor making it more accessible to cleavage [15]. Chemical digestion of the receptor was carried out on native and deglycosylated Ste2p. N-linked glycosylation of Ste2p was removed by treatment with PNGaseF (Glyko). Deglycosylation of the receptor was verified by SDS-PAGE with the deglycosylated receptor migrating approximately 2 kD smaller than the native receptor (Figure 9). Similar results of deglycosylation of Ste2p were shown previously by others [27, 28]. The observed doublet is most likely due to the fact that strain BJ2168pNED1 expresses both a native chromosomal copy of *STE2* which codes for 50 kD protein when glycosylated and an epitope-tagged, episomally-expressed *STE2* which codes for a 52 kD when glycosylated. BNPS-skatole, which cleaves at tryptophan residues, theoretically fragments the receptor into four pieces (**A** - 7.5 kD [1-70], **B** - 25 kD [71-295], **C** - 14.6 kD [296-424] and **D** - 3.6 kD [425-457]) (Figure 10A). The fragments **C** and **D** corresponding to residues [296-424] and [425-457] can be eliminated as prospective crosslinking sites as they make up the intracellular C-terminal tail which is not accessible to  $\alpha$ -

**Figure 9. Autoradiograph of SDS-PAGE 10-20% tricine gel analysis of BJ2168pNED1 membranes photolabeled with [Bpa<sup>1</sup>(<sup>125</sup>I)Tyr<sup>3</sup>Arg<sup>7</sup>Phe<sup>13</sup>]  $\alpha$ -factor.**

(A) photocrosslinked membranes - untreated (B) photocrosslinked membranes treated with PNGaseF to remove N-linked oligosaccharides. Arrows denote crosslinked Ste2p receptor indicating the 2 kD decrease in size of product in membranes treated with PNGaseF.

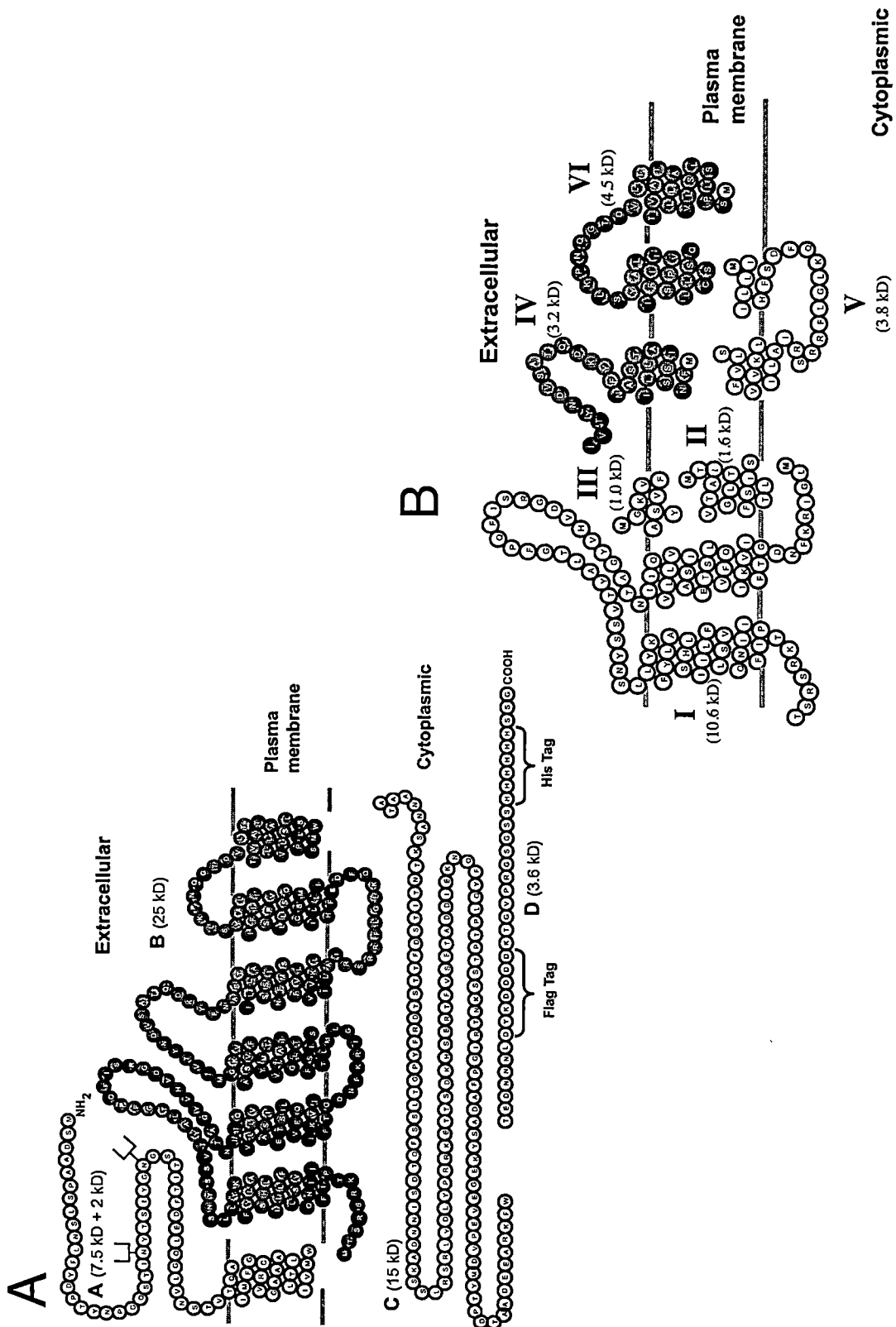


**Figure 10. Schematic of chemical cleavage of Ste2p.**

These figures represent the BNPS-Skatole and CNBr cleavage sites for the Ste2p receptor. Ste2p receptor is shown here using snake diagrams to represent the putative transmembrane domains. [Panel A] Cleavage of the receptor by BNPS-Skatole results in four fragments labeled A [1-70], B [71-295], C [296-424] and D [425-458] with their respective molecular weights given in parenthesis.

Fragment A contains the putative N-linked glycosylation sites as represented by the symbol  $\Psi$ . The oligosaccharides add 2 kD of mass to fragment A. [Panel B] Represents CNBr cleavage of fragment B from panel A and are designated: I [72-165], II [166-180], III [181-189], IV [190-218], V [219-250] and VI [251-294].

The carboxyl segment of Ste2p is not shown because it is known not to be involved in ligand binding. Shaded segments represent the fragment identified to be crosslinked to the photoprobe.



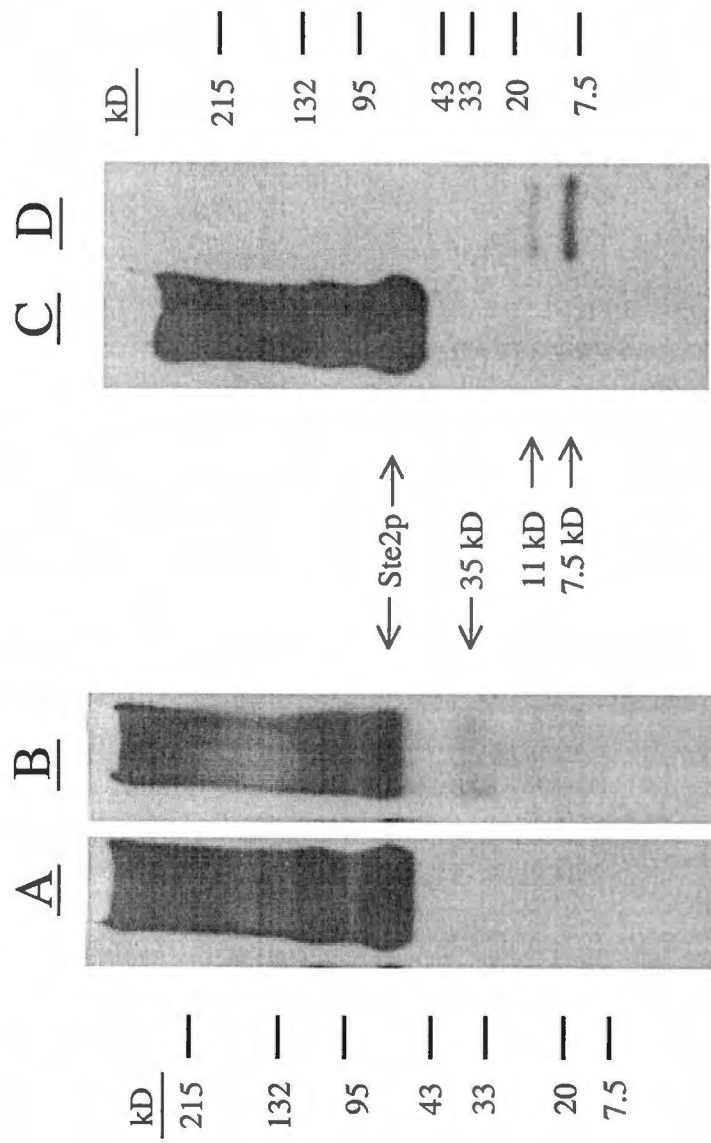


factor and whose removal has been shown to not affect  $\alpha$ -factor binding [27]. The 7.5 kD (A) and 25 kD (B) fragments remain as possible crosslinking sites. Western analysis of native receptor with polyclonal antibodies against residues 1-60 reveals that after two minutes in BNPS-skatole a broad band between 33 kD and 35 kD begins to appear (Figure 11, lanes A and B). The size of this band corresponds to glycosylated and deglycosylated forms of a fragment consisting of residues 1-295 (fragments A+B). After 24 hours, two fragments of 7.5 kD and 11 kD are detectable (Figure 11, lanes C and D). These bands likely correspond to glycosylated and deglycosylated forms of fragment A. These data indicate the receptor is cut to completion after treatment with BNPS-skatole under the conditions used.

Crosslinked receptor digested for 24 hours with BNPS-skatole was dissolved in tricine sample buffer and run on 16% and 10-20% gradient tricine gels. Phosphorimaging of the gels revealed two fragments of 27 kD and 6 kD (Figure 12, panel I). The 27 kD fragment corresponds to the 25 kD fragment (B) plus 2 kD for the radiolabeled probe. The 6 kD fragment is anomalous as it does not correspond to the 7.5 kD fragment (A) which would actually migrate to 9.5 kD with the attached probe and at 11.5 kD in the samples that had not been deglycosylated with PNGaseF. Additionally, deglycosylation of the receptor does not result in a shift of the 6 kD fragment (Figure 12-panel II lanes B and C). Based on this evidence, we believe that the 6 kD fragment is the result of aberrant

**Figure 11. Western blot analysis of BNPS-skatole digested BJ2168pNED1 membranes.**

BJ2168pNED1 membranes were digested with BNPS-skatole. At various timepoints, portions of the reaction mix were removed and dried down in a speedvac. Samples were then dissolved in tricine sample buffer (Novex) and run on gradient tricine gels (10-20%, 120V). Protein was transferred to Immobilon P membranes (Millipore) and probed with polyclonal antibodies that are specific for the first 60 amino acids of Ste2p. Blot is then probed with goat anti-rabbit secondary antibody conjugated to horseradish peroxidase. Antibody complex is detected by applying the chemiluminiscent ECL reagent from ICN to the blot and exposing blot to X-ray film. Lane A and C designate undigested membrane protein. Intact Ste2p is indicated in the figure. Lanes B and D represent 2 minute and 24 hour digestion with BNPS-skatole. The sizes of the detected fragments are designated by arrows.



**Figure 12. Autoradiograph of BJ2169pNED1 membranes photocrosslinked with [Bpa<sup>1</sup>(<sup>125</sup>I)Tyr<sup>3</sup>Arg<sup>7</sup>Phe<sup>13</sup>]  $\alpha$ -factor and treated with BNPS-Skatole.**

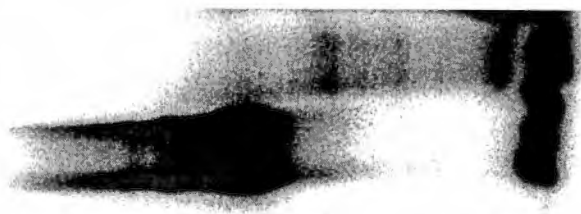
**I.** (A) untreated photocrosslinked membranes. (B) photocrosslinked membranes treated with BNPS-Skatole for 24 hours. Arrows designate intact Ste2p (54 kD) and 28 kD and 6.8 kD BNPS cleavage fragments of Ste2p. Molecular weights of markers are given.

**II.** (A) membranes treated with PNGaseF. (B) membranes cleaved with BNPS-Skatole and (C) membranes treated with BNPS-Skatole and PNGaseF. Arrows denote deglycosylated Ste2p (52 kD) and two fragments 27 kD and 6.5 kD.

I

A B

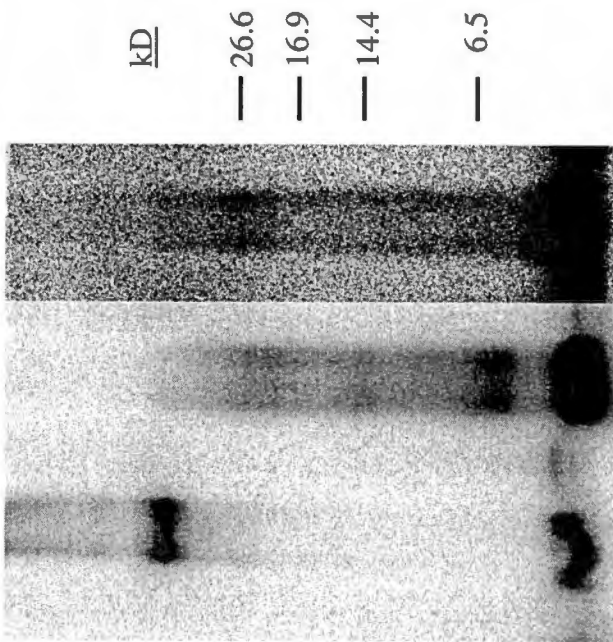
kD  
— 200  
— 116  
— 97  
— 66  
— 45  
— 31  
— 21  
— 14  
— 7



54 kD —  
28 kD —  
6 kD —

II

A B C



kD  
— 26.6  
— 16.9  
— 14.4  
— 6.5

52 kD —  
27 kD —  
6 kD —

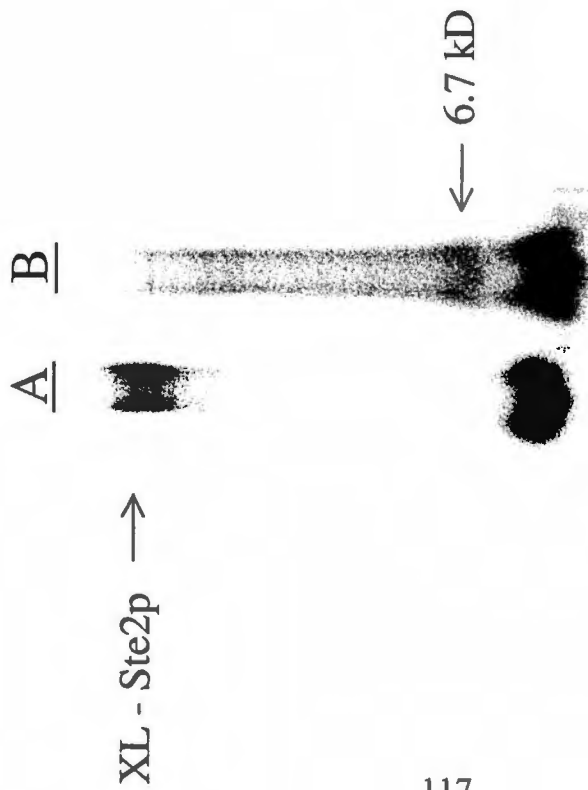
cleavage of the receptor by BNPS-skatole. It has been reported that slight impurities in BNPS-skatole can result in cleavage at methionines and cysteines [29]. These impurities can arise from incomplete removal of *N*-bromosuccinimide (NBS) substrate during the synthesis of BNPS-skatole. However, NBS contamination is usually only a small fraction of the total reagent. As a result, Trp residues are cleaved fast by BNPS-skatole while the Met and Cys residues are cleaved at a slower rate. Based on this information, it is believed that the 6kD fragment is generated by cleavage at sites other than Trp in the 27 kD fragment and would explain why the fragment is not detected in Western analysis by anti-N terminal Ste2p antibodies following BNPS cleavage.

Complete cleavage of the crosslinked receptor with CNBr yielded one labeled fragment of ~6 kD (Figure 13 panel I). There are three fragments that when crosslinked to the probe would be about 6 kD in size. These are fragments [190-218], [219-250] and [251-294]. Of the three fragments, only [190-218] and [251-294] are likely candidates for crosslinking sites as fragment [219-250] is buried deep in the membrane. This conclusion is further supported by incomplete CNBr digestion of crosslinked Ste2p. Incomplete CNBr digestion resulted in several fragments 31 kD, 22 kD, 9 kD and 6 kD in size (Figure 13 panel II). It is likely that the 22 kD, 9 kD and 6 kD fragments resulted from sequential cleavage at methionines in the 31 kD fragment. Based on CNBr fragment patterns of the receptor (Figure 10B), the size of the fragments from the incomplete digestion

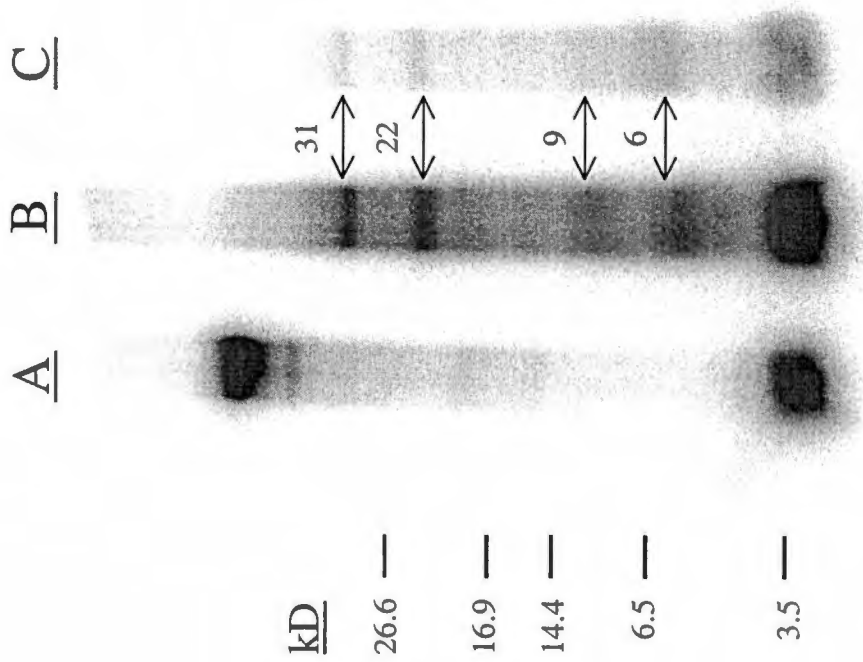
**Figure 13. Autoradiographs of BJ2169pNED1 membranes photocrosslinked with [Bpa<sup>1</sup>(<sup>125</sup>I)Tyr<sup>3</sup>Arg<sup>7</sup>Phe<sup>13</sup>]  $\alpha$ -factor and treated with cyanogen bromide.**

**I.** (A) untreated photocrosslinked membranes. (B) Complete digestion of photocrosslinked membranes with CNBr. Arrows indicate photolabeled Ste2p and 6.7 kD cleavage fragment of Ste2p. **II.** (A) untreated photocrosslinked membranes. (B) Incomplete digestion of photocrosslinked membranes. (C) PNGaseF treatment of membranes from lane B.

I



II





indicate that the probe crosslinked to 31 kD fragment which corresponds to fragments I through VI (Figure 10B) and an additional fragment [295-409]. Cleavage at M294 would result in a labeled 22 kD fragment. A single cleavage of the 22 kD fragment at M218 or double cleavage at M181 and M250 would result in a 9 kD fragment corresponding to fragments (V + VI) and (IV + V), respectively. The six kD fragment could then result from cleavage of V and VI or IV and V. Therefore, the pattern indicates that the probe crosslinks to either fragment [190-218] or [251-294]. The fact that none of the fragments identified by incomplete digestion with CNBr were glycosylated (Figure 13) (PNGaseF treatment did not result in a shift in molecular weight) further supports the findings that the crosslinked receptor fragment is not located in the N-terminal portion of the receptor.

## CHAPTER IV

### DISCUSSION

Photoaffinity labeling with Bpa has been shown to be a useful tool in elucidating direct contacts between ligands and their cognate receptors [8, 10, 11, 14, 15]. The majority of the photoaffinity studies, which include work on the secretin, integrin and nociceptin receptors, have used receptor digestion analysis to elucidate small fragments of the receptor 5-20 residues in length crosslinked to the photoactivatable ligand probe. Fragmentation analysis can then be followed by mutagenesis studies to identify specific residues in the crosslinked receptor fragment involved in ligand-receptor interaction.

The present study details the synthesis and testing of  $\alpha$ -factor analogs containing Bpa for use as photoprobes to elucidate binding sites on the Ste2p receptor. Bpa was incorporated into  $\alpha$ -factor analogs previously tested for their ability to be used as probes for Ste2p [25]. From that study, it was concluded that substitution of Phe for Tyr at position 13 in  $\alpha$ -factor has minimal to no effect on binding affinity and biological activity. Additionally, it was determined that Trp at the first position of  $\alpha$ -factor can be replaced by Tyr to produce a biologically active ligand that can be radioiodinated and used in Ste2p receptor binding studies. The hydrophobicity and structure of Bpa make it a good choice for replacement of

hydrophobic aromatic amino acids. As a result, most of the analogs tested in this study contained Bpa substituted for Trp and Tyr residues.

One of the analogs tested, [Bpa<sup>1</sup>Tyr<sup>3</sup>Arg<sup>7</sup>Phe<sup>13</sup>]  $\alpha$ -factor, was radiolabeled with <sup>125</sup>I and maintained a submicromolar binding affinity in competition binding assays. This analog also exhibited relatively good agonistic activity in two standard pheromone response assays (growth arrest and *FUS1-lacZ*). Binding of <sup>125</sup>I-[Bpa<sup>1</sup>Tyr<sup>3</sup>Arg<sup>7</sup>Phe<sup>13</sup>]  $\alpha$ -factor was found to be specific for the Ste2p receptor based on the ability of native  $\alpha$ -factor to displace <sup>125</sup>I-[Bpa<sup>1</sup>Tyr<sup>3</sup>Arg<sup>7</sup>Phe<sup>13</sup>] in a competition binding assay. Furthermore, photolabeling of Ste2p with <sup>125</sup>I-[Bpa<sup>1</sup>Tyr<sup>3</sup>Arg<sup>7</sup>Phe<sup>13</sup>] was competable by addition of excess cold  $\alpha$ -factor. Based on the biological and binding data, it appears that <sup>125</sup>I-[Bpa<sup>1</sup>Tyr<sup>3</sup>Arg<sup>7</sup>Phe<sup>13</sup>]  $\alpha$ -factor binds to the same site on Ste2p as native  $\alpha$ -factor and adopts a similar binding conformation.

SDS-PAGE analysis of photolabeling experiments with <sup>125</sup>I-[Bpa<sup>1</sup>Tyr<sup>3</sup>Arg<sup>7</sup>Phe<sup>13</sup>]  $\alpha$ -factor resulted in detection of one major radiolabeled product which migrated to the expected size of Ste2p covalently attached to the probe (54 kD). Deglycosylation of the crosslinked reaction resulted in a 2kD decrease in size of the product. This is comparable to the 2 kD shift of Ste2p observed in Western blots before and after deglycosylation with PNGaseF [27]. Additionally, the amount of the 54 kD product was reduced by 74% in the presence of excess cold  $\alpha$ -factor indicating that the majority of crosslinking was

specific for Ste2p. Based on these findings, which show the iodinated probe has biological and binding characteristics similar to native  $\alpha$ -factor especially in regards to specificity for Ste2p, we are confident that  $^{125}\text{I}$ -[Bpa<sup>1</sup>Tyr<sup>3</sup>Arg<sup>7</sup>Phe<sup>13</sup>]  $\alpha$ -factor can be used to determine the binding site contacts between  $\alpha$ -factor and its receptor.

Receptor crosslinked with the radiolabeled probe was semi-purified by SDS-PAGE, eluted from the gel and treated with various cleavage agents to identify a fragment(s) which was covalently attached to the radioprobe. The proteases Glu-C (V8) and Trypsin were used in initial studies to cleave the receptor. However, the reaction conditions required for these proteases did not allow for all cleavage sites on Ste2p to be accessible and resulted in incomplete digestion as determined by Western analysis. The number and sizes of the fragments generated by these enzymes would make incomplete digestion results problematic to interpret (data not shown). Therefore, we chose to use the chemical cleavage agents BNPS-skatole and cyanogen bromide to perform chemical cleavage in concentrated acid allowing for complete digestion of receptor.

Cleavage at the Trp residues of Ste2p with BNPS-skatole cleaves the receptor into four fragments (**A** - 7.5 kD [1-70], **B** - 25 kD [71-295], **C** - 14.6 kD [296-424] and **D** - 3.6 kD [425-457]). Previous studies by others have shown that the intracellular C-terminal tail of Ste2p has no effect on binding of  $\alpha$ -factor and

can actually be removed without loss of  $\alpha$ -factor binding to Ste2p. Based on this information, two of these fragments **C** and **D** were eliminated as possible sites for crosslinking as they make up the intracellular C-terminal tail of the receptor and are not accessible to  $\alpha$ -factor. SDS-PAGE analysis with high percentage tricine gels resulted in identification of two major radiolabeled products of 27 kD and 6 kD in size. The 27 kD fragment corresponds to fragment **B** (25 kD) plus the probe (2kD). The 6 kD fragment is unexpected in that it does not correspond to a crosslinked form of fragment **A** which would have an expected size of 11 kD (7.5 kD + 2 kD for the probe + 2 kD for the polysaccharides = 11.5 kD). The unexpected 6 kD fragment most likely corresponds to cleavage of receptor fragment **B** at methionines and/or cysteines due to reagent contamination. It should be noted that complete cleavage by CNBr which cleaves at methionines also results in a 6 kD fragment. A time course cleavage of the receptor and Western blot analysis using polyclonal antibodies against the first 60 amino acids of Ste2p indicate complete cleavage of the receptor by BNPS-skatole. Furthermore, fragment **A** (glycosylated and deglycosylated) could be detected but no band was detected which corresponded to a 4 kD fragment (6 kD minus 2 kD probe). The 2 kD difference between the two Fragment **A** bands detected by Western analysis indicate that only the N-terminus (Fragment **A**) is glycosylated.

Complete cleavage of the receptor with cyanogen bromide resulted in the identification of a single labeled band ~6 kD in size. Based on the BNPS-skatole

results the band should be part of fragment **B**. CNBr cleavage of Fragment **B** yields six fragments (**I** – 10.6 kD [72-165], **II** – 1.6 kD [166-180], **III** – 1.0 kD [181-189], **IV** – 3.2 kD [190-218], **V** – 3.8 kD [219-250], **VI** – 4.5 kD [251-294]). Of these, fragments **IV**, **V**, and **VI** when crosslinked to the probe would give sizes similar to the identified radiolabeled fragment. Incomplete digestion of the crosslinked receptor with CNBr yields 4 fragments. Based upon the sizes of these incomplete digestion fragments an order of cleavage of fragment **B** can be discerned in which the fragments **I**, **VII** are cleaved in sequence. Then fragment **III** is removed which also eliminates fragment **II**. Of the three remaining fragments, **IV** and **VI** can be formed by only one cleavage event whereas fragment **V** requires two cleavages to occur simultaneously. Therefore, as there are no detectable intermediates the final cleavage either cuts between **IV** and **V** leaving fragment **VI** or between **V** and **VI** leaving fragment **IV**. This observation is strengthened in that fragment **V** is deep within the membrane [19] and is less likely to be accessible by  $\alpha$ -factor. Based on these results the radiolabeled probe crosslinks to fragments **IV** and/or **VI**. Efforts are continuing to discern between fragments **IV** and **VI** as the binding site of the probe.

This study represents the first direct evidence of contact between the  $\alpha$ -factor ligand and a domain of the Ste2p receptor. Additionally, this is the first study to use Bpa photocrosslinkable probes to study ligand-receptor interaction in Class IV GPCRs. Future studies should allow for identification of a residue or

residues that crosslink to the  $\alpha$ -factor probe used in this study. These results along with planned studies to use a series of  $\alpha$ -factor probes that will place crosslinkable moieties at various positions in the pheromone should allow for mapping of the ligand binding site of the Ste2p receptor. Results from such studies have the potential to provide key insight into peptide ligand mediated activation of GPCRs by identifying contact residues. Identification of the contact residues will allow us to begin assigning structure-function relationships between the pheromone and Ste2p and compare the results to information gained from other classes of GPCRs.

## REFERENCES

1. Fong, T.M., M.A. Cascieri, H. Yu, A. Bansal, C. Swain, and C.D. Strader, *Amino-aromatic interaction between histidine 197 of the neurokinin-1 receptor and CP 96345*. *Nature*, 1993. **362**(6418): p. 350-3.
2. Huang, R.R., H. Yu, C.D. Strader, and T.M. Fong, *Interaction of substance P with the second and seventh transmembrane domains of the neurokinin-1 receptor*. *Biochemistry*, 1994. **33**(10): p. 3007-13.
3. Huang, R.R., P.P. Vicario, C.D. Strader, and T.M. Fong, *Identification of residues involved in ligand binding to the neurokinin-2 receptor*. *Biochemistry*, 1995. **34**(31): p. 10048-55.
4. Strader, C.D., T.M. Fong, M.P. Graziano, and M.R. Tota, *The family of G-protein-coupled receptors*. *FASEB J*, 1995. **9**(9): p. 745-54.
5. Dorman, G. and G.D. Prestwich, *Using photolabile ligands in drug discovery and development*. *Trends Biotechnol*, 2000. **18**(2): p. 64-77.



6. Dorman, G. and G.D. Prestwich, *Benzophenone photophores in biochemistry*. *Biochemistry*, 1994. **33**(19): p. 5661-73.
7. Prestwich, G.D., G. Dorman, J.T. Elliott, D.M. Marecak, and A. Chaudhary, *Benzophenone photoprobes for phosphoinositides, peptides and drugs*. *Photochem Photobiol*, 1997. **65**(2): p. 222-34.
8. Dong, M., Y.W. Asmann, M. Zang, D.I. Pinon, and L.J. Miller, *Identification of two pairs of spatially approximated residues within the carboxyl-terminus of secretin and its receptor*. *J Biol Chem*, 2000.
9. Dong, M., Y. Wang, E.M. Hadac, D.I. Pinon, E. Holicky, and L.J. Miller, *Identification of an interaction between residue 6 of the natural peptide ligand and a distinct residue within the amino-terminal tail of the secretin receptor*. *J Biol Chem*, 1999. **274**(27): p. 19161-7.
10. Dong, M., Y. Wang, D.I. Pinon, E.M. Hadac, and L.J. Miller, *Demonstration of a direct interaction between residue 22 in the carboxyl-terminal half of secretin and the amino-terminal tail of the secretin receptor using photoaffinity labeling*. *J Biol Chem*, 1999. **274**(2): p. 903-9.

11. Behar, V., A. Bisello, M. Rosenblatt, and M. Chorev, *Direct identification of two contact sites for parathyroid hormone (PTH) in the novel PTH-2 receptor using photoaffinity cross-linking*. *Endocrinology*, 1999. **140**(9): p. 4251-61.
12. Behar, V., A. Bisello, G. Bitan, M. Rosenblatt, and M. Chorev, *Photoaffinity cross-linking identifies differences in the interactions of an agonist and an antagonist with the parathyroid hormone/parathyroid hormone-related protein receptor*. *J Biol Chem*, 2000. **275**(1): p. 9-17.
13. Hadac, E.M., D.I. Pinon, Z. Ji, E.L. Holicky, R.M. Henne, T.P. Lybrand, and L.J. Miller, *Direct identification of a second distinct site of contact between cholecystinin and its receptor*. *J Biol Chem*, 1998. **273**(21): p. 12988-93.
14. Bisello, A., A.E. Adams, D.F. Mierke, M. Pellegrini, M. Rosenblatt, L.J. Suva, and M. Chorev, *Parathyroid hormone-receptor interactions identified directly by photocross-linking and molecular modeling studies*. *J Biol Chem*, 1998. **273**(35): p. 22498-505.

15. Bitan, G., L. Scheibler, Z. Greenberg, M. Rosenblatt, and M. Chorev, *Mapping the integrin alpha V beta 3-ligand interface by photoaffinity cross-linking*. *Biochemistry*, 1999. **38**(11): p. 3414-20.
16. Mouldous, L., C.M. Topham, H. Mazarguil, and J.C. Meunier, *Direct identification of a peptide binding region in the ORL1 receptor by photoaffinity labelling with [Bpa10, Tyr14]nociceptin*. *J Biol Chem*, 2000.
17. Koelle, M.R., *A new family of G-protein regulators - the RGS proteins*. *Curr Opin Cell Biol*, 1997. **9**(2): p. 143-7.
18. Dohlman, H.G., J. Song, D. Ma, W.E. Courchesne, and J. Thorner, *Sst2, a negative regulator of pheromone signaling in the yeast Saccharomyces cerevisiae: expression, localization, and genetic interaction and physical association with Gpa1 (the G-protein alpha subunit)*. *Mol Cell Biol*, 1996. **16**(9): p. 5194-209.
19. Dube, P., A. DeCostanzo, and J.B. Konopka, *Interaction between transmembrane domains five and six of the alpha-factor receptor*. *J Biol Chem*, 2000.

20. David, N.E., M. Gee, B. Andersen, F. Naider, J. Thorner, and R.C. Stevens, *Expression and purification of the Saccharomyces cerevisiae alpha-factor receptor (Ste2p), a 7-transmembrane-segment G protein-coupled receptor.* J Biol Chem, 1997. **272**(24): p. 15553-61.
21. Raths, S.K., F. Naider, and J.M. Becker, *Peptide analogues compete with the binding of alpha-factor to its receptor in Saccharomyces cerevisiae.* J Biol Chem, 1988. **263**(33): p. 17333-41.
22. Aletras, A., K. Barlos, D. Gatos, S. Koutsogianni, and P. Mamos, *Preparation of the very acid-sensitive Fmoc-Lys(Mtt)-OH. Application in the synthesis of side-chain to side-chain cyclic peptides and oligolysine cores suitable for the solid-phase assembly of MAPs and TASP.* Int J Pept Protein Res, 1995. **45**(5): p. 488-96.
23. Kaiser, E., R.L. Colescott, C.D. Bossinger, and P.I. Cook, *Color test for detection of free terminal amino groups in the solid-phase synthesis of peptides.* Anal Biochem, 1970. **34**(2): p. 595-8.

24. Breslav, M., J. Becker, and F. Naider, *Dithioketal formation during synthesis of Bpa containing peptides*. Tetrahedron Letters, 1997. **38**: p. 2219-2222.
25. Liu, S., L.K. Henry, B.K. Lee, S.H. Wang, B. Arshava, B. J.M., and F. Naider, *Position 13 analogs of the tridecapeptide mating pheromone from Saccharomyces cerevisiae: design of an iodinated ligand for receptor binding*. J. Peptide Res., 2000. **56**: p. 24-34.
26. Kippert, F., *A rapid permeabilization procedure for accurate quantitative determination of beta-galactosidase activity in yeast cells*. FEMS Microbiol Lett, 1995. **128**(2): p. 201-6.
27. Konopka, J.B., D.D. Jenness, and L.H. Hartwell, *The C-terminus of the S. cerevisiae alpha-pheromone receptor mediates an adaptive response to pheromone*. Cell, 1988. **54**(5): p. 609-20.
28. Bukusoglu, G. and D.D. Jenness, *Agonist-specific conformational changes in the yeast alpha-factor pheromone receptor*. Mol Cell Biol, 1996. **16**(9): p. 4818-23.

29. Fontana, A., *Modification of tryptophan with BNPS-skatole (2-(2-Nitrophenylsulfenyl)-3-methyl-3-bromoindolenine)*. *Methods Enzymol*, 1972. **25**: p. 419-423.

## **PART IV**

### **DESIGN, SYNTHESIS AND CHARACTERIZATION OF A NOVEL DIMERIC $\alpha$ -FACTOR LIGAND.**

Part IV represents collaborative work with the laboratory of Dr. Fred Naider at the City University of New York, Staten Island. Keith Henry performed all the studies in the part with the exception of synthesis of the peptides used in this study. The peptide syntheses were carried out by Dr. F. X. Ding in Dr. Naider's lab.

# CHAPTER I

## INTRODUCTION

Multivalent ligands are compounds that typically consist of multiple core ligand structures (also known as pharmacores) connected by bridging molecules and have been shown to be pharmacologically relevant in receptor-ligand complexes [1]. Increasingly, multivalent ligands are proving to be useful tools not only in the study of ligand-receptor interactions but also in development of super-active pharmacological agents [2-5].

Most of the information concerning multivalent ligands has centered around agonists and antagonists of the opioid and serotonin receptors, and the pharmacological importance of these ligands has been shown through this work [1, 3, 5-11]. For instance, a dimer of sumatriptan, a 5-HT<sub>1B</sub> (serotonin) receptor agonist, can be used as a potent, orally-active treatment for migraines [7]. Portoghese and others have reported using bivalent opioid agonists and antagonists as receptor probes to understand how ligands are presented to the active sites of opioid receptors [3]. A number of the multivalent ligands tested have shown heightened efficacy and specificity over their monomeric forms in vivo and in vitro. In one these studies, dimers of the neurotransmitter serotonin showed increased specificity for the 5-HT<sub>1A</sub> receptor vs. monomeric serotonin indicating



that these multivalent ligands could be used to decrease inappropriate cross activation of receptor sub-types [12].

There is convincing evidence that the length of the spacer used to connect the active groups in oligomeric ligands plays a major role in determining whether a ligand is super-active or has greater receptor specificity. This observation has far reaching implications for use of multivalent ligands as biochemical tools considering that oligomerization of G-protein coupled receptors (GPCRs) has recently become of interest in the understanding of receptor activation and regulation [13-17]. These reports suggest that GPCRs oligomerize upon agonist binding and the resulting complex is a signal for internalization leading to down regulation of the receptor from the plasma membrane. The phenomenon appears to be a common occurrence with GPCRs as receptor oligomerization has been observed from yeast to humans. Investigation of receptor oligomerization and its role in regulation could provide important insight into a major aspect of receptor signal desensitization.

Currently, the tools available for studying GPCR oligomerization are limited. The primary information on receptor complexes formation has come from mutational and FRET (fluorescence resonance energy transfer) analysis. But many questions still remain such as: what proteins are involved in this process and what is the stoichiometry of these oligomeric complexes? New approaches and tools

are needed to address these questions. It is possible that oligomeric ligands may be useful in the study of the phenomenon of receptor oligomerization.

In studies of the  $\alpha$ -factor peptide pheromone (WHWLQLKPGQPMY) and its receptor Ste2p in *Saccharomyces cerevisiae*, it has been determined that acetylation of  $\alpha$ -factor on the side chain of lysine at position seven resulted in a ligand with good binding affinity and biological activity (L.K. Henry, F. Naider, and J. Becker, unpublished data). These results as well as studies with  $\alpha$ -factor analogs constrained in a bent conformation using amino acid analogs [18, 19] indicate that the lysine at position 7 may be relatively exposed to the aqueous environment when  $\alpha$ -factor is bound to the receptor. Thus, our current model of  $\alpha$ -factor binding has the N and C termini buried into the hydrophobic receptor and the middle portion of the ligand exposed to the aqueous environment. As a result, modification of  $\alpha$ -factor at terminal residues would be expected to result in more dramatic effects on its binding and/or biological activity compared to modification at Lys<sup>7</sup>. These predictions have been validated as studies have shown that removal of the first two N-terminal amino acids resulted in a potent  $\alpha$ -factor antagonist and truncation of the C-terminal residues causes total loss of detectable binding [20].

To further investigate the nature of the environment of Lys<sup>7</sup> when  $\alpha$ -factor is bound to the receptor and possibly develop a tool to study receptor oligomerization, an  $\alpha$ -factor dimer was constructed by covalently linking the Lys<sup>7</sup> side chains of two  $\alpha$ -factor molecules via an aminohexanoic acid bridge. The

resulting dimeric  $\alpha$ -factor analog was then characterized by analyzing biological activity, binding affinity and peptide stability.

## CHAPTER II

### MATERIALS AND METHODS

#### *Synthesis and Construction of $\alpha$ -factor Dimer.*

*Materials:* Amino acid derivatives were purchased from Advanced ChemTech (Louisville, KY), Bachem Inc. (Torrance, CA), NovaBiochem (La Jolla, CA). Ethylene glycol-bis (succinic acid N-hydroxy succinimide ester) was purchased from Aldrich Chemical Co. (Milwaukee, WI). All reagents and solvents for solid phase peptide synthesis were analytical grade and were purchased from Aldrich Chemical Co. (Milwaukee, WI), Advanced ChemTech (Louisville, KY), VWR Scientific (Piscataway, NJ) and Richelieu Biotechnology (Montreal, Canada).

*$\alpha$ -factor dimer synthesis:* N- $\alpha$ -Fmoc alpha factor was synthesized on a stepwise manner in a 0.1mmol scale using an Applied Biosystems Inc. Model 433A synthesizer in the laboratory of Dr. Fred Naider, City University of New York, College of Staten Island. The synthesis commenced with a Wang resin preloaded with Tyr (Boc) (0.6mmol/g). HBTU/HOBt activation method was utilized and capping was accomplished with acetic anhydride in presence of DIEA. After the complete assembly of the peptide chain, the resin was treated with 95% TFA, 2.5% EDT and 2.5% deionized water at room temperature for 1.5

hours. The reaction mixture was filtered to remove the resin. The combined filtrate was concentrated on a rotary evaporator to a small volume. The crude peptides were precipitated by adding cold anhydrous ether to the concentrated filtrate. The obtained crude peptide purity was 70% by HPLC. The above crude peptide 30.5mg(0.01mmol) was dissolved in 3ml DMF, then N-methyl morpholine 11  $\mu$ l (0.1mmol) and Ethylene glycol-bis (succinic acid N-hydroxy succinimide ester) 2.3mg (0.005mmol) were added. The reaction mixture was stirred at room temperature for 24 hours. Piperidine 0.7 ml was added to the reaction mixture for deprotection of Fmoc and the reaction mixture was stirred at room temperature for 30 min. The reaction mixture was concentrated by speed vacuum to a small volume, cold anhydrous ether was added and crude peptide was precipitated.

*Purification and characterization of  $\alpha$ -factor dimer:* Purification and analysis of the peptides was accomplished by preparative reversed phase HPLC and performed on a Hewlett Packard 1050 HPLC system using Waters  $\mu$ -Bondapak-C18 (3.9 mm x 300mm for analytical analysis; 19 x 300mm for preparative purification). Analytical HPLC was run using a linear gradient of water (0.025% TFA) and acetonitrile (0.025% TFA) with acetonitrile from 10-100% over 30 min. Preparative HPLC was run using a linear gradient of water (0.025% TFA) and acetonitrile (0.025% TFA) with acetonitrile from 10-90% over 90 min. The monitoring was usually done at 220 nm. The peptide with greater than 95% purity was obtained after two preparative runs. The purity of the final

products was assessed by analytical RP-HPLC, thin-layer chromatography (TLC) and fast atom bombardment mass spectrometry (FAB-MS). The  $[M+1]^+$  molecular ion for  $\alpha$ -factor 3557.9 was in agreement with the calculated molecular weight 3558.1. FAB-MS was performed at Peptido Genic Research & Company, Livermore, CA. TLC was carried out on glass back silica gel plates (DC-Fertigplatten Kieselgel 60, Merk) using different solvent systems; ninhydrin spray and iodine were used for detection. Amino acid analyses were performed at the Biopolymer Laboratory, Brigham and Women's Hospital of Harvard Medical School, after acid hydrolysis with 6N HCl.

*Yeast Strains, Plasmids and Growth Conditions.* *S. cerevisiae* strains RC629 (*MAT $\alpha$  sst1-2*), RC631 (*MAT $\alpha$  sst2-1*) from R. Chan, University of Cincinnati [21] were grown in YEPD (Yeast Extract Peptone Dextrose). Strain DK102 (*MAT $\alpha$  ste2 $\Delta$* ) containing the *STE2* overexpression plasmid pNED1 was grown in MLT (medium lacking tryptophan)[yeast nitrogen base without amino acids (Difco), 6.7 g/L; casamino acids (Difco), 10 g/L; glucose, 20 g/L; adenine sulfate (ICN), 0.058 g/L; arginine, 0.026 g/L; asparagine, 0.058 g/L; aspartic acid, 0.14 g/L; glutamic acid, 0.14 g/L; histidine, 0.028 g/L; isoleucine, 0.058 g/L; leucine, 0.083 g/L; lysine, 0.042 g/L; methionine, 0.028 g/L, phenylalanine, 0.69 g/L; serine, 0.52 g/L; threonine, 0.28 g/L; tyrosine, 0.042 g/L; valine, 0.21 g/L; and uracil, 0.028 g/L [22]. DK102 control cells lacking the pNED1 plasmid and LM23-3az from Lorraine Marsh, Albert Einstein College of Medicine, New York

were grown on MLT supplemented with tryptophan (MWT). All strains were incubated at 30°C with agitation and harvested at the appropriate time for each assay.

*Growth Arrest Assay.* Cells were grown overnight in liquid medium, harvested by centrifugation, washed with sterile distilled water and resuspended in water. Cells were then tested as previously described [20] except the amount of peptide spotted was measured in nmoles of peptide rather than micrograms to account for the difference in molecular weight of the ligands.

*Effect of  $\alpha$ -factor Dimer on Gene Induction.* *S. cerevisiae* strain LM23-3az contains a chromosomal copy of the pheromone inducible *FUS1* gene fused to the  $\beta$ -galactosidase reporter gene. Cells were grown overnight to  $5 \times 10^6$  cells/ml in MWT medium, washed by centrifugation, and resuspended to  $1 \times 10^8$  cells/ml in MWT. Induction was initiated by addition of 250  $\mu$ l of peptide at various concentrations to 2.25 ml of concentrated cells. Peptide-cell suspensions were mixed by vortexing and incubated at 30°C with shaking for 2 hours. Assays for  $\beta$ -galactosidase activity were then performed using a modified standard protocol [23]

*Binding Competition Assay.* Binding competition experiments were performed with iodinated ligand [ $^{125}$ I-Y<sup>1</sup> Nle<sup>12</sup> F<sup>13</sup>] $\alpha$ -factor. DK102 pNED1 cells were grown in MLT medium, to  $1 \times 10^7$  cells/ml, harvested by centrifugation and resuspended to  $6.25 \times 10^7$  cells/ml in PPBi buffer [0.5M potassium phosphate

(pH6.24) containing 10mM TAME, 10mm sodium azide, 10 mM potassium fluoride and 1% BSA (fraction IV)] and placed at 4°C. [<sup>125</sup>I-Y<sup>1</sup> Nle<sup>12</sup> F<sup>13</sup> ]α-factor (2 x 10<sup>-9</sup>M final concentration) was pre-mixed with various concentrations of cold competitor. DK102pNED1 and DK102 cells in PPBi were then added to a final density of 6.25 X 10<sup>6</sup> cells/ml. Suspensions were mixed and incubated for 45 minutes at room temperature. Following incubation, reaction mixes were transferred (3 x 200 µl) to wells in a MultiScreen –HV 0.45 µm 96 well plate (Millipore MHVBN4510) pre-blocked with PBBi. Samples were vacuum filtered, washed with PBBi (2 x 200 µl) and counted on a LKB-Wallac CliniGamma 1272 gamma counter.

*Degradation Assays.* DK102pNED and RC631 cells were grown overnight in MLT medium, harvested by centrifugation and resuspended in fresh MLT medium to 1x10<sup>6</sup> cells/ml. Two ml of the cell suspension was transferred to a sterile siliconized tube containing 50 µg of α-factor or α-factor dimer and incubated at 30°C. At 0, 1, 2 and 3.5 hours 400 µl was removed from each reaction and filtered by centrifugation (13,000 × g) for 1 minute through a Millipore UltraFree-MC 0.45µM filter unit pre-washed with 400 µl of sterile H<sub>2</sub>O. Following centrifugation the filter was washed with 100 µl of 100% HPLC grade MeOH and re-centrifuged to elute any peptide that remained bound to the filter membrane. The filtrate and the MeOH wash was combined and diluted with 400 µl of HPLC grade H<sub>2</sub>O. Analysis of the filtrate was carried out on a Hewlett-



Packard 1100 Series HPLC by reverse phase using an analytical C8 Zorbax column ( $4.6 \times 150$ ;  $5 \mu\text{M}$ ) using a H<sub>2</sub>O/acetonitrile/0.025% trifluoroacetic acid gradient. Acetonitrile percentage was change from 20 to 60 over 45 minutes. Relevant fractions were analyzed at the Mass Spectrometry Facility, University of Tennessee, Knoxville, for mass using electrospray mass spectrometry on a Micromass Quattro II tandem electrospray spectrometer run in positive mode at 4 kV (scan range 0-2000 m/z).

## CHAPTER III

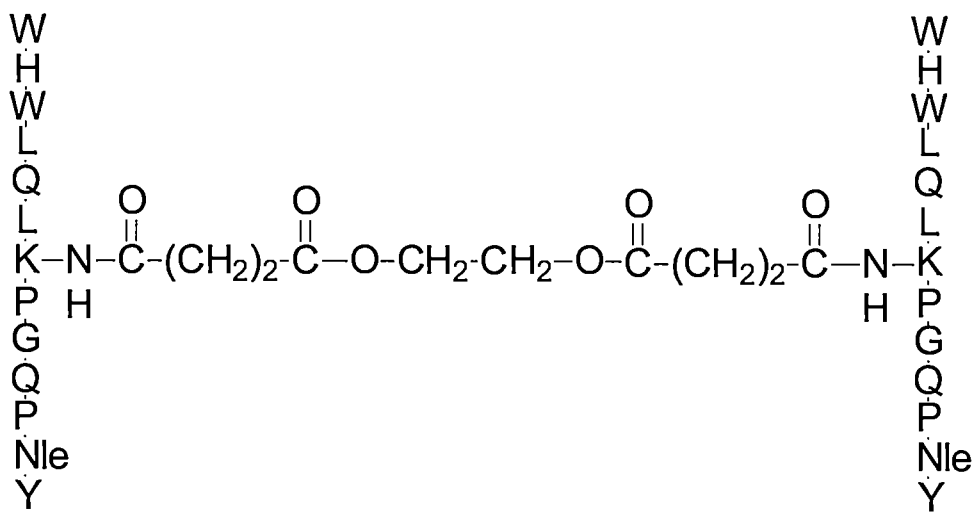
### RESULTS

*Synthesis of  $\alpha$ -factor dimer.* The  $\alpha$ -factor dimer was found to be >97% pure by HPLC analysis in a two solvent systems and amino acid analysis was within 10% of expected ratios (data not shown). A schematic of  $\alpha$ -factor dimer is shown in Figure 1.

*Bioactivity of  $\alpha$ -factor dimer.* The biological activity of the dimer was assessed using growth arrest and gene induction assays. Strains used in the bioactivity studies lacked the Bar1p protease which is known to functionally inactivate  $\alpha$ -factor by cleaving it between the Leu at position six and the Lys at position seven. In the growth arrest assay, sterile disks containing various amounts of ligand were placed on a lawn of cells. The diameter of the resulting zones of growth inhibition were graphed on a semilogarithmic plot versus nmoles of peptide spotted to produce a standard curve. The nmoles of peptide required to give a 15 mm halo was interpolated from the standard curve and used to rank the biological activities of the peptides. In the gene induction assay, the strain LM23-3AZ, which contains a chromosomal copy of the lacZ reporter gene driven by the

**Figure 1. Diagram of primary structure of  $\alpha$ -factor dimer.**

Diagram represents the primary structure of  $\alpha$ -factor dimer showing the amino acid sequence of two  $\alpha$ -factor moieties and the chemical structure of aminohexanoic acid used to bridge the two peptides via the lysine at position seven.



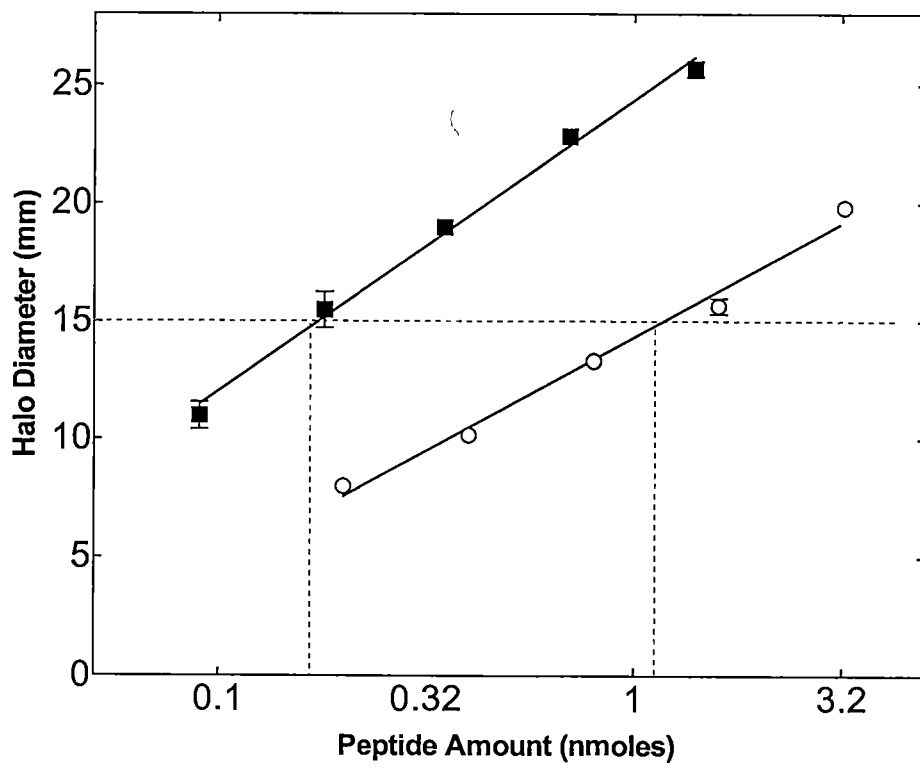
*FUSI* promoter, is incubated with various amounts of peptide. The *FUSI* gene is induced quickly following receptor mediated activation of the pheromone signal transduction pathway and has been shown to be very sensitive in measuring activation of the Ste2p receptor [24].

As shown in Figure 2, the plots of the growth arrest data were linear and resulted in almost parallel slopes. Based on these data, 1.17 nmoles of  $\alpha$ -factor dimer were required to form a 15 mm halo compared to 0.17 nmoles of  $\alpha$ -factor, a 6.9 fold difference. In the gene induction (*FUSI*-lacZ) assay, expression of the lacZ gene was reported in Miller units and plotted versus molar concentration of peptide (Figure 3). LacZ activity for  $\alpha$ -factor appeared to saturate at around 4400 Miller Units giving an Emax (efficacy or maximum response) of  $1 \times 10^{-7}$  M and an EC<sub>50</sub> (potency) of  $2.5 \times 10^{-8}$  M. The dimer did not saturate at the concentrations tested but appeared to be reaching a maximum similar to  $\alpha$ -factor. This indicated that the dimer is able to maximally activate *FUSI* to levels comparable to those seen with  $\alpha$ -factor. Based on the EC<sub>50</sub>, the dimer has an apparent potency of  $2.9 \times 10^{-7}$  M, a 12-fold decrease compared to  $\alpha$ -factor. This is comparable to the 6.9-fold reduction in activity seen with the growth arrest assay.

*Binding affinity of  $\alpha$ -factor dimer.* Binding affinity of the dimer was established by measuring its ability to displace  $^{125}\text{I}$ -[Y<sup>1</sup>F<sup>13</sup>] $\alpha$ -factor from the Ste2p receptor [25]. As shown in Figure 4, Bmax values for the dimer and  $\alpha$ -factor were similar and both peptides were able to reduce binding of the radioligand >90%.

**Figure 2. Growth arrest assay of *S. cerevisiae* by  $\alpha$ -factor and  $\alpha$ -factor dimer.**

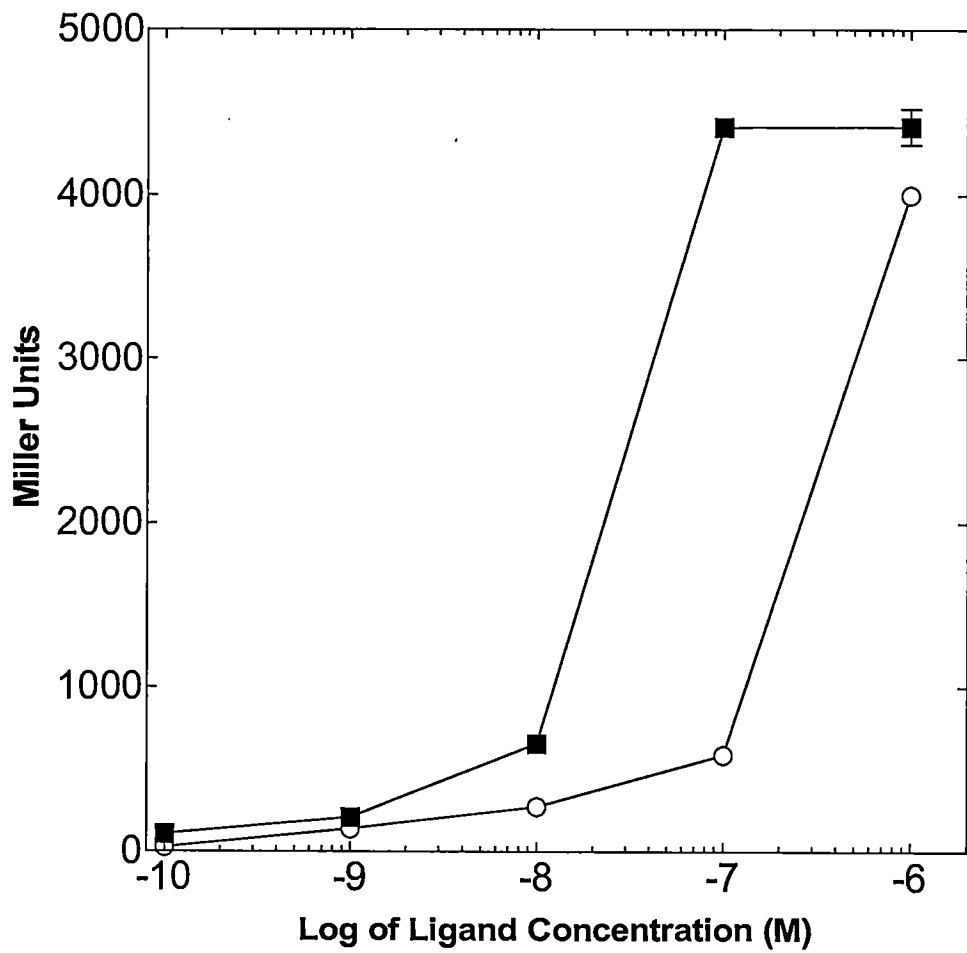
Halo diameters were measured and plotted in relationship to the nmoles of peptide spotted on the disk. The peptides are:  $\alpha$ -factor (■) and  $\alpha$ -factor dimer (○). The nmoles of peptide required to obtain a 15 mm halo was determined from linear regression of the plotted values.



**Figure 3. Dose response to  $\alpha$ -factor and  $\alpha$ -factor dimer by reporter gene lacZ ( $\beta$ -galactosidase).**

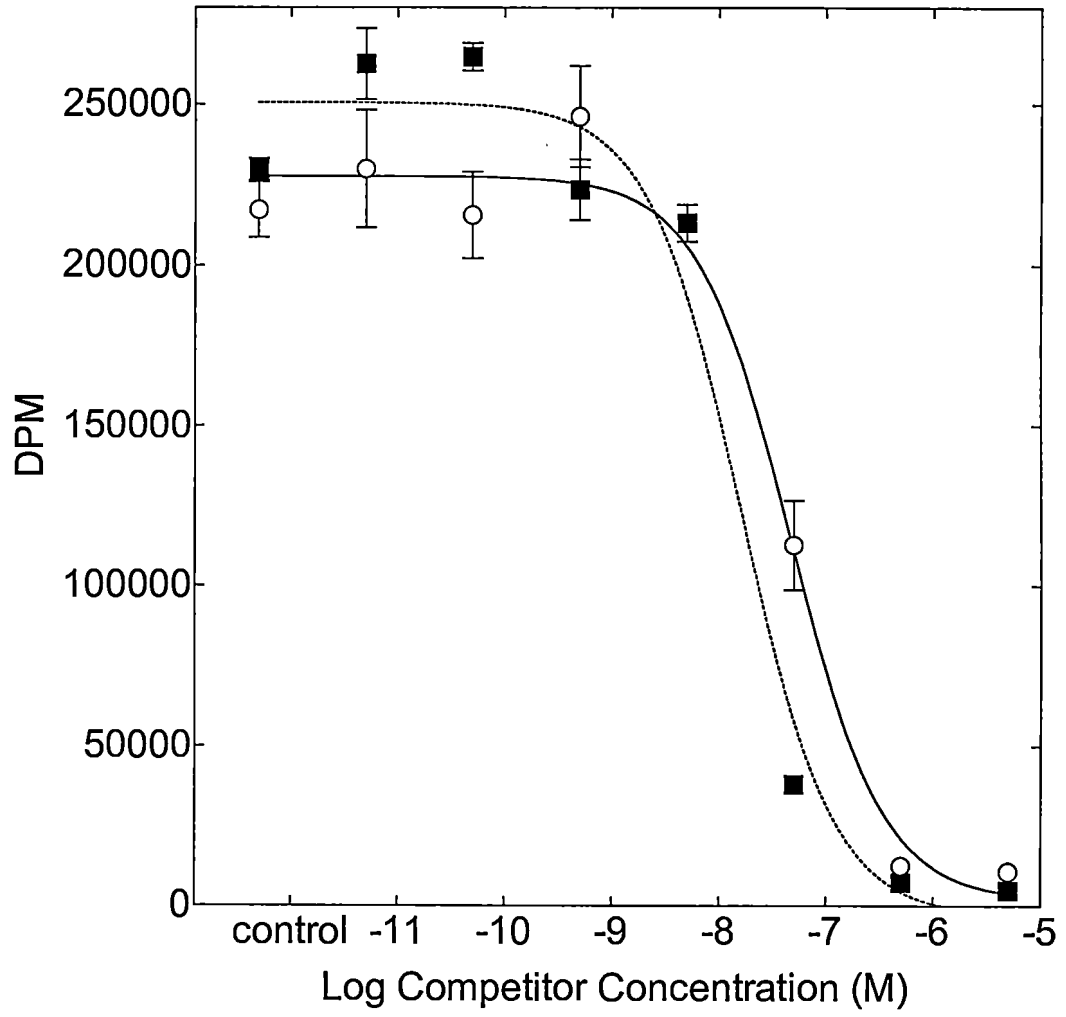
$\beta$ -galactosidase activity is given in Miller units and was measured in cultures incubated with various amounts peptide as shown:  $\alpha$ -factor (■) and  $\alpha$ -factor dimer (○).





**Figure 4. Competition binding assay with [Tyr<sup>1</sup>(<sup>125</sup>I) Phe<sup>13</sup>]  $\alpha$ -factor.**

Cells were incubated with radioactive pheromone ( $2 \times 10^{-9}$  M) and increasing amounts of cold competitor as indicated in graph. The peptides are:  $\alpha$ -factor (■ - dashed line) and  $\alpha$ -factor dimer (○ - solid line).



Using the equation by Cheng and Prusoff [26],  $K_i$ 's of  $4.7 \times 10^{-8}$  M and  $1.6 \times 10^{-8}$  M were determined for the dimer and  $\alpha$ -factor, respectively, a difference of only 2.9-fold. The  $K_i$  of  $\alpha$ -factor is comparable to  $K_i$  values obtained in previous studies with iodinated and tritiated  $\alpha$ -factor [25, 27].

*Synergist and antagonist affect on dimer activity.* If the dimer is binding to Ste2p and activating the signal transduction pathway in a manner similar to  $\alpha$ -factor, it is reasonable to predict that analogs that modify the activity of  $\alpha$ -factor should have a comparable affect on the dimer. Two  $\alpha$ -factor analogs, a synergist and an antagonist, were tested to determine their affect on the biological activity of the dimer. The synergist peptide [WHWLQLKPGQP] is a truncated  $\alpha$ -factor analog which is unable to activate the mating response alone. However, when used in combination with native  $\alpha$ -factor, the resulting response is greater than with the same concentration of  $\alpha$ -factor alone [20]. The antagonist is an N-terminal truncated  $\alpha$ -factor analog [WLQLKPGQPMY] which has been shown to competitively inhibit  $\alpha$ -factor binding and subsequent activation of Ste2p. The synergist was tested by spotting  $\alpha$ -factor dimer alone or in combination with the  $\alpha$ -factor synergist onto a paper disk (Difco, 6 mm diameter), placing the disks on a lawn of RC629 or RC631 cells and observing the resulting zone of growth inhibition. The results are summarized in Table 1. With RC629 cells,  $\alpha$ -factor and dimer alone resulted in halos of 11 and 7 mm, respectively. However, upon

**Table 1. Synergist effect on growth arrest activity of  $\alpha$ -factor dimer in *S. cerevisiae* strains RC629 and RC631.**

Compound	Halo diameter (mm)			
	RC629 ( <i>bar1</i> )		RC631 ( <i>sst2</i> )	
	synergist <sup>a</sup>		synergist <sup>a</sup>	
$\alpha$ -factor <sup>b</sup>	11	19	18	22
$\alpha$ -factor dimer <sup>c</sup>	7	12	12	20
Synergist <sup>a</sup>	<6 <sup>d</sup>	NA	7	NA

<sup>a</sup> The peptide [desM<sup>12</sup>desY<sup>13</sup>] $\alpha$ -factor at 15 nmoles was used as synergist in this assay and was co-spotted with test compounds where indicated.

<sup>b</sup> 0.35 nmoles of  $\alpha$ -factor was spotted on disk

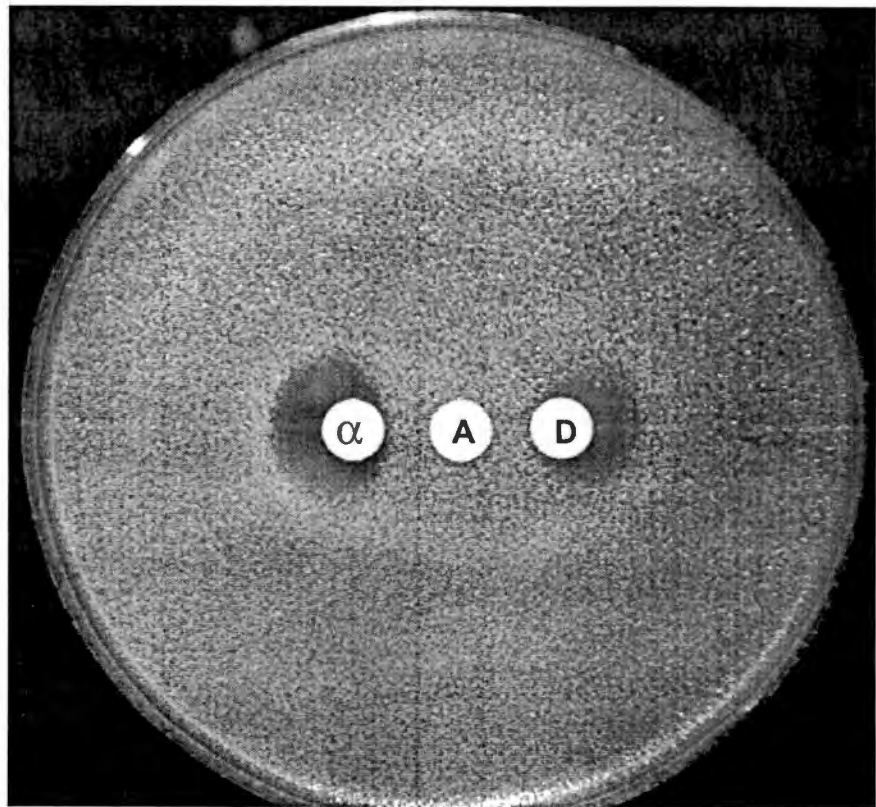
<sup>c</sup> 0.7 nmoles of  $\alpha$ -factor dimer was spotted on disk

<sup>d</sup> No growth arrest was observed. Analysis is limited by size of concentration disk.  
NA- not applicable

co-application of synergist, the halos for  $\alpha$ -factor (19 mm) and the dimer (12 mm) increased by 8 mm and 5 mm, respectively. No halo was detected around disks spotted with synergist alone. A similar pattern is seen in the *sst2* mutant strain RC631. However, in this strain background, the synergist can act as an agonist at high concentrations. As expected from previous testing of RC631 [20], the halo sizes with RC631 were larger than those with RC629. However, the same trend was observed where addition of synergist was able to enhance activity of  $\alpha$ -factor (18→22 mm) and dimer (12→20 mm). To test the  $\alpha$ -factor antagonist [desW<sup>1</sup>desH<sup>2</sup>]  $\alpha$ -factor (WLQLKPGQPMY), antagonist was spotted onto a disk and placed between two other disks that contained either native  $\alpha$ -factor or  $\alpha$ -factor dimer on a lawn of RC629 cells (Figure 5). The desW<sup>1</sup>desH<sup>2</sup> antagonist reduced the ability of both  $\alpha$ -factor dimer and native  $\alpha$ -factor to cause growth inhibition as illustrated by the characteristic bean shaped halos. The antagonist diffuses and competes with  $\alpha$ -factor and dimer for binding to Ste2p resulting in a reduced arrest response by the cells and consequently leads to a filling in of the halo near the disk containing antagonist. The ability of the dimer to activate the pheromone signal transduction pathway and the fact that an  $\alpha$ -factor synergist and antagonist are able to modulate the dimer's activity in a similar manner to that of  $\alpha$ -factor strongly suggest that the dimer is binding and activating Ste2p in the same manner as native  $\alpha$ -factor.

**Figure 5. Affect of the  $\alpha$ -factor antagonist desW<sup>1</sup>desH<sup>2</sup>  $\alpha$ -factor on  $\alpha$ -factor and  $\alpha$ -factor dimer in growth arrest assay.**

Peptides were pipetted onto sterile disks and placed on a lawn of RC629 cells and incubated for 24 hours. Peptides spotted are: ( $\alpha$ )  $\alpha$ -factor [0.18 nmoles], (**D**)  $\alpha$ -factor dimer [1.6 nmoles] and (**A**) desW<sup>1</sup>desH<sup>2</sup>  $\alpha$ -factor [3.8 nmoles].



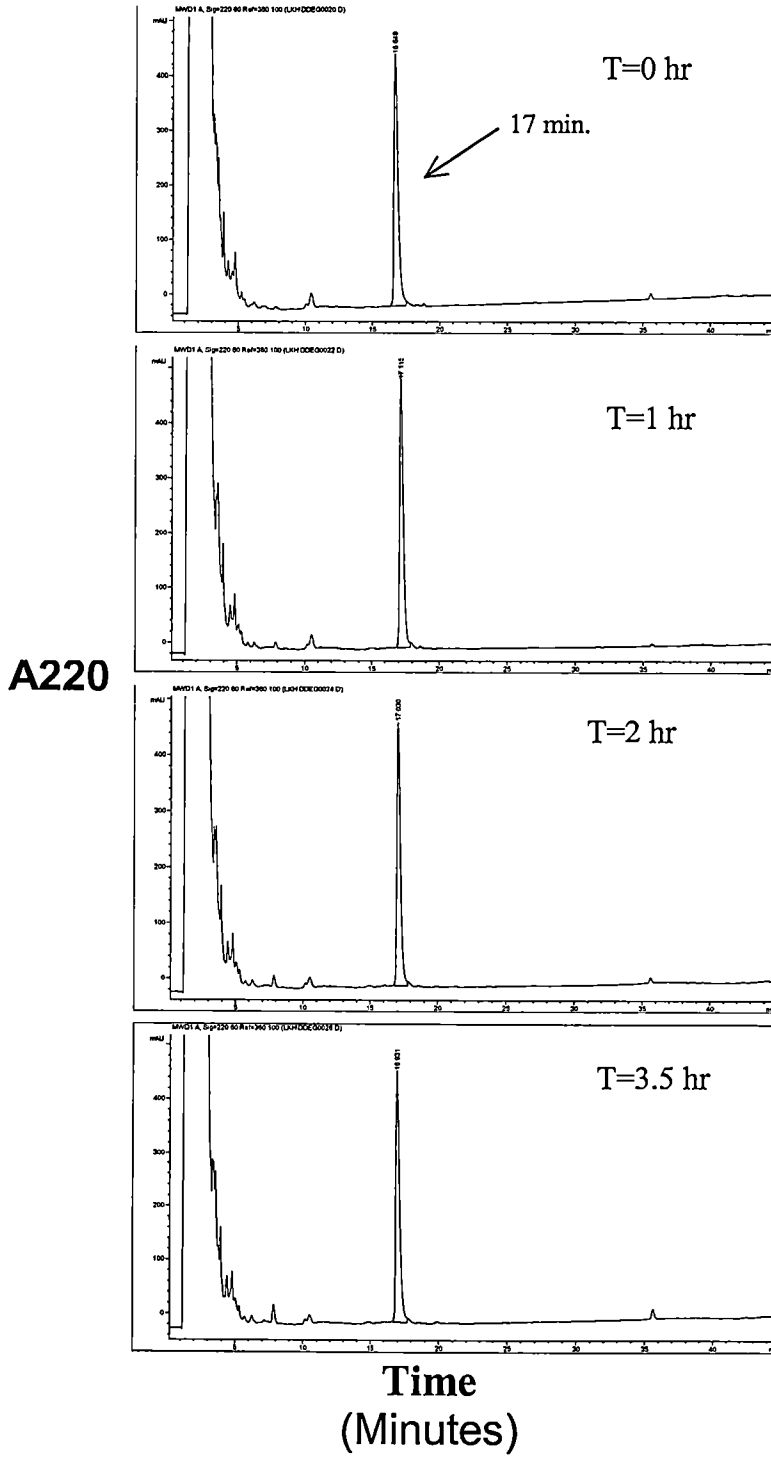


*Stability of  $\alpha$ -factor dimer.* To test whether the biological and binding activity observed was indeed due to dimeric  $\alpha$ -factor and not monomeric breakdown products,  $\alpha$ -factor dimer was incubated in the presence of whole cells and the supernatant was analyzed by HPLC for dimer breakdown products. All fractions corresponding to pertinent HPLC peaks were analyzed by electrospray mass spectrometry (ESMS) to verify mass. The dimer and native  $\alpha$ -factor were tested with strain DK102pNED (used in binding analysis) which, like strains RC629 (used in growth arrest assays) and LM23-3az (used in *FUS1-lacZ* assays), lacked the Bar1p protease and strain RC631 which has a functional Bar1p protease and served as a positive control. The HPLC analysis of the timepoints is shown in Figures 6A, 6B, 6C and 6D. As expected,  $\alpha$ -factor when incubated with bar1<sup>-</sup> strain DK102pNED remains intact over the 3.5 hour incubation as evidenced by detection of one major peak at 17 minutes (Figure 6A). The peak shows the same relative intensity (mAU) over the entire time course of the experiment. However, when  $\alpha$ -factor is incubated with bar1<sup>+</sup> cells (RC631), a gradual decrease of the 17 minute peak is observed and coincides with the appearance of a 19 minute peak until both are of relatively the same intensity at 3.5 hours (Figure 6B). Based on hydrophobicity, the 19 minute peak was predicted to be the liberated  $\alpha$ -factor fragment WHWLQL following Bar1p digestion and was found to have the corresponding mass by ESMS (data not shown). The other fragment resulting from cleavage of  $\alpha$ -factor (KPGQPNIeY) cannot be detected because it is more

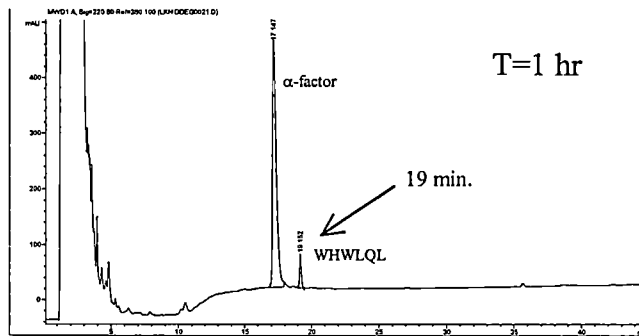
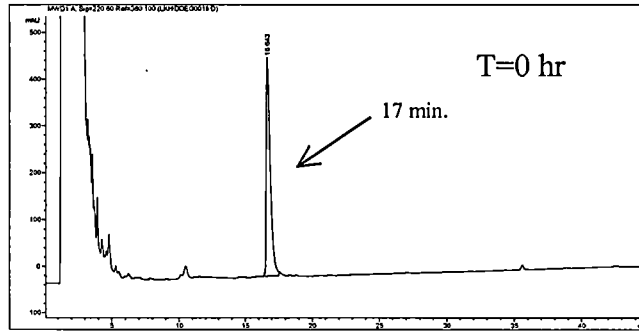
**Figure 6. HPLC analysis of  $\alpha$ -factor and  $\alpha$ -factor dimer following incubation with RC629 and DK102pNED1 cells.**

Supernatant from cells incubated with different peptides was analyzed over time and processed by HPLC reverse phase analysis on a C8 Eclipse column (4.6 x 150; 5  $\mu$ M)(Zorbax) using a H<sub>2</sub>O/acetonitrile/0.025% trifluoroacetic acid gradient (20 to 60% over 45 minutes). Flowthrough was monitored at 220 nm. Arrows represent peak retention times. T denotes the length of time peptides were incubated in the presence of cells. Samples are as follows: (A)  $\alpha$ -factor incubated with Dk102pNED1 (*bar1*) cells, (B)  $\alpha$ -factor incubated with RC631 (*sst2*) cells, (C)  $\alpha$ -factor dimer incubated with Dk102pNED1 (*bar1*) cells and (D)  $\alpha$ -factor dimer incubated with RC631 (*sst2*).

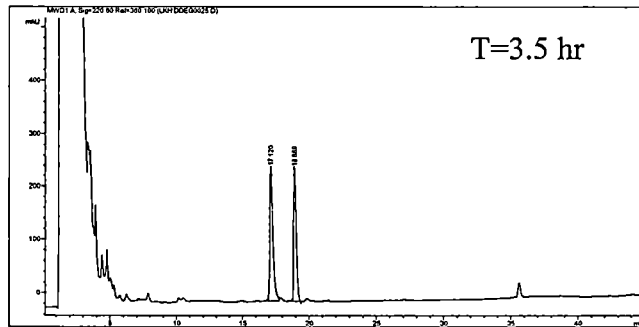
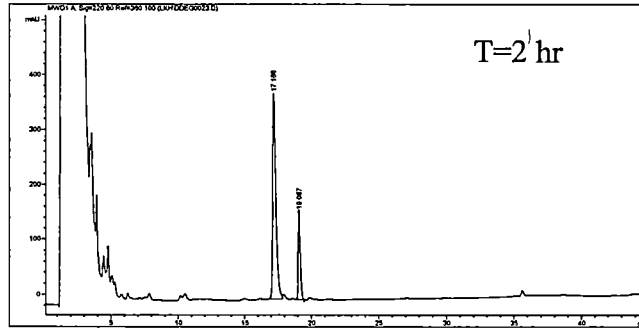
**A** Dk102pNED (bar1<sup>-</sup>)



**B** RC631 (BAR1<sup>+</sup>)

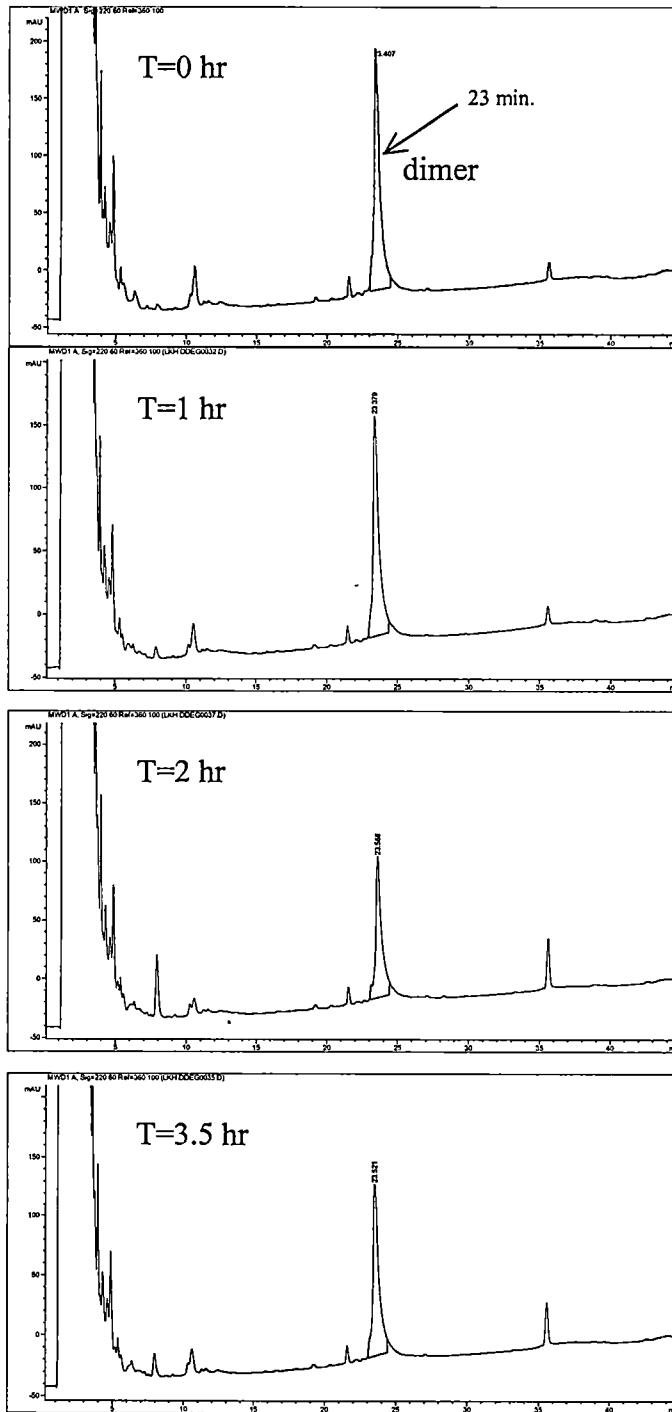


**A220**



**Time  
(Minutes)**

# C Dk102pNED (bar1<sup>-</sup>)

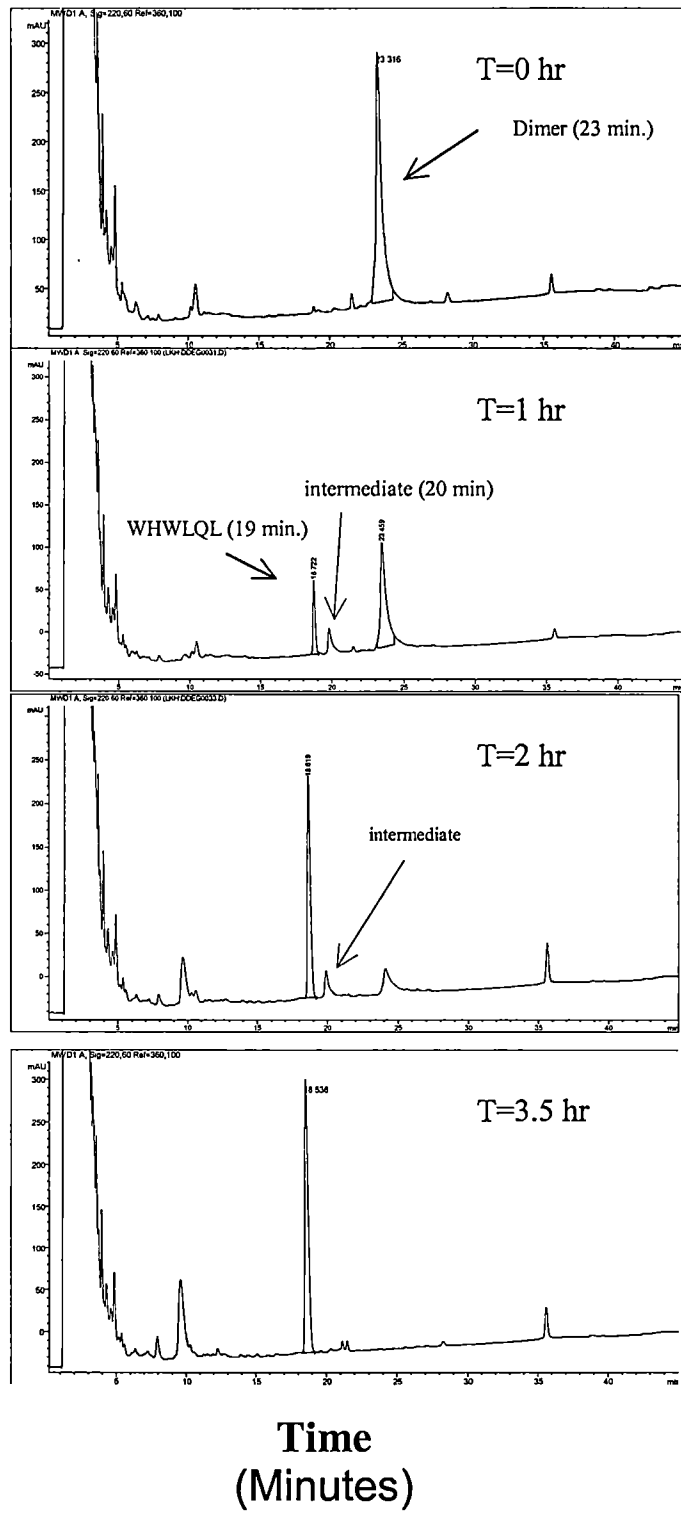


A220

Time  
(Minutes)

# D RC631 Cells (BAR1<sup>+</sup>)

A220



hydrophilic and elutes with the reaction medium. According to the HPLC column's manufacturer, the unexpected longer retention time of the WHWLQL fragment compared to  $\alpha$ -factor was apparently due to a previously observed interaction of the column matrix with very short peptides due to their increased rigidity versus longer peptides. These data show that  $\alpha$ -factor is stable when using Bar1p minus cells.

The dimer showed a similar pattern of degradation (Figure 6 C and 6D). In the presence of bar1<sup>-</sup> cells, the dimer (retention time 23 minutes) was the major peak observed and remained at relatively the same intensity throughout the experiment. There was a slight reduction of intensity at 2 hours. However, the intensity goes back up at 3.5 hours and no new peaks were observed indicating that the lower intensity at that point was probably due to lack of full recovery of filtrate and not degradation of the dimer. This occasional fluctuation of recovery was observed infrequently at other time-points in repeats of this assay. In the presence of bar1<sup>+</sup> cells, the dimer was quickly converted to two breakdown species with retention times of 19 and 20 minutes and after 3.5 hours only one breakdown product (19 minutes) remains resulting in complete disappearance of the dimer. As expected, ESMS analysis shows that the peak at 19 minutes has the same mass as the 19 minute peak seen in degradation of  $\alpha$ -factor (WHWLQL). This fragment would result from both  $\alpha$ -factor molecules in the dimer being cleaved by Bar1p. Due to the transient nature of the peak at 20 minutes, we were unable to obtain

sufficient quantities of the fraction to determine mass using ESMS. It is likely that the peak at 20 minutes represents an  $\alpha$ -factor dimer intermediate where only one of the  $\alpha$ -factor molecules has been cleaved by Bar1p resulting in two fragments [ fragment 1 -(WHWLQL) and fragment 2- (WHWLQLK(-AHA-KPGQPNleY)PGQPNleY)]. This intermediate (fragment 2) was then cleaved as indicated by its disappearance at 3.5 hours to give only the 19 minute fragment. Also, note that the 19 minute peak after 3.5 hours is of the same relative intensity as the dimer at time zero. Interestingly, after 3.5 hours only half of the  $\alpha$ -factor was degraded based on relative peak heights of intact  $\alpha$ -factor vs. the WHWLQL fragment (Figure 6B) whereas all of the  $\alpha$ -factor dimer was converted to the WHWLQL peptide after the same amount of time (Figure 6D). It is possible that the total amount of Bar1p enzyme was different between the  $\alpha$ -factor and dimer samples leading to different levels of cleavage. Alternatively, it is conceivable that the addition of the AHA spacer on the Lys<sup>7</sup> residues make the dimer more susceptible to Bar1p mediated cleavage compared to  $\alpha$ -factor.



## CHAPTER IV

### DISCUSSION

In this study, we present synthesis and characterization of a novel dimeric  $\alpha$ -factor analog. The analog was constructed using an aminohexanoic acid bridge to connect two  $\alpha$ -factor molecules via the epsilon amine of lysine at position seven on the  $\alpha$ -factor peptide.

Studies examining biological activity show that the  $\alpha$ -factor dimer exhibits only a marginal decrease in the ability to arrest growth (7-fold reduction) and induction of the *FUS1-lacZ* reporter construct (12-fold) when compared to native  $\alpha$ -factor. Though binding affinity and biological activity have not always correlated in previous studies with  $\alpha$ -factor analogs [24, 25], the decrease in biological activity is likely due to the lower binding affinity of the dimer compared to  $\alpha$ -factor.  $K_i$  values for the dimer and  $\alpha$ -factor determined by competition binding assays revealed that the dimer ( $K_i = 4.7 \times 10^{-8}$  M) bound with 3-fold less affinity as compared to  $\alpha$ -factor ( $K_i = 1.6 \times 10^{-8}$  M). Furthermore, like  $\alpha$ -factor, the dimer was able to displace binding of radiolabeled  $^{125}\text{I}$ -[Y<sup>1</sup>R<sup>7</sup>F<sup>13</sup>]  $\alpha$ -factor by >90% indicating that it was specific for binding to the Ste2p receptor.

In addition to the dimer having biological activity and binding affinity similar to  $\alpha$ -factor, dimer-mediated activation of the pheromone signal transduction pathway was affected by previously characterized Ste2p synergistic

and antagonistic peptides. The  $\alpha$ -factor synergist (WHWLQLKPGQP), which by itself has no agonistic activity, was able to enhance growth arrest when applied together with the dimer. The synergist has the same enhancing effect on  $\alpha$ -factor mediated growth arrest. Likewise, the  $\alpha$ -factor antagonist [desH<sup>1</sup>desW<sup>2</sup>]  $\alpha$ -factor (WLQLKPGQPMY) inhibited the ability of both the dimer and  $\alpha$ -factor to induce growth arrest. When considered together, the biological activity, binding affinity and response to  $\alpha$ -factor antagonistic and synergistic peptides clearly show that the dimer binds to and activates the Ste2p receptor in a manner very similar to  $\alpha$ -factor.

It was possible that the  $\alpha$ -factor dimer was either breaking down or being broken down into monomeric units corresponding to  $\alpha$ -factor which were able to bind to the receptor and activate the pheromone signal cascade. However, HPLC and ESMS analysis of the dimer and  $\alpha$ -factor incubated with yeast cells showed that the peptides were stable as long as the cells used in the assay lacked the Bar1p protease which functions to inactivate  $\alpha$ -factor by cleaving it in half.

Based on the results of this study, the  $\alpha$ -factor peptide can function as a dimer when linked through the epsilon amine of lysine at position seven by aminohexanoic acid. The structural information that can be gleaned from this data support previous predictions concerning the location of the Lys<sup>7</sup>  $\alpha$ -factor when bound to Ste2p. It is thought that the N and C termini of  $\alpha$ -factor, which are

relatively hydrophobic, are buried into the receptor and that the middle of the peptide is relatively exposed to the surface. The dimer study supports these predictions by indicating that the lysine at position seven is not buried in the receptor because tethering an  $\alpha$ -factor molecule to this lysine only results in a 3-fold decrease in binding affinity versus native  $\alpha$ -factor. The idea of Lys<sup>7</sup> being relatively exposed to the solvent face when  $\alpha$ -factor is bound to Ste2p is also supported by recent data using fluorescent probes attached to K<sup>7</sup> in  $\alpha$ -factor to study its local the environment when bound to the receptor (Ding and Lee, personal communication).

Biological studies with the dimer did not result in the discovery of a super-active agonist or antagonist as has been found with some pharmacologically relevant dimeric ligands [2, 7, 8, 28, 29]. However, this does not preclude that such enhanced ligands will not be found in the future with other dimeric  $\alpha$ -factor analogs. In many of the previous studies involving oligomeric ligands, it has been found that the length of the spacer played an essential role in determining whether or not an oligomeric ligand exhibited hyper-activity. Increasing spacer length between the  $\alpha$ -factor moieties in the dimer could allow for correct presentation of the second  $\alpha$ -factor moiety following initial binding of the first  $\alpha$ -factor moiety to a Ste2p receptor and result in a dimer with increased activity. This concept of signaling two receptors with one  $\alpha$ -factor dimer is even more plausible considering the latest data suggesting the Ste2p receptor is present as oligomeric

complexes in the plasma membrane [17]. Future studies with  $\alpha$ -factor dimers may lead to analogs that can be used as tools for looking at receptor oligomeric complexes in the plasma membrane. For instance, the affect of longer or shorter spacers on binding could provide information concerning the distance between Ste2p receptors in the membrane. In addition, it is possible that future multivalent  $\alpha$ -factor analogs could be designed to incorporate fluorescent labels and/or crosslinkable moieties such as Bpa (benzoylphenylalanine) to begin addressing issues such as receptor stoichiometry in these oligomeric complexes. It is also possible that a dimeric  $\alpha$ -factor antagonist analog could be used to bring two Ste2p receptors in close proximity to one another to determine whether formation of the oligomeric receptor complexes is a density dependent phenomenon where the receptors only need to come in contact with one another to oligomerize or whether it requires active signaling to occur.  $\alpha$ -factor dimers formed from spacers between amino acids at positions other than Lys<sup>7</sup> in  $\alpha$ -factor and the resulting affect on binding and biological activity could provide useful information concerning the environment of the amino acids in  $\alpha$ -factor when it is bound to Ste2p.

In conclusion, studies with oligomeric ligands have led to many valuable insights concerning ligand specificity, binding site co-operativity, and ligand presentation to receptors indicating their use as tools in the analysis of structure-function relationships between receptors and ligands. This study represents the

first example of a multimeric  $\alpha$ -factor agonist for the  $\alpha$ -factor pheromone receptor, Ste2p. Based on my results,  $\alpha$ -factor dimers have the potential to be used for investigation of multiple aspects of Ste2p function.

## REFERENCES

1. Bolognesi, M.L., W.H. Ojala, W.B. Gleason, J.F. Griffin, F. Farouz-Grant, D.L. Larson, A.E. Takemori, and P.S. Portoghese, *Opioid antagonist activity of naltrexone-derived bivalent ligands: importance of a properly oriented molecular scaffold to guide "address" recognition at kappa opioid receptors*. J Med Chem, 1996. **39**(9): p. 1816-22.
2. Shuker, S.B., P.J. Hajduk, R.P. Meadows, and S.W. Fesik, *Discovering high-affinity ligands for proteins: SAR by NMR*. Science, 1996. **274**(5292): p. 1531-4.
3. Portoghese, P.S., D.L. Larson, L.M. Sayre, C.B. Yim, G. Ronsisvalle, S.W. Tam, and A.E. Takemori, *Opioid agonist and antagonist bivalent ligands. The relationship between spacer length and selectivity at multiple opioid receptors*. J Med Chem, 1986. **29**(10): p. 1855-61.

4. Hubble, J., *A model of multivalent ligand-receptor equilibria which explains the effect of multivalent binding inhibitors*. Mol Immunol, 1999. **36**(1): p. 13-8.
5. Halazy, S., M. Perez, C. Fourrier, I. Pallard, P.J. Pauwels, C. Palmier, G.W. John, J.P. Valentin, R. Bonnafous, and J. Martinez, *Serotonin dimers: application of the bivalent ligand approach to the design of new potent and selective 5-HT(1B/1D) agonists*. J Med Chem, 1996. **39**(25): p. 4920-7.
6. Shimohigashi, Y., T. Costa, H.C. Chen, and D. Rodbard, *Dimeric tetrapeptide enkephalins display extraordinary selectivity for the delta opiate receptor*. Nature, 1982. **297**(5864): p. 333-5.
7. Perez, M., P.J. Pauwels, C. Fourrier, P. Chopin, J.P. Valentin, G.W. John, M. Marien, and S. Halazy, *Dimerization of sumatriptan as an efficient way to design a potent, centrally and orally active 5-HT<sub>1B</sub> agonist*. Bioorg Med Chem Lett, 1998. **8**(6): p. 675-80.
8. Portoghese, P.S., G. Ronsisvalle, D.L. Larson, C.B. Yim, L.M. Sayre, and A.E. Takemori, *Opioid agonist and antagonist bivalent ligands as receptor probes*. Life Sci, 1982. **31**(12-13): p. 1283-6.

9. Portoghese, P.S., D.L. Larson, C.B. Yim, L.M. Sayre, G. Ronsisvalle, A.W. Lipkowski, A.E. Takemori, K.C. Rice, and S.W. Tam, *Stereostructure-activity relationship of opioid agonist and antagonist bivalent ligands. Evidence for bridging between vicinal opioid receptors*. J Med Chem, 1985. **28**(9): p. 1140-1.
10. Portoghese, P.S., H. Nagase, K.E. MaloneyHuss, C.E. Lin, and A.E. Takemori, *Role of spacer and address components in peptidomimetic delta opioid receptor antagonists related to naltrindole*. J Med Chem, 1991. **34**(5): p. 1715-20.
11. Portoghese, P.S., A. Garzon-Aburbeh, H. Nagase, C.E. Lin, and A.E. Takemori, *Role of the spacer in conferring kappa opioid receptor selectivity to bivalent ligands related to norbinaltorphimine*. J Med Chem, 1991. **34**(4): p. 1292-6.
12. Perez, M., C. Jorand-Lebrun, P.J. Pauwels, I. Pallard, and S. Halazy, *Dimers of 5HT1 ligands preferentially bind to 5HT1B/1D receptor subtypes*. Bioorg Med Chem Lett, 1998. **8**(11): p. 1407-12.



13. Jordan, B.A. and L.A. Devi, *G-protein-coupled receptor heterodimerization modulates receptor function*. Nature, 1999. **399**(6737): p. 697-700.
14. Cvejic, S. and L.A. Devi, *Dimerization of the delta opioid receptor: implication for a role in receptor internalization*. J Biol Chem, 1997. **272**(43): p. 26959-64.
15. Chan, J.S., J.W. Lee, M.K. Ho, and Y.H. Wong, *Preactivation permits subsequent stimulation of phospholipase C by G(i)- coupled receptors*. Mol Pharmacol, 2000. **57**(4): p. 700-8.
16. Yesilaltay, A. and D.D. Jenness, *Homo-oligomeric complexes of the yeast alpha factor pheromone receptor are functional units of endocytosis*. Mol. Biol. Cell, 2000. **11**: p. 2873-2884.
17. Overton, M.C. and K.J. Blumer, *G-protein-coupled receptors function as oligomers in vivo*. Curr Biol, 2000. **10**(6): p. 341-4.
18. Xue, C.B., A. McKinney, H.F. Lu, Y. Jiang, J.M. Becker, and F. Naider, *Probing the functional conformation of the tridecapeptide mating*

- pheromone of Saccharomyces cerevisiae through study of disulfide-constrained analogs. Int J Pept Protein Res, 1996. 47(3): p. 131-41.*
19. Yang, W., A. McKinney, J.M. Becker, and F. Naider, *Systematic analysis of the Saccharomyces cerevisiae alpha-factor containing lactam constraints of different ring size. Biochemistry, 1995. 34(4): p. 1308-15.*
  20. Eriotou-Bargiota, E., C.B. Xue, F. Naider, and J.M. Becker, *Antagonistic and synergistic peptide analogues of the tridecapeptide mating pheromone of Saccharomyces cerevisiae. Biochemistry, 1992. 31(2): p. 551-7.*
  21. Chan, R.K. and C.A. Otte, *Isolation and genetic analysis of Saccharomyces cerevisiae mutants supersensitive to G1 arrest by a factor and alpha factor pheromones. Mol Cell Biol, 1982. 2(1): p. 11-20.*
  22. David, N.E., M. Gee, B. Andersen, F. Naider, J. Thorner, and R.C. Stevens, *Expression and purification of the Saccharomyces cerevisiae alpha-factor receptor (Ste2p), a 7-transmembrane-segment G protein-coupled receptor. J Biol Chem, 1997. 272(24): p. 15553-61.*

23. Kippert, F., *A rapid permeabilization procedure for accurate quantitative determination of beta-galactosidase activity in yeast cells*. FEMS Microbiol Lett, 1995. **128**(2): p. 201-6.
24. Marsh, L., *Substitutions in the hydrophobic core of the alpha-factor receptor of Saccharomyces cerevisiae permit response to Saccharomyces kluyveri alpha-factor and to antagonist*. Mol Cell Biol, 1992. **12**(9): p. 3959-66.
25. Liu, S., L.K. Henry, B.K. Lee, S.H. Wang, B. Arshava, B. J.M., and F. Naider, *Position 13 analogs of the tridecapeptide mating pheromone from Saccharomyces cerevisiae: design of an iodinated ligand for receptor binding*. J. Peptide Res., 2000. **56**: p. 24-34.
26. Cheng, Y. and W.H. Prusoff, *Relationship between the inhibition constant (K<sub>i</sub>) and the concentration of inhibitor which causes 50 per cent inhibition (I<sub>50</sub>) of an enzymatic reaction*. Biochem Pharmacol, 1973. **22**(23): p. 3099-108.

27. Rath, S.K., F. Naider, and J.M. Becker, *Peptide analogues compete with the binding of alpha-factor to its receptor in Saccharomyces cerevisiae*. J Biol Chem, 1988. **263**(33): p. 17333-41.
  
28. Kitajima, Y., K.J. Catt, and H.C. Chen, *Enhanced biological activity of dimeric gonadotropin releasing hormone*. Biochem Biophys Res Commun, 1989. **159**(3): p. 893-8.
  
29. Posner, R.G., K. Subramanian, B. Goldstein, J. Thomas, T. Feder, D. Holowka, and B. Baird, *Simultaneous cross-linking by two nontriggering bivalent ligands causes synergistic signaling of IgE Fc epsilon RI complexes*. J Immunol, 1995. **155**(7): p. 3601-9.

## PART V

### CHARACTERIZATION OF A NOVEL GROUP OF SYNERGISTIC LIGANDS FOR Ste2p, THE $\alpha$ -FACTOR RECEPTOR IN *SACCHAROMYCES CEREVISIAE*.

Part V represents collaborative work with the laboratory of Dr. Fred Naider at the City University of New York, Staten Island. Keith Henry performed all the studies in the part with the exception of synthesis of the peptides used in this study. The peptide syntheses were carried out by members of Dr. Naider's lab.

## CHAPTER I

### INTRODUCTION

Ligand analogs have long been used to study structure-function relationships between receptors and their ligands. Ligand analogs can be structural analogs, which are structurally similar to the parent compound, or functional analogs, which are able to bind to the receptor but may be very different structurally from the native ligand. The structural changes of analogs can lead to stronger or weaker agonists or even antagonists and often times provide important insight into how the “natural” ligand interacts with its receptor. The use of ligand analogs has been especially beneficial in studies of G-protein coupled receptors (GPCRs). For example, a unique group of compounds have been discovered and termed *privileged structures* based on their ability to bind and activate a diverse range of GPCRs while being structurally dissimilar to the native ligand(s) [1]. The usefulness of privileged structures is in understanding the contact points between these compounds and the receptor and how these contacts are able to mimic the function of the native ligand. Use of privileged structures can lead to valuable information concerning structure-function relationships and possibly lead to chemical modification of the privileged structures or native ligand to result in compounds that have much greater specificity, potency and/or efficacy. This

phenomenon is true not only for small GPCR ligands such as monoamines but also for peptidyl ligands. For instance, the privileged structure concept was used to design clinically useful agonists (small synthetic peptides and non-peptidyl compounds L692,429 and MK-0677) for the human growth hormone secretagogue receptors [1-4]. These studies are only a few examples of how ligand analogs can be used to study structure-function relationships between receptors and ligands and how those relationships can be used to gain greater understanding of how GPCRs work.

While studying the effects of truncation on the biological activity and binding affinity of the tridecapeptide pheromone  $\alpha$ -factor [WHWLQLKPGQPMY] from *Saccharomyces cerevisiae*, a novel ligand analog was discovered that shows activity distinct from any other ligand known for any GPCR [5]. As each amino acid was removed from  $\alpha$ -factor, the resulting peptide was tested for agonistic and antagonistic activity. Truncation of Trp at position one resulted in a peptide with about 5-fold less biological activity. Removal of both Trp<sup>1</sup> and His<sup>2</sup> produced a ligand that was biologically inactive but was found to be a potent  $\alpha$ -factor antagonist with only 5-fold less binding affinity compared to  $\alpha$ -factor. Truncation of the Tyr at position 13 resulted in a peptide that was >40-fold less active than  $\alpha$ -factor in ability to arrest growth [5]. Unexpectedly, when a C-terminally truncated peptide lacking residues M<sup>12</sup> and Y<sup>13</sup> was tested for antagonism of  $\alpha$ -factor, the truncated peptide appeared to enhance the biological

activity of  $\alpha$ -factor in pheromone mediated growth arrest assays. Further testing showed the [desM<sup>12</sup>desY<sup>13</sup>]  $\alpha$ -factor peptide itself was unable to elicit biological response in yeast cells but when combined with  $\alpha$ -factor was able to enhance biological activity in growth arrest and mating projection formation assays. Due to its enhancing activity but lack of agonistic activity, the peptide was termed a synergist.

In competition binding assays, the synergist was unable to displace binding of [<sup>3</sup>H]  $\alpha$ -factor even when a 10,000-fold excess of synergist was added indicating that the synergist bound Ste2p very weakly, if at all. Binding analysis of  $\alpha$ -factor in the presence of synergist showed that the K<sub>d</sub> of  $\alpha$ -factor was not altered in comparison to  $\alpha$ -factor alone suggesting that the synergist did not alter the binding affinity of  $\alpha$ -factor for the Ste2p receptor. Biological testing of the synergist using  $\alpha$ -factor supersensitive strains RC629 (supersensitivity to  $\alpha$ -factor due to elimination of  $\alpha$ -factor inactivating protease, Bar1p) and RC631 (supersensitivity to  $\alpha$ -factor due to loss of G-protein activation suppressor protein Sst2p) [6] revealed that the synergist was a weak agonist only in an *sst2* mutant background. Mutants of Sst2p, the first RGS (regulator of G-protein coupled signaling) family member discovered [7-10], are 100 times more sensitive to  $\alpha$ -factor compared to wild-type cells and 5 times more sensitive than *bar1* supersensitive mutants. The synergist's ability to act as an agonist in the *sst2* strain background suggested the



synergist had at least a weak interaction with the Ste2p receptor undetectable by normal assays in wild type strains but unmasked in a supersensitive strain.

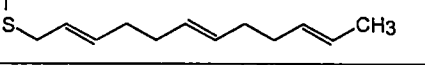

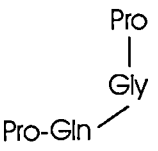
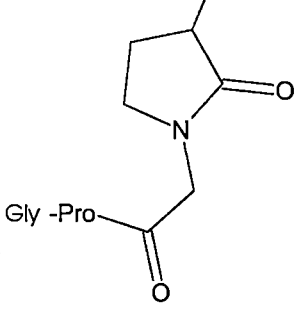
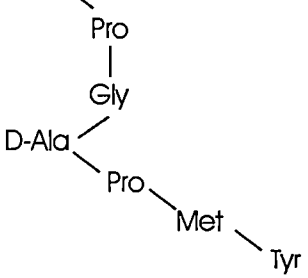
In addition to [desM<sup>12</sup>desY<sup>13</sup>]  $\alpha$ -factor synergist, other  $\alpha$ -factor analogs with synergistic activity have also been identified. It has been proposed that  $\alpha$ -factor forms a bend between residues 8 and 10 and that this bend is important for binding of  $\alpha$ -factor to Ste2p. To investigate whether this proposed bend was relevant to  $\alpha$ -factor activity several analogs of  $\alpha$ -factor were synthesized which were constrained into a bent conformation by substituting amino acids 8-10 with a  $\gamma$ -lactam moiety (termed D-Block<sup>8-10</sup>). [desM<sup>12</sup> desY<sup>13</sup> D-block<sup>8-10</sup>]  $\alpha$ -factor, was found to exhibit synergistic activity similar to [desM<sup>12</sup> desY<sup>13</sup>]  $\alpha$ -factor but like [desM<sup>12</sup> desY<sup>13</sup>]  $\alpha$ -factor, binding of [desM<sup>12</sup> desY<sup>13</sup> D-block<sup>8-10</sup>]  $\alpha$ -factor was not detectable in a competition binding assay with [<sup>3</sup>H]  $\alpha$ -factor .

Another synergist was discovered while testing alanine scanned analogs of the  $\alpha$ -factor peptide to investigate individual amino acid contribution to binding and biological activity of the pheromone. Each residue of  $\alpha$ -factor was replaced with either L-alanine or D-alanine, and one of these analogs, [D-Ala<sup>10</sup>]  $\alpha$ -factor, exhibited synergistic activity. Unlike [desM<sup>12</sup> desY<sup>13</sup>]  $\alpha$ -factor and [D-Block<sup>8-10</sup> desM<sup>12</sup> desY<sup>13</sup>]  $\alpha$ -factor which were truncated at the eleventh residue, [D-Ala<sup>10</sup>]  $\alpha$ -factor was a full-length  $\alpha$ -factor analog that had a replacement of Glu at position 10 with D-alanine. Interestingly, the commonality between the three

synergistic analogs is the altered C-terminal portion of the peptide as [desM<sup>12</sup> desY<sup>13</sup>]  $\alpha$ -factor and [D-Block<sup>8-10</sup> desM<sup>12</sup> desY<sup>13</sup>]  $\alpha$ -factor peptides lack the last two C-terminal residues and substitution of L-Ala with D-Ala in the [D-Ala<sup>10</sup>]  $\alpha$ -factor analog likely results in perturbed conformation of this  $\alpha$ -factor peptide (See Table 1 for ligand structures).

The synergists all show very similar characteristics. [D-Ala<sup>10</sup>]  $\alpha$ -factor like [desM<sup>12</sup> desY<sup>13</sup>]  $\alpha$ -factor and [D-Block<sup>8-10</sup> desM<sup>12</sup> desY<sup>13</sup>]  $\alpha$ -factor, was unable to displace [<sup>3</sup>H]  $\alpha$ -factor binding to Ste2p. However, in structure-function studies where cells harboring mutant Ste2p receptors were screened for their biological response to a variety of  $\alpha$ -factor analogs, [D-Ala10]  $\alpha$ -factor exhibited agonistic activity in cells expressing the Ste2p [F55V] mutant. [D-Ala10]  $\alpha$ -factor was able to arrest growth and induce expression of the FUS1-lacZ reporter gene, which is commonly used to monitor activation of the pheromone transduction pathway. Furthermore, [D-Ala10]  $\alpha$ -factor exhibited detectable binding to Ste2p [F55V] as the analog was able to compete for binding of [3H]  $\alpha$ -factor in the mutant receptor background with a Ki only 10-fold lower than that of  $\alpha$ -factor. The biological activity and binding affinity of [D-Ala10]  $\alpha$ -factor for this gain of function receptor mutant indicates a possible direct interaction between the C-terminus of the  $\alpha$ -factor peptide and residues around F55 in Ste2p and is providing

**Table 1. Ligand Structures**

A	a-factor	Tyr-Ile-Ile-Lys-Gly-Val-Phe-Trp-Asp-Pro-Ala-Cys-OCH <sub>3</sub>
		
B	α-factor	Trp-His-Trp-Leu-Gln-Leu-Lys
		
C	desMY Synergist	Trp-His-Trp-Leu-Gln-Leu-Lys
		
D	D-Block Synergist	Trp-His-Trp-Leu-Gln-Leu-Lys-HN
		
E	D-Ala <sup>10</sup> Synergist	Trp-His-Trp-Leu-Gln-Leu-Lys
		

NOTE: Biochemical data strongly supports the above conformation of alpha-factor. However, the remaining structures are an artistic representation to represent structure changes by amino acid substitution.

experimental direction for ongoing receptor mutagenesis and ligand analog studies looking at ligand-receptor interactions.

An understanding of how these synergistic ligands function to enhance  $\alpha$ -factor activity could provide important insight into peptidyl ligand-receptor interactions as well as regulation of signal propagation following receptor activation. This study details the further characterization of the synergist phenomenon in *S. cerevisiae*. Unless otherwise stated, the term synergist will refer to the peptide [desM<sup>12</sup> desY<sup>13</sup>]  $\alpha$ -factor.

## CHAPTER II

### MATERIALS AND METHODS

*Organisms.* Growth arrest assays were performed using (a) *S. cerevisiae* DK102 [*MATa ste2::HIS3 bar1 leu2 ura3 lys2 ade2 his3 trp1*] cells transformed with the pNED1 plasmid which overexpresses the Ste2p receptor [11], (b) RC629 [*MATa sst1-2*] (supersensitive to pheromone due to deletion of the  $\alpha$ -factor protease gene *BAR1* which is allelic to *SST2*) [6] and (c) RC631 [*MATa sst2-1*] (supersensitive to  $\alpha$ -factor through deletion of the RGS protein *sst2*) [6]. Rate of association and dissociation studies of  $\alpha$ -factor for Ste2p were performed using membrane preparations [11] from *S. cerevisiae* BJ2168 [*MATa prc1-407 prb1-1122 pep4-3 leu2 trp1 ura3-52*] cells transformed with pNED1. Saturation and competition binding assays with [ $^3\text{H}$ ]  $\alpha$ -factor were performed using *S. cerevisiae* A1111 [*MATa STE2 bar1 far1 ura3 leu2 sst2 his4 lys2 TRP1 tyr1 ade2*] cells provided by Mark Dumont, University of Rochester as three independent isolates designated A1111A, A1111B and A1111C.

*Determination of  $k_{on}$  for  $\alpha$ -factor to Ste2p.* Membrane preparations from exponentially growing BJ2168pNED1 cells were suspended in YM1+i [12] to 24  $\mu\text{g/ml}$  of protein with or without  $8 \times 10^{-6}\text{M}$  [ $\text{desM}^{12}\text{Y}^{13}$ ]  $\alpha$ -factor and allowed to equilibrate to 18°C for 10 minutes. 540  $\mu\text{l}$  of the membrane suspension was

combined with 60  $\mu$ l of [ $^3$ H]  $\alpha$ -factor [ $2 \times 10^{-7}$ M] in a siliconized microfuge tube and vortexed. At 0.25, 0.5, 1, 1.5, 2, 2.5, 3, 3.5, 4, and 4.5 minutes, 50  $\mu$ l was removed and added to 2 ml of ice cold YM1+i and filtered over 25 mm GF/F Whatman glass fibre filters pre-blocked with 0.3% (v/v) polyethyleneimine. The filter was washed twice with 2 ml of ice cold YM1+i. Filters were air dried, placed in 2ml of scintillation cocktail, allowed to dissolve for at least 2 hours and counted on a Wallac Liquid Scintillation Counter Model 1409.

*Determination of  $k_{off}$  for  $\alpha$ -factor to Ste2p.* Membrane preparations from exponentially growing BJ2168pNED1 cells were suspended in YM1+i to 2200  $\mu$ g/ml of protein with or without  $8 \times 10^{-6}$ M desMY synergist. [ $^3$ H]  $\alpha$ -factor [ $7 \times 10^{-8}$ M] was added and reaction allowed to equilibrate to 18°C for 20 minutes. The reaction (0.5ml) was diluted into 100 ml of YM1+i pre-equilibrated to 18°C with constant stirring using a magnetic stir bar. At times 0.5, 2, 4, 8, 10, 15, 20 30, 45, 60, 90 and 120 minutes post dilution, one ml was added to 2 ml of ice cold YM1+i and filtered over 25 mm GF/F Whatman glass fiber filters pre-soaked for 2 hours with 0.3% (v/v) polyethyleneimine. The filter was washed twice with 2 ml of ice cold YM1+i. Filters were air-dried, placed in 2ml of Cytoscint scintillation cocktail (ICN) allowed to dissolve for at least 2 hours and counted on a Wallac Liquid Scintillation Counter Model 1409. Percent bound radiolabel was calculated by averaging 0.5 minute values and setting that time point to 100%. All

other time points were normalized to the 0.5 minute timepoint. Assay was performed in triplicate.

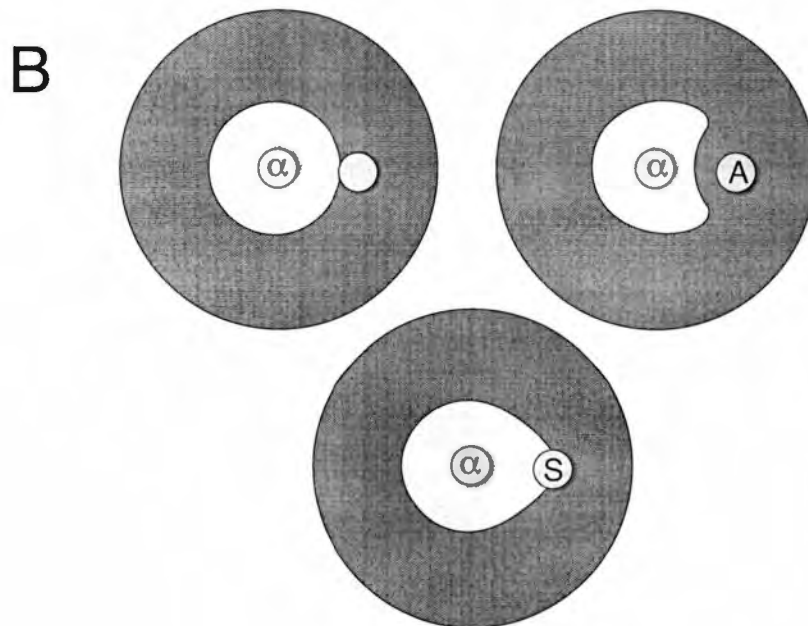
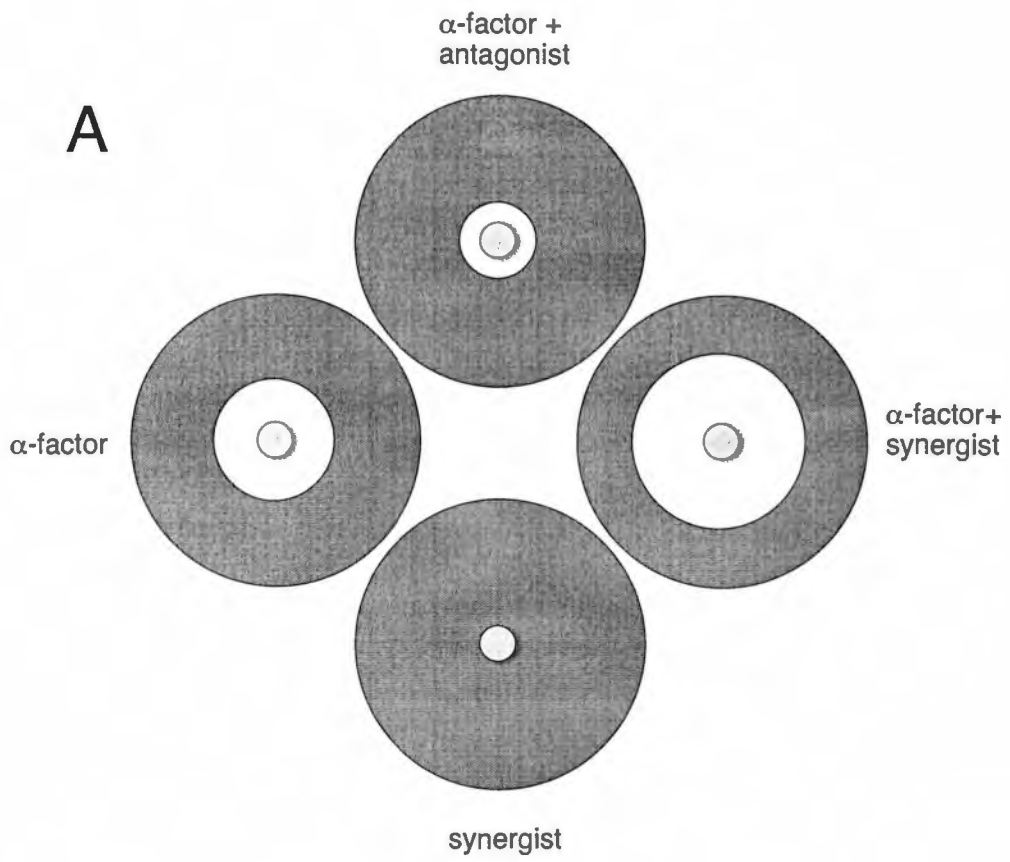
*Growth Arrest Assays.* Paper disks (concentration disks from Difco), 8 mm in diameter, were saturated with 10  $\mu$ l portions of peptide solutions at various concentrations and placed onto the overlay. Synergist peptide was either (1) added to the same disk as  $\alpha$ -factor and placed on a lawn of cells or (2) spotted on a disk and placed next to a disk containing  $\alpha$ -factor such that the synergist containing disk was near the periphery of the expected  $\alpha$ -factor induced zone of inhibition (Figure 1). The plates were incubated at 30<sup>0</sup>C for 24 -36 h and then observed for clear zones (halos) around the disks. The data were expressed as the diameter of the halo including the diameter of the disk. Therefore, a minimum value for growth arrest is 9 mm, which represents the disk diameter (8 mm) and a small zone of inhibition. All assays were carried out at least three times with no more than a 2 mm variation in halo size at a particular amount applied for each peptide. The values reported represent the mean of these tests.

*Trypsinization Protection Assays.* Assays were performed as described by Jenness [13] with only slight alteration. For the purpose of this dissertation the full protocol is described below. BJ2168pNED1 membranes prepared as above were pelleted in a microfuge at top speed, washed once and resuspended to 0.8 mg/ml of protein in 500  $\mu$ l of digestion buffer (1mM Mg Acetate; 0.1 mM DTT; 0.1 mM EDTA; 7.6% glycerol; 10 mM MOPS, pH 7.0). 100  $\mu$ l portions of the

**Figure 1. Illustration of growth arrest assays used to characterize the activity of  $\alpha$ -factor analogs.**

Exogenous application of  $\alpha$ -factor results in growth arrest of cells in affected area. Dark circles represent lawns of cells. Small gray circles represent paper disks to which peptide has been applied. White circles represent zones of growth inhibition. Panel A illustrates typical results obtained when a peptide analog and  $\alpha$ -factor are applied to the same disk. Antagonists compete with  $\alpha$ -factor to give a reduced growth arrest response as shown by a decrease in halo size. Co-application of synergist and  $\alpha$ -factor results in enhanced growth arrest as noted by the larger zone of growth inhibition while synergist alone results in no growth arrest. Panel B shows an alternative method for characterizing analog activity.  $\alpha$ -factor is applied to a disk ( $\alpha$ ) and a separate disk containing an analog is placed a predetermined distance away from the  $\alpha$ -factor disk such that it will be at the edge of the expected  $\alpha$ -factor zone of growth inhibition. When a disk containing an  $\alpha$ -factor antagonist (A) is placed adjacent to the disk containing  $\alpha$ -factor,  $\alpha$ -factor mediated growth arrest is inhibited around the disk containing the antagonist resulting in a bean shaped halo. When synergist (S) is used in place of antagonist, the halo around the disk containing  $\alpha$ -factor extends towards the disk containing synergist indicating enhanced growth arrest where synergist and  $\alpha$ -factor are present together.





membranes were then transferred to four microfuge tubes.  $\alpha$ -factor at  $2 \times 10^{-6}$  M and synergist at  $2 \times 10^{-4}$  M were added. The amounts of  $\alpha$ -factor and synergist were chosen based on amounts used in growth arrest assays where synergy was detected. Trypsin was added to a final concentration of 30  $\mu$ g/ml. At various time points, 20  $\mu$ l of reaction was transferred to a microfuge tube containing 3.25  $\mu$ l of 0.1N HCl to halt the digestion. 10  $\mu$ l of Laemmli sample buffer [14] was added and samples run on 10% SDS-PAGE gels (35 mAmps) and separated proteins were electrophoretically transferred (1 hour at 400 mAmps) to PVDF membranes (Immobilon P, Millipore) using a modified Towbin Transfer Buffer (25 mM Tris; 200 mM glycine; 15% methanol; 0.01% SDS) in a Hoeffer tank blotter. Western analysis to detect N-terminal fragments of Ste2p was performed by probing blotted membranes with polyclonal antibodies (diluted 1/50 in tris buffered saline plus tween [TBST, 20 mM Tris; 500 mM NaCl, and 0.1% Tween-20]) against the first 60 amino acids of Ste2p. The antibodies were provided by James Konopka [15]. Goat anti-rabbit antibodies from Promega diluted 1/15,000 in TBST were used as secondary antibodies and the resulting complex was detected using ECL (enhanced chemiluminescence) reagent (Amersham Pharmacia Biotech) and exposed to X-ray film.

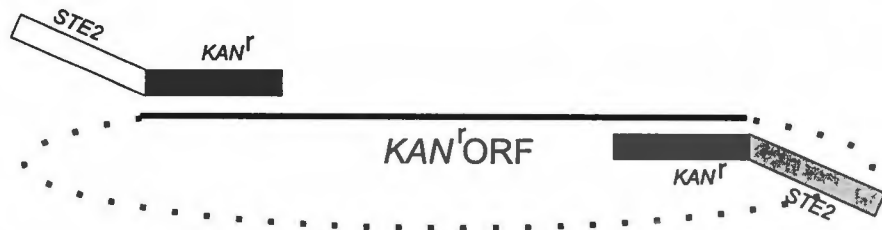
*Deletion of Ste2p in RC631.* Deletion of *STE2* was carried out by replacing the ORF with the *kan<sup>r</sup>* dominant selectable marker using the pUG6 vector as the source for *kan<sup>r</sup>* gene [16] (Figure 2). Forward and reverse binary oligonucleotide

**Figure 2. Schematic for disruption of the *STE2* open reading frame using a PCR amplified disruption cassette of the selectable *kan<sup>r</sup>* resistance gene.**

PCR primers were designed to amplify the kanamycin resistance gene (*KAN<sup>r</sup>*).

These primers also contain homologous sequence of the *STE2* gene allowing the amplified product to be transformed into yeast cells and recombine with the chromosomal copy of *STE2* to replace the *STE2* open reading frame with the selectable marker gene *kan<sup>r</sup>*.

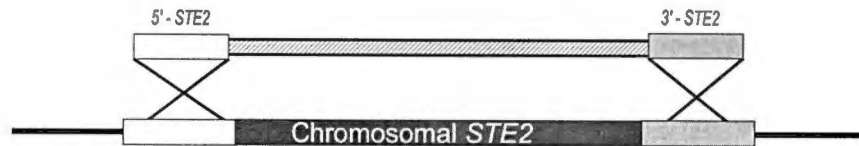
pUG6  
Vector



↓ PCR



↓ Transformation



↓ Recombination



primers were constructed which contained homologous sequence to the ends of the *STE2* ORF and priming sequence to amplify the *kan<sup>r</sup>* gene from the pUG6 vector resulting in the replacement of the entire *STE2* gene. The forward and reverse primers (*STE2* sequence - all caps; pUG6 sequence - lower case) used to amplify the *STE2* deletion cassette were: Forward-ATGTCTGATGCGGCTCCTTCATTG AGCAATCTATTTTATG cagctgaagcttcgtacgc and Reverse-TCATAAATTATTA TTATCTTCAGTCCAGAACTTTCTGGCTgcataggccactagtgatct. PCR amplification using these primers yielded a product with the expected fragment size. RC631 cells transformed with this fragment were screened for resistance to G418. Three candidate transformants were confirmed by PCR analysis of genomic DNA using check primers (Forward – CACCGTTAAGAACCATATCCA; Reverse – CGAAATTACTIONTTTTCAAAGCC). PCR confirmed deletion candidates were then tested for biological activity in an  $\alpha$ -factor growth arrest assay. KHSYN1, one of the transformants confirmed to be a null mutant for *STE2* was tested further against response to synergist in the presence and absence of  $\alpha$ -factor in a dose response growth arrest assay as previously described.

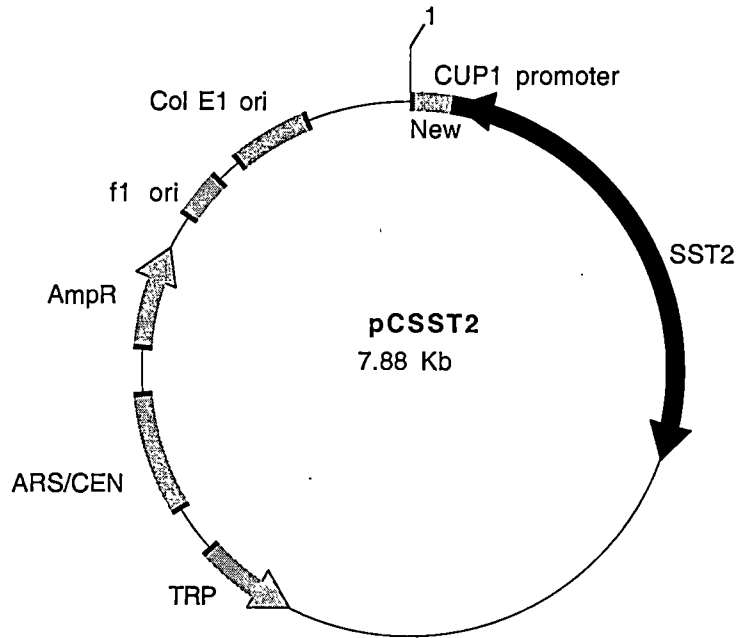
*Saturation Binding Assays.* Assays were performed using tritiated  $\alpha$ -factor prepared by reduction of [dehydroproline<sup>8</sup>, Nle<sup>12</sup>]  $\alpha$ -factor as described previously [12]. Cells were grown overnight at 30°C to a cell density of 1 x 10<sup>7</sup> cells/ml and harvested by centrifugation for 10 minutes 5,000 x g at 4°C. Cell pellets were

washed twice with ice-cold potassium phosphate buffer with inhibitors (PPBi; pH 6.24) containing 10 mM TAME, 10 mM sodium azide, 10 mM potassium fluoride, 1% BSA (fraction IV) [17] and placed at 4°C. Tritiated  $\alpha$ -factor was added to siliconized microfuge tubes such that the final density of cells was  $6.25 \times 10^7$  cells/ml. The reaction tubes containing cells and labeled peptide were incubated at room temperature for 30 minutes. Following incubation, the reaction mixes were transferred (3 x 200  $\mu$ l) to a 96 well plate and filtered and washed over glass fiber filtermats using the Standard Cell Harvester (Skatron Instruments, Sterling, VA). Filters were placed in scintillation vials for counting.

*Construction of SST2 Overexpression Vector.* The plasmid pCSST2 (Figure 3), which regulates expression of *SST2* by copper titration in the medium, was created by inserting the *SST2* gene into the copper inducible expression vector, YATAG200 [18-20], using an in vivo ligation method as described by Degryse *et al.* [21]. The primers (Forward 5'-ccaccatgtaccatacagacgttccagactacgctgtggat aaaaataggacgtt - 3' and Reverse - 5'-cctttcttagcagaaccggccttgaattgctcagacctga agatgagtaagactct - 3' ) were used to amplify the integration cassette from strain RC629 [6]. The integration cassette was used to transform strain LM23-3AZ (*sst2*) using the Geitz protocol [22]. Transformants were initially screened by their ability to grow on medium lacking Tryptophan (expressed from vector) and subsequently by their sensitivity to  $\alpha$ -factor in a halo assay (transformants which showed greater than a 10-fold decrease in sensitivity were believed to contain a

**Figure 3. Map of pCSST2 plasmid used for overexpression of *SST2*.**

The pCSST2 plasmid was constructed by inserting the *SST2* gene into the YATAG200 yeast expression vector [Lieberman, 1995, genbank submission] such that the expression of *SST2* was controlled by the *CUP1* promoter which is induced by  $\text{CuSO}_4$ .





functional *SST2* gene. Plasmids were recovered from yeast and shuttled to *E. coli* using a Zymoprep kit from Zymo Research. Plasmid DNA from *E. coli* transformants was prepared using a Qiagen Mini-Prep Kit (Qiagen) and sequenced using an automated DNA sequencing (ABI Fluorescence DNA Sequencer).

*SST2 Overexpression Studies.* Strains LM23-3AZ [*MATa bar1 FUS1-lacZ trp1 met1 ura3-52/URA3*] (from Lorraine Marsh, Albert Einstein University, New York and JE114-8A [*MATa leu2-3, 112 ura3-52 trp1 his3Δ1 sst2-1 ste2Δ::LEU2*] (from K. Blumer) [23] were used in these assays. Strains transformed with pCSST2 were tested on CAA+AU medium (0.2% Casamino Acids; 2% glucose; 2% agar; 6.7g/L Yeast Nitrogen Base without amino acids; 20 μg/ml Adenine, 20 μg/ml Uracil) containing increasing amounts of copper sulfate ( $\text{CuSO}_4 \cdot 5\text{H}_2\text{O}$ ). Tryptophan at 20 μg/ml was added to the medium for growth of control strains lacking the pCSST2 plasmid. Halo assays were performed as described above with  $\alpha$ -factor or  $\alpha$ -factor co-applied with the synergistic [*desM*<sup>12</sup> *desY*<sup>13</sup>]  $\alpha$ -factor analog.

## CHAPTER III

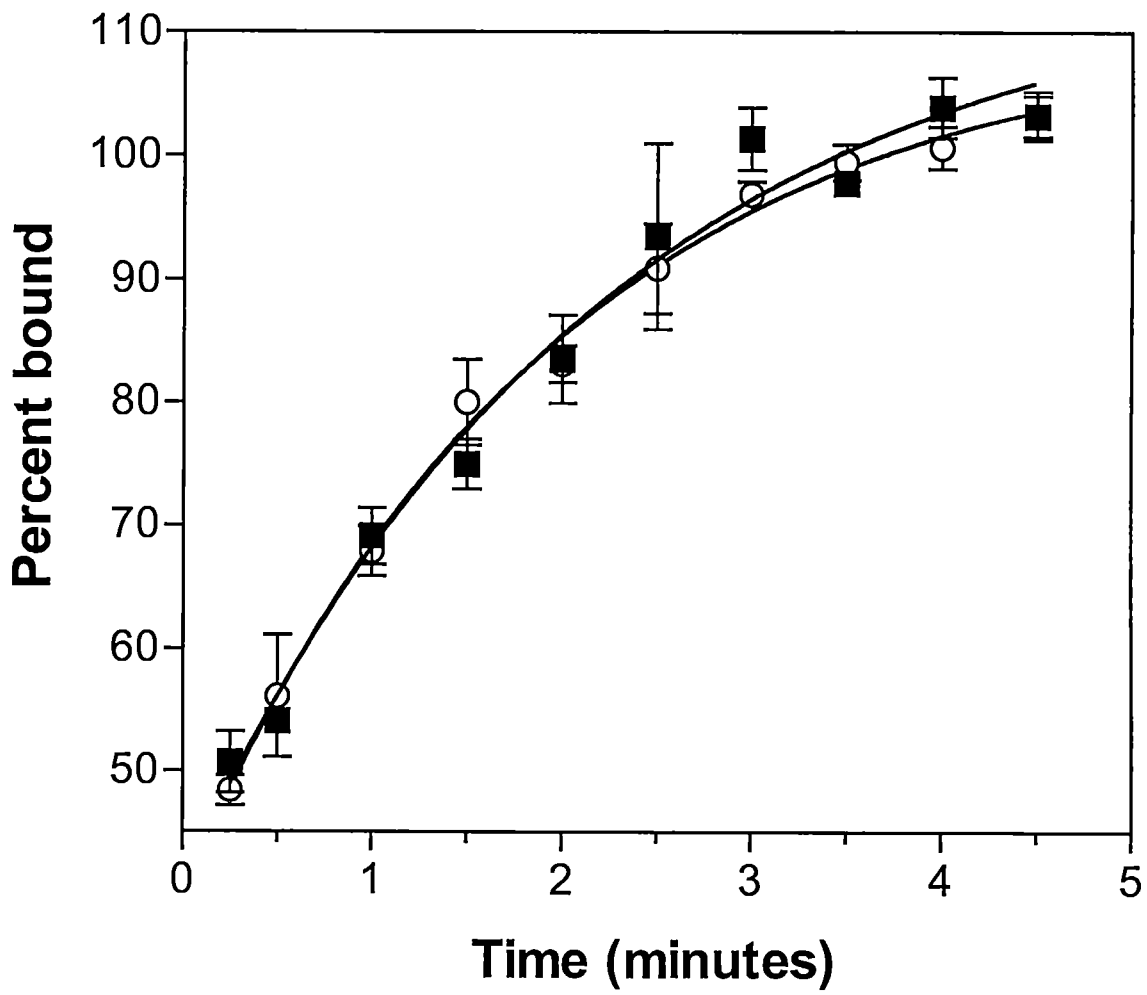
### RESULTS

Initial characterization of the synergist peptide [desM<sup>12</sup> desY<sup>13</sup>]  $\alpha$ -factor by Eriotou-Bargiota *et al.* [5] indicated that the K<sub>d</sub> of  $\alpha$ -factor did not change in the presence or absence of the synergist peptide. The dissociation constant K<sub>d</sub> is related by the equation  $K_d = k_{off}/k_{on}$  such that the K<sub>d</sub> is a ratio of the rates of ligand dissociation and association to the receptor. Therefore, it is possible that the synergist could proportionally change the  $k_{on}$  and  $k_{off}$  rates in such a way as to modulate how long the receptor is bound and therefore activated by  $\alpha$ -factor without changing the observed K<sub>d</sub>. Therefore, the rates of association and dissociation of  $\alpha$ -factor were determined in the presence and absence of the [desM<sup>12</sup> desY<sup>13</sup>]  $\alpha$ -factor peptide.

*Synergist effect on rate of association of  $\alpha$ -factor to Ste2p.* To determine whether synergist affected the  $k_{on}$  of  $\alpha$ -factor, the rate of association of [<sup>3</sup>H] $\alpha$ -factor was examined in the presence and absence of synergist. Binding of  $\alpha$ -factor alone showed a characteristic curve representative of exponential binding that leveled off by four minutes indicating saturation conditions (Figure 4). There was no apparent difference in association of  $\alpha$ -factor when the same experiment was carried out in the presence of  $8 \times 10^{-6}$  M synergist ( $8 \times 10^{-6}$  M was sufficient to

**Figure 4. Rate of association of [<sup>3</sup>H]  $\alpha$ -factor in the presence and absence of synergist ([desM<sup>12</sup>W<sup>13</sup>]  $\alpha$ -factor).**

BJ2168pNED1 membranes were incubated with  $2 \times 10^{-8}$  M [<sup>3</sup>H]  $\alpha$ -factor with or without synergist ( $8 \times 10^{-6}$  M). Aliquots were removed over time and counted for radioactivity associated to Ste2p. CPM values were normalized to percent bound by setting Bmax values to 100%. The plot shows percent bound radioactivity versus time. The plots represent  $\alpha$ -factor (■) and coincubation of  $\alpha$ -factor and synergist (○). Data were fit to exponential association binding equation (see text).



give enhanced activity in halo assays [5]. The curves shown in Figure 4 are virtually superimposable indicating that the synergist has no detectable effect on the  $k_{on}$  of  $\alpha$ -factor for Ste2p. The experiment was performed in triplicate under temperature controlled conditions with similar results. However, the relatively high affinity of the  $\alpha$ -factor peptide ( $9 \times 10^{-9}$  M) would likely prevent small changes in  $k_{on}$  from being observed as the rate of association of high affinity ligands is faster than the rate of peptide diffusion. Therefore, an effect by addition of the synergist may not be detectable. However, due to the relationship between  $K_d$ ,  $k_{on}$ , and  $k_{off}$ , measurement of  $k_{off}$  may be able to pick up differences that cannot be seen by measuring  $k_{on}$  alone.

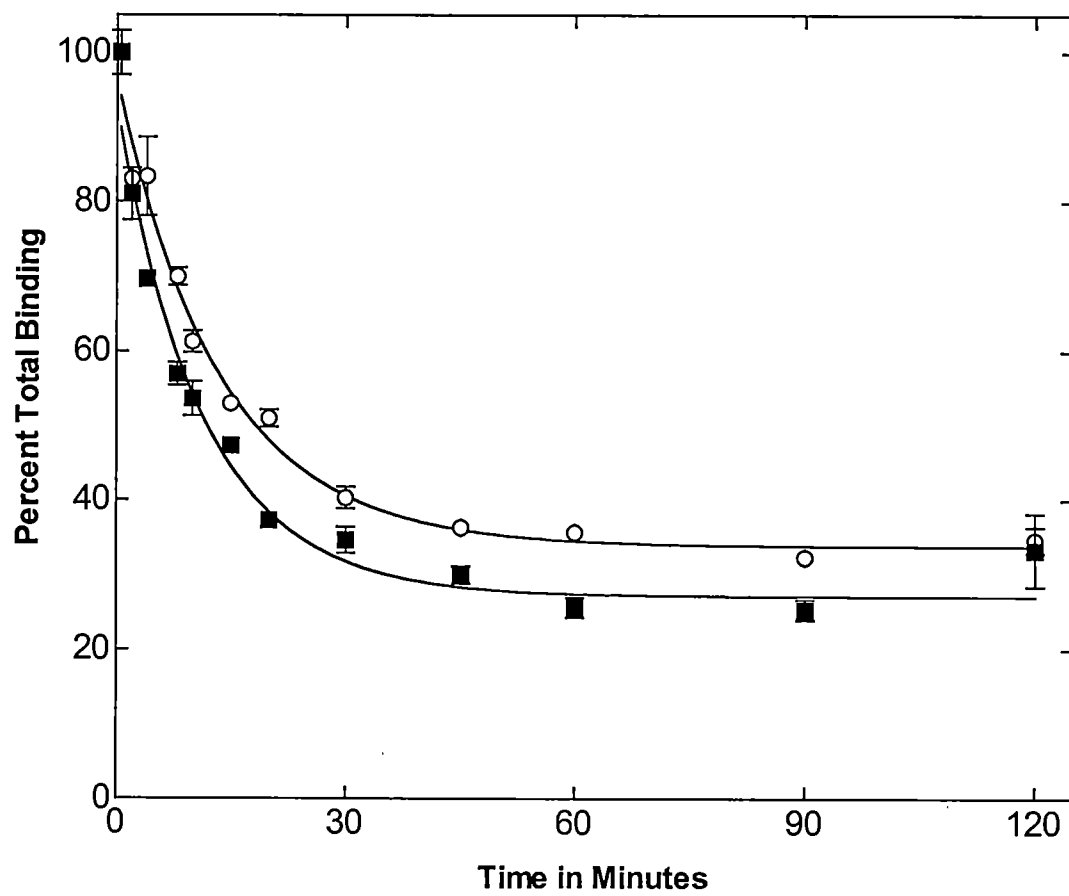
Another hypothesis for synergist action is that the synergist somehow functions to create a higher proportion of ligand-binding competent receptors and thereby increases signaling potency. However, the  $B_{max}$  (binding maximum) of  $\alpha$ -factor is equivalent in the presence or absence of synergist. The  $B_{max}$  is a representation of the total number of  $\alpha$ -factor molecules bound to Ste2p. Previous binding analysis of Ste2p has shown that each receptor molecule only binds one molecule of  $\alpha$ -factor[24]. The fact that the  $B_{max}$  values are the same in samples with and without synergist indicates that the synergist does not act by allowing more receptors to bind  $\alpha$ -factor.

*Synergist effect on rate of dissociation of  $\alpha$ -factor from Ste2p.* To test whether synergist had an effect on the rate of dissociation of  $\alpha$ -factor from the Ste2p receptor, membranes from BJ2168pNED1 were incubated with [ $^3\text{H}$ ]  $\alpha$ -factor under saturating conditions and subjected to “infinite” dilution. The amount of bound ligand was monitored over time and the resulting graph is shown in Figure 5. The graph was analyzed by graphing software (Prism 3 for Macintosh, Graphpad, Inc) using a one phase exponential decay equation. The rate of dissociation of  $\alpha$ -factor alone was  $0.088 (\pm 0.0086) \text{ min}^{-1}$ , while the K for  $\alpha$ -factor plus synergist was  $0.074 (\pm 0.0048) \text{ min}^{-1}$  indicating that synergist has no statistically discernable affect at a 95% competency level on dissociation of  $\alpha$ -factor from the receptor. This can be visualized by noting the similarity in slope of the lines at any point along the length of the curves. The slight difference between the plateaus of the plots is likely due to small differences in total protein amounts in each sample.

*Trypsinization Protection Assays.* A previous study by Bukusoglu *et al.* [13] showed that trypsin mediated fragmentation patterns of the Ste2p receptor were distinctly different in the presence and absence of the  $\alpha$ -factor ligand. Additionally, trypsinization of Ste2p in the presence of a known  $\alpha$ -factor antagonist, [desW<sup>1</sup> desH<sup>2</sup>]  $\alpha$ -factor, resulted in a fragmentation pattern dissimilar to that seen in the presence of  $\alpha$ -factor or in the absence of any ligand. This study indicated that trypsin mediated fragmentation of Ste2p receptor can be used to

**Figure 5. Rate of dissociation of [<sup>3</sup>H]  $\alpha$ -factor in the presence and absence of synergist ([desM<sup>12</sup>W<sup>13</sup>]  $\alpha$ -factor).**

BJ2168pNED1 membranes were incubated with  $7 \times 10^{-8}$  M [<sup>3</sup>H]  $\alpha$ -factor with or without synergist ( $8 \times 10^{-6}$  M) and allowed to come to equilibrium binding conditions. Reaction was infinitely diluted and aliquots were removed over time and counted for radioactivity associated to membranes. CPM values were normalized to percent bound by setting the first time point to 100%. The plot shows percent bound radioactivity versus time. The plots represent  $\alpha$ -factor (■) and coincubation of  $\alpha$ -factor and synergist (○). The plots were fit to an exponential decay equation to determine K<sub>off</sub> (see text).

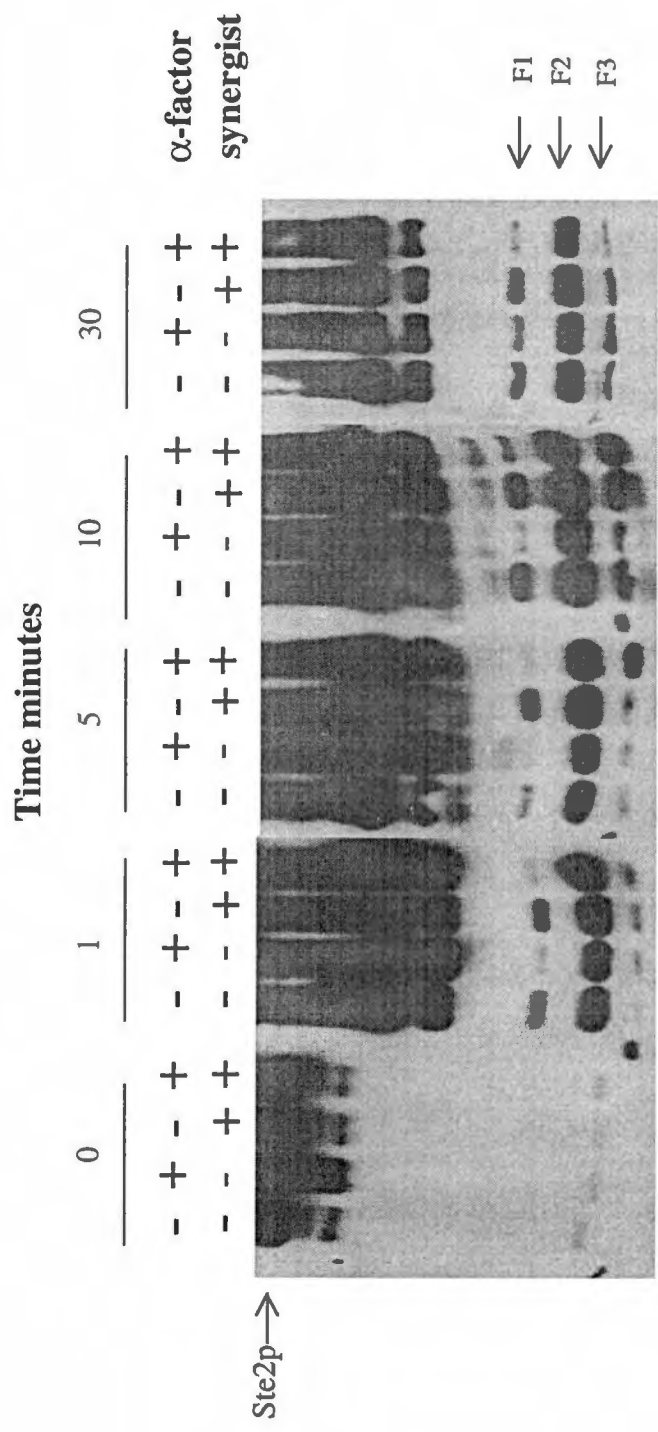




detect ligand induced conformational changes in the receptor. Using this procedure, the synergist peptide was tested to determine if the synergist could induce a conformational change in the receptor distinct from unbound or  $\alpha$ -factor bound receptor. In these studies, BJ2168pNED membranes were incubated with  $\alpha$ -factor ( $2 \times 10^{-6}$  M) or  $\alpha$ -factor plus synergist ( $2 \times 10^{-4}$  M) and allowed to come to saturation (45 minutes). The membranes were then treated with TPCK-treated trypsin (TPCK treatment eliminates chymotrypsin activity). The polyclonal antibodies used in Western analysis of the Ste2p fragments were the same as those used by Bukusoglu *et al.* [13] and are specific for the first 60 amino acids of Ste2p. Because the antibodies are specific for the N-terminus, only fragments of Ste2p containing all or part of the first 60 amino acids will be detected. The assay was repeated at least three times. A representative Western blot is shown in Figure 6. The Western blot was overexposed in order to visualize the smaller Ste2p fragments following digestion. At time point zero, the majority of Ste2p is intact and can be seen in its monomeric form. Two bands which are likely degradation products of Ste2p can be seen at time zero. These Ste2p degradation products are commonly seen by others during this membrane purification process [11]. After one minute of trypsin digestion, Ste2p is cleaved into several smaller fragments. The only fragment that shows appreciable difference between the positive (with  $\alpha$ -factor) and negative (without  $\alpha$ -factor) control is designated by F1 and is consistent with results from Bukusoglu *et al.* [13]. The difference in

**Figure 6. Western blot analysis of trypsin digest of Ste2p over time in the presence and absence of  $\alpha$ -factor and/or synergist.**

BJ2168pNED1 membranes were incubated with peptides and subjected to trypsin digestion aliquots were removed over time, separated on by SDS-PAGE and transferred to PVDF membrane for Western analysis with a polyclonal antibody which recognizes the first 60 amino acids of Ste2p. Addition of synergist ( $8 \times 10^{-6}$  M) and/or  $\alpha$ -factor ( $2 \times 10^{-6}$  M) is designated by plus symbols. Trypsin incubation times are indicated on figure. Full length Ste2p and the F1, F2, and F3 Ste2p trypsin digestion fragments designated by arrows.



intensity of this band can be seen clearly at 1, 5, and 10 minutes post addition of trypsin. At 30 minutes, the difference becomes much less apparent. According to Bukusoglu *et al.* [13], the low intensity of the F1 band in the  $\alpha$ -factor treated samples at 1, 5 and 10 minutes was due to the F1 fragment being more susceptible to trypsin cleavage when  $\alpha$ -factor was bound to Ste2p resulting in rapid conversion of F1 to the smaller fragments. However, when  $\alpha$ -factor was not bound, fragment F1 was less susceptible to cleavage thereby increasing its half-life and resulting in a build-up. As more and more of the larger fragments are cleaved, the build-up of fragment F1 will slowly reduce and therefore result in less difference between the  $\alpha$ -factor bound and unbound samples which is seen at the 30 minute time point.

When synergist was added alone a pattern similar to the negative control (without  $\alpha$ -factor) was observed, indicating that synergist alone was unable to cause the same conformational change as that caused by  $\alpha$ -factor. Finally, synergist and  $\alpha$ -factor when added simultaneously gave similar results as adding  $\alpha$ -factor alone indicating that when combined, the two ligands do not cause a change in the receptor distinct from that of  $\alpha$ -factor alone.

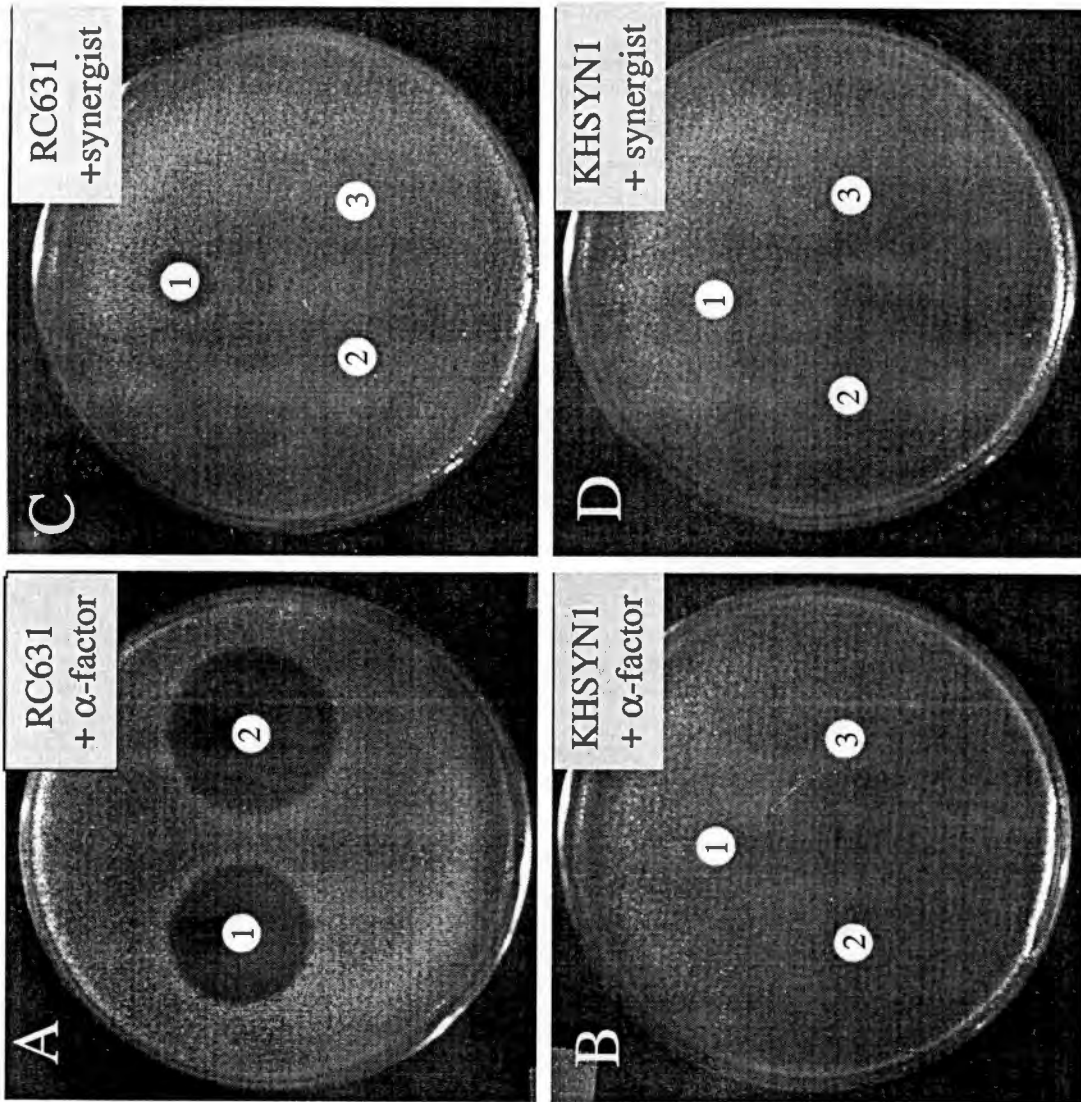
*Deletion of Ste2p in RC631.* One of the previous observations made by Eriotou-Bargiota *et al.* [5] was that the synergist has agonistic activity by itself in an *sst2* deficient strain. In this same report, it was shown that an *sst2* mutant strain that harboured a temperature sensitive *ste2<sup>ts</sup>* gene responded to synergist only at

the permissive temperature ( $STE2^+$ ) and not at the restrictive temperature. In order to further verify that the synergist acts through Ste2p, and that the lack of activity of the synergist was not due to temperature variations in the assays studying the Ste2p<sup>ts</sup> mutant, the *STE2* gene was deleted from RC631, an *sst2* mutant strain. The resulting strain KHSYN1 (*ste2 sst2*) was tested for response to synergist and  $\alpha$ -factor in a growth arrest assay. Photographs of the plates are shown in Figure 7. Robust halos can be seen around disks spotted with either 1 or 5  $\mu$ g of  $\alpha$ -factor on a lawn of RC631 cells (Figure 7A) whereas no halos can be seen around disks spotted with 5, 10 or 40  $\mu$ g of  $\alpha$ -factor on a lawn of KHSYN1 cells (Figure 7B). A similar pattern to that seen in Figure 7B can be seen when synergist is used instead of  $\alpha$ -factor (Figure 7D). A small halo of growth arrest is observed around the disk spotted with 32  $\mu$ g of synergist on the lawn of RC631 cells (Figure 7C) but no halo is observed with the KHSYN1 cells even at 32  $\mu$ g of synergist (Figure 7D). The inability of KHSYN1 to respond to both  $\alpha$ -factor and synergist are compelling data indicating that KHSYN1 has integrated the *kan<sup>r</sup>* cassette at the *STE2* locus. In addition, this data corroborates the previous findings with the temperature sensitive mutant that Ste2p is required for agonistic activity of the synergist in *sst2* minus strains.

*Effect of SST2 overexpression on synergist activity.* Based on current data discussed above, the synergist has no detectable binding affinity for the wild-type Ste2p receptor and does not have an effect on the binding of  $\alpha$ -factor to Ste2p as

**Figure 7. Biological testing of KHSYN1 Ste2p deletion strain using growth arrest assay.**

Sterile concentration disks were spotted with peptide and placed on a lawn of cells and incubated for 24-36 hours. **A-** RC631 cells tested with (1) 1  $\mu\text{g}$  and (2) 5  $\mu\text{g}$  of  $\alpha$ -factor. **B -** KHSYN1 cells tested with (1) 40  $\mu\text{g}$  (2) 10  $\mu\text{g}$  and (3) 5  $\mu\text{g}$  of  $\alpha$ -factor. **C-** RC631 tested with (1) 32  $\mu\text{g}$  (2) 10  $\mu\text{g}$  and (3) 5  $\mu\text{g}$  of [desM<sup>12</sup>desY<sup>13</sup>]  $\alpha$ -factor synergist. **D -** KHSYN1 cells tested with (1) 32  $\mu\text{g}$  (2) 10  $\mu\text{g}$  and (3) 5  $\mu\text{g}$  of [desM<sup>12</sup>desY<sup>13</sup>]  $\alpha$ -factor synergist.



neither the  $K_d$ ,  $k_{on}$ ,  $k_{off}$  nor  $B_{max}$  for  $\alpha$ -factor change in the presence or absence of synergist. The agonistic activity of the synergist in an *sst2* null background is evidence that the synergist may act as a very weak agonist. Therefore, it is possible that during initial binding of  $\alpha$ -factor to Ste2p, Sst2p becomes limiting after a certain threshold number of receptors have been activated. Under these conditions, Ste2p receptors could be activated by both  $\alpha$ -factor and synergist because there would be no unsequestered Sst2p available to prevent synergist bound receptors from signaling. Based on these observations the following hypothesis was proposed: Overexpression of *SST2* would reduce and eventually eliminate synergist activity. Therefore, the following experiment was designed to test whether overexpression of Sst2p alters the action of the synergist.

Overexpression of *SST2* was accomplished by cloning the *SST2* open reading frame into the YATAG200 plasmid such that *SST2* expression was driven by the copper inducible promoter *CUP1* [25]. The resulting plasmid was named pCSST2 (see map in Figure 3). pCSST2 was transformed into strain LM23-3AZ (*bar1*) for use in growth arrest and *FUS1*-lacZ assays. LM23-3AZ [pCSST2] transformed cells were plated on media containing various concentrations of  $CuSO_4$  and tested for response to synergist and  $\alpha$ -factor in a growth arrest assay. The diameter of the resulting zones of growth inhibition were measured and plotted versus the  $CuSO_4$  concentration used in the medium. The results are shown in Table 2.

Enhancement of growth arrest by the synergist can be seen by comparing columns



**Table 2. Effect of Overexpression of SST2 on action of synergist and  $\alpha$ -factor in growth arrest assay with strain LM23-3AZ.**

CuSO <sub>4</sub> Conc. [ $\mu$ M]	LM23-3AZ <sup>a</sup>	LM23-3AZ <sup>a</sup> [pCSST2]	LM23-3AZ <sup>a</sup> + synergist [10 $\mu$ g]	LM23-3AZ [pCSST2] <sup>a</sup> + synergist [10 $\mu$ g]
0	12.5	12	20	19
50	10	10	19	16
100	10	9	17	14
150	9	<6	16	13
200	9	<6	15	12
250	8	<6	14	11

<sup>a</sup> -  $\alpha$ -factor was spotted on all disks at 0.2  $\mu$ g; numbers represent diameter of halo in mm.

two and four and columns three and five. However, it appears that  $\text{CuSO}_4$  itself had an effect on response to  $\alpha$ -factor alone as decrease in halo size was proportional to  $\text{CuSO}_4$  concentration in the medium (column two) indicating that the  $\text{Cu}^+$  cation may have a detrimental affect on  $\alpha$ -factor binding to Ste2p. The ability of  $\text{Cu}^+$  to affect binding of  $\alpha$ -factor to Ste2p makes these data uninterpretable.

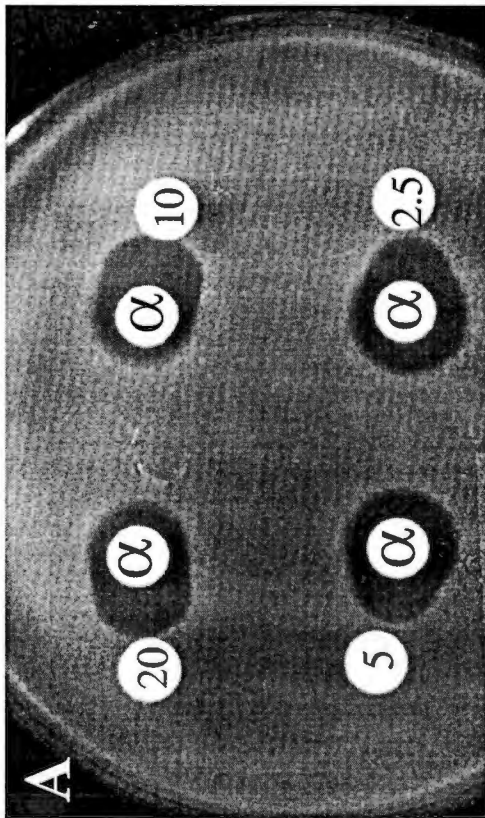
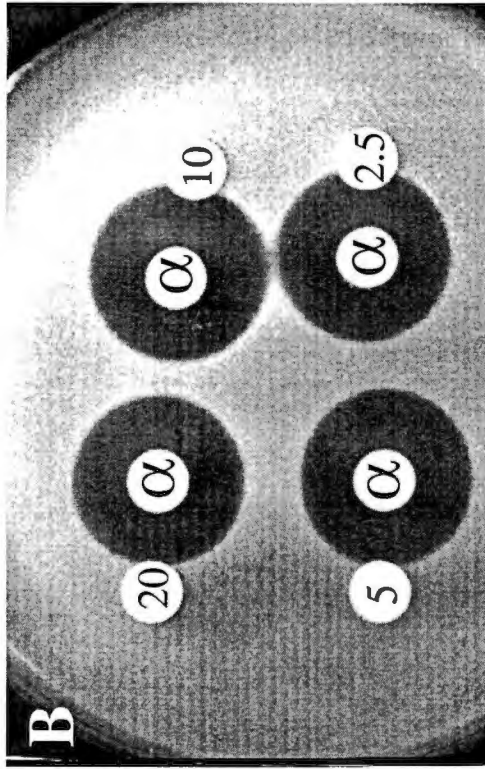
*Synergist activity is concentration dependent on  $\alpha$ -factor.* Binding experiments have been unable to detect synergist binding to the Ste2p receptor. However, studies with the Ste2p null mutant show that the synergist acts through Ste2p. Therefore, it is likely that the synergist does bind to Ste2p but with a very poor binding affinity. While the above expression studies were not as revealing as hoped, the working hypothesis does predict an interesting observation that was made during our investigations. At high  $\alpha$ -factor concentrations (above threshold necessary for activation), synergist would have no contribution on pheromone pathway activation due to the synergist's low binding affinity for Ste2p. When  $\alpha$ -factor concentrations are well below threshold levels, synergist would not be able to contribute to activation because sufficient Sst2p would be present to prevent "weak" activation of the receptor. Therefore, there would be a small window of  $\alpha$ -factor concentrations close to threshold levels where Sst2p would be limiting and free  $\alpha$ -factor concentration was insufficient to compete out binding of synergist. Under these, conditions the synergist would act to increase the overall

'agonist' concentration resulting in enhanced activity. If this were true, activity of the synergist should be concentration dependent on  $\alpha$ -factor. In previous studies, peptides were tested for synergistic activity by placing a disk spotted with the peptide just outside of the edge of the expected halo from a disk spotted with  $\alpha$ -factor (Figure 1). If the peptide were a synergist, the halo from the  $\alpha$ -factor spotted disk protruded towards the disk containing the test peptide, and the synergistic peptide would not show any agonistic activity (halo) on the side of the disk opposite the  $\alpha$ -factor disk (See Figure 8A for visual reference). Typically, putative synergists are tested in growth arrest assays using strain RC629.

Interestingly, when strain LM23-3AZ was used to test the synergist, no enhancing activity was observed (Figure 8B). This was surprising given that LM23-3AZ had been used successfully to test synergistic activation and antagonistic inhibition of *FUS-lacZ* gene induction (H. F. Lu and Becker, personal communication). It is possible that the inability to detect synergy in the LM23-3AZ strain by growth arrest assay may have been due to a limitation of the assay itself. Therefore, the following experiment was performed. A constant amount of the synergist (10  $\mu$ g) was added to a series of disks. Then increasing amounts of  $\alpha$ -factor were spotted on the same series of disks. The diameter of the resulting halos were compared with spotting of  $\alpha$ -factor alone. The experiment was conducted with both RC629 and LM23-3AZ cells. The results are shown in Figure 9. Considering strain RC629, notice that at each concentration of  $\alpha$ -factor, addition of synergist resulted

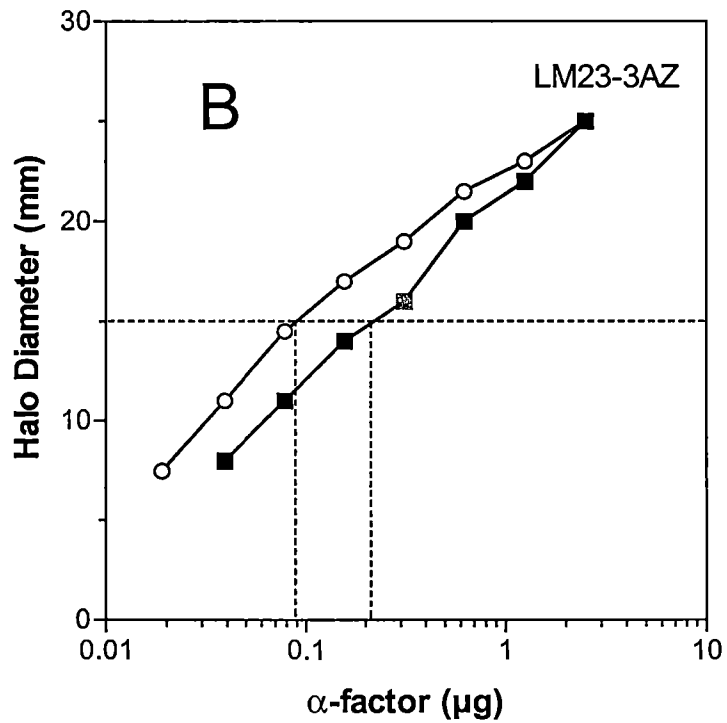
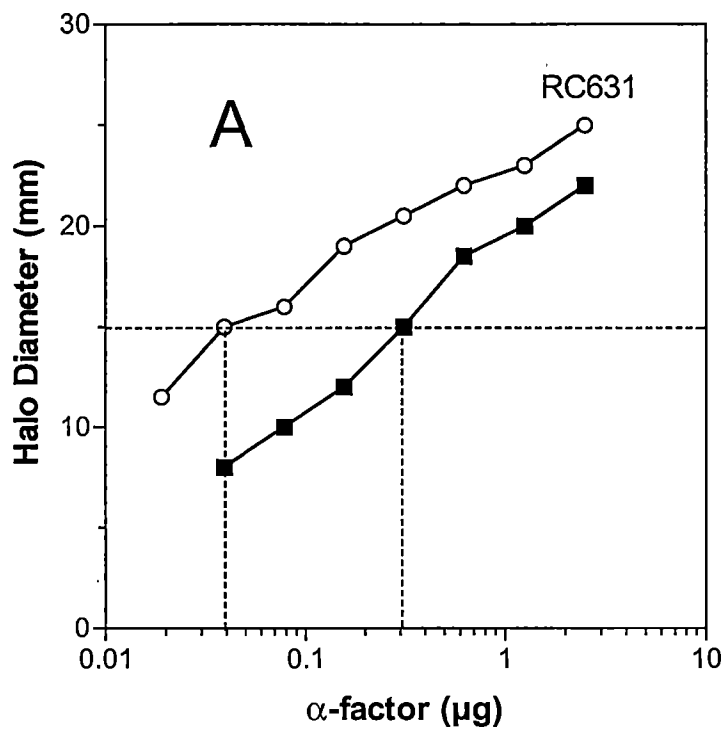
**Figure 8. Test of synergist in growth arrest assay with various strains of *S. cerevisiae*.**

Sterile paper disks were spotted with peptide and placed on a plate overlaid with a lawn of cells. Disks containing the  $\alpha$ -factor synergist, [desM<sup>12</sup>desY<sup>13</sup>]  $\alpha$ -factor, were placed adjacent to disks spotted with  $\alpha$ -factor. Disks containing the synergist peptide are denoted with numbers indicating the  $\mu\text{g}$  of peptide spotted on the disk.  $\alpha$ -factor containing disks are denoted by the ( $\alpha$ ) symbol and were spotted with 0.4  $\mu\text{g}$  of peptide. Panel (A) shows assay with RC629 cells while panel (B) shows LM23-3AZ cells.



**Figure 9. Dose response growth arrest assay by co-spotting of  $\alpha$ -factor and synergist in strains RC629 and LM23-3AZ.**

Sterile paper disks containing peptide were placed on plates overlaid with either RC629 or LM23-3AZ cells. Plates were incubated 24-36 hours. The diameter of the zones of growth inhibition were measured and plotted versus  $\mu\text{g}$  of  $\alpha$ -factor spotted as indicated in graph. A constant amount of synergist ( $10\mu\text{g}$ ) was added when co-spotted with  $\alpha$ -factor. Panel A shows data from strain RC629. Panel B shows results when strain LM23-3AZ. The plots represent  $\alpha$ -factor (■) and cospotting of  $\alpha$ -factor and synergist (○).



in increased halo size. As  $\alpha$ -factor concentration increased the total enhancement caused by the synergist appeared to decrease. However, this was likely due to the fact that the relationship between diameter of halo and volume of halo is not linear. As a result, it takes much more peptide to increase a halo from 25 mm to 26 mm than it would to increase a 10 mm halo to 11 mm. However, there is a substantial difference between the strains in regards to the amount of  $\alpha$ -factor and  $\alpha$ -factor plus synergist necessary to give a 15 mm halo (designated by dotted lines). With strain RC629, 0.3  $\mu\text{g}$  of  $\alpha$ -factor results in a 15 mm halo while only 0.04  $\mu\text{g}$  of  $\alpha$ -factor is necessary to yield a 15 mm halo in the presence of synergist, a difference of 7.5-fold. In contrast, a 15 mm halo using LM23-3AZ requires 0.2  $\mu\text{g}$  of  $\alpha$ -factor without synergist and 0.09  $\mu\text{g}$  with synergist, a difference of only 2-fold. Notice also that the amount of  $\alpha$ -factor alone necessary to give a 15 mm halo differs between the two strains (0.3  $\mu\text{g}$  for RC629 vs. 0.2  $\mu\text{g}$  for LM23-3AZ) indicating that the cells have an inherent difference in sensitivity to  $\alpha$ -factor. This difference in sensitivity means that the end point, defined here as the concentration of  $\alpha$ -factor at the edge of a halo, is lower for the LM23-3AZ strain than for RC629. Therefore, since no synergy was observed with strain LM23-3AZ when the  $\alpha$ -factor and synergist disks were placed adjacent to one another but was observed when the two peptides were added to a single disk, the synergy must be occurring closer in towards the disk and not at the periphery, confounding the ability to observe synergy in the assay presented in Figure 8B .

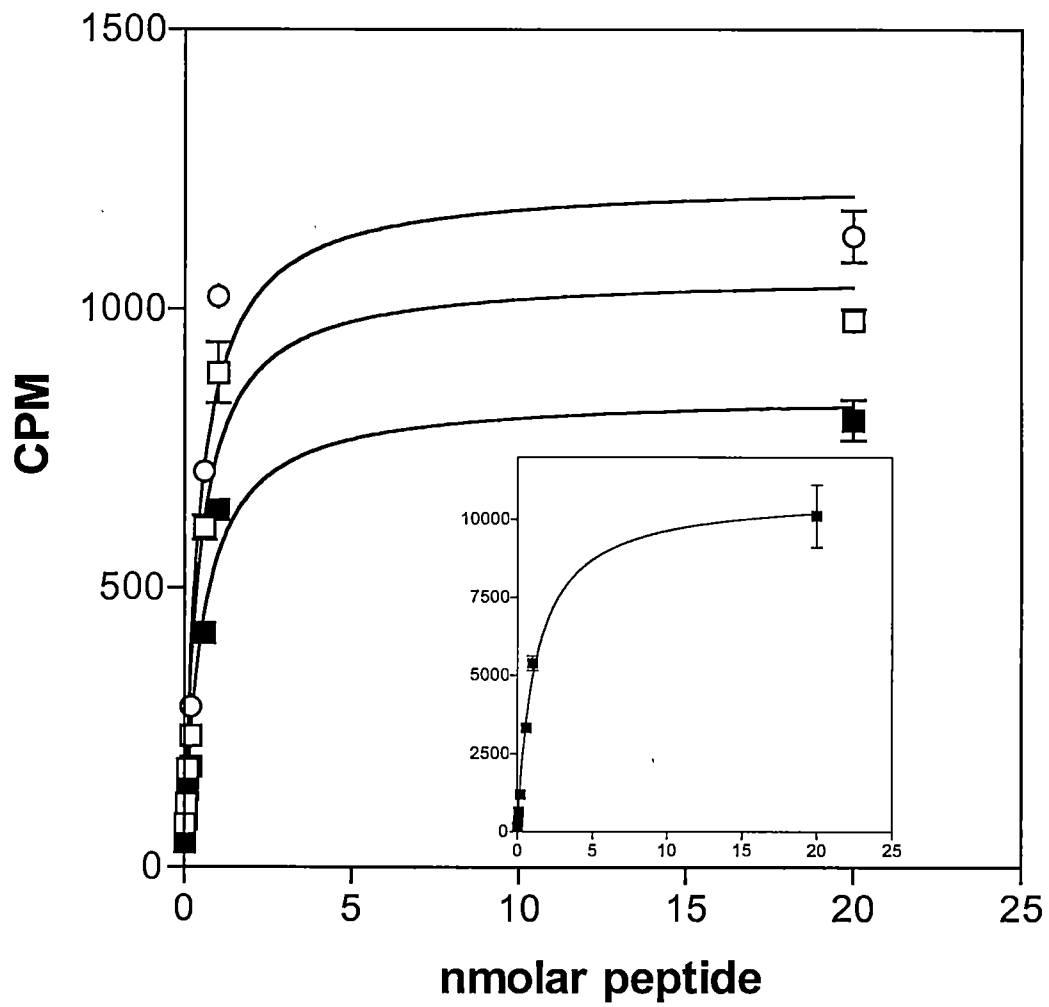


*Binding of  $\alpha$ -factor to bar1 sst2 far1 null strain.* With the evidence that Sst2p may play a crucial role in the synergist phenomenon, efforts were undertaken to construct a strain to better study the affect of Sst2 on receptor signaling. To that end, it would be advantageous to have a strain that lacked *SST2* and *BAR1* ( $\alpha$ -factor protease) so that agonistic activity of the synergist could be studied without having the problem of Bar1p mediated cleavage of the synergist. However, it has been observed by us and other investigators that *sst2 bar1* mutants were not viable. It is thought that a-cells produce very small amounts of  $\alpha$ -factor that is able to auto-activate the a-cell in an autocrine-like manner resulting in activation of growth arrest unless at least one of the two genes (*SST2* or *BAR1*) is functional. The inability to “knock-out” both genes creates a problem in effectively studying the action of the synergist as it, like  $\alpha$ -factor, is susceptible to inactivation by the Bar1p protease. Recently, however, this problem has been partially overcome by deletion of the *FAR1* gene. Upon activation of the pheromone cascade, the Far1p kinase phosphorylates the cell cyclin Cdk1p causing the cells to arrest growth at G1 of the cell cycle. Deletion of *FAR1* prior to double deletion of *SST2* and *BAR1* allows the cell to remain viable because Far1p is not present to inactivate Cdk1p upon activation of the pheromone signal cascade. The triple knockout strain A1111 (*far1 bar1 sst2*) was provided to us by Mark Dumont (University of Rochester) as three independently derived isolates designated A1111A, A1111B and A1111C. Using the A1111 isolates,  $\alpha$ -factor

binding was tested by saturation binding assay with [ $^3\text{H}$ ]  $\alpha$ -factor. RC631 and DK102pNED1 were used as control strains. Binding was performed in triplicate and the results, shown in Figure 10, were analyzed by Prism software using the one site binding equation. Isolates A, B and C showed slightly different Bmax values indicating a possible difference in the total number of binding-competent receptors expressed in the plasma membrane. However, the binding affinity between the isolates was similar as isolates A, B and C exhibited  $K_d$  values of 1.0, 1.2, and 1.6 nM, respectively. The control strain DK102pNED binds with a  $K_d$  value of 1.2 nM. These data indicate that deletion of both *BARI* and *SST2* has no affect on binding of  $\alpha$ -factor to the receptor. It should be noted that this strain contained the reporter construct *FUS1-lacZ* [17] which was going to be used in to monitor propagation of the pheromone signal transduction pathway because it is not affected by the loss of Far1p. However, the *FUS1-lacZ* reporter construct was found to be maximally induced even in the absence of exogenous pheromone, negating its use as an effective reporter to study synergist activation of the pheromone signal cascade.

**Figure 10. Saturation binding analysis with various strains of *S. cerevisiae*.**

Increasing amounts of tritiated  $\alpha$ -factor as indicated on graph were added to cells of A1111 A (■), B (□) and C (○) or DK102pNED (inset). CPM are plotted in relation to peptide concentration (nmolar).



## CHAPTER IV

### DISCUSSION

Previous studies by Erioutou-Bargiota *et al.* [5] concentrated on the initial characterization of the synergistic analog [desM<sup>12</sup>desY<sup>13</sup>]  $\alpha$ -factor. This analog did not show agonistic activity in a wild-type strain but had the ability to enhance the biological activity of  $\alpha$ -factor when added simultaneously with  $\alpha$ -factor. In that initial characterization it was shown that the binding affinity of  $\alpha$ -factor did not change in the presence of synergist and that the synergist acted as an agonist in an *sst2* mutant background. The binding affinity of the synergist was below detectable levels ( $<10^{-4}$ M) under the conditions of the assay used. The current report describes continued characterization of the synergy phenomenon.

The rates of association and dissociation were determined for  $\alpha$ -factor in the presence and absence of synergist. While it was known that the  $K_d$  of  $\alpha$ -factor did not change in the presence of synergist, it was possible that the synergist interacted with the Ste2p in such a way as to cause a change in the rates of association or dissociation of  $\alpha$ -factor to the receptor. However, the results show that the  $k_{on}$  of  $\alpha$ -factor was not affected by synergist. The  $k_{on}$  for  $\alpha$ -factor to Ste2p is quite fast reaching saturation within 4 minutes post addition of radiolabeled peptide. Therefore, the observed rate of  $k_{on}$  is actually measuring the rate of

diffusion of the peptide and only a dramatic reduction in association would allow for a difference to be observed. However, the rate of association and dissociation are related to one another by the  $K_d$  where  $K_d = k_{off}/k_{on}$  so by knowing the  $K_d$  and  $k_{off}$ , the correct value for  $k_{on}$  can be determined. Analysis of the  $k_{off}$  showed that synergist did not statistically change (at 95 % confidence levels) the rate of dissociation of  $\alpha$ -factor. Therefore, since the  $K_d$  and  $k_{off}$  do not change, by definition, the  $k_{on}$  did not change. Based on these data, the synergist did not alter the affinity of  $\alpha$ -factor for Ste2p.

Ligand-induced conformational change of Ste2p was detected by Bukusoglu *et al.* [13] by following altered trypsin fragmentation of the receptor in the presence and absence of  $\alpha$ -factor and an antagonist. The same assay was used here to determine whether synergist alone or synergist plus  $\alpha$ -factor altered the conformation of Ste2p in such a manner that it could be detected by trypsin fragmentation. While we were able to reproduce the findings of Bukusoglu *et al.* [13] by showing that binding of  $\alpha$ -factor resulted in altered trypsin fragmentation, addition of synergist did not result in an altered fragmentation pattern. Fragmentation of Ste2p in the presence of synergist was the same as with no  $\alpha$ -factor added and fragmentation of the receptor in the presence of synergist and  $\alpha$ -factor was the same as adding  $\alpha$ -factor alone. These results suggest that the synergist did not induce a change in receptor conformation or affect  $\alpha$ -factor's

ability to do so. It is possible that the synergist caused subtle changes in the receptor structure that could not be detected using this experimental protocol.

Previous studies with a Ste2p temperature sensitive mutant, that was also mutant for Sst2p, linked synergist activity to the Ste2p receptor [5]. In this study, Ste2p was completely deleted in an *sst2* minus background and tested for response to synergist. The results which showed that there was no agonistic activity of synergist against the *ste2 sst2* background strain and confirmed the earlier study showing that agonistic activity of the synergist in an *sst2* minus background was mediated through Ste2p.

The finding that the synergist acts as an agonist in cell backgrounds that lack Sst2p suggests a link between Sst2p and the synergy phenomenon. To further investigate this apparent link, attempts were made to overexpress Sst2p to determine the affect it would have on synergist activity. To accomplish this the vector pCSST2 was constructed to obtain regulated overexpression of *SST2* by linking the *SST2* open reading frame to the *CUP1* promoter in the YATAG200 yeast expression vector. The use of the *CUP1* expression system had been used successfully by others in our lab to study expression of proteins involved in peptide transport (G. Anderson and J. Becker, personal communication). However, the CuSO<sub>4</sub> added to the medium to drive expression from the *CUP1* promoter appeared to have a negative effect on the cell's ability to respond to  $\alpha$ -factor that

was directly proportional to the amount of  $\text{CuSO}_4$  added. This unexpected effect of  $\text{CuSO}_4$  made interpretation of the results impossible.

One of the most interesting findings from this study was the apparent concentration dependency between synergist and  $\alpha$ -factor. Observations that some strain backgrounds did not show response to synergist during the growth arrest assay led to an alternative method of testing for synergy. Application of the synergist and  $\alpha$ -factor on one disk resulted in obvious enhanced growth arrest that was not apparent in certain strains when  $\alpha$ -factor and synergist were spotted separately on adjacent paper disks. It was also found that the strain (LM23-3AZ) that would not respond to synergist in the two-disk assay was almost 2-fold more sensitive to  $\alpha$ -factor than strain RC629 which responded to synergist in both the two-disk and one disk assays. There are several explanations for this observation. First, enhancement of biological activity by the synergist occurred only at a particular concentration ratio of synergist to  $\alpha$ -factor. Alternatively, synergist is active only after  $\alpha$ -factor has reached a certain threshold concentration. Either of these could explain why synergy was observed in LM23-3AZ when synergist and  $\alpha$ -factor was applied to the same disk but not when placed on separate disks adjacent to one another.

Efforts to study the synergist have been hampered by the inability to construct a *bar1 sst2* strain. The synergist, like  $\alpha$ -factor, is cleaved and inactivated by the Bar1p protease making it difficult to make direct correlation



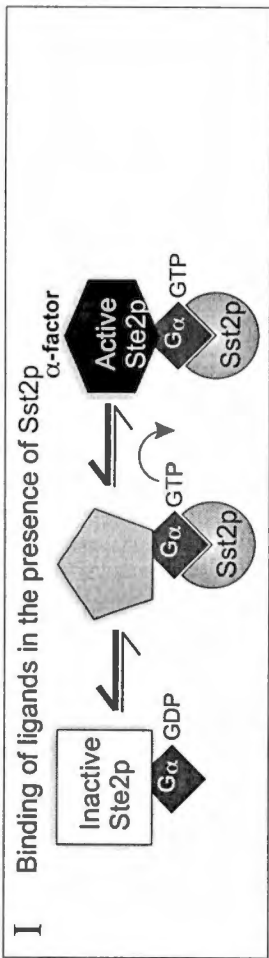
between biological activity and amount of synergist used in an experiment. As Bar1p mediated degradation of the synergist is a time dependent phenomenon, correlating results between assays that take place over very different time periods becomes problematic. For example, the growth arrest assay takes place over a 24-36 hour time period compared to the FUS1-lacZ gene induction assay, which takes only two hours. Recently, the strain A1111 was obtained from the lab of Mark Dumont which is *far1* minus allowing for disruption of *sst2* and *bar1* in the same strain background. Due to the *far1* mutation, this strain cannot be used in  $\alpha$ -factor growth arrest assays. And while A1111 contains a genomic *FUS1*-lacZ reporter construct, the absence of both Bar1p and Sst2p allow for the small amount of  $\alpha$ -factor produced by the a-cell to fully activate the lacZ reporter. As a result, it is not useful as a reporter strain for synergist mediated activation of the pheromone transduction pathway. However, the strain can be used to study peptide receptor interactions. The strain was tested to determine if a *bar1 sst2* mutant altered the  $K_d$  of  $\alpha$ -factor for the receptor. The  $K_d$  did not change and was the same as the control strain DK102pNED (*bar1*).

Finally, presented here are the current models for how the synergist works based on the data collected thus far. The *Sst2p Sequestration Model* (Figure 11) will be considered first. There is strong evidence that Sst2p is directly related to the synergist phenomenon. It has already been shown that Sst2p determined whether the synergist acts as an agonist or as an enhancer only [5]. Therefore, it is

**Figure 11. Model I – Sst2p sequestration**

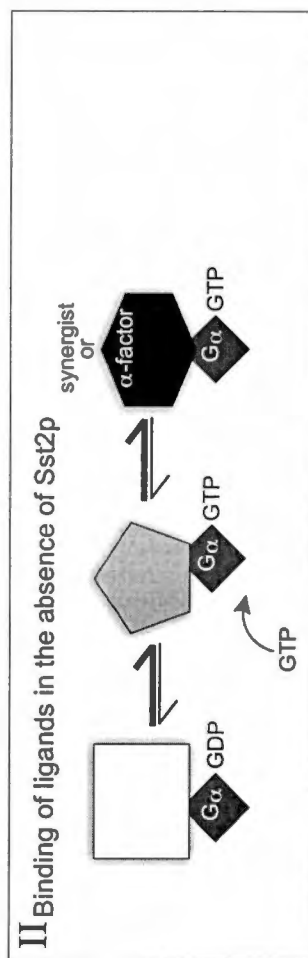
I. a limited number of receptors are stimulated. Sst2p levels are high enough to push the equilibrium back towards the resting state. Synergist even at high concentrations is not able to overcome the affect of Sst2p.

II. When sufficient  $\alpha$ -factor is present to allow for activation of a larger number of receptors Sst2p becomes limiting, leaving unactivated receptors vulnerable for activation by synergist. This acts to increase the overall concentration of agonistic peptide.

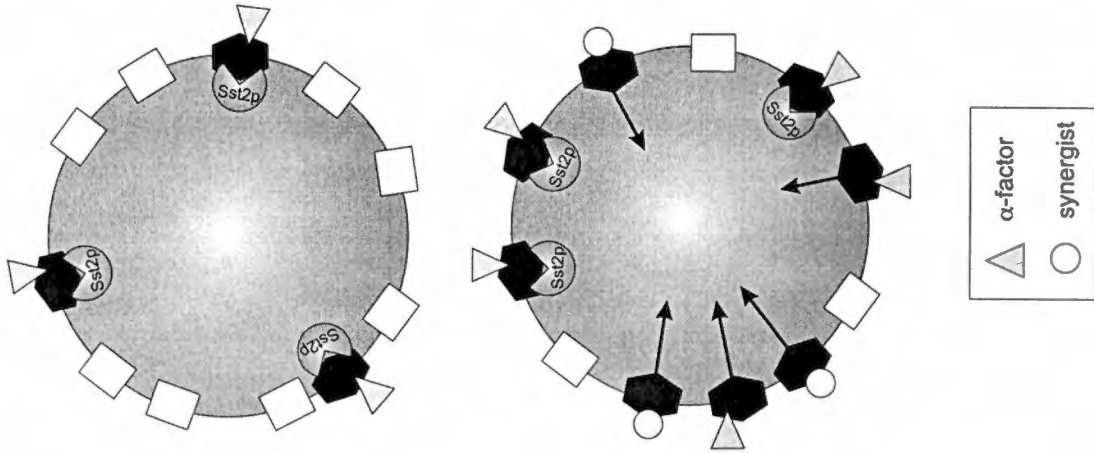


When Ste2p is in the active conformation G $\alpha$  binds GTP. Sst2p recognizes this complex and binds to G $\alpha$  increasing GTPase activity. This shifts the equilibrium to favor an inactive Ste2p/G $\alpha$ -GDP complex as indicated by the size of the reaction arrows. This enables the cell to ensure that low level signaling of the receptor does not result in signal propagation.

However, in the absence of Sst2p, there is no enhancement of the GTPase activity of G $\alpha$  and the equilibrium is shifted toward an active Ste2p/G $\alpha$ -GTP. This not only increases the population of active receptors but also the length of time they spend in the active form.



In this model, propagation of the pheromone signal cascade occurs when the number of Sst2p molecules per activated receptor becomes limiting. After this threshold is reached, additional activated receptors will not be subject to the negative regulation of Sst2p. These receptors will then remain in an active conformation long enough to propagate the pheromone signal. As the synergist is thought to have a low affinity for the receptor, the extended time of the active form of the receptor may allow for synergist binding.

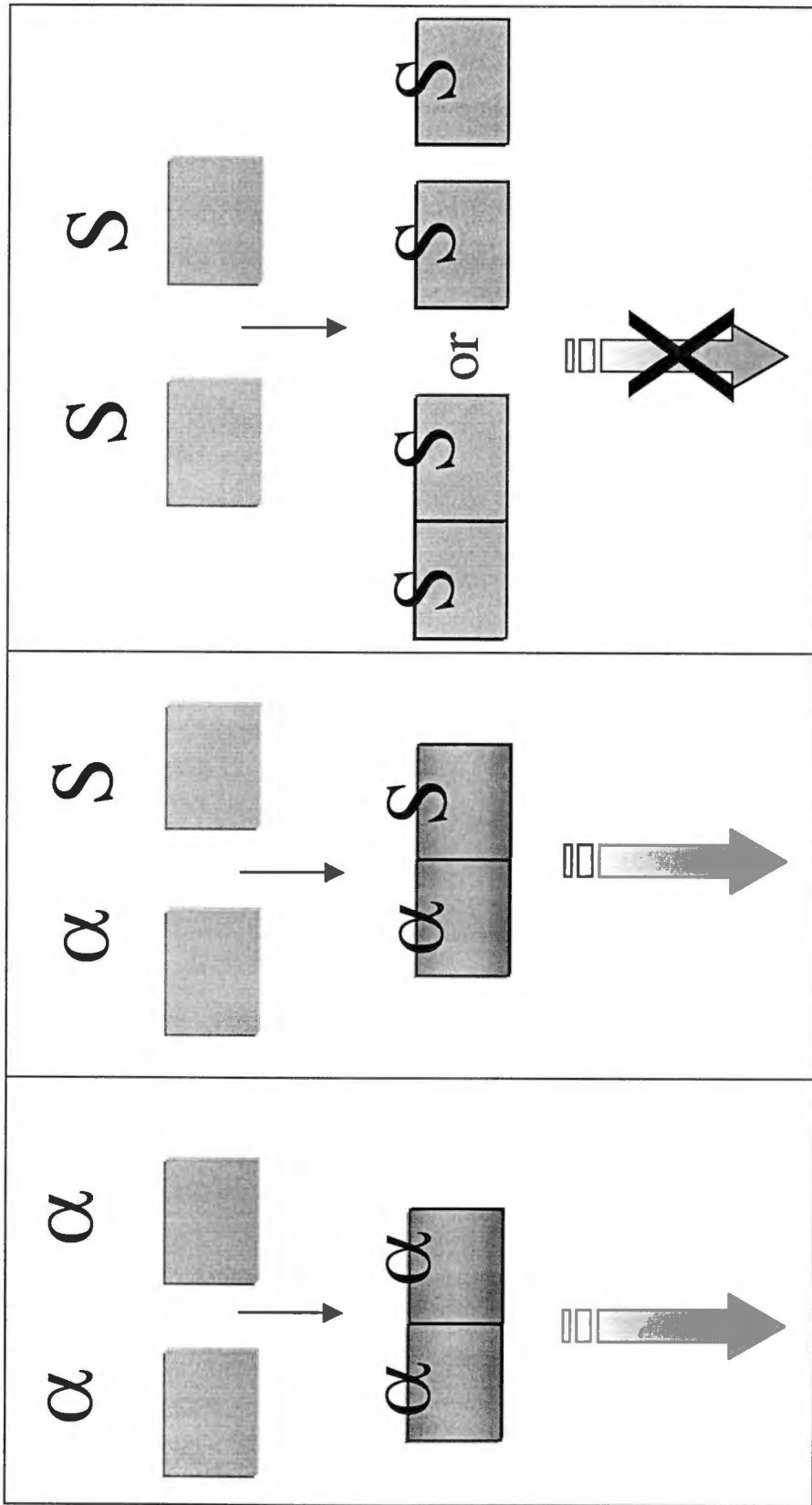


hypothesized that as Ste2p molecules are bound and activated by  $\alpha$ -factor, Sst2p is recruited to the activated receptor to down inactivate the  $G\alpha$  subunit. As more and more Ste2p receptors are activated a point is reached where Sst2p becomes limiting. Then when additional unbound receptors are activated they are not subjected to the inhibitory affects of Sst2p due to its sequestration and can therefore be activated by  $\alpha$ -factor or synergist. Under these conditions, synergist acts as an agonist and increases the total concentration of agonistic peptide [synergist +  $\alpha$ -factor] resulting in more cells being activated *i.e.* enhanced activity. This model predicts that there would be a specific concentration ratio of  $\alpha$ -factor to synergist that would allow for synergy to occur. In other words, if the  $\alpha$ -factor to synergist ratio is too high,  $\alpha$ -factor would readily displace synergist from the receptor making synergist affect on activity negligible. On the other hand, conditions where the  $\alpha$ -factor concentration was below a certain threshold would result in unsequestered Sst2p which would inactivate any receptors activated by the synergist. This leaves a small window of conditions for synergy were the  $\alpha$ -factor concentration is sufficient to sequester the majority of Sst2p proteins but not too high to compete all of the synergist from binding.

The second model is based upon evidence that Ste2p exists as an oligomer in the plasma membrane and is presented in Figure 12. It has been long been noted that when Ste2p is analyzed by Western blot, the receptor runs in monomeric, and multiple oligomeric forms [13, 24]. While the oligomerization

**Figure 12. Model II – heteroactivation of Ste2p dimer.**

Dimers of Ste2p can be activated by two molecules of  $\alpha$ -factor (I) or one  $\alpha$ -factor and one synergist molecule (II). However, binding of synergist alone to either monomeric or dimeric receptor does not result in signal propagation (III).



could be due to sample preparation, recent studies have provided strong evidence using FRET (fluorescence resonance energy transfer) that Ste2p exists at least at some point as an oligomer in the plasma membrane [26]. While most of the evidence indicates that the oligomerization is formed after activation of the receptor, we cannot rule out that the synergist may be acting through an oligomeric complex of Ste2p. For simplicity, I will present the model with a dimeric Ste2p but it can be translated into higher oligomeric forms. If these Ste2p dimers form, it is possible that the transduction cascade could be activated by binding of (1) two molecules of  $\alpha$ -factor or (2) one synergist molecule and one  $\alpha$ -factor molecule. However, binding of two synergist molecules to the Ste2p dimer does not result in signal propagation. The removal of the inhibitory effects of Sst2p in an *sst2* minus strain, would allow the synergist to activate the pheromone cascade. This model also predicts the same concentration dependency between  $\alpha$ -factor and the synergist as stated above. But again this is the less likely of the two models because experimental evidence suggests that oligomerization is not necessary for signaling.

Future studies of the synergist phenomenon may include disruption of the *MF $\alpha$ 1* and *MF $\alpha$ 2* genes that code for  $\alpha$ -factor in A1111 in an attempt to eliminate the autocrine-like activation of Ste2p. Such a strain would be useful as a starting point for experiments to study the effect of *SST2* expression on synergist action. Also, alternative methods to overexpress *SST2* should be investigated such as

using a constitutive promoter such as the alcohol dehydrogenase promoter (ADH) to drive *SST2* expression. The results of this study indicated a concentration relationship between the synergist and  $\alpha$ -factor. This phenomenon could be investigated by performing *FUS1-lacZ* studies using a grid method to look at various ratios of synergist to  $\alpha$ -factor and the affect these ratios have on activation of the pheromone signal cascade.



## REFERENCES

1. Wess, J., *Structure-function analysis of G protein-coupled receptors*. Receptor biochemistry and methodology. 1999, New York: Wiley-Liss. xii, 412 , [8] of plates.
2. Momany, F.A., C.Y. Bowers, G.A. Reynolds, D. Chang, A. Hong, and K. Newlander, *Design, synthesis, and biological activity of peptides which release growth hormone in vitro*. Endocrinology, 1981. **108**(1): p. 31-9.
3. Bowers, C.Y., F. Momany, G.A. Reynolds, D. Chang, A. Hong, and K. Chang, *Structure-activity relationships of a synthetic pentapeptide that specifically releases growth hormone in vitro*. Endocrinology, 1980. **106**(3): p. 663-7.
4. Patchett, A.A., R.P. Nargund, J.R. Tata, M.H. Chen, K.J. Barakat, D.B. Johnston, K. Cheng, W.W. Chan, B. Butler, G. Hickey, and et al., *Design and biological activities of L-163,191 (MK-0677): a potent, orally active growth hormone secretagogue*. Proc Natl Acad Sci U S A, 1995. **92**(15): p. 7001-5.

5. Eriotou-Bargiota, E., C.B. Xue, F. Naider, and J.M. Becker, *Antagonistic and synergistic peptide analogues of the tridecapeptide mating pheromone of Saccharomyces cerevisiae*. *Biochemistry*, 1992. **31**(2): p. 551-7.
6. Chan, R.K. and C.A. Otte, *Isolation and genetic analysis of Saccharomyces cerevisiae mutants supersensitive to G1 arrest by a factor and alpha factor pheromones*. *Mol Cell Biol*, 1982. **2**(1): p. 11-20.
7. Dohlman, H.G., J. Song, D. Ma, W.E. Courchesne, and J. Thorner, *Sst2, a negative regulator of pheromone signaling in the yeast Saccharomyces cerevisiae: expression, localization, and genetic interaction and physical association with Gpa1 (the G-protein alpha subunit)*. *Mol Cell Biol*, 1996. **16**(9): p. 5194-209.
8. Koelle, M.R., *A new family of G-protein regulators - the RGS proteins*. *Curr Opin Cell Biol*, 1997. **9**(2): p. 143-7.
9. Hajdu-Cronin, Y.M., W.J. Chen, G. Patikoglou, M.R. Koelle, and P.W. Sternberg, *Antagonism between G(o)alpha and G(q)alpha in Caenorhabditis elegans: the RGS protein EAT-16 is necessary for*

- G(o)alpha signaling and regulates G(q)alpha activity.* Genes Dev, 1999. 13(14): p. 1780-93.
10. Dong, M.Q., D. Chase, G.A. Patikoglou, and M.R. Koelle, *Multiple RGS proteins alter neural G protein signaling to allow C. elegans to rapidly change behavior when fed.* Genes Dev, 2000. 14(16): p. 2003-2014.
  11. David, N.E., M. Gee, B. Andersen, F. Naider, J. Thorner, and R.C. Stevens, *Expression and purification of the Saccharomyces cerevisiae alpha-factor receptor (Ste2p), a 7-transmembrane-segment G protein-coupled receptor.* J Biol Chem, 1997. 272(24): p. 15553-61.
  12. Raths, S.K., F. Naider, and J.M. Becker, *Peptide analogues compete with the binding of alpha-factor to its receptor in Saccharomyces cerevisiae.* J Biol Chem, 1988. 263(33): p. 17333-41.
  13. Bukusoglu, G. and D.D. Jenness, *Agonist-specific conformational changes in the yeast alpha-factor pheromone receptor.* Mol Cell Biol, 1996. 16(9): p. 4818-23.

14. Laemmli, U.K., *Cleavage of structural proteins during the assembly of the head of bacteriophage T4*. *Nature*, 1970. **227**(259): p. 680-5.
15. Konopka, J.B., D.D. Jenness, and L.H. Hartwell, *The C-terminus of the S. cerevisiae alpha-pheromone receptor mediates an adaptive response to pheromone*. *Cell*, 1988. **54**(5): p. 609-20.
16. Guldener, U., S. Heck, T. Fielder, J. Beinhauer, and J.H. Hegemann, *A new efficient gene disruption cassette for repeated use in budding yeast*. *Nucleic Acids Res*, 1996. **24**(13): p. 2519-24.
17. Liu, S., L.K. Henry, B.K. Lee, S.H. Wang, B. Arshava, B. J.M., and F. Naider, *Position 13 analogs of the tridecapeptide mating pheromone from Saccharomyces cerevisiae: design of an iodinated ligand for receptor binding*. *J. Peptide Res.*, 2000. **56**: p. 24-34.
18. Lieberman, B., *Yeast CUP1 expression-CEN/ARS cloning vector YATAG200 with the hemagglutinin tag sequence, complete sequence*. Genbank submission, 1995.

19. Thiele, D.J., C.F. Wright, M.J. Walling, and D.H. Hamer, *Function and regulation of yeast copperthionein*. *Experientia Suppl*, 1987. **52**: p. 423-9.
20. Mascorro-Gallardo, J.O., A.A. Covarrubias, and R. Gaxiola, *Construction of a CUP1 promoter-based vector to modulate gene expression in Saccharomyces cerevisiae*. *Gene*, 1996. **172**(1): p. 169-70.
21. Degryse, E., B. Dumas, M. Dietrich, L. Laruelle, and T. Achstetter, *In vivo cloning by homologous recombination in yeast using a two-plasmid-based system*. *Yeast*, 1995. **11**(7): p. 629-40.
22. Gietz, R.D., R.H. Schiestl, A.R. Willems, and R.A. Woods, *Studies on the transformation of intact yeast cells by the LiAc/SS- DNA/PEG procedure*. *Yeast*, 1995. **11**(4): p. 355-60.
23. Reneke, J.E., K.J. Blumer, W.E. Courchesne, and J. Thorner, *The carboxy-terminal segment of the yeast alpha-factor receptor is a regulatory domain*. *Cell*, 1988. **55**(2): p. 221-34.

24. Blumer, K.J., J.E. Reneke, and J. Thorner, *The STE2 gene product is the ligand-binding component of the alpha-factor receptor of Saccharomyces cerevisiae*. J Biol Chem, 1988. **263**(22): p. 10836-42.
25. Fujita, V.S., D.J. Thiele, and M.J. Coon, *Expression of alcohol-inducible rabbit liver cytochrome P-450 3a (P-450IIE1) in Saccharomyces cerevisiae with the copper-inducible CUP1 promoter*. DNA Cell Biol, 1990. **9**(2): p. 111-8.
26. Overton, M.C. and K.J. Blumer, *G-protein-coupled receptors function as oligomers in vivo*. Curr Biol, 2000. **10**(6): p. 341-4.

**PART VI**

**GENERAL CONCLUSIONS AND DISCUSSION**

This dissertation details how novel  $\alpha$ -factor analogs have been used to gain better understanding of the structure-function relationships between the  $\alpha$ -factor peptide pheromone and its receptor Ste2p in *S. cerevisiae*. Given below are the major findings from these studies and discussions of possible future experiments.

*Replacement of tyrosine at position 13 in the  $\alpha$ -factor peptide pheromone with phenylalanine results in a ligand with biological activity and binding affinity similar to that of native  $\alpha$ -factor.* Previous literature implied that the phenolic group of Tyr<sup>13</sup> in the  $\alpha$ -factor peptide pheromone was absolutely required for biological activity of the peptide [1]. We have re-evaluated these claims in an attempt to produce a radiolabeled  $\alpha$ -factor ligand with high specific activity (>1000 Ci/mmol) that could be used to study structure-function relationships between  $\alpha$ -factor and Ste2p, a G-protein coupled receptor (GPCR) in the yeast *Saccharomyces cerevisiae*. Labeling of tyrosines in peptides and proteins with <sup>125</sup>I can result in radioactive products with specific activity >2000 Ci/mmol. However, attempts to label Tyr<sup>13</sup> in the  $\alpha$ -factor pheromone resulted in a biologically inactive peptide. We investigated the possibility of replacing Tyr<sup>13</sup> with another amino acid or amino acid analog while still maintaining biological activity. Effective substitution of Tyr<sup>13</sup> would allow Tyr to be placed elsewhere in  $\alpha$ -factor where subsequent iodination would not result in loss of biological activity.



Testing of biological activity and binding affinity of various position 13 analogs revealed that Tyr<sup>13</sup> in  $\alpha$ -factor could be replaced by *p*-F-Phe, *m*-F-Phe, *p*-NO<sub>2</sub>-Phe, *p*-NH<sub>2</sub>-Phe or Phe with at most a 2-fold decrease in biological activity and binding affinity to Ste2p. Substitution of Ser at position 13 resulted in a 6-fold reduction in binding affinity and >100-fold reduction in binding affinity versus  $\alpha$ -factor indicating serine at this position is not tolerated well.

Based on these results, a second generation of peptides was synthesized and characterized starting with [Phe<sup>13</sup>]  $\alpha$ -factor as the parent compound and Tyr, (I) Tyr, or (I<sub>2</sub>)Tyr substituted for Trp at positions 1 or 3. From this study, it was found that [Tyr<sup>1</sup> Arg<sup>7</sup> Phe<sup>13</sup>]  $\alpha$ -factor could be radio-iodinated (specific activity – 2159 Ci/mmol) with only a 3-fold reduction in biological activity and 8-fold reduction in binding affinity. Saturation and competition binding assays with <sup>125</sup>I-[Tyr<sup>1</sup> Arg<sup>7</sup> Phe<sup>13</sup>]  $\alpha$ -factor indicated binding specificity for Ste2p.

*The photoactivatable, crosslinking amino acid analog benzoylphenylalanine (Bpa) can be incorporated into radioiodinatable  $\alpha$ -factor analogs.* Bpa is a UV-activatable crosslinker [2] that can be incorporated into synthetic peptides that can be subsequently radioiodinated. Radioiodinated Bpa photoprobes have been used in a growing number of studies to identify contacts between peptide ligands and the GPCRs they bind [3-10].

Bpa and Tyr were substituted at various residues in the [Arg<sup>7</sup> Phe<sup>13</sup>]  $\alpha$ -factor peptide and the resulting analogs tested for biological activity, binding

affinity and ability to be radioiodinated. One iodinated analog, [Bpa<sup>1</sup> Tyr<sup>3</sup> Arg<sup>7</sup> Phe<sup>13</sup>]  $\alpha$ -factor could be radioiodinated and exhibited relatively good biological activity and binding affinity and was used in Ste2p receptor crosslinking studies.

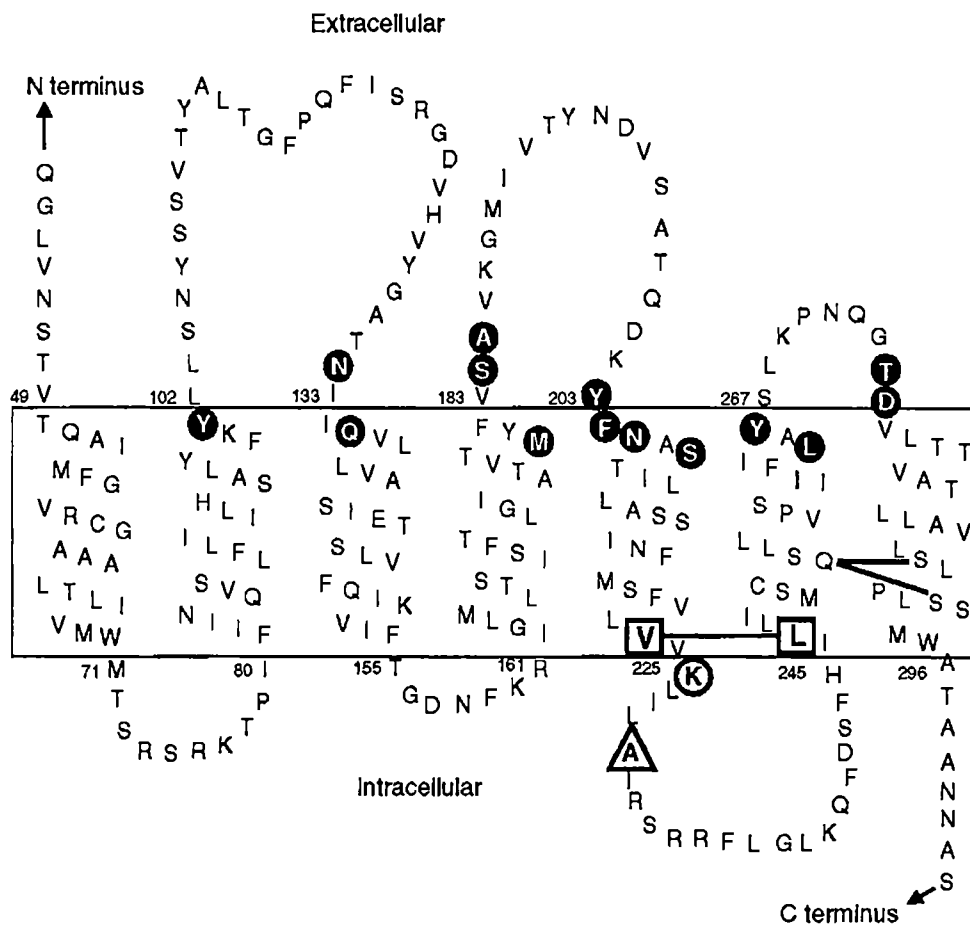
*[Bpa<sup>1</sup> Tyr<sup>3</sup> (<sup>125</sup>I) Arg<sup>7</sup> Phe<sup>13</sup>]  $\alpha$ -factor specifically crosslinks to the Ste2p receptor in membrane preparations.* Photoactivated crosslinking of [Bpa<sup>1</sup> Tyr<sup>3</sup> (<sup>125</sup>I) Arg<sup>7</sup> Phe<sup>13</sup>]  $\alpha$ -factor to membrane preparations of BJ2168 cells transformed with the high level Ste2p expression plasmid, pNED1 [11], resulted in one major radiolabeled band of 54 kD by SDS-PAGE analysis. Furthermore, the intensity of this radiolabeled band was reduced in the presence of excess non-radiolabeled  $\alpha$ -factor indicating specific crosslinking of the radioligand to the Ste2p receptor. No crosslinking was observed in membrane preparations that were not UV photoactivated.

*The photoprobe [Bpa<sup>1</sup> Tyr<sup>3</sup> (<sup>125</sup>I) Arg<sup>7</sup> Phe<sup>13</sup>]  $\alpha$ -factor crosslinks to a fragment of the receptor corresponding to amino acid residues [190-295].*

Chemical digestion of the crosslinked Ste2p- [Bpa<sup>1</sup> Tyr<sup>3</sup> (<sup>125</sup>I) Arg<sup>7</sup> Phe<sup>13</sup>]  $\alpha$ -factor complex with cyanogen bromide and BNPS-skatole followed by SDS-PAGE analysis indicated that the Bpa moiety in the photoprobe crosslinked into an 11 kD fragment of the Ste2p receptor [amino acids [190-295]] comprising extracellular loop two through transmembrane domain VII. This fragment contains two cyanogen bromide cleavage sites, which when cleaved, results in three fragments of 3.2 kD, 3.8 kD, and 4.5 kD in size. Current analysis of the fragmentation

patterns following cyanogen bromide cleavage of the receptor-photoprobe complex does not allow for definitive identification of one of these smaller fragments as the site for covalent attachment of the photoprobe. However, the fact that the 3.8 kD fragment is predicted to be buried deep within the plasma membrane and comprises intracellular loop three makes it a less likely site for crosslinking of the photoprobe.

The 3.2 kD and 4.5 kD fragments mentioned above comprise the second and third extracellular loop domains and are plausible sites for crosslinking as they should be accessible to the photoprobe. The interaction of  $\alpha$ -factor with extracellular loop domains of the receptor is consistent with recent GPCR photoaffinity labeling studies which have discovered direct contacts between peptide ligands and receptor extracellular loop domains [3, 5, 6, 9]. A recent study by Dube *et al.* [12] looking at interaction between the fifth and sixth transmembrane domains of Ste2p using cysteine mutagenesis and crosslinking studies resulted in refinement of the two-dimensional structure of Ste2p in the plasma membrane (Figure 1). Mapping of dominant-negative Ste2p mutants that exhibit defective  $\alpha$ -factor binding [13, 14], revealed that the majority of these residues proposed to be important for  $\alpha$ -factor binding reside within the 3.2 kD and 4.5 kD fragments identified in my crosslinking studies with [Bpa<sup>1</sup> Tyr<sup>3</sup> (<sup>125</sup>I) Arg<sup>7</sup> Phe<sup>13</sup>]  $\alpha$ -factor. The residues corresponding to the dominant negative mutations



**FIG. 1. Predicted membrane topology of the  $\alpha$ -factor receptor.** The central amino acids of the 431-residue long  $\alpha$ -factor receptor are indicated by the *one-letter code*. The *black line* between TMD5 and TMD6 highlights the positions of Val<sup>223</sup> and Leu<sup>247</sup> that are predicted by the results of this study to be in close proximity. A *set of lines* between Gln<sup>253</sup> in TMD6 and Ser<sup>288</sup> and Ser<sup>292</sup> in TMD7 mark the predicted intramolecular contact that was identified by analysis of constitutive mutants. *Black circles* indicate the residues affected by dominant-negative mutations. The *open circle* indicates the position of Lys<sup>225</sup>, and the *triangle* indicates the position of Ala<sup>229</sup>; these are sites of Cys substitutions that caused loss of function and super-sensitivity, respectively. Source: Dube *et al.*, 2000 *J. Biol. Chem.*

within the 3.2 kD and 4.5 kD fragments serve as key starting points for mutagenesis and its affect on crosslinking of [Bpa<sup>1</sup> Tyr<sup>3</sup> (<sup>125</sup>I) Arg<sup>7</sup> Phe<sup>13</sup>]  $\alpha$ -factor.

Future studies should attempt to map the crosslinking of the photoprobe to smaller fragments of the receptor and eventually identify the actual residue(s) in the receptor crosslinked to Bpa in the probe. To accomplish this, it may be possible to use a series of receptor mutants in which single methionines residues in the receptor are mutated to alanine or leucine (E. Arevalo, personal communication). Crosslinking analysis of these mutants and subsequent fragmentation with cyanogen bromide may be able to determine which of the three Ste2p fragments (3.2 kD, 3.8 kD, and 4.5 kD) mentioned above is crosslinked by the photoprobe. Once the smaller fragment is identified, single amino acid mutagenesis of the receptor could be performed to identify the residue(s) involved in crosslinking. While enzymatic cleavage of Ste2p with Glu-C and trypsin did not give sufficient fragmentation to be beneficial in determining the site of crosslinking, it may be possible to use alternative enzymes such as kallikrein [9], Arg-C , and Lys-C [5] to digest the receptor as they have been used with success in other receptor crosslinking studies.

The long-term goal of these studies is to map the  $\alpha$ -factor binding site in Ste2p. One approach to accomplish this is to create a series of  $\alpha$ -factor analogs placing a photoactivatable moiety at each residue. Such an analog series could be used in crosslinking studies to map the contact sites of the Ste2p receptor for each

residue in the  $\alpha$ -factor ligand. For instance, the  $\alpha$ -factor analog [ $Y^1$  ( $I_2$ )  $R^7$   $Bpa^{13}$ ]  $\alpha$ -factor, discussed in Part III of this dissertation, bound to the Ste2p receptor at submicromolar levels ( $K_i$  of 315 nM). It may be possible to radioiodinate the [ $Y^1$   $R^7$   $Bpa^{13}$ ]  $\alpha$ -factor peptide and use it in receptor crosslinking and fragmentation studies. Fruition of crosslinking studies with [ $Bpa^1$   $Y^3$   $R^7$   $F^{13}$ ]  $\alpha$ -factor and [ $Y^1$   $R^7$   $Bpa^{13}$ ]  $\alpha$ -factor could allow the N and C termini of  $\alpha$ -factor to be mapped to the receptor and simplify mapping the binding sites for the other residues in the ligand. Mapping the entire binding site of the  $\alpha$ -factor peptide should provide information on the structure of the active state of Ste2p. Such a map in combination with what is known about the different functional domains of  $\alpha$ -factor (*i.e.* activation domain (N-terminus), bend region (residues 8-10) and binding domain (C-terminus)) could identify individual domains in the Ste2p receptor that play specific roles in ligand binding or signal transduction. While the crosslinking studies with photoactivatable  $\alpha$ -factor analogs are promising to provide direct contacts between the  $\alpha$ -factor ligand and Ste2p, studies with other  $\alpha$ -factor analogs can be quite useful in understanding the structure-function relationships in activation of Ste2p.

*Characterization of a dimeric  $\alpha$ -factor ligand suggests that Lys at position 7 of the peptide is relatively exposed to solvent when  $\alpha$ -factor is bound to the Ste2p receptor.* A dimeric  $\alpha$ -factor molecule formed by bridging side chains of

Lys<sup>7</sup> with an aminohexanoic acid spacer resulted in a ligand with good binding affinity and biological activity. Like  $\alpha$ -factor, the dimer was able to arrest growth and induce expression of the *FUS1-lacZ* reporter gene in pheromone responsive cells. The binding affinity of the dimer was reduced by only 2.9-fold compared to  $\alpha$ -factor. The meager reduction in binding affinity considering the size of the covalent attachment of another  $\alpha$ -factor molecule indicates that the Lys<sup>7</sup> residue is exposed to solvent and not buried in the binding pocket of the receptor as a more dramatic change in binding affinity of the dimer would be expected from steric interactions if the Lys<sup>7</sup> residue were buried deep in the receptor-binding pocket.

*The dimeric  $\alpha$ -factor ligand does not exhibit superactivity in biological or binding assays.* Previous study of ligand analogs of the opioid and serotonin receptors has resulted in the identification of multivalent ligands with superactivity and/or increased receptor subtype specificity [15-24]. The superactivity of these multivalent ligands appeared to be determined by the length of the spacer bridging the molecules and whether that length was sufficient for proper presentation of each active group to its binding site. So, while the  $\alpha$ -factor dimer tested here did not exhibit enhanced activity over native  $\alpha$ -factor, it may be possible to construct a superactive  $\alpha$ -factor dimer by varying the length of the spacer used to connect the  $\alpha$ -factor molecules. Such a study could give information concerning the spacing of Ste2p receptors in the plasma membrane as recent reports have found that Ste2p can exist as oligomeric complexes in the plasma membrane [25, 26].

Receptor oligomers have been proposed to play an important role in signal transduction of some GPCRs [27]. Dimeric  $\alpha$ -factor ligands could be used to test whether Ste2p oligomeric complexes have any effect on signal transduction. What effect would an  $\alpha$ -factor heterodimer in which one-half of the molecule is  $\alpha$ -factor and the other half is the [desW<sup>1</sup> desH<sup>2</sup>]  $\alpha$ -factor antagonist have on signal transduction? Would this heterodimer act similar to the  $\alpha$ -factor dimer or would it act to inhibit signaling? What would be the effect with an antagonist/antagonist homodimer? The effect these multivalent analogs have on signal propagation could provide insight into the role of Ste2p oligomerization in signal transduction.

Overall, conclusions from the studies with the  $\alpha$ -factor dimer allow us to predict local environment of Lys<sup>7</sup> when  $\alpha$ -factor is bound to the receptor. Currently, studies using fluorescent groups attached to the epsilon amine of Lys<sup>7</sup> via spacers of various lengths are underway to investigate the local environment of Lys<sup>7</sup> in receptor-bound  $\alpha$ -factor (X. Ding, B. Lee, F. Naider and J. Becker, personal communication). Information gained from these studies concerning the local environment of Lys<sup>7</sup> residue can be used in combination with data from crosslinking studies to map the  $\alpha$ -factor binding site in Ste2p and make predictions about  $\alpha$ -factor structure and orientation when bound to Ste2p.

The studies discussed above offer insight into the structure-function relationship between  $\alpha$ -factor and the Ste2p receptor using ligands which fit into



the well defined groups of agonist or antagonist. However, many times profound understanding of a problem can come from studying exceptions to the rule.

In the studies of  $\alpha$ -factor-Ste2p interaction, several  $\alpha$ -factor analogs have been discovered which display activity that has not been reported for any other ligand of a GPCR. These peptides, termed synergists, when used in combination with  $\alpha$ -factor resulted in an overall increase in biological activity. However, when used alone the synergists were unable to elicit activation of the pheromone signal transduction pathway. Mode of action studies of the synergistic peptides has yielded the following conclusions.

*The synergists do not act to enhance the observed biological activity of  $\alpha$ -factor by modulating the binding affinity, rate of association or rate of dissociation of  $\alpha$ -factor to Ste2p.* My studies have shown that the  $K_{on}$  (rate of association) and  $K_{off}$  (rate of dissociation) of  $\alpha$ -factor do not change in the presence or absence of synergist. This observation in combination with previous data showing no affect of synergist on the  $K_d$  of  $\alpha$ -factor for Ste2p [28], rule out the hypothesis that  $\alpha$ -factor synergists act by altering  $\alpha$ -factor binding to the receptor.

*Synergists likely act through interaction with Ste2p.* The synergists were able to act as agonists in an *sst2* minus which is 100-fold more sensitive to  $\alpha$ -factor than wild-type strains. However, a previous study [28] and a study presented in Part V of this dissertation show that the agonistic activity of the

synergists is lost in the absence of a functional Ste2p receptor. These findings suggest that the synergists act by interaction with the Ste2p receptor even though binding studies have been unable to detect synergist binding to the receptor. It is possible that synergist binding of Ste2p is too weak to be detected by current binding analysis techniques.

*Enhancement of biological activity by synergist peptides is dependent upon  $\alpha$ -factor concentration.* In growth arrest assays studying the response of *S. cerevisiae* to synergist peptides an interesting observation was made. Strains which displayed different levels of sensitivity to  $\alpha$ -factor also exhibited differential response to synergistic peptides. The original method used to test for synergy was a growth arrest assay which entailed application of  $\alpha$ -factor and synergist to separate paper disks which were placed adjacent to one another on a lawn of cells. The resulting halo of growth arrest around the disk with  $\alpha$ -factor would be noticeably extended towards the disk containing synergist indicating enhanced biological response [28]. However, I found that the extension of the halo towards the disk containing synergist did not occur when using certain *S. cerevisiae* strains. These "synergist unresponsive" strains were tested and displayed an innate 2-fold greater sensitivity to  $\alpha$ -factor than strains that responded to synergist in the above assay. This observation was surprising because one of the synergist unresponsive strains had been used previously to show that synergist peptides were able to enhance  $\alpha$ -factor mediated induction of

the *FUS1-lacZ* reporter gene used to monitor pheromone signaling. To understand why synergist enhancement of growth arrest was not seen with some strains, the growth assay and the information it provides was closely evaluated.

The concentration of  $\alpha$ -factor at the edge of the halo in growth arrest assays is indicative of the minimum concentration of  $\alpha$ -factor required to induce growth arrest for that strain. The synergist responsive and unresponsive strains mentioned above have a respective 2-fold difference in sensitivity to  $\alpha$ -factor. This correlates to a 2-fold difference in the concentration of  $\alpha$ -factor at the edge of the growth arrest halo. This observation led me to believe that the ability of the synergist to enhance the observed biological response may be dependant upon the presence of a particular amount of  $\alpha$ -factor. To test this hypothesis, the growth arrest assay was modified such that  $\alpha$ -factor and synergist were both applied to the same disk instead of separate disks. Under these conditions, co-application of  $\alpha$ -factor and synergist resulted in an observable increase of halo size over use of  $\alpha$ -factor alone in both synergist responsive and synergist unresponsive strains. These results suggest that synergist mediated enhancement of growth arrest in the synergist unresponsive strains was occurring at higher  $\alpha$ -factor concentrations closer to the disk and not at the periphery of the halo as seen with the synergist responsive strains. These findings indicate that the enhancing effect of the synergist is modulated by  $\alpha$ -factor concentration.

While studies of the synergists have failed to provide a clear mechanism for synergist activity, they have ruled out several previous hypotheses and have led to two current models that could explain the synergist phenomenon (See Part V of this dissertation). Model one (*Sst2p sequestration*) focuses on the possible role of Sst2p in synergy as the presence or absence of Sst2p modulates the activity of the synergists from enhancers to agonists. The second model (*Ste2p oligomerization*) suggests that synergist activity may be linked to receptor oligomerization such that interaction between two Ste2p receptors may allow for illicit activation of the signal cascade by synergist.

Future studies should concentrate on testing the validity of these two proposed models. For example, it is known that upon activation of the pheromone signal cascade, Sst2p levels in the cell rapidly decrease [29]. Constitutive overexpression of *SST2* may keep levels of Sst2p relatively high following activation of the pheromone response pathway. Under conditions where Sst2p levels are not limiting, the Sst2p sequestration model predicts that synergist mediated enhancement of pheromone response will be lost. To investigate this hypothesis, studies presented in Part V of dissertation were initiated to evaluate *SST2* expression levels on synergist activity, but the results were inconclusive. The  $\text{CuSO}_4$  used to drive *SST2* expression from the *CUP1* copper inducible promoter had an unforeseen inhibitory effect on  $\alpha$ -factor mediated growth arrest. However, alternative methods of overexpressing *SST2* should be investigated such

as driving expression of *SST2* using the high-level, constitutive glyceraldehyde 3-phosphate dehydrogenase promoter (GPD) which was used successfully in overexpression of Ste2p [11].

It may be possible to determine the nature of the relationship between synergist activity and  $\alpha$ -factor concentration using the 96 well format *FUS1-lacZ* gene induction reporter assay detailed in this dissertation (Part III). The ease of testing multiple samples at one time in this 96 well format would allow for evaluation of the effect various ratios and amounts of  $\alpha$ -factor and synergist had on the ability of synergist to enhance biological activity. Results from such an experiment could provide greater understanding of the synergy phenomenon as to whether a specific amount of  $\alpha$ -factor is required for synergy to be observed or whether a particular ratio of  $\alpha$ -factor and synergist is needed.

It would be interesting to test the biological activity of a synergist/ $\alpha$ -factor dimer created from bridging an  $\alpha$ -factor peptide to a synergist peptide similar to the dimers described in Part IV of this dissertation. Evaluating the biological activity of such dimers could give insight into whether receptor oligomers play a role in the synergist phenomenon. In addition, a crosslinkable synergist or synergist/ $\alpha$ -factor dimer could be used to determine direct interaction of the synergist with Ste2p.

In conclusion, this dissertation describes the synthesis and characterization of a number of new  $\alpha$ -factor analogs and their subsequent use to evaluate

structure-function relationships between the  $\alpha$ -factor pheromone and its receptor, Ste2p. Results with these analogs detail the first report of: (1) direct contact between the first residue in the  $\alpha$ -factor peptide and a fragment of the Ste2p receptor using photo-affinity labeling and (2) synthesis and characterization of an  $\alpha$ -factor dimer which led to evidence that Lys<sup>7</sup> is relatively exposed to solvent and not buried in the receptor when  $\alpha$ -factor is bound to Ste2p. This dissertation also details the further characterization of a novel class of  $\alpha$ -factor analogs termed synergists and has resulted in the creation of hypothetical models to describe synergist action.

## REFERENCES

1. Masui, Y., T. Tanaka, N. Chino, H. Kita, and S. Sakakibara, *Amino acid substitution of mating factor of Saccharomyces cerevisiae structure-activity relationship*. Biochem Biophys Res Commun, 1979. **86**(4): p. 982-7.
2. Dorman, G. and G.D. Prestwich, *Benzophenone photophores in biochemistry*. Biochemistry, 1994. **33**(19): p. 5661-73.
3. Behar, V., A. Bisello, M. Rosenblatt, and M. Chorev, *Direct identification of two contact sites for parathyroid hormone (PTH) in the novel PTH-2 receptor using photoaffinity cross-linking*. Endocrinology, 1999. **140**(9): p. 4251-61.
4. Behar, V., A. Bisello, G. Bitan, M. Rosenblatt, and M. Chorev, *Photoaffinity cross-linking identifies differences in the interactions of an agonist and an antagonist with the parathyroid hormone/parathyroid hormone-related protein receptor*. J Biol Chem, 2000. **275**(1): p. 9-17.
5. Bisello, A., A.E. Adams, D.F. Mierke, M. Pellegrini, M. Rosenblatt, L.J. Suva, and M. Chorev, *Parathyroid hormone-receptor interactions*

- identified directly by photocross-linking and molecular modeling studies.* J Biol Chem, 1998. **273**(35): p. 22498-505.
6. Bitan, G., L. Scheibler, Z. Greenberg, M. Rosenblatt, and M. Chorev, *Mapping the integrin alpha V beta 3-ligand interface by photoaffinity cross-linking.* Biochemistry, 1999. **38**(11): p. 3414-20.
  7. Dong, M., Y. Wang, E.M. Hadac, D.I. Pinon, E. Holicky, and L.J. Miller, *Identification of an interaction between residue 6 of the natural peptide ligand and a distinct residue within the amino-terminal tail of the secretin receptor.* J Biol Chem, 1999. **274**(27): p. 19161-7.
  8. Dong, M., Y. Wang, D.I. Pinon, E.M. Hadac, and L.J. Miller, *Demonstration of a direct interaction between residue 22 in the carboxyl-terminal half of secretin and the amino-terminal tail of the secretin receptor using photoaffinity labeling.* J Biol Chem, 1999. **274**(2): p. 903-9.
  9. Mouldous, L., C.M. Topham, H. Mazarguil, and J.C. Meunier, *Direct identification of a peptide binding region in the ORL1 receptor by photoaffinity labelling with [Bpa10, Tyr14]nociceptin.* J Biol Chem, 2000.



10. Prestwich, G.D., G. Dorman, J.T. Elliott, D.M. Marecak, and A. Chaudhary, *Benzophenone photoprobes for phosphoinositides, peptides and drugs*. Photochem Photobiol, 1997. **65**(2): p. 222-34.
11. David, N.E., M. Gee, B. Andersen, F. Naider, J. Thorner, and R.C. Stevens, *Expression and purification of the Saccharomyces cerevisiae alpha-factor receptor (Ste2p), a 7-transmembrane-segment G protein-coupled receptor*. J Biol Chem, 1997. **272**(24): p. 15553-61.
12. Dube, P., A. DeCostanzo, and J.B. Konopka, *Interaction between transmembrane domains five and six of the alpha-factor receptor*. J Biol Chem, 2000.
13. Leavitt, L.M., C.R. Macaluso, K.S. Kim, N.P. Martin, and M.E. Dumont, *Dominant negative mutations in the alpha-factor receptor, a G protein-coupled receptor encoded by the STE2 gene of the yeast Saccharomyces cerevisiae*. Mol Gen Genet, 1999. **261**(6): p. 917-32.
14. Dosil, M., L. Giot, C. Davis, and J.B. Konopka, *Dominant-negative mutations in the G-protein-coupled alpha-factor receptor map to the*

- extracellular ends of the transmembrane segments*. Mol Cell Biol, 1998. 18(10): p. 5981-91.
15. Patchett, A.A., R.P. Nargund, J.R. Tata, M.H. Chen, K.J. Barakat, D.B. Johnston, K. Cheng, W.W. Chan, B. Butler, G. Hickey, and et al., *Design and biological activities of L-163,191 (MK-0677): a potent, orally active growth hormone secretagogue*. Proc Natl Acad Sci U S A, 1995. 92(15): p. 7001-5.
16. Pauwels, P.J., D.S. Dupuis, M. Perez, and S. Halazy, *Dimerization of 8-OH-DPAT increases activity at serotonin 5-HT1A receptors*. Naunyn Schmiedebergs Arch Pharmacol, 1998. 358(4): p. 404-10.
17. Perez, M., P.J. Pauwels, C. Fourrier, P. Chopin, J.P. Valentin, G.W. John, M. Marien, and S. Halazy, *Dimerization of sumatriptan as an efficient way to design a potent, centrally and orally active 5-HT1B agonist*. Bioorg Med Chem Lett, 1998. 8(6): p. 675-80.
18. Perez, M., C. Jorand-Lebrun, P.J. Pauwels, I. Pallard, and S. Halazy, *Dimers of 5HT1 ligands preferentially bind to 5HT1B/1D receptor subtypes*. Bioorg Med Chem Lett, 1998. 8(11): p. 1407-12.

19. Perez, M., P.J. Pauwels, I. Pallard-Sigogneau, C. Fourrier, P. Chopin, C. Palmier, V. Colovray, and S. Halazy, *Design and synthesis of new potent, silent 5-HT1A antagonists by covalent coupling of aminopropanol derivatives with selective serotonin reuptake inhibitors*. *Bioorg Med Chem Lett*, 1998. **8**(23): p. 3423-8.
20. Portoghese, P.S., G. Ronsisvalle, D.L. Larson, C.B. Yim, L.M. Sayre, and A.E. Takemori, *Opioid agonist and antagonist bivalent ligands as receptor probes*. *Life Sci*, 1982. **31**(12-13): p. 1283-6.
21. Portoghese, P.S., D.L. Larson, C.B. Yim, L.M. Sayre, G. Ronsisvalle, A.W. Lipkowski, A.E. Takemori, K.C. Rice, and S.W. Tam, *Stereostructure-activity relationship of opioid agonist and antagonist bivalent ligands. Evidence for bridging between vicinal opioid receptors*. *J Med Chem*, 1985. **28**(9): p. 1140-1.
22. Portoghese, P.S., D.L. Larson, L.M. Sayre, C.B. Yim, G. Ronsisvalle, S.W. Tam, and A.E. Takemori, *Opioid agonist and antagonist bivalent ligands. The relationship between spacer length and selectivity at multiple opioid receptors*. *J Med Chem*, 1986. **29**(10): p. 1855-61.

23. Portoghese, P.S., H. Nagase, K.E. MaloneyHuss, C.E. Lin, and A.E. Takemori, *Role of spacer and address components in peptidomimetic delta opioid receptor antagonists related to naltrindole*. J Med Chem, 1991. 34(5): p. 1715-20.
24. Portoghese, P.S., A. Garzon-Aburbeh, H. Nagase, C.E. Lin, and A.E. Takemori, *Role of the spacer in conferring kappa opioid receptor selectivity to bivalent ligands related to norbinaltorphimine*. J Med Chem, 1991. 34(4): p. 1292-6.
25. Overton, M.C. and K.J. Blumer, *G-protein-coupled receptors function as oligomers in vivo*. Curr Biol, 2000. 10(6): p. 341-4.
26. Yesilaltay, A. and D.D. Jenness, *Homo-oligomeric complexes of the yeast alpha factor pheromone receptor are functional units of endocytosis*. Mol. Biol. Cell, 2000. 11: p. 2873-2884.
27. Hebert, T.E. and M. Bouvier, *Structural and functional aspects of G protein-coupled receptor oligomerization*. Biochem Cell Biol, 1998. 76(1): p. 1-11.

28. Eriotou-Bargiota, E., C.B. Xue, F. Naider, and J.M. Becker, *Antagonistic and synergistic peptide analogues of the tridecapeptide mating pheromone of Saccharomyces cerevisiae*. *Biochemistry*, 1992. **31**(2): p. 551-7.
29. Dohlman, H.G., J. Song, D. Ma, W.E. Courchesne, and J. Thormer, *Sst2, a negative regulator of pheromone signaling in the yeast Saccharomyces cerevisiae: expression, localization, and genetic interaction and physical association with Gpa1 (the G-protein alpha subunit)*. *Mol Cell Biol*, 1996. **16**(9): p. 5194-200

laboratory

Cellular, Molecular and

He has accepted a postdoc

Nashville, Tennessee where he will be working in the

Blakely studying the regulation of serotonin transporters in the human brain.

Wilmington, Virginia.

Wilmington, North Carolina

graduated from

University of

Master of Science

technician in the

program

University in

Dr. Randy

28. Eriotou-Bargiota, E., C.B. Xue, F. Naider, and J.M. Becker, *Antagonistic and synergistic peptide analogues of the tridecapeptide mating pheromone of Saccharomyces cerevisiae*. *Biochemistry*, 1992. **31**(2): p. 551-7.
  
29. Dohlman, H.G., J. Song, D. Ma, W.E. Courchesne, and J. Thorner, *Sst2, a negative regulator of pheromone signaling in the yeast Saccharomyces cerevisiae: expression, localization, and genetic interaction and physical association with Gpa1 (the G-protein alpha subunit)*. *Mol Cell Biol*, 1996. **16**(9): p. 5194-209.

## VITA

L. Keith Henry was born November 12, 1968 in Newport News, Virginia. He spent the first thirteen years of his life living near Wilmington, North Carolina and moved to Tennessee as a freshman in high school. He graduated from Rutledge High School in Rutledge, Tennessee and attended the University of Tennessee, Knoxville in the Fall of 1987 where he obtained a Bachelor of Science in Cell Biology in 1992. He worked for two years as a research technician in the laboratory of Dr. Jeffrey M. Becker and then entered the doctoral program in Cellular, Molecular and Developmental Biology.

He has accepted a postdoctoral research position at Vanderbilt University in Nashville, Tennessee where he will be working in the laboratory of Dr. Randy Blakely studying the regulation of serotonin transporters in the human brain.